iScience

CellPress

Article

Synthesis of Biaryls via Decarbonylative Palladium-Catalyzed Suzuki-Miyaura Cross-Coupling of Carboxylic Acids

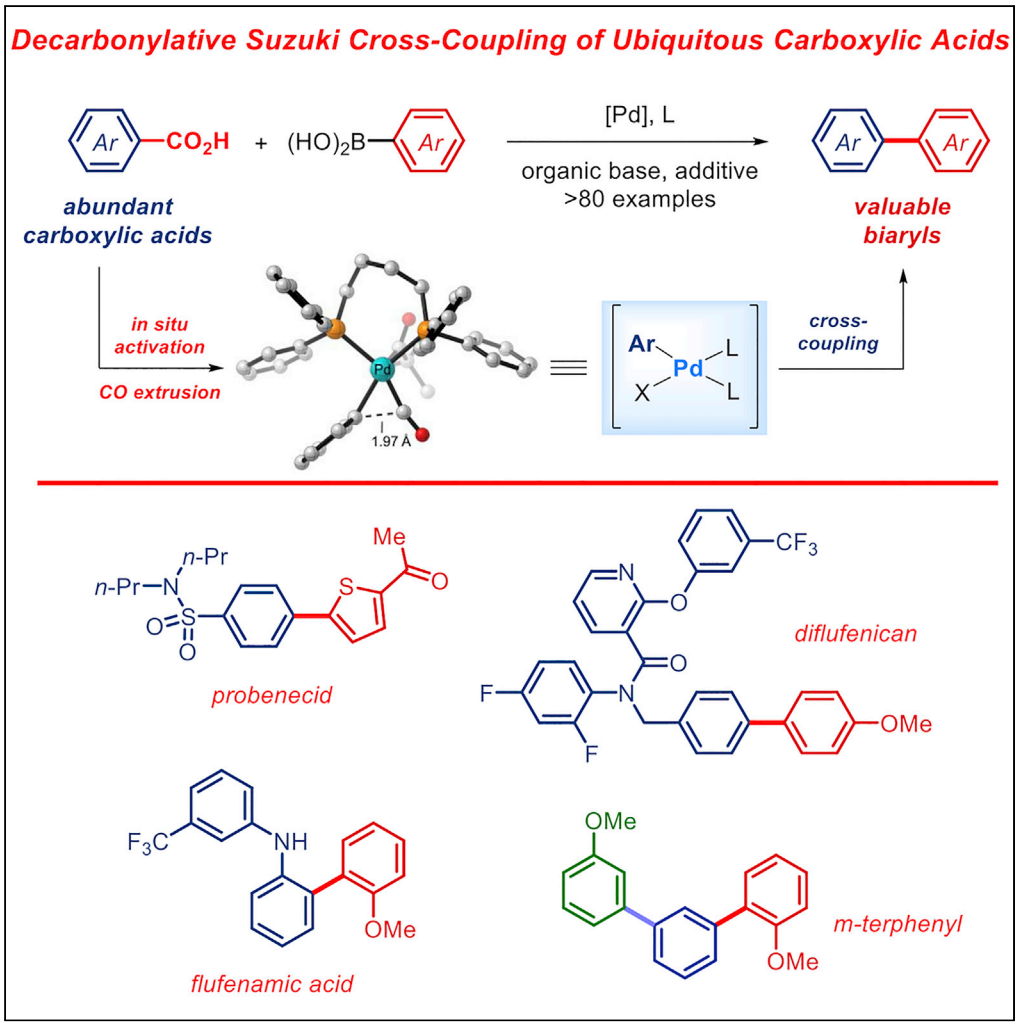

Chengwei Liu, Chong-Lei Ji, Zhi-Xin Qin, Xin Hong, Michal Szostak

hxchem@zju.edu.cn (X.H.)
michal.szostak@rutgers.edu (M.S.)

HIGHLIGHTS

First decarbonylative Suzuki cross-coupling of carboxylic acids via Pd catalysis

Rapid synthesis of functionalized biaryls from ubiquitous carboxylic acids

Mechanistic insights from DFT studies point at the origin of high selectivity

CO loss as a strategy for expanding access to aryl metals (cf. CO_2 loss)

Liu et al., iScience 19, 749–759
September 27, 2019
https://doi.org/10.1016/j.isci.2019.08.021

iScience

CellPress

Article

Synthesis of Biaryls via Decarbonylative Palladium-Catalyzed Suzuki-Miyaura Cross-Coupling of Carboxylic Acids

Chengwei Liu,[2] Chong-Lei Ji,[3] Zhi-Xin Qin,[3] Xin Hong,[3,*] and Michal Szostak[1,2,4,*]

SUMMARY

The biaryl motif is a building block in many drugs, agrochemicals, and materials, and as such it is highly desirable as a synthesis target. The state-of-the-art process for biaryl synthesis from ubiquitous carboxylic acids is decarboxylative cross-coupling involving loss of carbon dioxide (CO_2). However, the scope of these methods is severely limited, mainly due to specific substitution required to promote decarboxylation. The present report implements a decarbonylative version with loss of carbon monoxide (CO) that enables to directly engage carboxylic acids in a Suzuki-Miyaura cross-coupling to produce biaryls as a general method with high cross-coupling selectivity using a well-defined Pd(0)/(II) catalytic cycle. This protocol shows a remarkably broad scope (>80 examples) and is performed in the absence of exogenous inorganic bases. In a broader context, the approach shows promise for routine applications in the synthesis of biaryls by carefully controlled decarbonylation of prevalent carboxylic acids.

INTRODUCTION

The biaryl motif is a privileged subunit in chemical science (Hassan et al., 2002; Horton et al., 2003; Burke and Marques, 2015). The importance of biaryls is highlighted by the wide presence in pharmaceuticals, functional materials, and natural products in both industrial and academic research (Brown and Boström, 2016; Yet, 2018). The biaryl architecture is at the heart of widely prescribed antihypertensive and anticancer agents, which, in addition to the huge economic benefit, save the lives of millions of patients annually (Figure 1A) (Urquahart, 2018). The tremendous success of the conventional Suzuki-Miyaura cross-coupling of aryl halides has provided multiple avenues to generate biaryl architectures of key significance to the chemical industry (Miyaura and Suzuki, 1995; Lennox and Lloyd-Jones, 2014; Molander et al., 2013; Colacot, 2015). Since the 2010 Nobel Prize in Chemistry (Suzuki, 2011), more than 12,000 publications address the improvements to the conventional Suzuki-Miyaura cross-coupling, signifying the great advantage of implementing this transformation (Scifinder, 2019). Although effective, the conventional Suzuki-Miyaura cross-coupling of aryl halides suffers from major limitations, including (1) the use of less available aryl halides, (2) the requirement for stoichiometric inorganic base to trigger transmetallation, and (3) generation of toxic halide waste.

The major breakthrough in using ubiquitous carboxylic acids as substrates for the synthesis of biaryls was achieved in 2006 involving the extrusion of carbon dioxide (–CO_2, Figure 1B; Gooßen et al., 2006). In this carefully engineered design, the use of a copper(I) co-catalyst lowers the decarboxylation barrier and delivers aryl nucleophiles to [Ar–Pd–X] intermediates (X = Cl, Br). Despite severe limitations mainly with respect to the reaction scope, this seminal report has sparked new interest in decarboxylative cross-couplings of ubiquitous carboxylic acids as advantageous substrates in homogeneous catalysis (Gooßen et al., 2008; Dzik et al., 2012). Recent years have witnessed the development of unconventional precursors for the biaryl synthesis, including aryl ethers (Tobisu et al., 2008), acetates (Guan et al., 2008), pivalates (Quasdorf et al., 2008), carbamates (Quasdorf et al., 2011), sulfamates (Quasdorf et al., 2011), and ammonium salts (Blakey and MacMillan, 2003; Tasker et al., 2014). Further progress has been realized in using aroyl precursors, including anhydrides (Gooßen and Paetzold, 2004), esters (Muto et al., 2015), amides (Shi et al., 2016; Ji and Hong, 2017), and acyl fluorides (Malapit et al., 2018) under Rh and Ni catalysis. In an alternative direction, the combined use of photocatalysis and Ni catalysis has effectively addressed the limitation of cross-coupling of C(sp^3) centers (Tellis et al., 2014; Zuo et al., 2014), whereas fundamental studies on ligand design have tackled the challenge of enantiodivergent (Zhao et al., 2018) and conjunctive (Zhang et al., 2016) Pd-catalyzed Suzuki cross-coupling. However, none of these methods have the key

[1]College of Chemistry and Chemical Engineering and Key Laboratory of Auxiliary Chemistry and Technology for Chemical Industry, Ministry of Education, Shaanxi University of Science and Technology, Xi'an 710021, China

[2]Department of Chemistry, Rutgers University, 73 Warren Street, Newark, NJ 07102, USA

[3]Department of Chemistry, Zhejiang University, Hangzhou 310027, China

[4]Lead Contact

*Correspondence: hxchem@zju.edu.cn (X.H.), michal.szostak@rutgers.edu (M.S.)

https://doi.org/10.1016/j.isci.2019.08.021

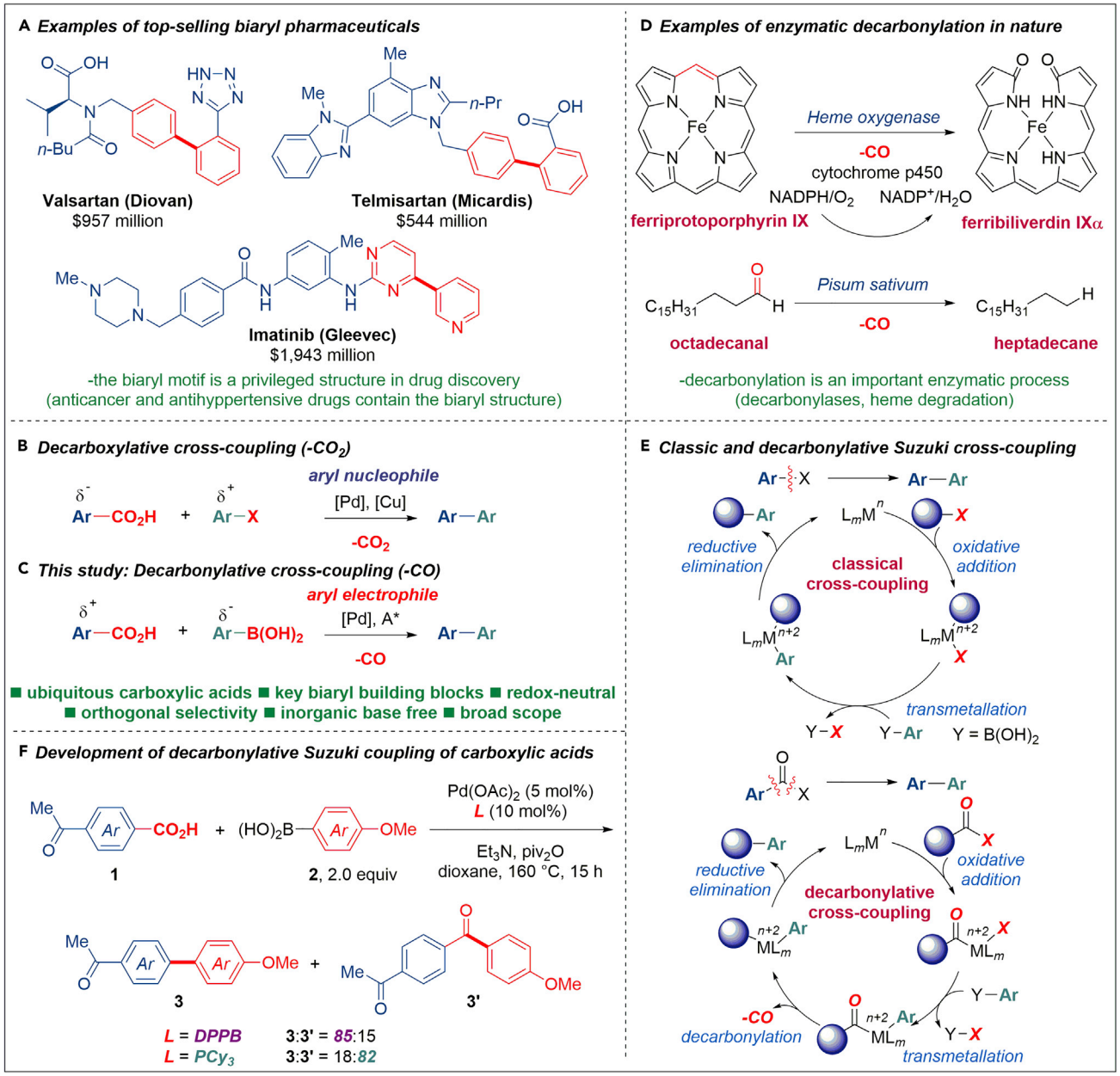

Figure 1. Background and Reaction Development

(A) Examples of top-selling pharmaceuticals containing the biaryl structure.

(B) Enzymatic decarbonylation in nature.

(C) Decarboxylative cross-coupling of carboxylic acids (loss of CO_2): current state of the art.

(D) Proposed decarbonylative cross-coupling of carboxylic acids (loss of CO).

(E) Mechanism of the classic and decarbonylative Suzuki cross-coupling.

(F) Development of decarbonylative Suzuki cross-coupling. Dppb, 1,4-bis(diphenylphosphino)butane; PCy_3, tricyclohexylphosphine; piv, pivaloyl.

advantage of directly engaging the pervasive carboxylic acid functional group in the Suzuki-Miyaura cross-coupling to generate highly useful biaryls.

This report implements a decarbonylative version of Suzuki-Miyaura cross-coupling with loss of carbon monoxide that enables to directly engage carboxylic acids in a redox-neutral pathway to generate biaryls with high selectivity using a well-defined Pd(0)/(II) catalytic cycle (–CO, Figure 1C) (Zhao and Szostak, 2019).

As (1) significantly more carboxylic acids than aryl halides are commercially available and (2) carboxylic acids form an intrinsic part of advanced bioactive products and functional materials, undoubtedly the direct Suzuki-Miyaura cross-coupling of carboxylic acids as electrophilic components represents a modular approach to precisely construct biaryl building blocks. Furthermore, the orthogonal properties of carboxylic acids and the exploitation of carbon monoxide loss (CO versus CO_2, carbon dioxide) offer unique opportunities for catalysis. The C–C bond formation by cross-coupling of boronic acids is a fundamental reaction in organic synthesis that has found widespread application in various areas of chemistry. This report demonstrates the first example of a general utilization of ubiquitous carboxylic acids in the Suzuki cross-coupling for the synthesis of biaryls.

RESULTS AND DISCUSSION

We anticipated that carboxylic acids can be galvanized into the decarbonylative (Murphy et al., 2015; Ryter and Tyrrell, 2000; Cheesbrough and Kolattukudy, 1984) Suzuki-Miyaura manifold (Figures 1D and 1E) through *in situ* activation, a process that is reminiscent of the classical activation of carboxylic acid derivatives in organic synthesis and has been utilized to great effect in decarboxylative cross-couplings of C(sp^3) electrophiles (Qin et al., 2016; Edwards et al., 2017; Fawcett et al., 2017). We targeted Pd catalysis and *in situ* activation as two key design elements to execute high catalytic efficiency, modularity, and practical significance. Studies showed that oxidative addition of a C–O bond of anhydrides occurs with high selectivity (Gooßen et al., 2008; Dzik et al., 2012); however, unselective decarbonylation and transmetallation lead to ketone products. Given this challenge, we hypothesized that a union of a sterically hindered O-acyl group and a bidentate ligand would favor decarbonylation (*vide infra*, **TS7**, Figure 2B), providing a simple and practical access to biaryls directly from carboxylic acids. Extensive optimization identified two catalytic systems that led to vastly different outcomes in the cross-coupling of 4-acetyl-benzoic acid with 4-MeO(C_6H_4)-B($OH)_2$ (2.0 equiv.) as the model reaction (Figure 1F and Supplemental Information): (1) Pd($OAc)_2$ (5 mol %)/1,4-bis(diphenylphosphino)butane [dppb] (10 mol %), piv_2O (2.0 equiv.), Et_3N (2.0 equiv.), dioxane, 160°C: biaryl: ketone = 85:15 selectivity (82% yield of the biaryl); (2) Pd($OAc)_2$ (5 mol %)/PCy_3 (10 mol %), piv_2O (2.0 equiv.), Et_3N (2.0 equiv.), dioxane, 160°C: biaryl: ketone = 18:82 selectivity (68% yield of the ketone). Selected key optimization results are presented in Table 1. It is noteworthy that an inorganic base is not required (entries 3–6), establishing a practical parallel to the Ni(0)-catalyzed method (Malapit et al., 2018) and that there is a good correlation between the efficiency and the ligand bite angle (entries 9–15) (Miyaura and Suzuki, 1995; Lennox and Lloyd-Jones, 2014). Note that the absence of piv_2O resulted in no reaction, in agreement with our design (not shown).

At this point, extensive density functional theory (DFT) studies were conducted to provide insight into the origin of the reaction selectivity and determine the reaction pathway (Figure 2, for the Cartesian coordinates, see Data S1, related to Figure 2). Note that the reaction is efficient in the absence of an inorganic base (Lennox and Lloyd-Jones, 2013; Malapit et al., 2018), which implies generation of the transmetallation-active [Ar–Pd–X] intermediate that could directly engage in transmetallation with a boronic acid under functional-group-tolerant inorganic-base-free conditions. The computed reaction energy profile with Pd/dppb catalyst is shown in Figure 2A (see the Supplemental Information for DFT calculation details). From the substrate-coordinated complex **4**, the acyl C–O bond cleavage via **TS5** generates the LPd(acyl) (OPiv) intermediate **6**. This acylpalladium intermediate undergoes decarbonylation through **TS7**, and subsequent CO extrusion leads to the arylpalladium species **9**. From **9**, the boronic acid coordinates to allow the transmetallation via **TS11**, leading to intermediate **12**. In **TS11**, the pivalic leaving group acts as an intramolecular base, which transfers the boronic acid to the corresponding boronate and promotes the transmetallation process. This suggests that the overall transformation does not require an external base, which is consistent with the experimental conditions. Therefore, the design of anhydride not only controls the desired C–O bond activation but also plays a critical role in the base-free transmetallation. After the transmetallation, **12** dissociates PivOB($OH)_2$ to form intermediate **13**, which undergoes C–C reductive elimination through **TS14** to generate the product-coordinated complex **15**. Final product liberation of **15** produces the biaryl cross-coupling product and regenerates the active palladium catalyst. Based on the computed free energy profile, the acylpalladium species **6** is the on-cycle resting state, and the transmetallation step via **TS11** is the rate-limiting step with a 31.8 kcal/mol overall barrier (**6** to **TS11**).

The mechanistic model provides a rationale for the ligand-controlled chemoselectivity of competing arylation and acylation. The computed chemoselectivities of dppb ligand are included in Figure 2B. From the acylpalladium intermediate **6**, decarbonylation and transmetallation determines the chemoselectivity (**TS7** versus **TS17**) if the CO extrusion is considered irreversible from a reaction kinetics perspective. Our

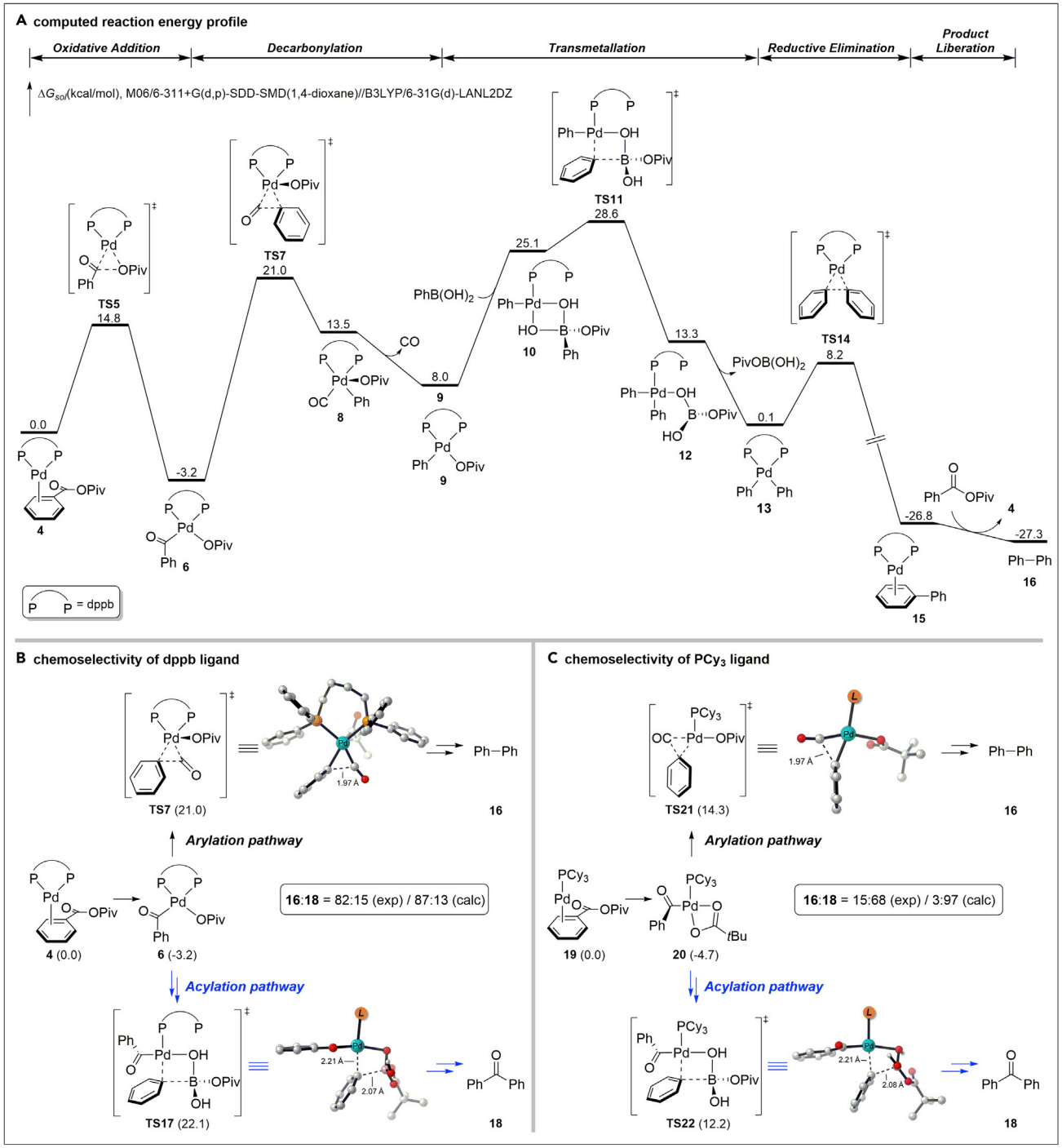

Figure 2. DFT-Calculated Reaction Energy Profile and Chemoselectivities of Pd-Catalyzed Decarbonylative Suzuki-Miyaura Cross-Coupling of Benzoic Pivalic Anhydride

(A) Computed reaction energy profile.

(B) Chemoselectivity of dppb ligand.

(C) Chemoselectivity of PCy_3 ligand.

All energies are in kcal/mol. Hydrogens are omitted for clarity in the transition state diagrams. DFT calculation details are provided in Transparent Methods in the Supplemental Information.

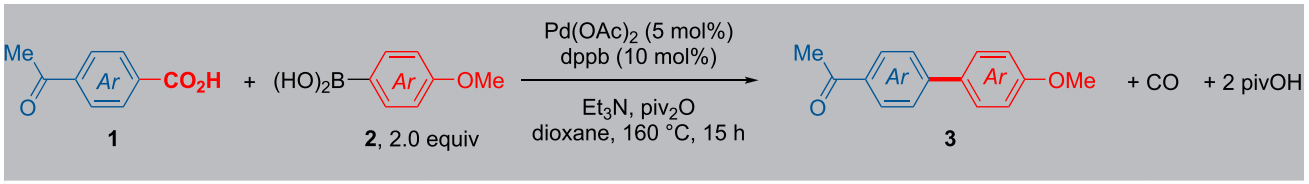

Entry	Variation from Standard Conditions	Yield (%)[a,b]
1	No change	82 (15)
2	No H_3BO_3	49 (9)
3	Na_2CO_3 instead of Et_3N	52 (15)
4	K_2CO_3 instead of Et_3N	51 (23)
5	Added Na_2CO_3	80 (12)
6	Added K_2CO_3	71 (13)
7	Pyridine instead of Et_3N	43 (6)
8	DMAP instead of Et_3N	43 (<2)
9	PPh_3 instead of dppb	24 (61)
10	PCy_3HBF_4 instead of dppb	15 (68)
11	DavePhos instead of dppb	<2 (<2)
12	dppp instead of dppb	<10 (<2)
13	dpppe instead of dppb	44 (21)
14	BINAP instead of dppb	27 (27)
15	XantPhos instead of dppb	26 (3)

Table 1. Summary of Optimization and Control Reaction Conditions

Standard conditions: Carboxylic acid (1.0 equiv.), Ar–B(OH)$_2$ (2.0 equiv.), Pd(OAc)$_2$ (5 mol %), dppb (10 mol %), Et_3N (2.0 equiv.), piv$_2$O (2.0 equiv.), H_3BO_3 (2.0 equiv.), dioxane, 160°C, 15 h.

GC< gas chromatography; NMR, nuclear magnetic resonance; dppb, 1,4-bis(diphenylphosphino)butane; piv, pivaloyl; Et_3N, triethylamine; DMAP, 4-dimethylaminopyridine; dppp, 1,3-bis(diphenylphosphino)propane; dppe, 1,2-bis(diphenylphosphino)ethane; BINAP, 2,2′-bis(diphenylphosphino)-1,1′-binaphthalene.

[a]Determined by GC/^{1}H NMR.

[b]Yields of the ketone product are shown in parentheses. See Table S2 in Supplemental Information for details.

computations indicate that **TS7** is 1.1 kcal/mol more favorable than **TS17**, which agrees well with the experimental observations that dppb ligand leads to arylation product. In contrast, for PCy_3 ligand, the acylation pathway is more favorable by 2.1 kcal/mol (**TS21** versus **TS22**, Figure 2C). The detailed free energy profile of PCy_3 ligand is included in the Supporting Information. This reversed selectivity is due to the denticity change of the ligands. Bidentate dppb ligand favors the decarbonylation step, because **TS7** has two phosphine coordinations, whereas **TS17** only has one phosphine coordination. This change of ligation does not exist for monodentate PCy_3 ligand because both transition states **TS21** and **TS22** have one phosphine coordination, which is why the chemoselectivity is reversed. Therefore, the ligand denticity is a useful approach to control the chemoselectivity in the Pd-catalyzed Suzuki-Miyaura cross-coupling of carboxylic acids (see the Supplemental Information for additional studies on the mechanism).

Synthetically, the key advantage of this approach is that carboxylic acids are directly engaged in the synthesis of biaryls without separate preactivation steps. The released by-products in the process are CO and a mild organic acid pivOH (pK_a = 5.0), which alleviate the potential side reactions, while at the same time this approach obviates toxic and more expensive activating reagents (e.g., TFFH [tetramethyl fluoroformamidinium hexafluorophosphate]) (Malapit et al., 2018) and, importantly, is performed on the benchtop using commercially available, air- and moisture-stable reagents, which supersedes previous methods using air-sensitive Ni(0). This results in a broadly applicable gateway to the Suzuki-Miyaura cross-coupling of carboxylic acids under redox-neutral conditions.

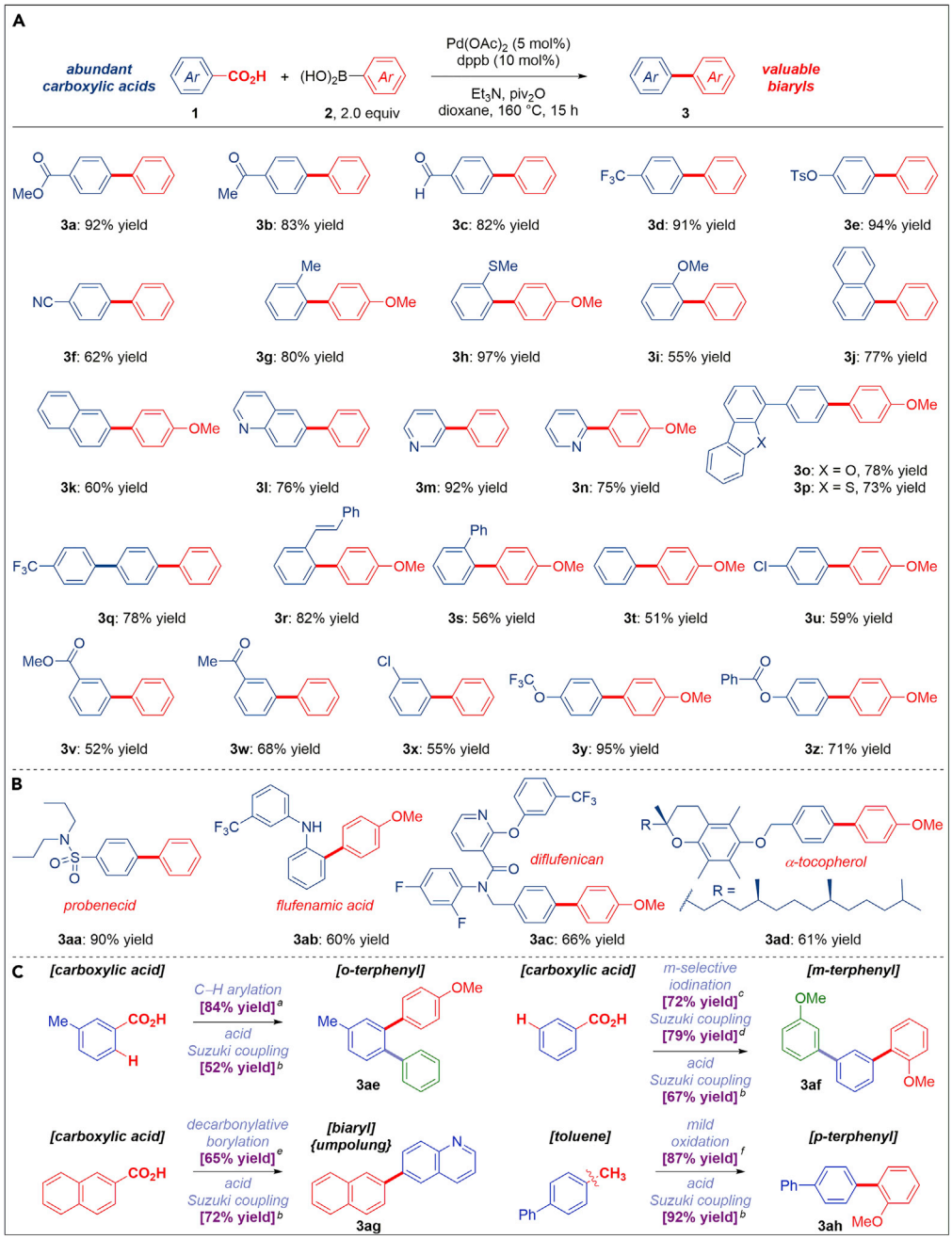

Figure 3. Scope of the Decarbonylative Suzuki-Miyaura Cross-Coupling of Carboxylic Acids: Carboxylic Acid Scope

(A) Scope of carboxylic acids.

(B) Late-stage functionalization.

(C) Sequential cross-coupling.

Conditions: Carboxylic acid (1.0 equiv.), Ar–$B(OH)_2$ (2.0 equiv.), $Pd(OAc)_2$ (5 mol %), dppb (10 mol%), Et_3N (1.5 equiv.), piv_2O (1.5 equiv.), H_3BO_3 (1.5 equiv.), dioxane, 160°C, 15 h. dppb, 1,4-bis(diphenylphosphino)butane; piv, pivaloyl.

The scope of this process is remarkably broad. In all examples, carboxylic acids were used directly without any preactivation steps. As shown in Figure 3A, a wide range of carboxylic acid substrates are compatible, including tolerance to many functional groups that might be exploited in a myriad of downstream transformations. Esters (**3a**), ketones (**3b**), aldehydes (**3c**), trifluoromethyl groups (**3d**), tosylates (**3e**), and nitriles (**3f**)

provide the biaryl products in high yields. Steric substitution, including *ortho*-alkyl (**3g**), *ortho*-thiomethyl (**3h**), *ortho*-methoxy (**3i**), as well as 1-naphthyl (**3j**), proved compatible. Note that decarboxylative biaryl syntheses typically require an activating substituent to favor decarboxylation (Gooßen et al., 2006, 2008; Dzik et al., 2012), whereas this is not needed in the present process. Polyaromatic (**3k**) and heterocyclic substrates (**3l–3p**), such as naphthalene, quinoline, pyridines, benzofuran, and benzothiophene, gave the cross-coupling adducts with high selectivity. Notably, owing to the activating role of carboxylic acids in the conventional cross-coupling strategies (Miyaura and Suzuki, 1995; Lennox and Lloyd-Jones, 2014), the present process can be readily utilized in the synthesis of terphenyls, including push-pull compounds (**3q**), and conjugated stilbenes (**3r**), which are widely exploited in the synthesis of functional materials (Beller and Blaser, 2012). Furthermore, electronically unactivated carboxylic acids (**3t**) as well as reactive functional groups, such as chloro (**3u**), ester (**3v**), ketone (**3w**), trifluoromethyl ether (**3y**), and phenolic ester (**3z**), also delivered the corresponding biaryls in good to excellent yields. The latter example is particularly noteworthy as it highlights compatibility of the present process with highly activated phenolic esters, which can be reacted under forcing Ni catalysis (Muto et al., 2015). This unique selectivity is predicated on selective activation of carboxylic acid derivatives enabled by transition metal catalysis (resonance energy, PhC(O)–Opiv = 5.1 kcal/mol versus PhC(O)–OPh, 9.3 kcal/mol, barrier to rotation) (Zhao and Szostak, 2019).

The synthetic potential of this method is showcased in the direct functionalization of pharmaceuticals and bioactive natural products (Figure 3B), including probenecid (**3aa**), flufenamic acid (**3ab**), diflufenican (**3ac**), and tocopherol (**3ad**), highlighting the potential impact of the present protocol for late-stage introduction of biaryl architectures directly exploiting the carboxylic acid functional group. The utility of this direct cross-coupling strategy is further emphasized by the unique capacity of carboxylic acids to act as traceless activating groups (Figure 3C). To this end, metal-catalyzed C–H functionalizations directed by a carboxylic acid (**3ae**) as well as metal-free electrophilic halogenation (**3af**) significantly expand the pool of carboxylic acid precursors available for cross-coupling (Twilton et al., 2017; Knappke and Jacobi von Wangelin, 2010). The combination with decarbonylative borylation (Liu et al., 2018) to furnish organoboranes directly from carboxylic acids (**3ag**) and valorization of toluenes (**3ah**) (Figure 3C) offers a new opportunity for adopting in synthetic processes.

The scope of the method with respect to the boronic acid coupling partner was also investigated, as shown in Figure 4. Pleasingly, we found that a wide range of aryl boronic acids are amenable to this biaryl Suzuki-Miyaura cross-coupling process, including deactivated electron-deficient boronic acids bearing an array of sensitive functional groups poised for further modification, such as ketones (**3ai**), esters (**3aj**), aldehydes (**3ak**), and nitriles (**3am**). Furthermore, electron-rich boronic acids that could lead to a competing ketone formation (**3an**) (Malapit et al., 2018) as well as fluorinated (**3ao-3aq**) (Campbell and Ritter, 2015) and sterically hindered boronic acids (**3ar**) are effectively coupled in this protocol. Substitution at the unconjugated 3-position was well-tolerated (**3at-3av**). Moreover, we found that various heterocyclic as well as polyaromatic substrates cross-couple in this redox-neutral protocol with high efficiency (**3aw-3ba**). The utility of this method is further demonstrated in the direct synthesis of biaryls bearing electrophilic carbonyl (**3bb-3bi**) and halogen handles (**3bj-3bm**) for subsequent manipulation by the traditional nucleophilic addition or cross-coupling strategies.

Studies were conducted to determine steric limits of the current protocol (Figure 4B). *Ortho*-substituted biaryls are important structural motifs in biologically active products and functional materials. We found that 2,6-disubstitution on the boronic acid component is well-tolerated, including various useful functional groups on the carboxylic acid cross-coupling partner (**3bn-3bs**). The steric limits of the present protocol are reached with tri-*ortho*-substituted biaryls (**3bu**) as well as with 2,2′-bis-*ortho*-substituted biaryls (**3bv**). These results bode well for future catalyst optimization efforts to promote decarbonylative coupling toward multiply *ortho*- substituted biaryls. Finally, to further demonstrate the powerful opportunity in late-stage derivatization of pharmaceuticals (Blakemore et al., 2018), we conducted a series of direct reactions with probenecid (**3bw-3cc**) and flufenamic acid (**3cd-3ce**) that allow for selective modification of the active core. Clearly, the ubiquity of the carboxylic acid unit in biologically active molecules highlights the advantage of the direct decarbonylative biaryl cross-coupling strategy.

Several additional points are to be noted. (1) In analogy to the classical Pd-catalyzed Suzuki-Miyaura cross-coupling of aryl halides electron-rich boronic acids couple preferentially, whereas electron-deficient electrophiles are more reactive, consistent with facility of metal insertion. (2) Sterically hindered electrophiles and boronic acids are more reactive, consistent with decarbonylation favored by steric demand of acylmetals. It should be noted that more electron-deficient carboxylic acids are also likely to undergo faster

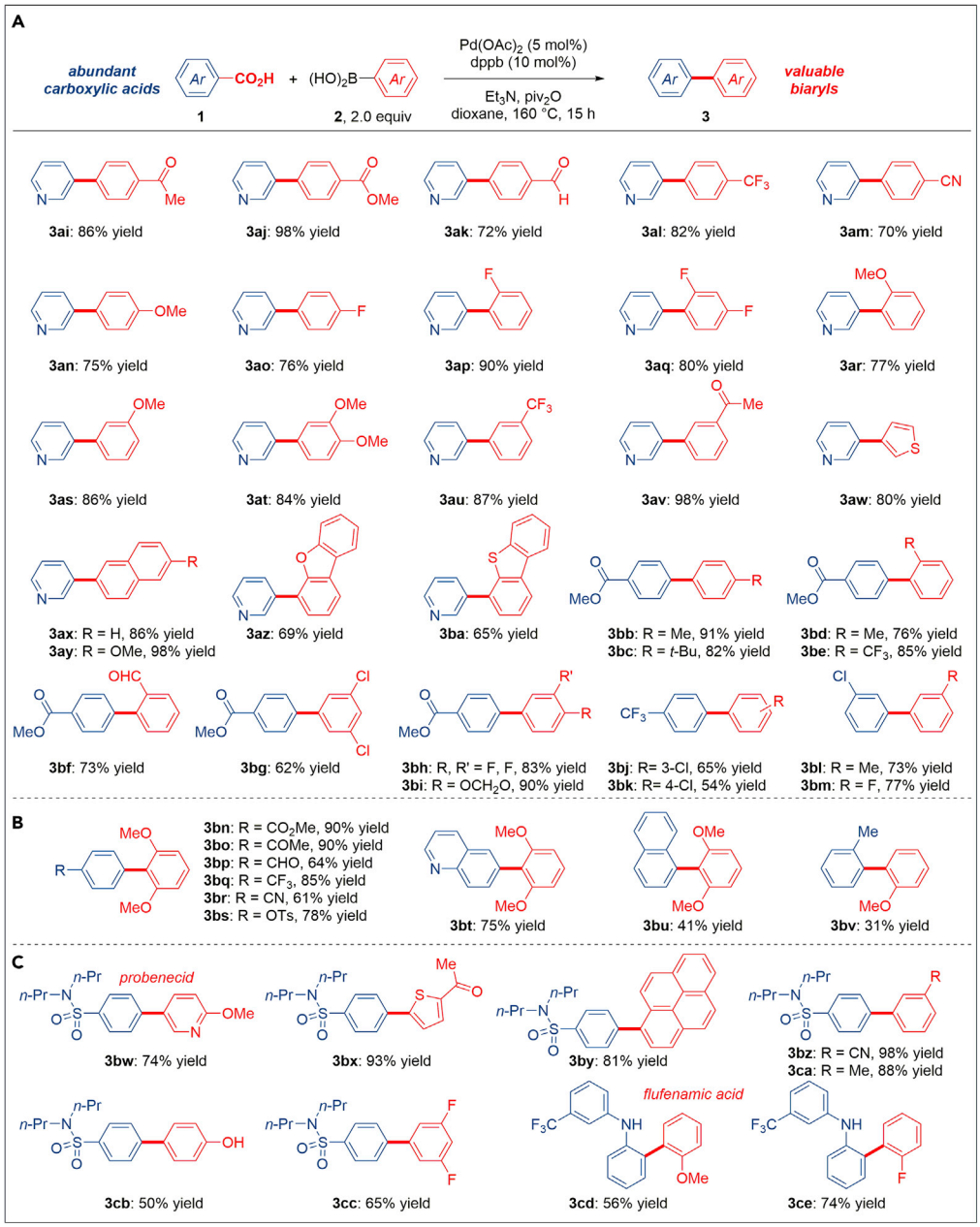

Figure 4. Scope of the Decarbonylative Suzuki-Miyaura Cross-Coupling of Carboxylic Acids: Boronic Acid Scope

(A) Scope of boronic acids.

(B) Cross-coupling of ortho-substituted boronic acids.

(C) Late-stage functionalization.

Conditions: Carboxylic acid (1.0 equiv.), Ar–$B(OH)_2$ (2.0 equiv.), $Pd(OAc)_2$ (5 mol %), dppb (10 mol %), Et_3N (1.5 equiv.), piv_2O (1.5 equiv.), H_3BO_3 (1.5 equiv.), dioxane, 160°C, 15 h. The extension of scope/conditions in passing from Ni to Pd, including functional group tolerance to sulfonates, phenols, anilines, ortho-biphenyls, trifluoromethylethers, and benchtop setup using air-stable catalysts and reagents, low catalyst loading (see Scheme S6), as well as a simple one-pot procedure should be noted.

oxidative addition. (3) The reaction is scalable (86% yield on gram scale) and efficient at low catalyst loading (81% yield, 0.25 mol% [Pd]). (4) Finally, the reaction setup can be further simplified by using commercially available precatalyst ($PdCl_2$(dppb), 5 mol%, 70% yield). These facts bode well for a broad spectrum of applications in various aspects of synthetic chemistry.

Furthermore, it is worthwhile to note that the vast majority of biaryl products reported here cannot be synthesized using currently available methods engaging ubiquitous carboxylic acids. Typically, only ortho-substituted or electronically biased benzoic acids are suitable substrates for decarboxylative Suzuki cross-coupling, whereas the present method could be employed for any functionalized position on the benzene ring of carboxylic acids as well as for electron-donating, electron-neutral, or electron-withdrawing carboxylic acid substrates. In the same vein, decarboxylative Suzuki cross-coupling typically requires bimetallic catalysis, whereas the present catalytic system only needs palladium single metal catalyst as a consequence of well-controlled decarbonylation. The absence of an exogeneous base represents a significant advantage because it enables much broader scope and generality. The prevalence and orthogonal nature of carboxylic acids enable the preparation of biaryls that are not easily accessible by other cross-coupling methods using halides or pseudohalides as cross-coupling partners. The use of palladium represents a significant advantage because it enables much broader tolerance and is more universally applicable than nickel. As a key design strategy, the present method involves a one-pot process directly involving ubiquitous carboxylic acids in which all reaction components are combined at the same time, which enables operational simplicity and rapid testing not available by other methods.

In conclusion, decarbonylative biaryl synthesis from carboxylic acids represents a powerful tool for the synthesis of complex biaryls using ubiquitous and orthogonal carboxylic acid cross-coupling partners. This decarbonylative strategy embodies a complementary approach to the traditional loss of carbon dioxide. The broad substrate scope, operational simplicity, and the potential to apply in complex molecule synthesis make it evident that decarbonylative cross-couplings (Stephan et al., 1998; Zhang et al., 2018; Meng and Szostak, 2015; Liu et al., 2019) will likely have a major impact in the modern era of organic synthesis. Future studies will focus on expanding the scope of the present protocol and mechanistic investigations of decarbonylative cross-coupling protocols involving carboxylic acids.

Limitations of the Study

Tetra-substituted biaryls as well as aryl bromides are not suitable, which supports similar rate of the oxidative addition step of C–Br and C–O bonds. H_3BO_3 is required for the efficient biaryl synthesis, which supports O-protonation and prevents protodeboronation. Although cross-coupling of electron-rich arenes is feasible (**3h**, **3i**), this also shows some limitations of the method. Future studies will focus on the development of more active catalyst systems to expand the substrate scope of the decarbonylative coupling.

METHODS

All methods can be found in the accompanying Transparent Methods supplemental file.

SUPPLEMENTAL INFORMATION

Supplemental Information can be found online at https://doi.org/10.1016/j.isci.2019.08.021.

ACKNOWLEDGMENTS

We thank Rutgers University (M.S.), the NSF (CAREER CHE-1650766, M.S.), NSFC (21702182 and 21873081, X.H.), the Chinese "Thousand Youth Talents Plan" (X.H.), and Zhejiang University (X.H.) for generous financial support. The Bruker 500 MHz spectrometer used in this study was supported by the NSF-MRI grant (CHE-1229030). Calculations were performed on the high-performance computing system at the Department of Chemistry, Zhejiang University.

AUTHOR CONTRIBUTIONS

M.S. and X.H. conceived the project and designed the experiments. C.L., C.-L.J., and Z.-X.Q. performed the experiments and analyzed the data. M.S. and X.H. wrote the manuscript. All the authors discussed the results and commented on the manuscript.

DECLARATION OF INTERESTS

The authors declare no competing interests.

Received: June 24, 2019
Revised: July 31, 2019
Accepted: August 13, 2019
Published: September 27, 2019

REFERENCES

Beller, M., and Blaser, H.U. (2012). Organometallics as Catalysts in the Fine Chemicals Industry (Springer-Verlag).

Blakemore, D.C., Castro, L., Churcher, I., Rees, D.C., Thomas, A.W., Wilson, D.M., and Wood, A. (2018). Organic synthesis provides opportunities to transform drug discovery. Nat. Chem. *10*, 383–394.

Blakey, S.B., and MacMillan, D.W.C. (2003). The first Suzuki cross-couplings with aryltrimethylammonium salts. J. Am. Chem. Soc. *125*, 6046–6047.

Brown, D.G., and Boström, J. (2016). Analysis of past and present synthetic methodologies on medicinal chemistry: where have all the new reactions gone? J. Med. Chem. *59*, 4443–4458.

Burke, A.J., and Marques, C. (2015). Catalytic Arylation Methods: From the Academic Lab to Industrial Processes (Wiley).

Campbell, M., and Ritter, T. (2015). Modern carbon–fluorine bond forming reactions for aryl fluoride synthesis. Chem. Rev. *115*, 612–633.

Cheesbrough, T.M., and Kolattukudy, P.E. (1984). Alkane biosynthesis by decarbonylation of aldehydes catalyzed by a particulate preparation from Pisum sativum. Proc. Natl. Acad. Sci. U S A *81*, 6613–6617.

Colacot, T.J. (2015). New Trends in Cross-Coupling: Theory and Applications (RSC).

Dzik, W.I., Lange, P.P., and Gooßen, L.J. (2012). Carboxylates as sources of carbon nucleophiles and electrophiles: comparison of decarboxylative and decarbonylative pathways. Chem. Sci. *3*, 2671–2678.

Edwards, J.T., Merchant, R.R., McClymont, K.S., Knouse, K.W., Qin, T., Malins, L.R., Vokits, B., Shaw, S.A., Bao, D.H., We, F.L., et al. (2017). Decarboxylative alkenylation. Nature *545*, 213–218.

Fawcett, A., Pradeilles, J., Wang, Y., Mutsuga, T., Myers, E.L., and Aggarwal, V.K. (2017). Photoinduced decarboxylative borylation of carboxylic acids. Science *357*, 283–286.

Gooßen, L.J., and Paetzold, J. (2004). New synthesis of biaryls via Rh-catalyzed decarbonylative Suzuki-coupling of carboxylic anhydrides with arylboroxines. Adv. Synth. Catal. *346*, 1665–1668.

Gooßen, L.J., Deng, G., and Levy, L.M. (2006). Synthesis of biaryls via catalytic decarboxylative coupling. Science *313*, 662–664.

Gooßen, L.J., Rodriguez, N., and Gooßen, K. (2008). Carboxylic acids as substrates in homogeneous catalysis. Angew. Chem. Int. Ed. *47*, 3100–3120.

Guan, B.T., Wang, Y., Li, B.J., Yu, D.G., and Shi, Z.J. (2008). Biaryl construction via Ni-catalyzed C–O activation of phenolic carboxylates. J. Am. Chem. Soc. *130*, 14468–14470.

Hassan, J., Sevignon, M., Gozzi, C., Schulz, E., and Lemaire, M. (2002). Aryl-aryl bond formation one century after the discovery of the Ullmann reaction. Chem. Rev. *102*, 1359–1470.

Horton, D.A., Bourne, G.T., and Smythe, M.L. (2003). The combinatorial synthesis of bicyclic privileged structures or privileged substructures. Chem. Rev. *103*, 893–930.

Ji, C.L., and Hong, X. (2017). Factors controlling the reactivity and chemoselectivity of resonance destabilized amides in Ni-catalyzed decarbonylative and nondecarbonylative Suzuki-Miyaura coupling. J. Am. Chem. Soc. *139*, 15522–15529.

Knappke, C.E.I., and Jacobi von Wangelin, A. (2010). A synthetic double punch: Suzuki–Miyaura cross-coupling mates with C–H functionalization. Angew. Chem. Int. Ed. *49*, 3568–3570.

Lennox, A.J.J., and Lloyd-Jones, G.C. (2013). Transmetalation in the Suzuki–Miyaura coupling: the fork in the trail. Angew. Chem. Int. Ed. *52*, 7362–7370.

Lennox, A.J.J., and Lloyd-Jones, G.C. (2014). Selection of boron reagents for Suzuki-Miyaura coupling. Chem. Soc. Rev. *43*, 412–443.

Liu, C., Ji, C.L., Hong, X., and Szostak, M. (2018). Palladium-catalyzed decarbonylative borylation of carboxylic acids: tuning reaction selectivity by computation. Angew. Chem. Int. Ed. *57*, 16721–16726.

Liu, C., Qin, Z.X., Ji, C.L., Hong, X., and Szostak, M. (2019). Highly-chemoselective step-down reduction of carboxylic acids to aromatic hydrocarbons via palladium catalysis. Chem. Sci. *10*, 5736–5742.

Malapit, C.A., Bour, J.R., Brigham, C.E., and Sanford, M.S. (2018). Base-free nickel-catalysed decarbonylative Suzuki-Miyaura coupling of acid fluorides. Nature *563*, 100–104.

Meng, G., and Szostak, M. (2015). General olefin synthesis by the palladium-catalyzed heck reaction of amides: sterically controlled chemoselective N–C activation. Angew. Chem. Int. Ed. *54*, 14518–14522.

Miyaura, N., and Suzuki, A. (1995). Palladium-catalyzed cross-coupling reactions of organoboron compounds. Chem. Rev. *95*, 2457–2483.

Molander, G.A., Wolfe, J.P., and Larhed, M. (2013). Science of Synthesis: Cross-Coupling and Heck-type Reactions (Thieme).

Murphy, S.K., Park, J.W., Cruz, F.A., and Dong, V.M. (2015). Rh-catalyzed C–C bond cleavage by transfer hydroformylation. Science *347*, 56–60.

Muto, K., Yamaguchi, J., Musaev, D.G., and Itami, K. (2015). Decarbonylative organoboron cross-coupling of esters by nickel catalysis. Nat. Commun. *6*, 7508.

Qin, T., Cornella, J., Li, C., Malins, L.R., Edwards, J.T., Kawamura, S., Maxwell, B.D., Eastgate, M.D., and Baran, P.S. (2016). A general alkyl-alkyl cross-coupling enabled by redox-active esters and alkylzinc reagents. Science *352*, 801–805.

Quasdorf, K.W., Tian, X., and Garg, N.K. (2008). Cross-coupling of aryl pivalates with boronic acids. J. Am. Chem. Soc. *130*, 14422–14423.

Quasdorf, K.W., Antoft-Finch, A., Liu, P., Silberstein, A.L., Komaromi, A., Blackburn, T., Ramgren, S.D., Houk, K.N., Snieckus, V., and Garg, N.K. (2011). Suzuki–miyaura cross-coupling of aryl carbamates and sulfamates: experimental and computational studies. J. Am. Chem. Soc. *133*, 6352–6363.

Ryter, S.W., and Tyrrell, R.M. (2000). The heme synthesis and degradation pathways: role in oxidant sensitivity. Free Radic. Biol. Med. *28*, 289–309.

Scifinder search for "Suzuki coupling". Accessed on 6/24/2019.

Shi, S., Meng, G., and Szostak, M. (2016). Synthesis of biaryls through nickel-catalyzed Suzuki-Miyaura coupling of amides by carbon-nitrogen bond cleavage. Angew. Chem. Int. Ed. *55*, 6959–6963.

Stephan, M.S., Teunissen, A.J.J.M., Verzijl, G.K.M., and de Vries, J.G. (1998). Heck reactions without salt formation: aromatic carboxylic anhydrides as arylating agents. Angew. Chem. Int. Ed. *37*, 662–664.

Suzuki, A. (2011). Cross-coupling reactions of organoboranes: an easy way to construct C–C bonds (Nobel Lecture). Angew. Chem. Int. Ed. *50*, 6722–6737.

Tasker, S.Z., Standley, E.A., and Jamison, T.F. (2014). Recent advances in homogeneous nickel catalysis. Nature *509*, 299–309.

Tellis, J.C., Primer, D.N., and Molander, G.A. (2014). Single-electron transmetalation in organoboron cross-coupling by photoredox/nickel dual catalysis. Science *345*, 433–436.

Tobisu, M., Shimasaki, T., and Chatani, N. (2008). Nickel-catalyzed cross-coupling of aryl methyl ethers with aryl boronic esters. Angew. Chem. Int. Ed. *47*, 4866–4869.

Twilton, J., Le, C.C., Zhang, P., Shaw, M.H., Evans, R.W., and MacMillan, D.W.C. (2017). The merger of transition metal and photocatalysis. Nat. Rev. Chem. *1*, 52.

Urquahart, L. (2018). Market watch: top drugs and companies by sales in 2017. Nat. Rev. Drug Discov. *17*, 232.

Yet, L. (2018). Privileged Structures in Drug Discovery: Medicinal Chemistry and Synthesis (Wiley).

Zhang, L., Lovinger, G.J., Edelstein, E.K., Szymaniak, A.A., Chierchia, M.P., and Morken, J.P. (2016). Catalytic conjunctive cross-coupling enabled by metal-induced metallate rearrangement. Science *351*, 70–74.

Zhang, X., Jordan, F., and Szostak, M. (2018). Transition-metal-catalyzed decarbonylation of carboxylic acids to olefins: exploiting acyl C–O activation for the production of high value products. Org. Chem. Front *5*, 2515–2521.

Zhao, Q., and Szostak, M. (2019). Redox-neutral decarbonylative cross-couplings coming of age. ChemSusChem *12*, 2983–2987.

Zhao, S., Gensch, T., Murray, B., Niemeyer, Z.L., Sigman, M.S., and Biscoe, M.R. (2018). Enantiodivergent Pd-catalyzed C–C bond formation enabled through ligand parametrization. Science *362*, 670–674.

Zuo, Z., Ahneman, D.T., Chu, L., Terrett, J.A., Doyle, A.G., and MacMillan, D.W.C. (2014). Merging photoredox with nickel catalysis: coupling of α-carboxyl sp^3-carbons with aryl halides. Science *345*, 437–440.

ISCI, Volume *19*

Supplemental Information

Synthesis of Biaryls via Decarbonylative Palladium-Catalyzed Suzuki-Miyaura Cross-Coupling of Carboxylic Acids

Chengwei Liu, Chong-Lei Ji, Zhi-Xin Qin, Xin Hong, and Michal Szostak

Figure S1. DFT-calculated reaction energy profile of the Pd/PCy_3-catalyzed Suzuki-Miyaura cross-coupling of benzoic pivalic anhydride with C–O bond cleavage of pivalic acid, related to **Figure 2**

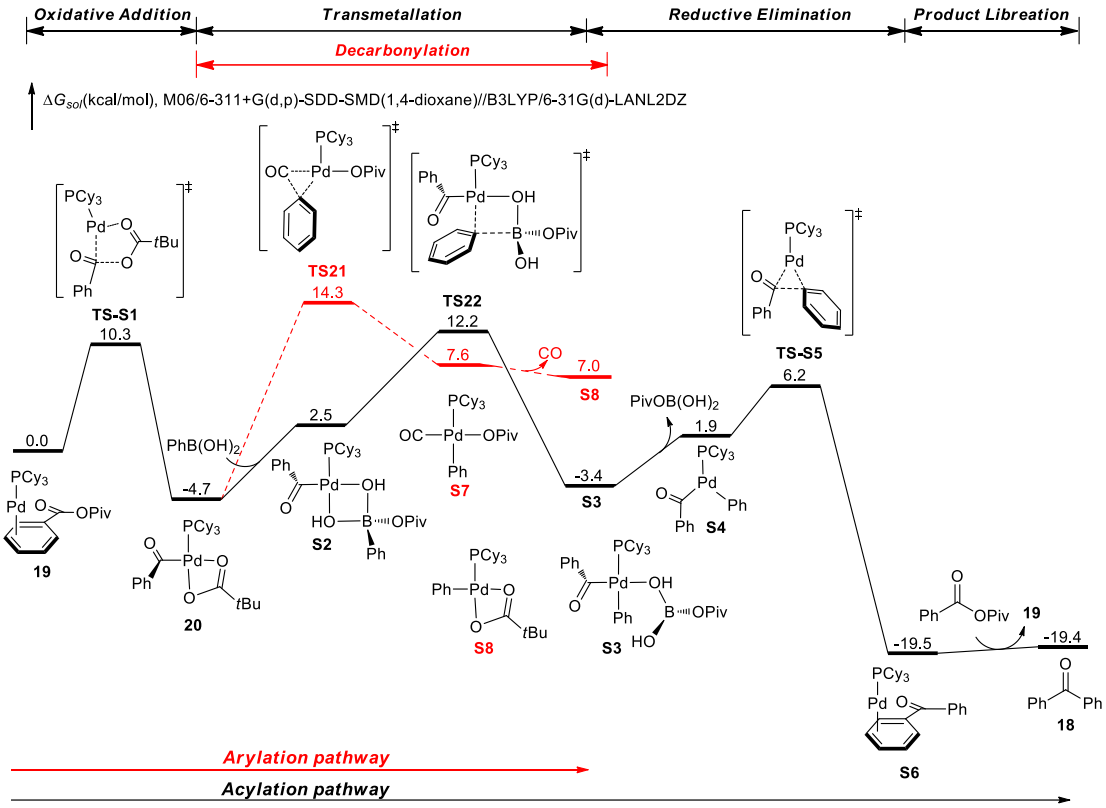

Figure S2. ^{1}H NMR spectrum of **3a**, related to **Figure 3**

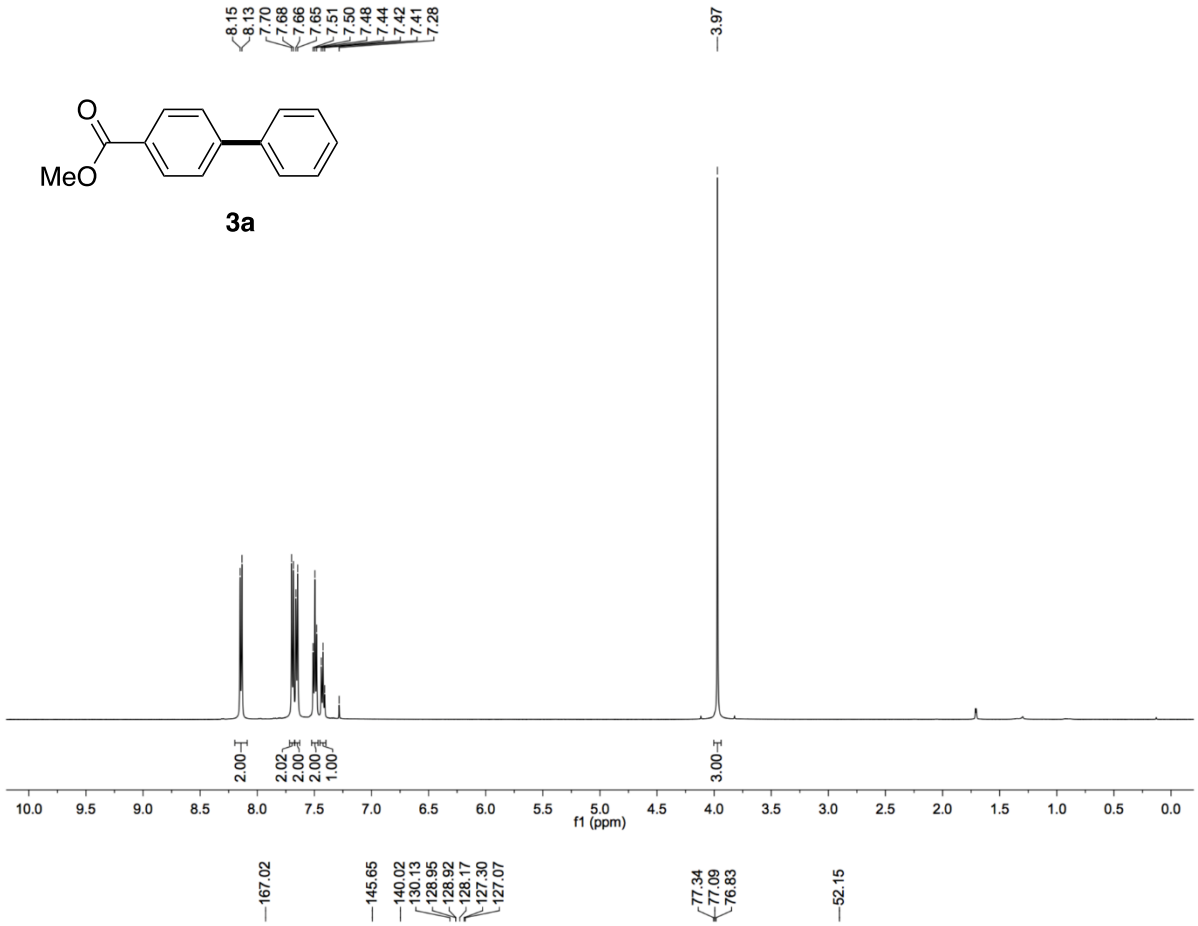

Figure S3. ^{13}C NMR spectrum of **3a**, related to **Figure 3**

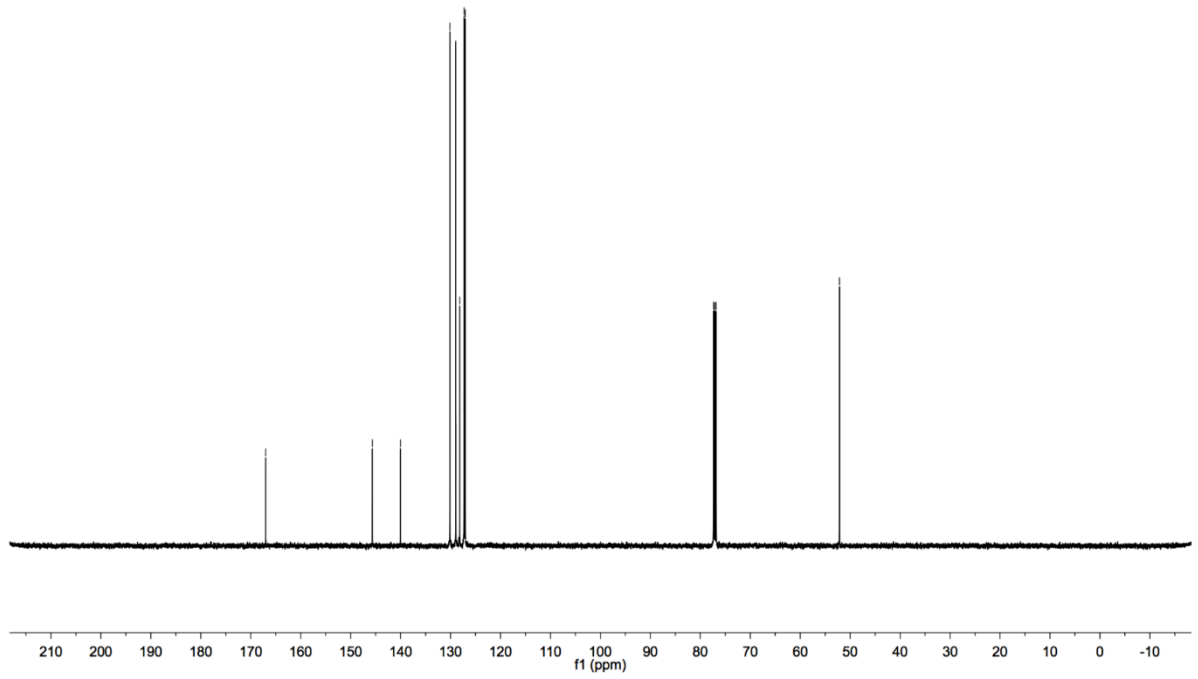

Figure S4. ^{1}H NMR spectrum of **3b**, related to **Figure 3**

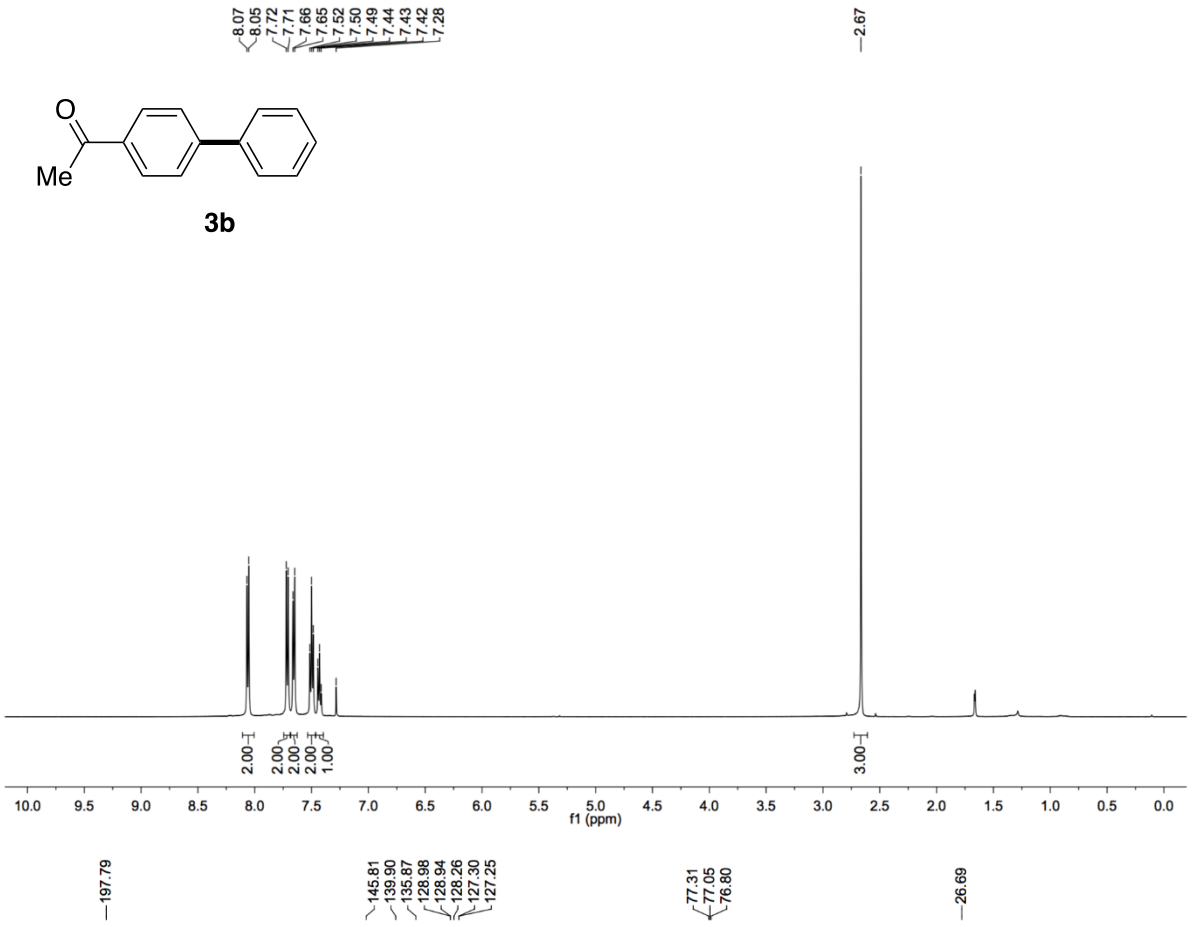

Figure S5. ^{13}C NMR spectrum of **3b**, related to **Figure 3**

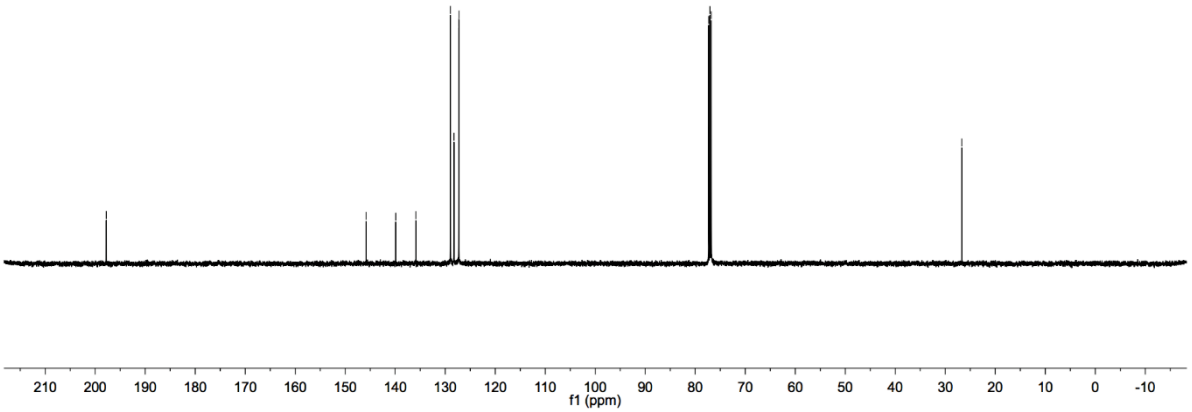

Figure S6. ^{1}H NMR spectrum of **3c**, related to **Figure 3**

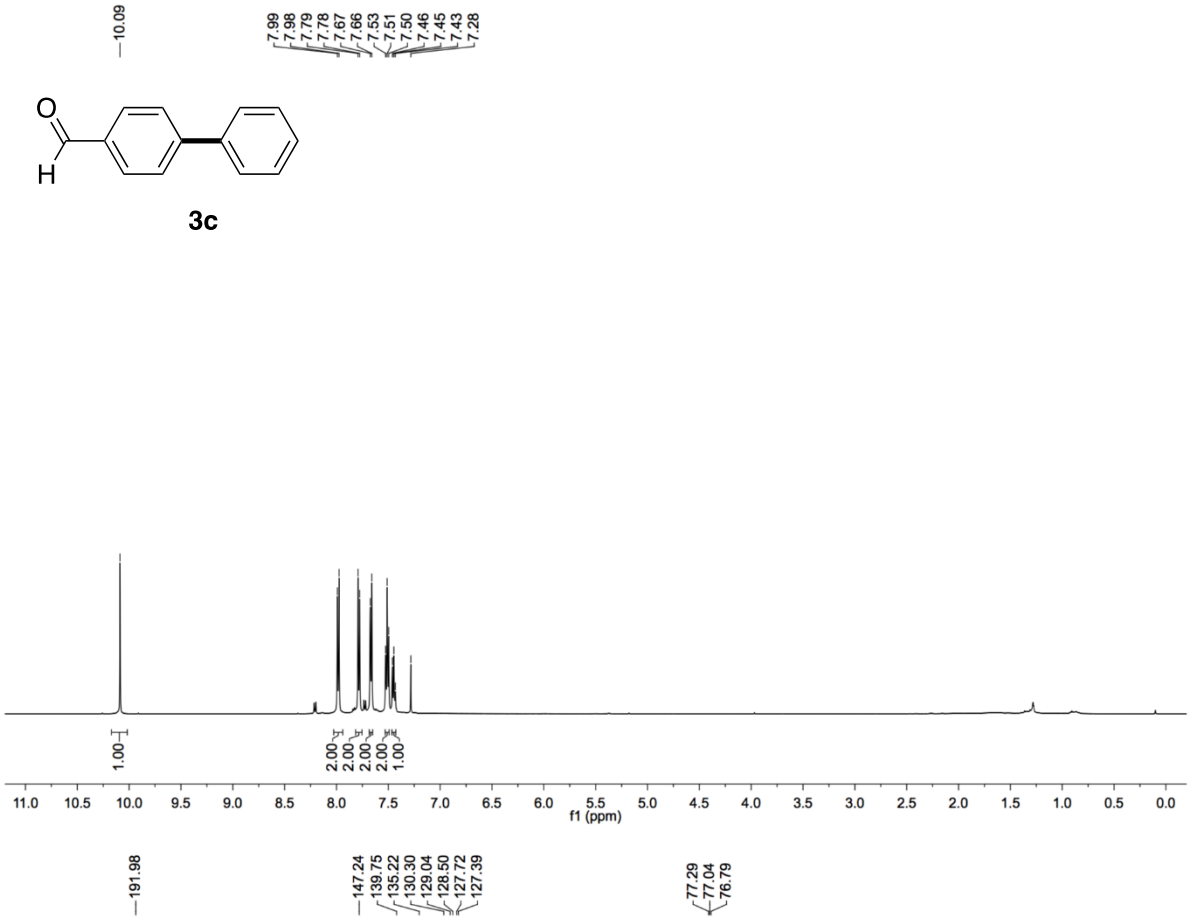

Figure S7. ^{13}C NMR spectrum of **3c**, related to **Figure 3**

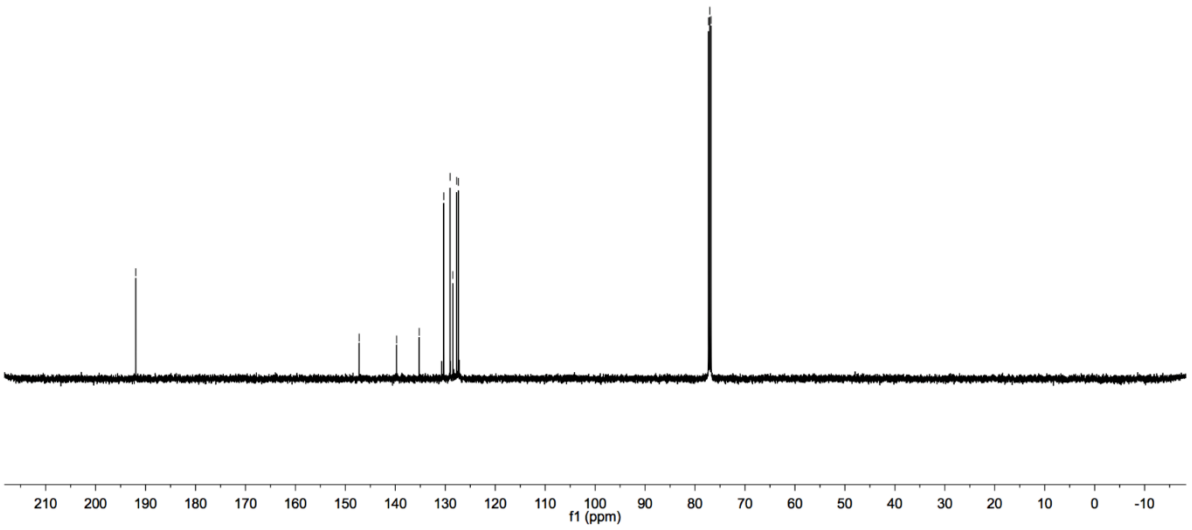

Figure S8. ^{1}H NMR spectrum of **3d**, related to **Figure 3**

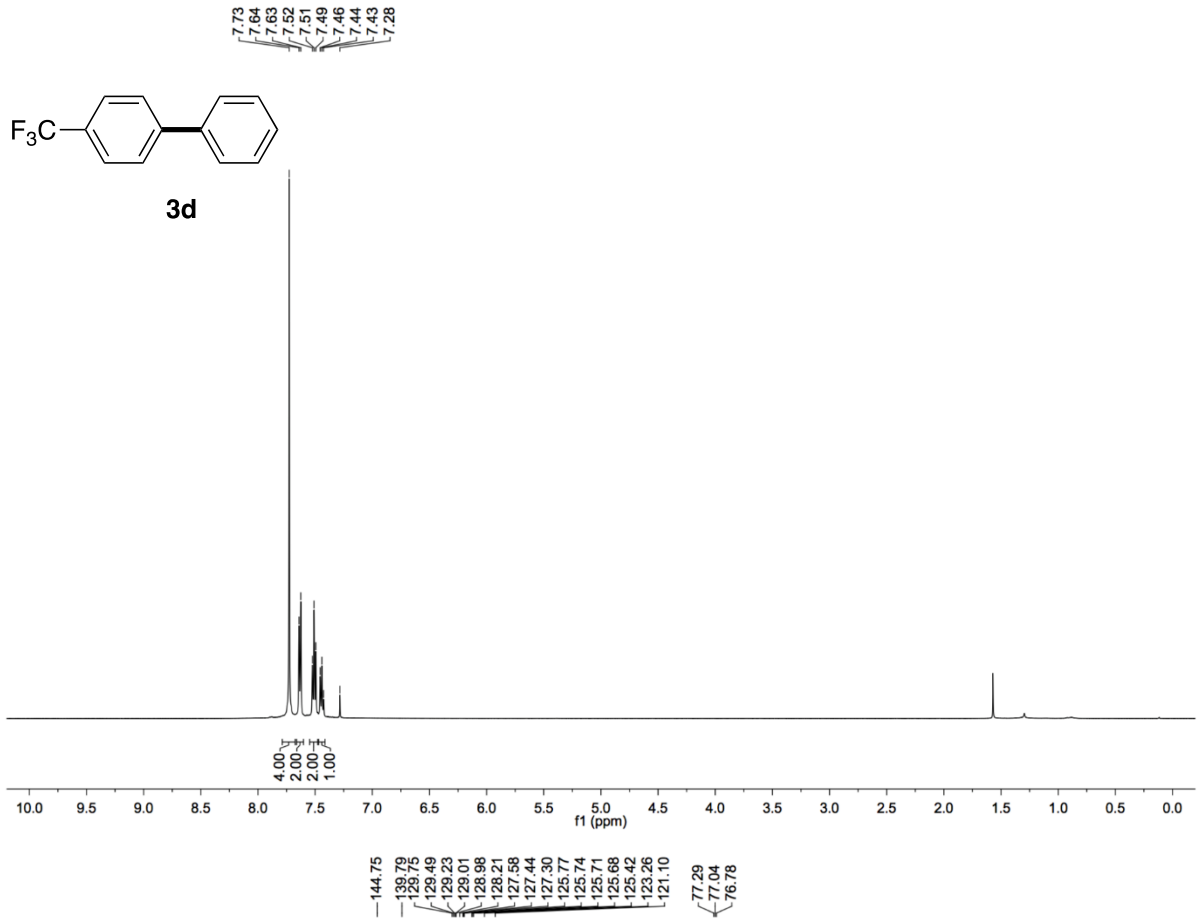

Figure S9. ^{13}C NMR spectrum of **3d**, related to **Figure 3**

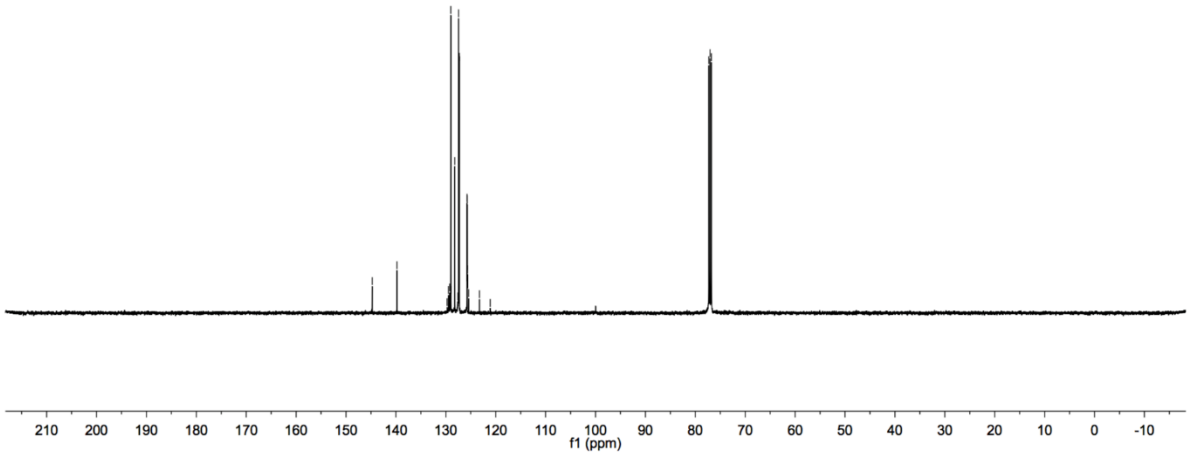

Figure S10. ^{19}F NMR spectrum of **3d**, related to **Figure 3**

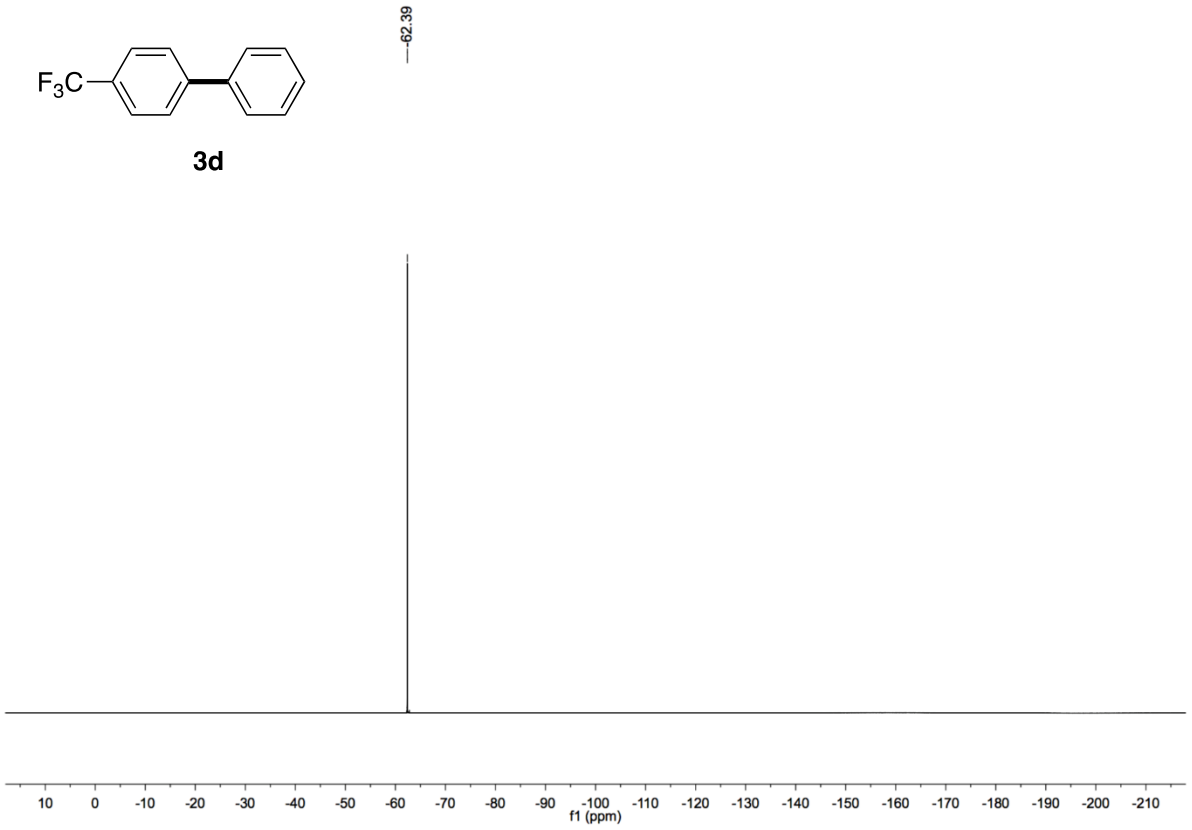

Figure S11. ^{1}H NMR spectrum of **3e**, related to **Figure 3**

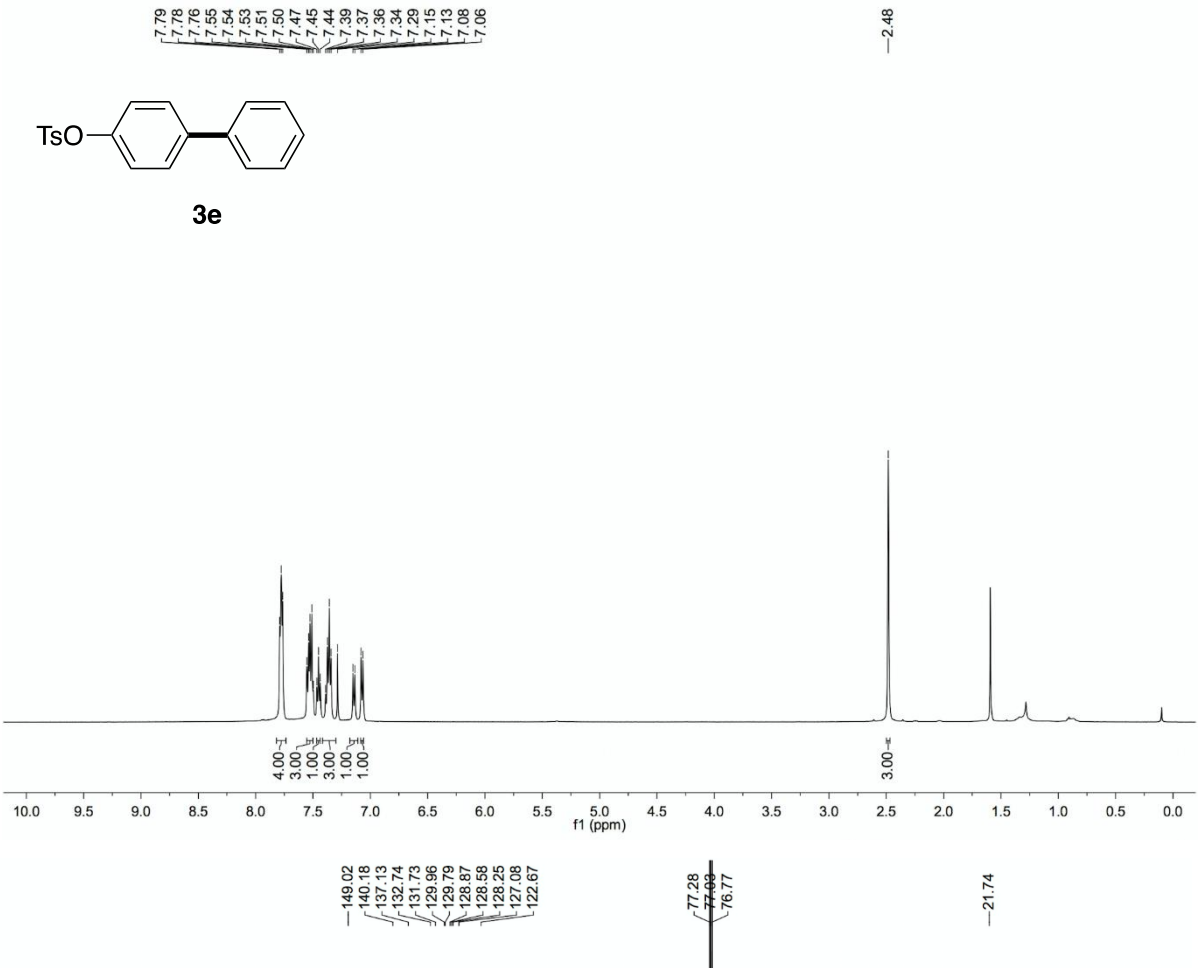

Figure S12. ^{13}C NMR spectrum of **3e**, related to **Figure 3**

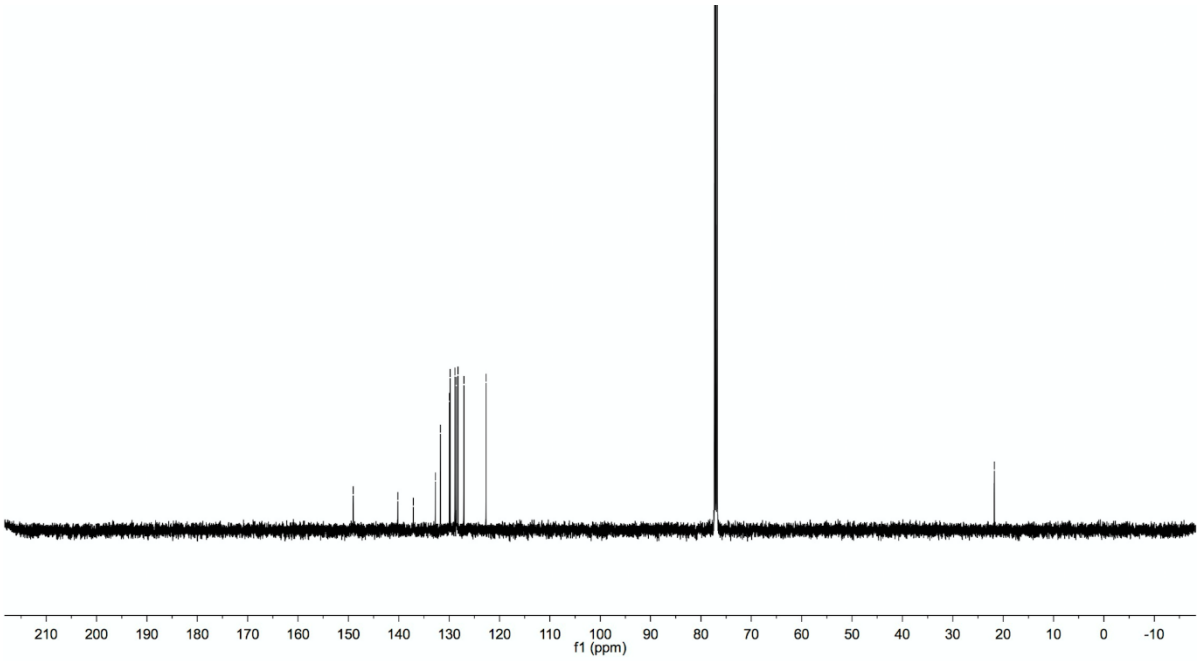

Figure S13. ^{1}H NMR spectrum of **3f**, related to **Figure 3**

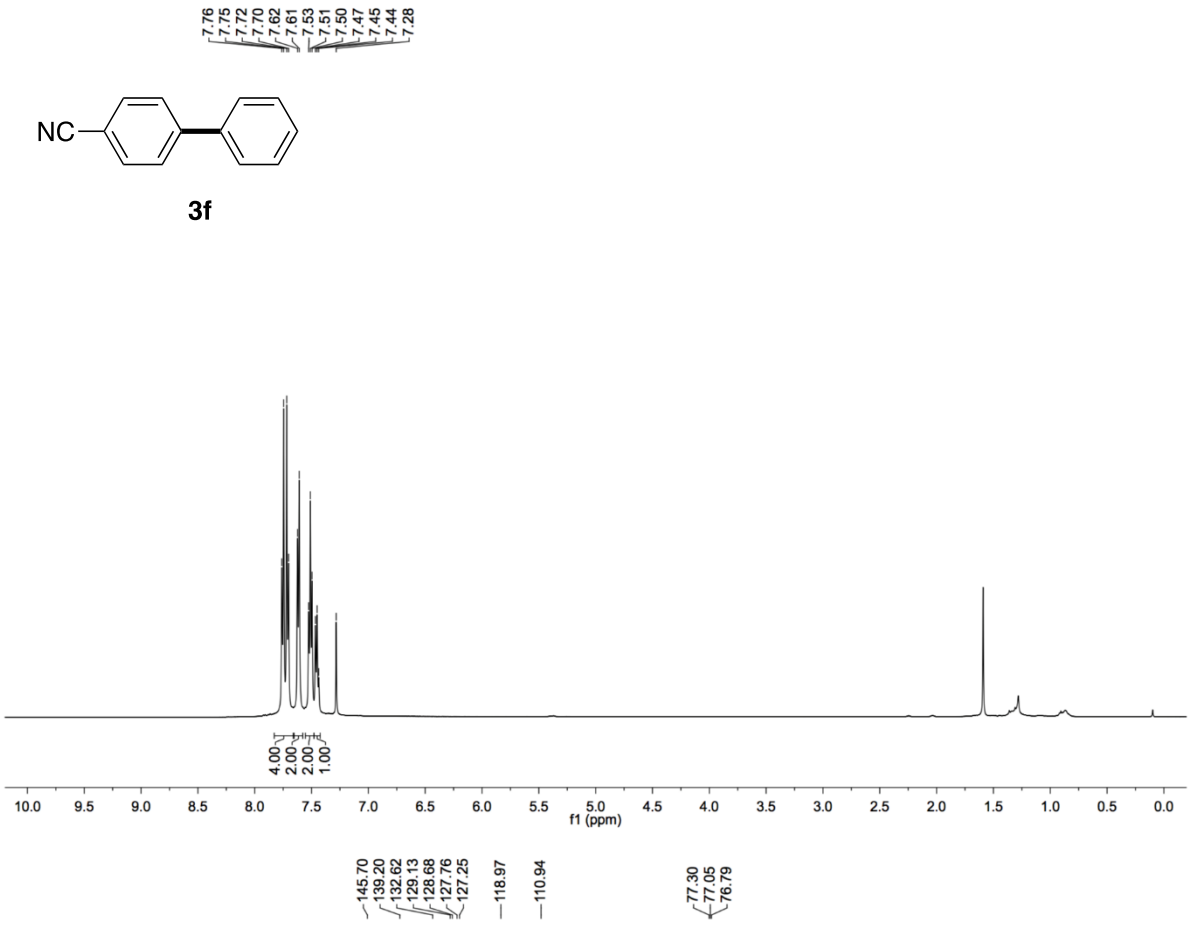

Figure S14. ^{13}C NMR spectrum of **3f**, related to **Figure 3**

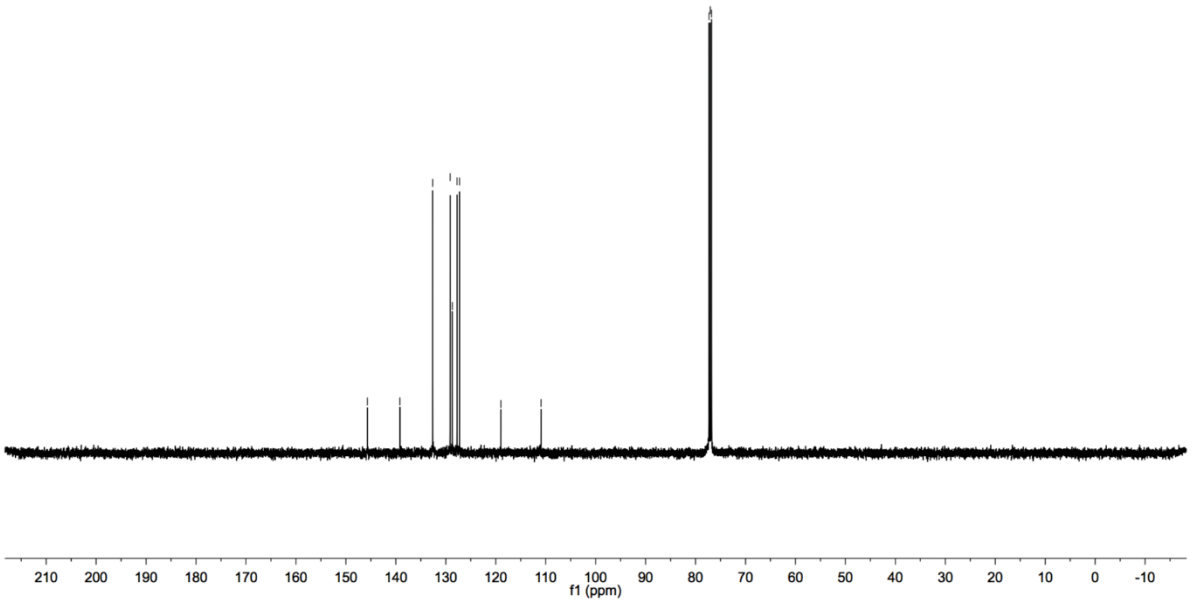

Figure S15. ^{1}H NMR spectrum of **3g**, related to **Figure 3**

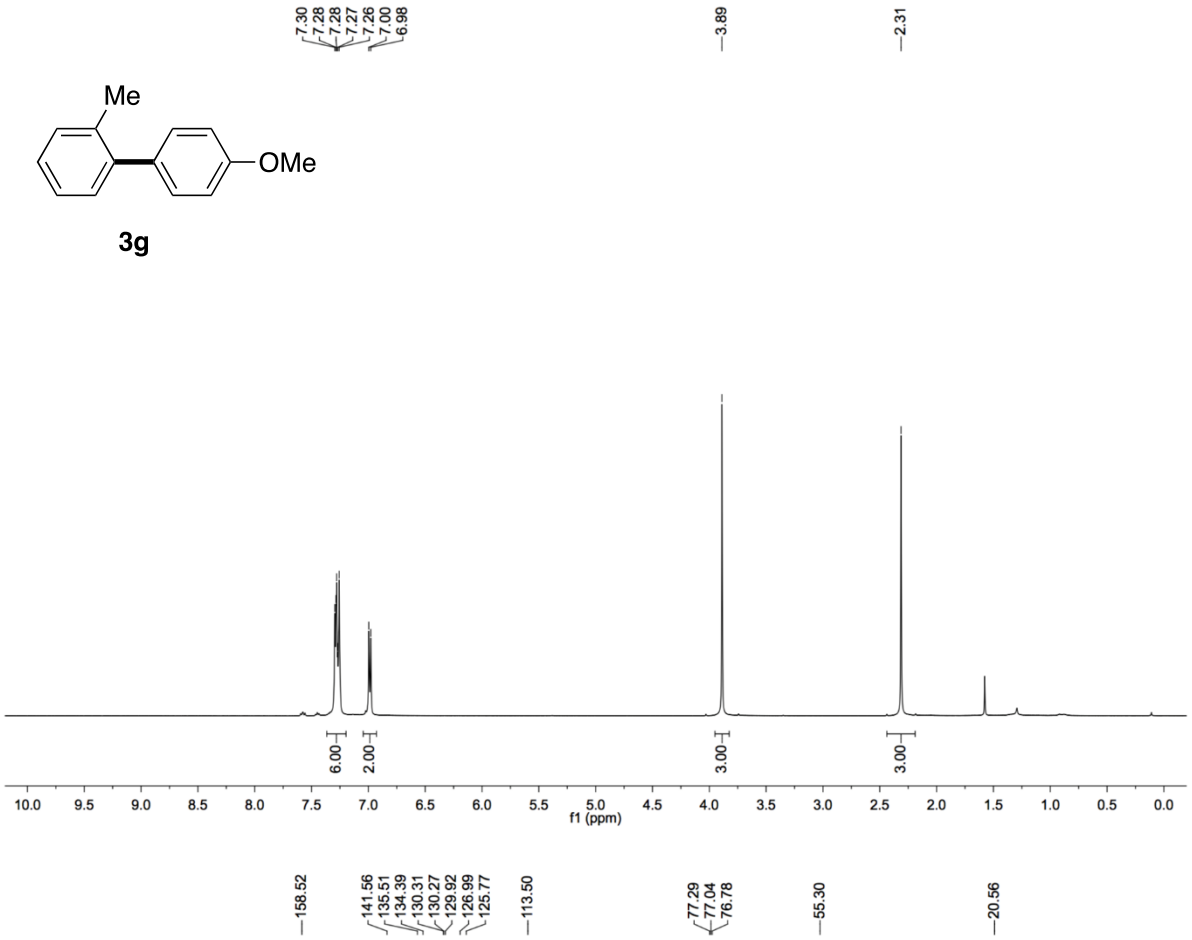

Figure S16. ^{13}C NMR spectrum of **3g**, related to **Figure 3**

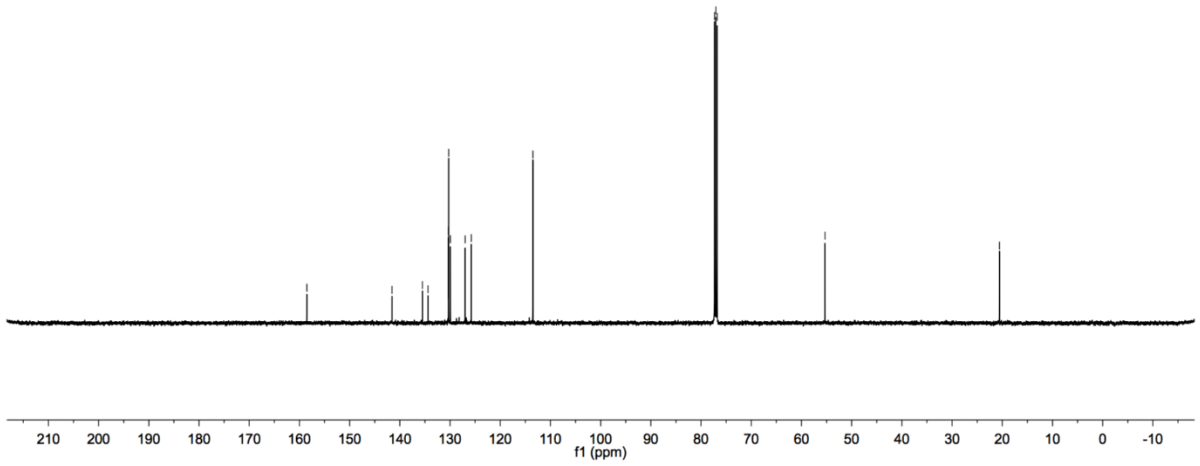

Figure S17. ^{1}H NMR spectrum of **3h**, related to **Figure 3**

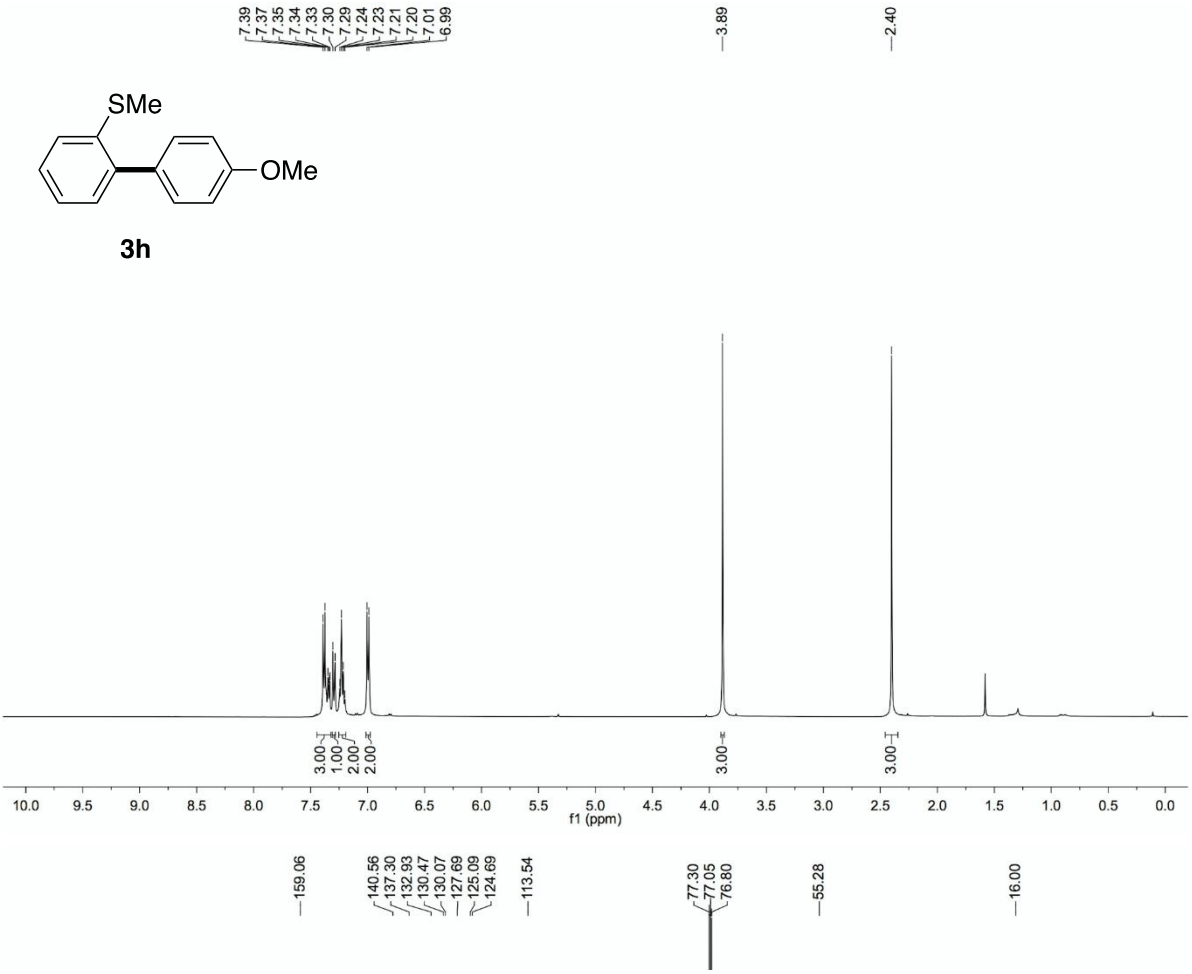

Figure S18. ^{13}C NMR spectrum of **3h**, related to **Figure 3**

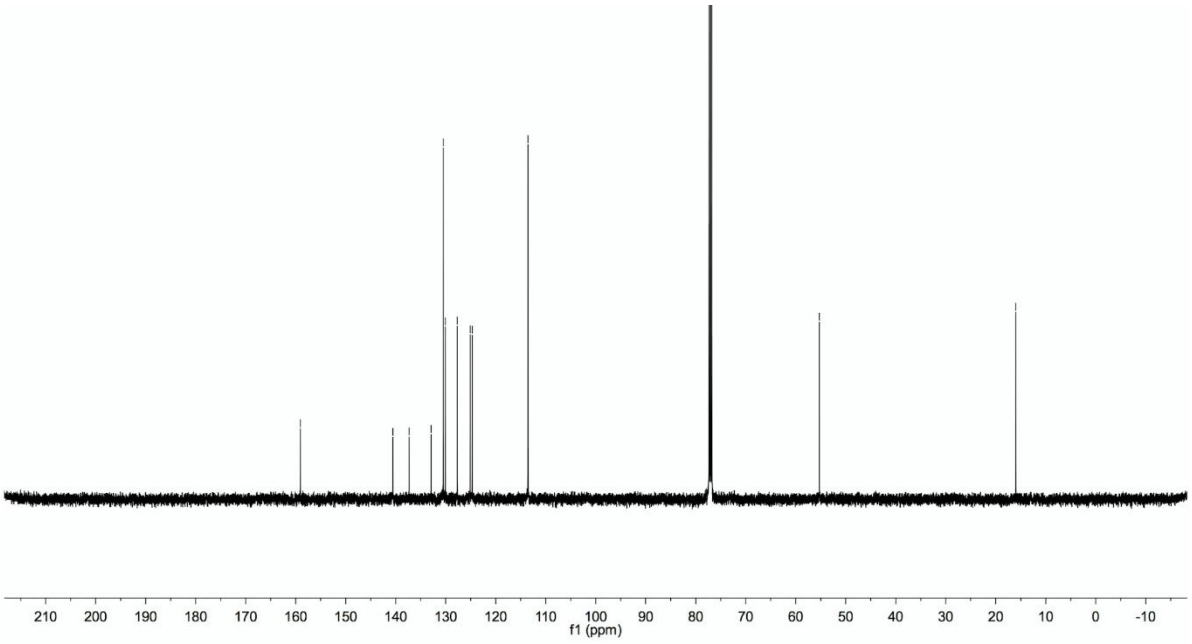

Figure S19. ^{1}H NMR spectrum of **3i**, related to **Figure 3**

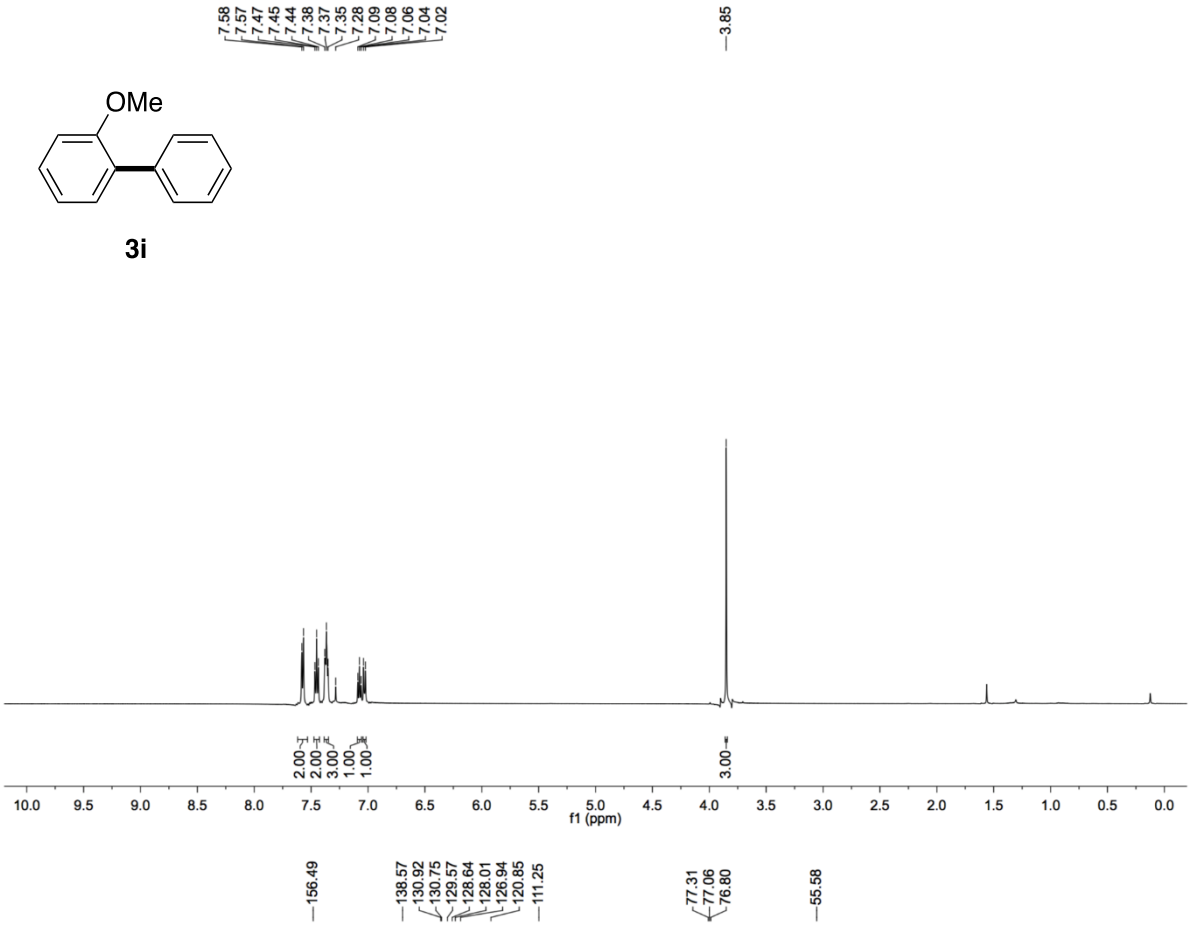

Figure S20. ^{13}C NMR spectrum of **3i**, related to **Figure 3**

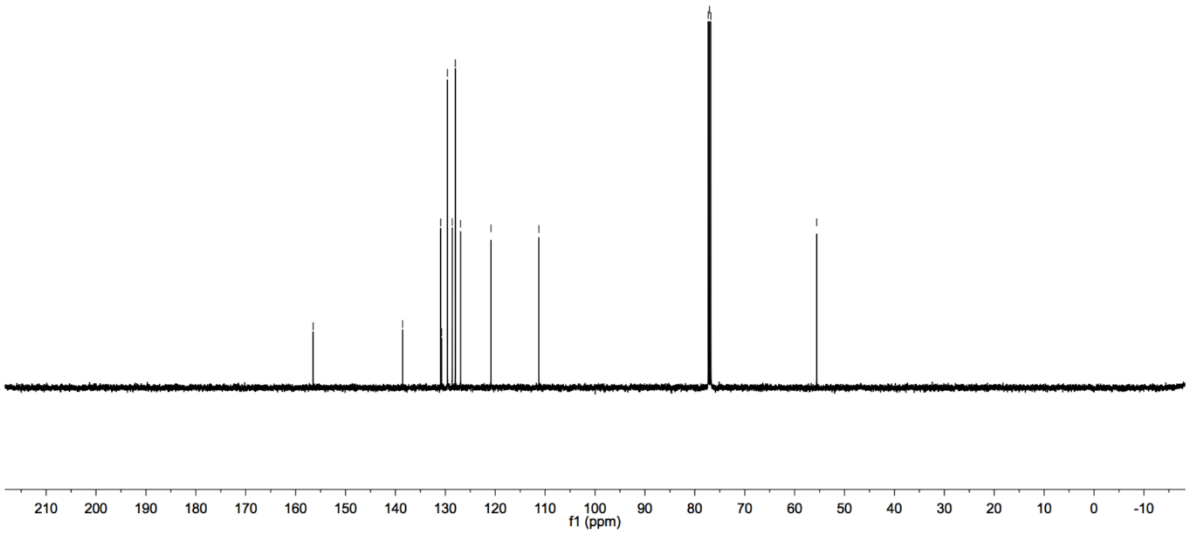

Figure S21. ^{1}H NMR spectrum of **3j**, related to **Figure 3**

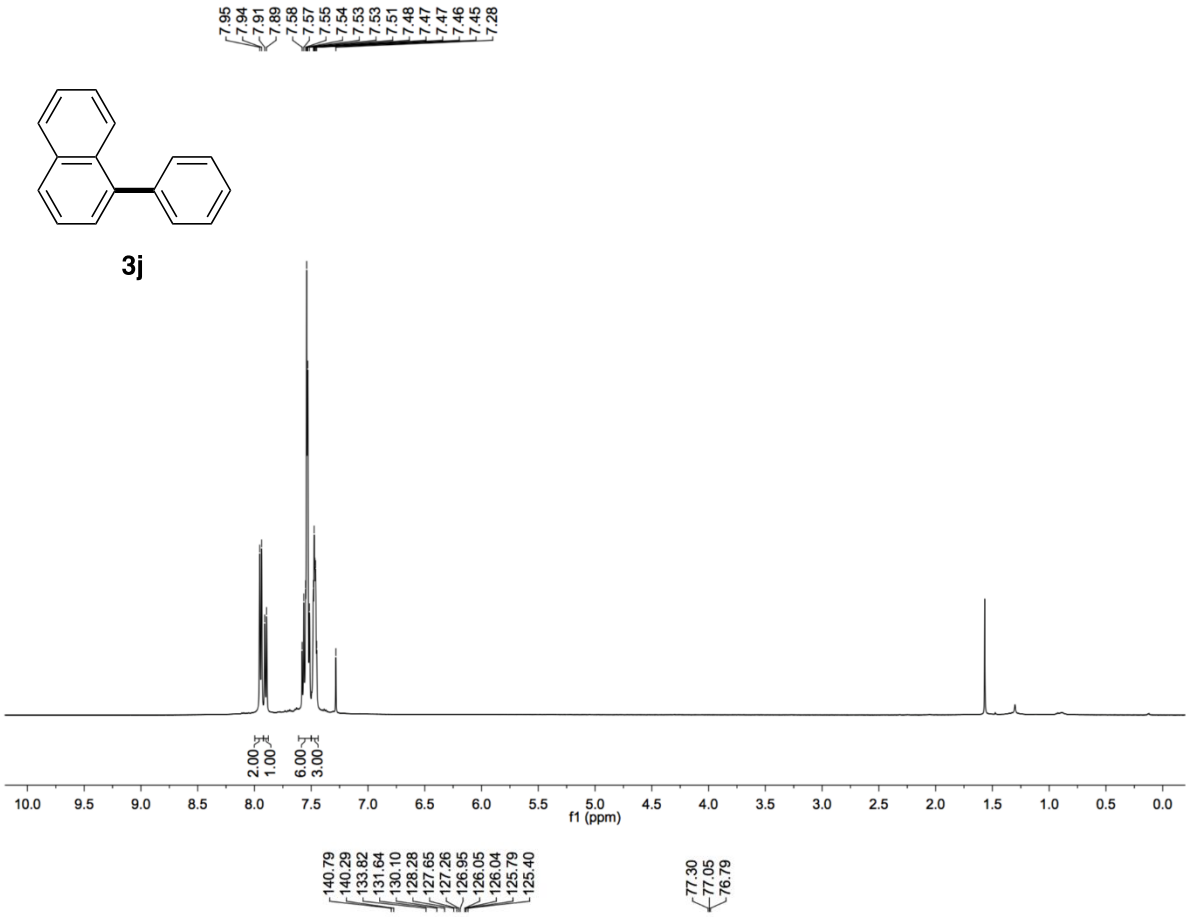

Figure S22. ^{13}C NMR spectrum of **3j**, related to **Figure 3**

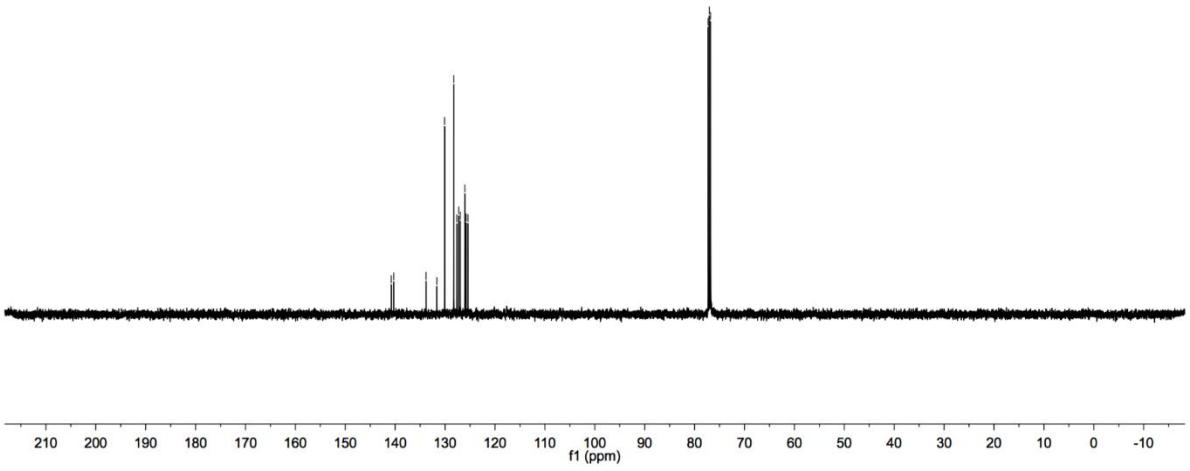

Figure S23. ^{1}H NMR spectrum of **3k**, related to **Figure 3**

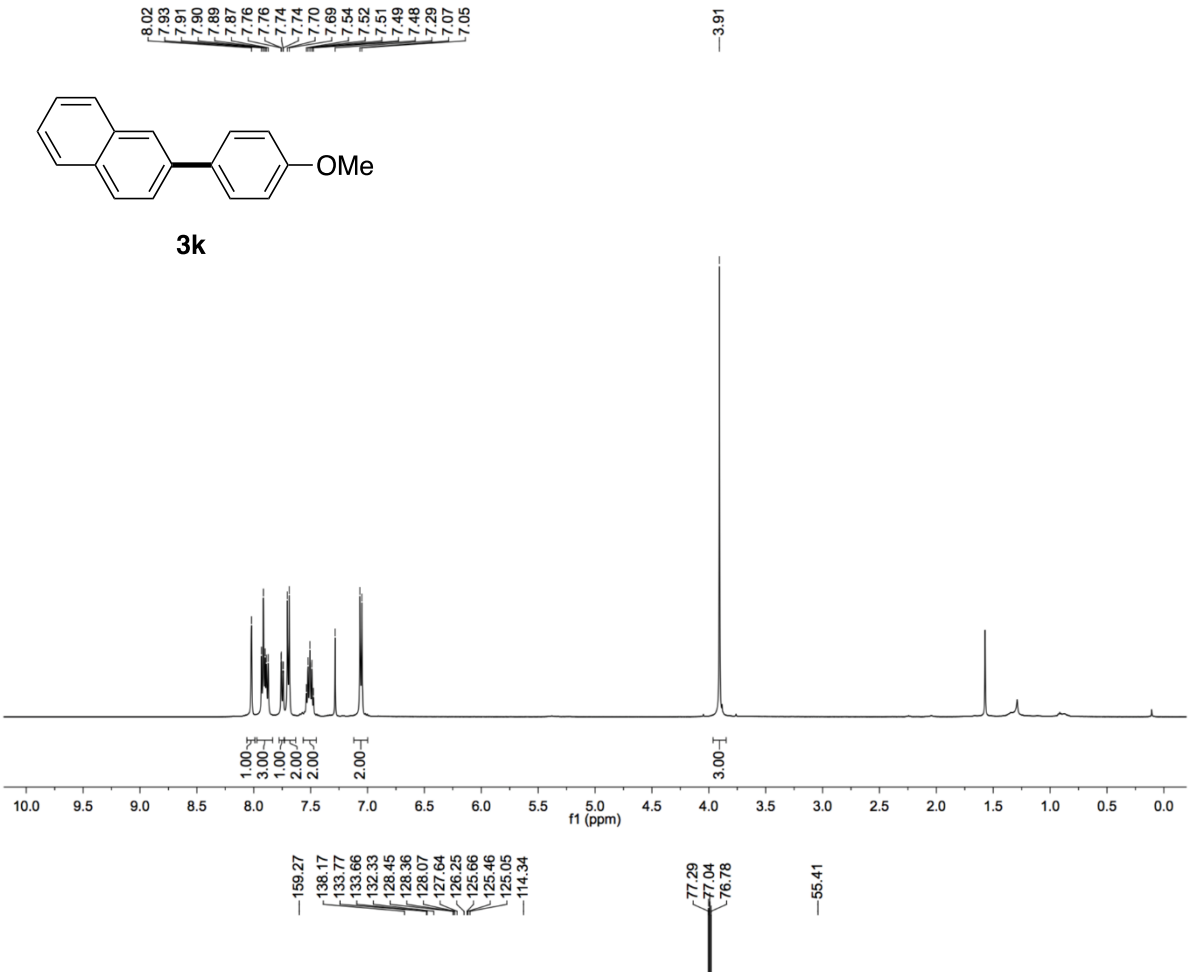

Figure S24. ^{13}C NMR spectrum of **3k**, related to **Figure 3**

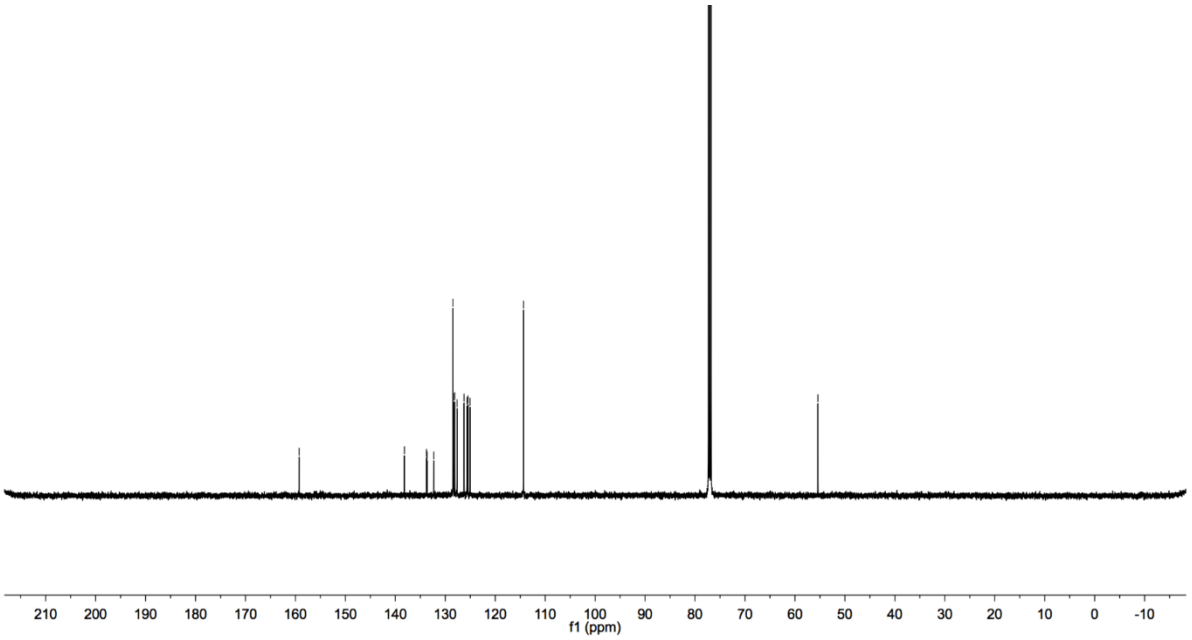

Figure S25. ^{1}H NMR spectrum of **3l**, related to **Figure 3**

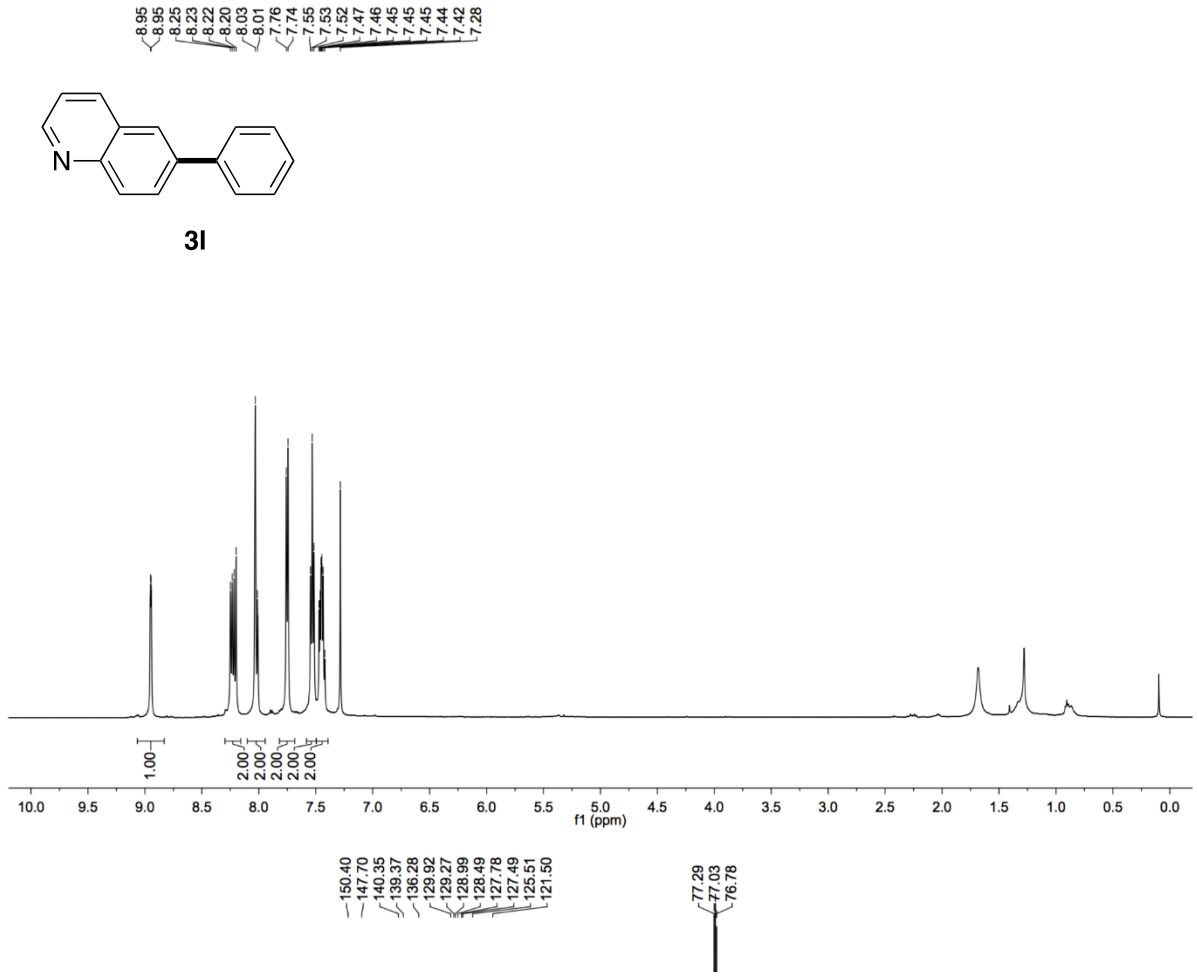

Figure S26. ^{13}C NMR spectrum of **3l**, related to **Figure 3**

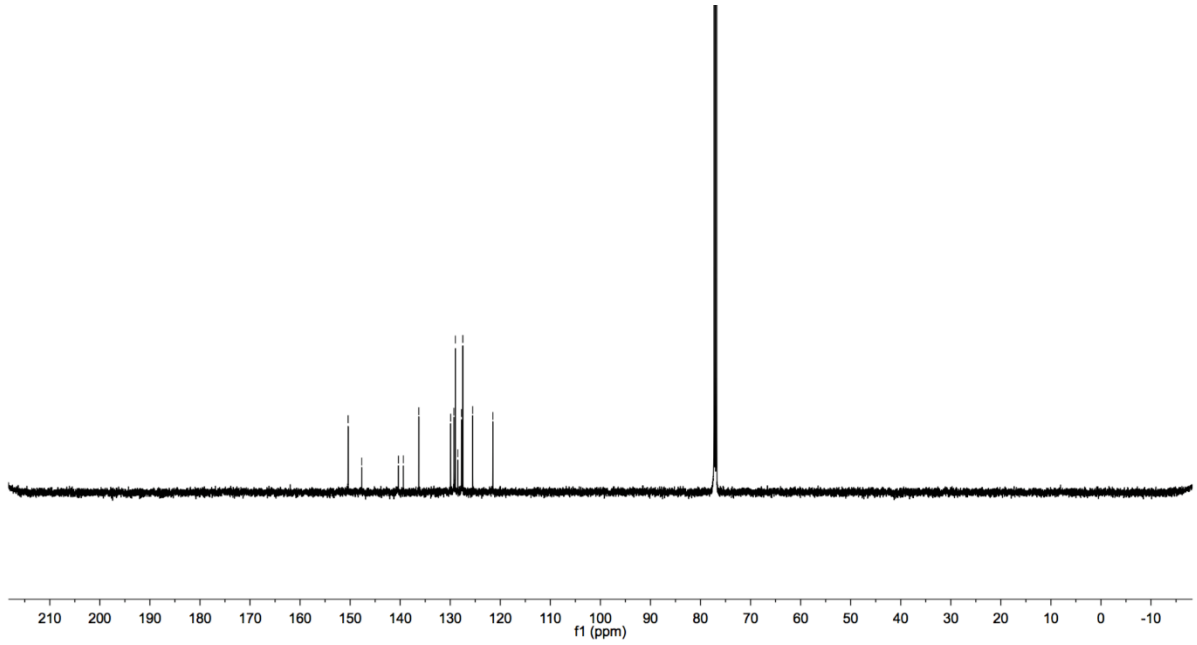

Figure S27. ^{1}H NMR spectrum of **3m**, related to **Figure 3**

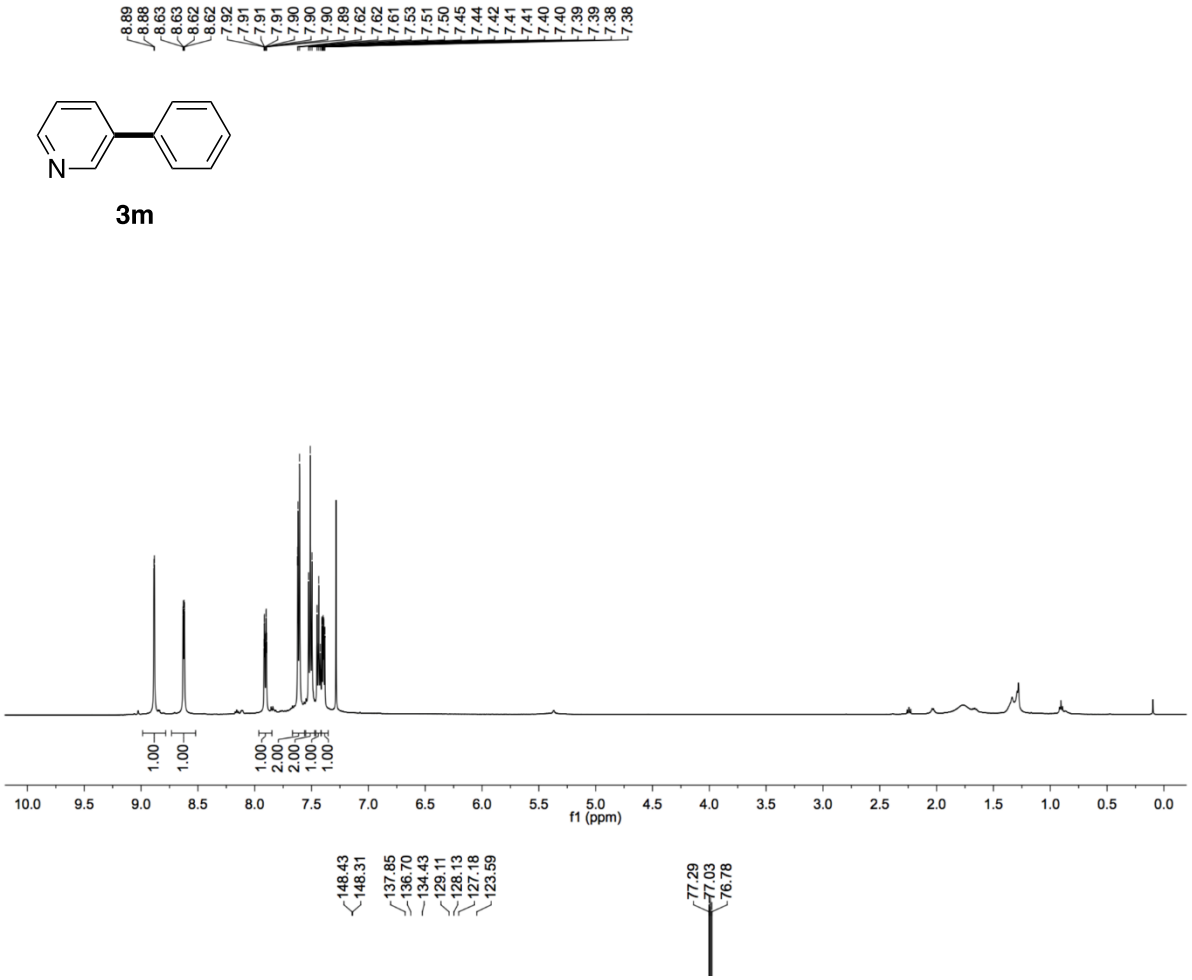

Figure S28. ^{13}C NMR spectrum of **3m**, related to **Figure 3**

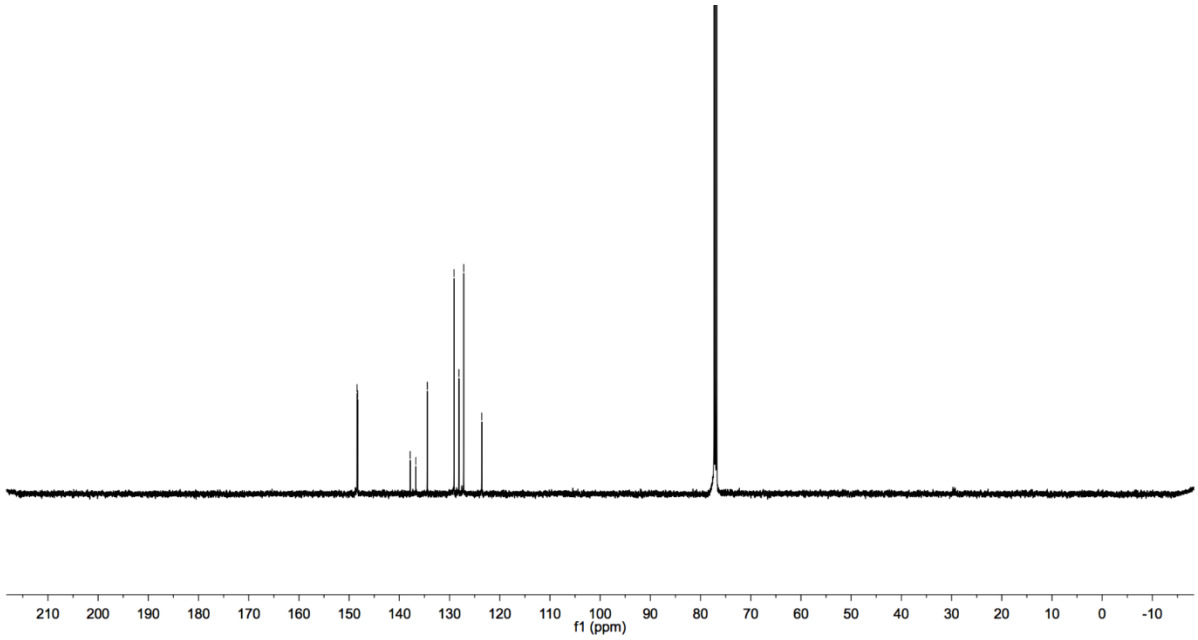

Figure S29. ^{1}H NMR spectrum of **3n**, related to **Figure 3**

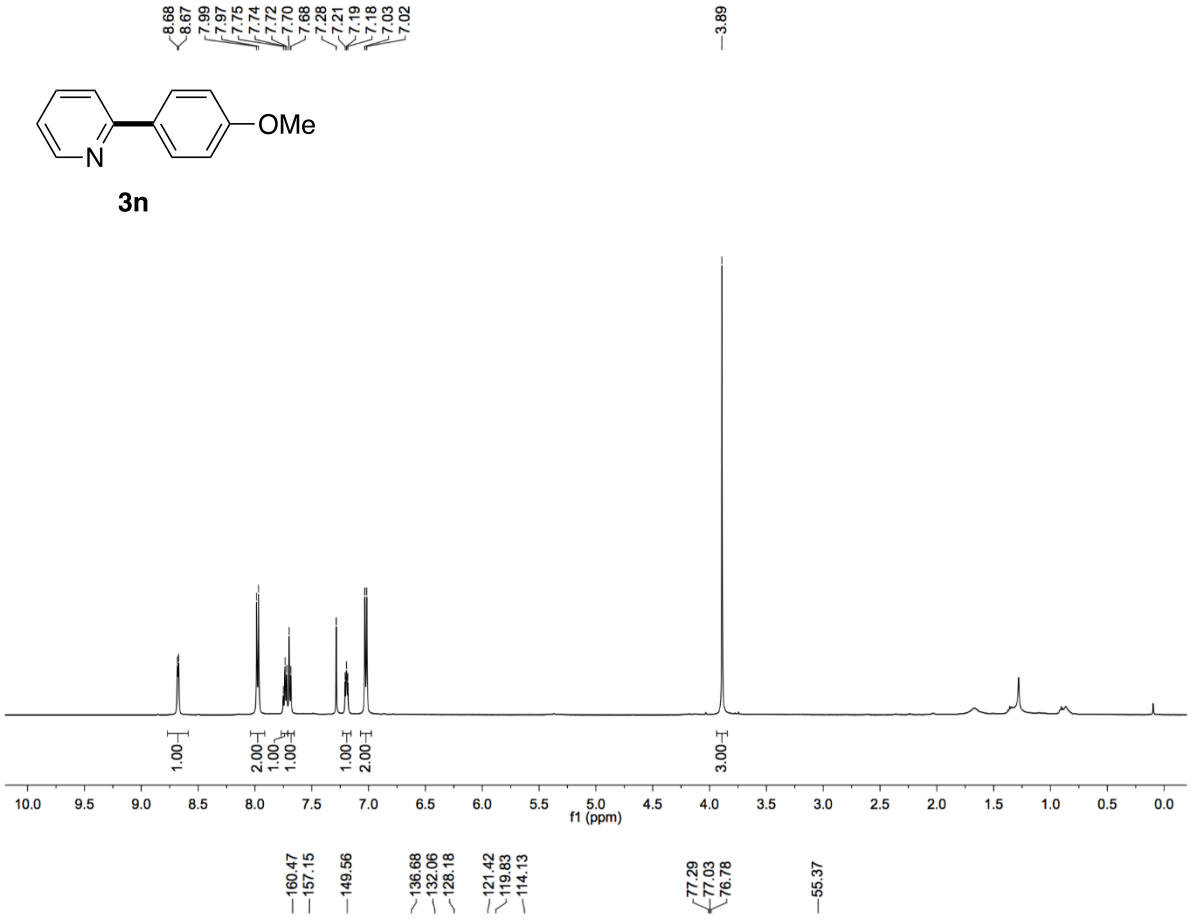

Figure S30. ^{13}C NMR spectrum of **3n**, related to **Figure 3**

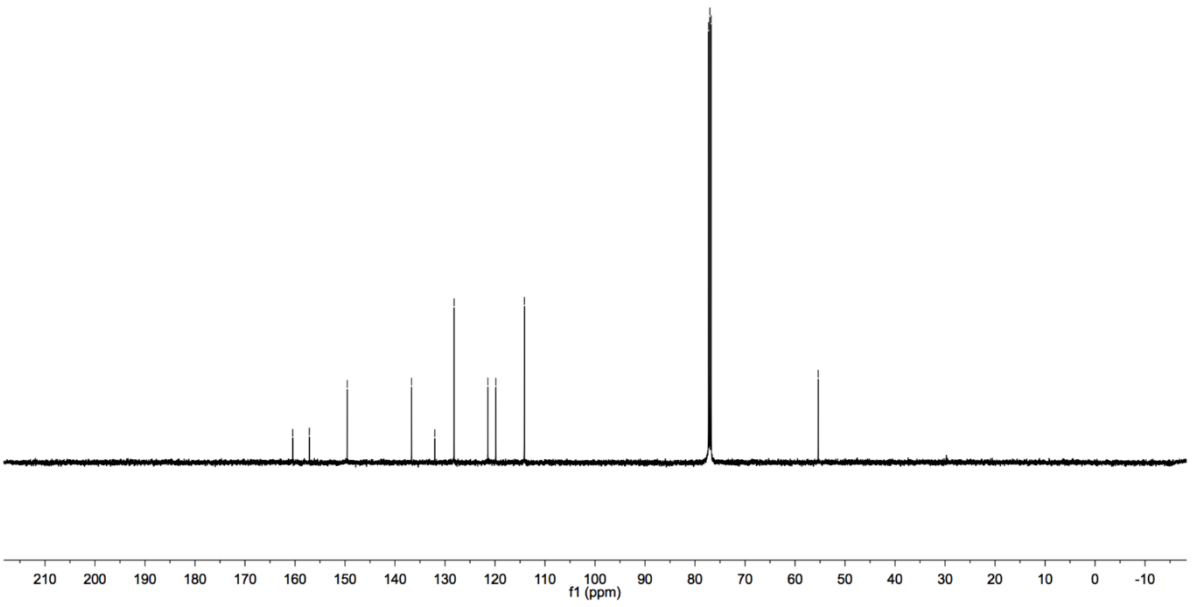

Figure S31. ^{1}H NMR spectrum of **3o**, related to **Figure 3**

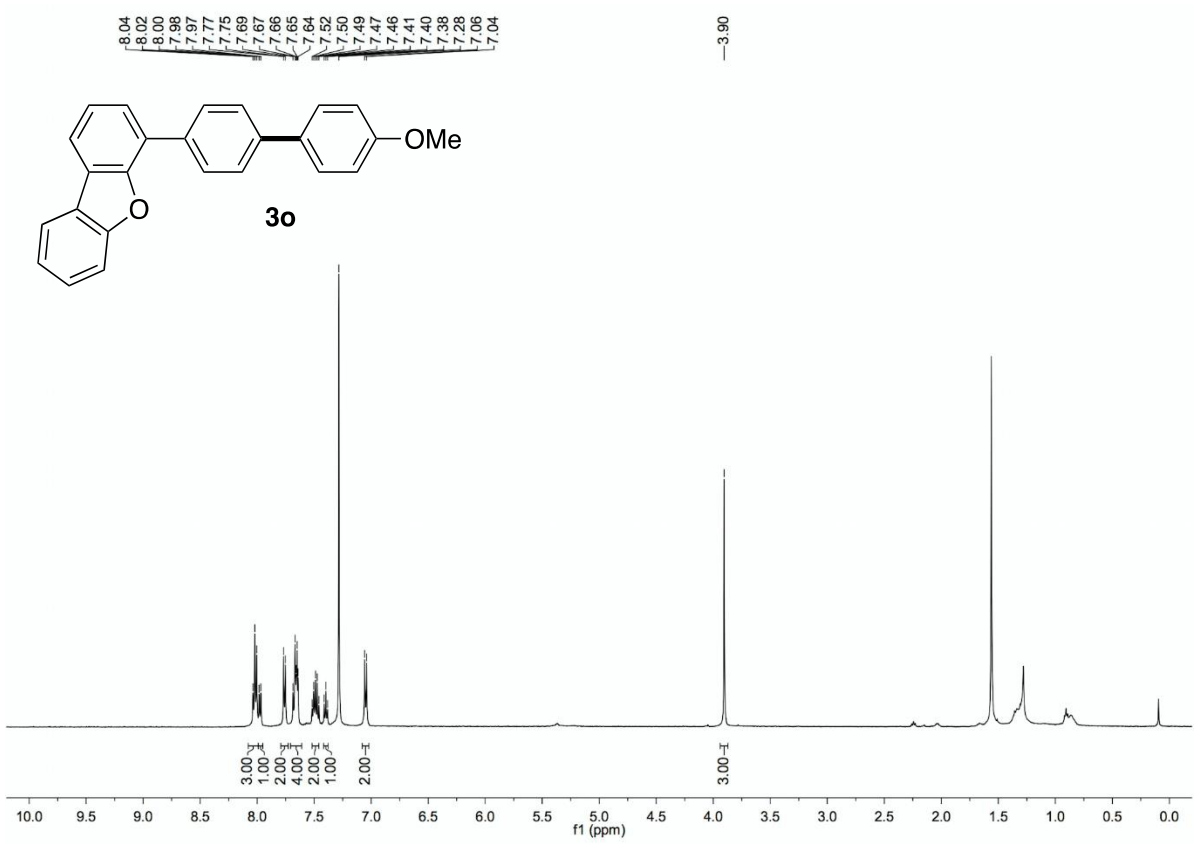

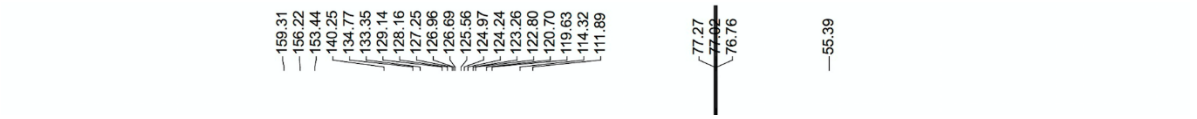

Figure S32. ^{13}C NMR spectrum of **3o**, related to **Figure 3**

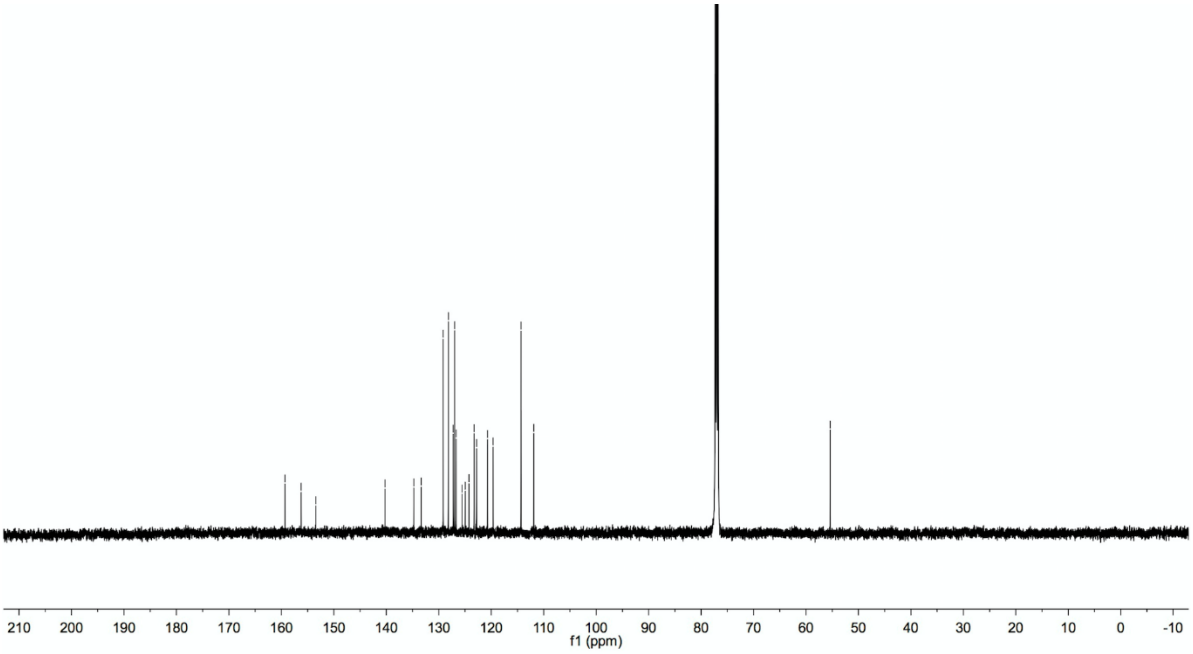

Figure S33. ^{1}H NMR spectrum of **3p**, related to **Figure 3**

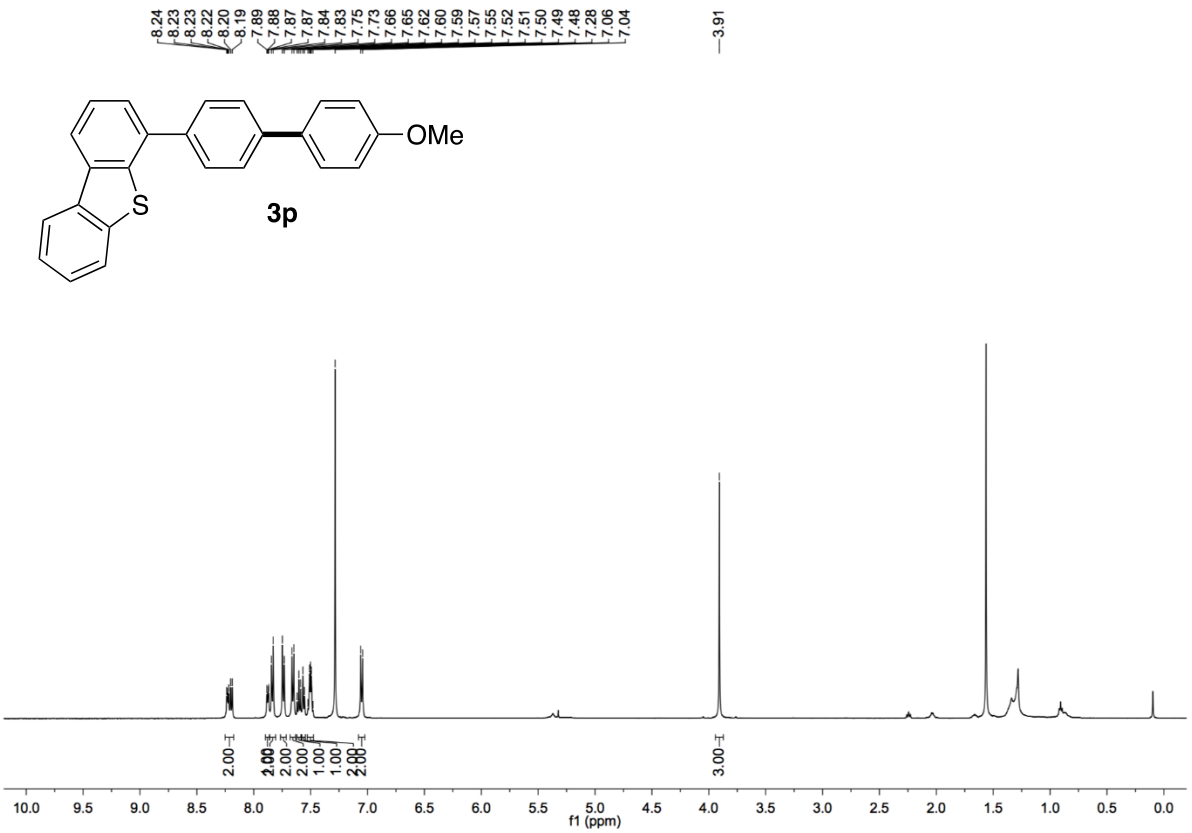

Figure S34. ^{13}C NMR spectrum of **3p**, related to **Figure 3**

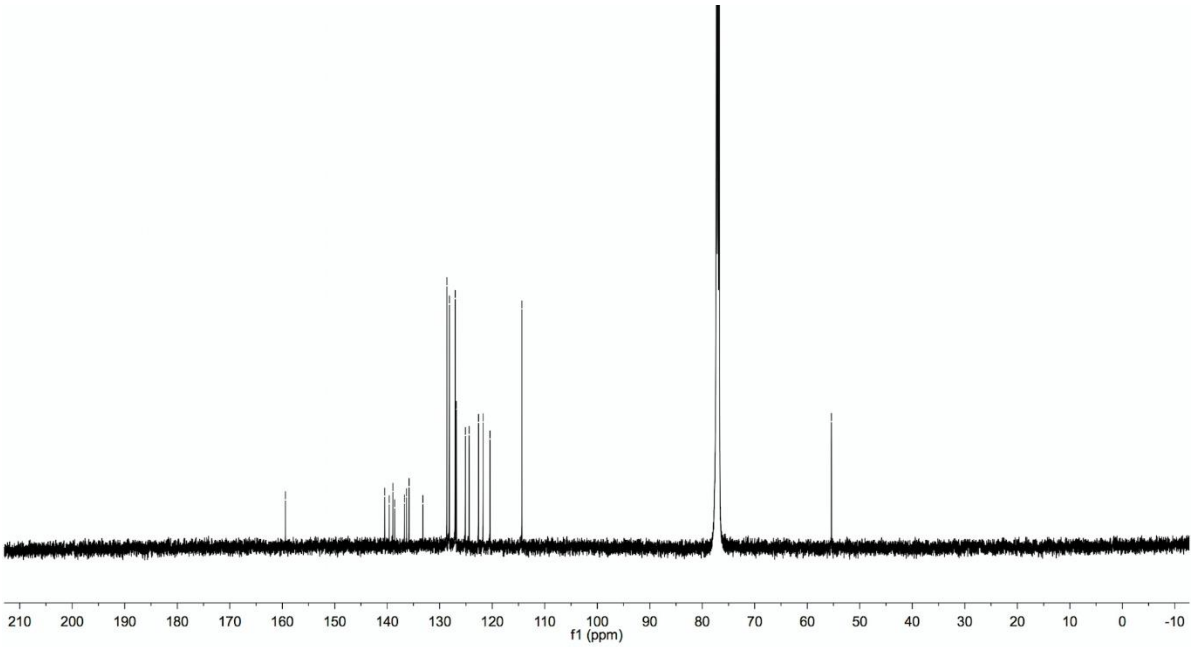

Figure S35. ^{1}H NMR spectrum of **3q**, related to **Figure 3**

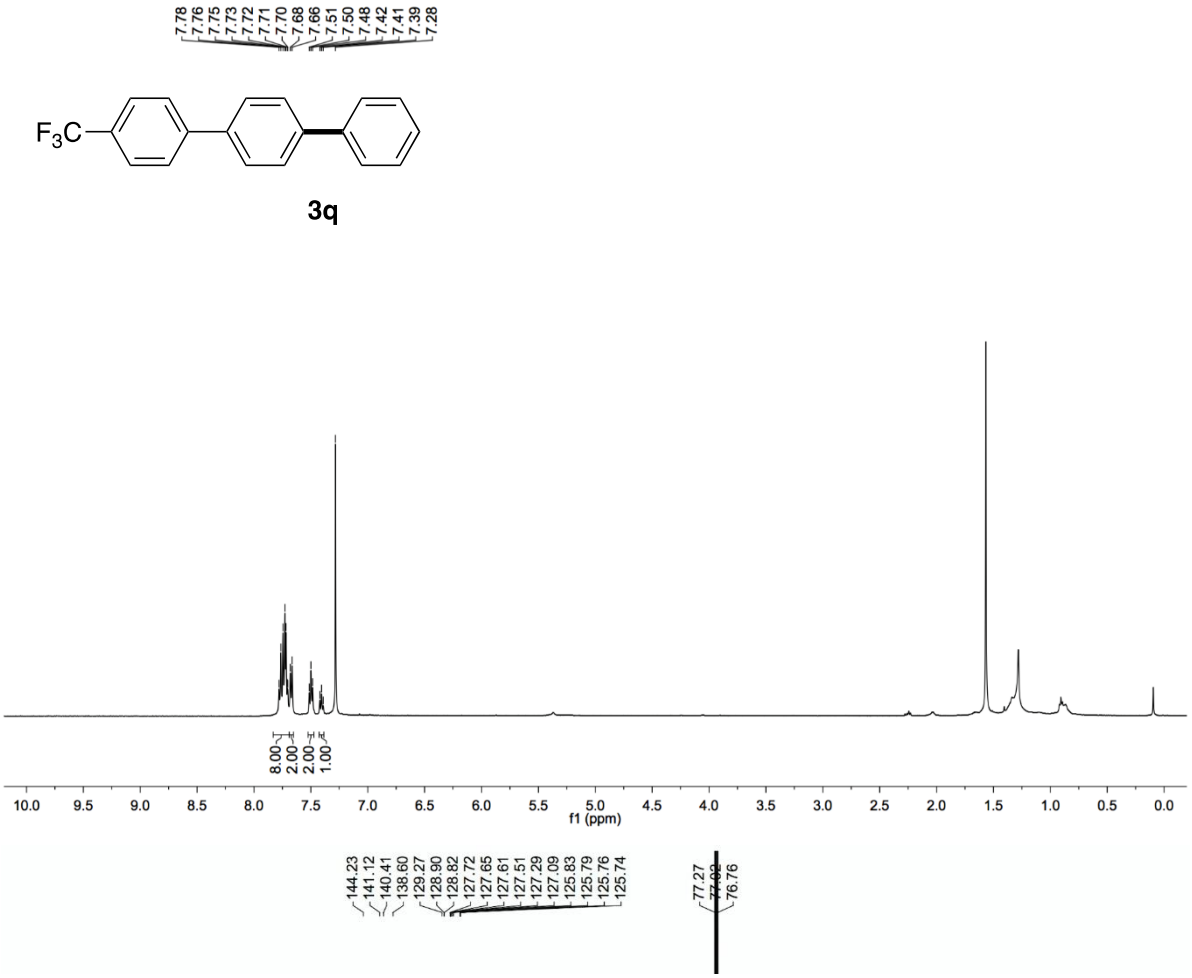

Figure S36. ^{13}C NMR spectrum of **3q**, related to **Figure 3**

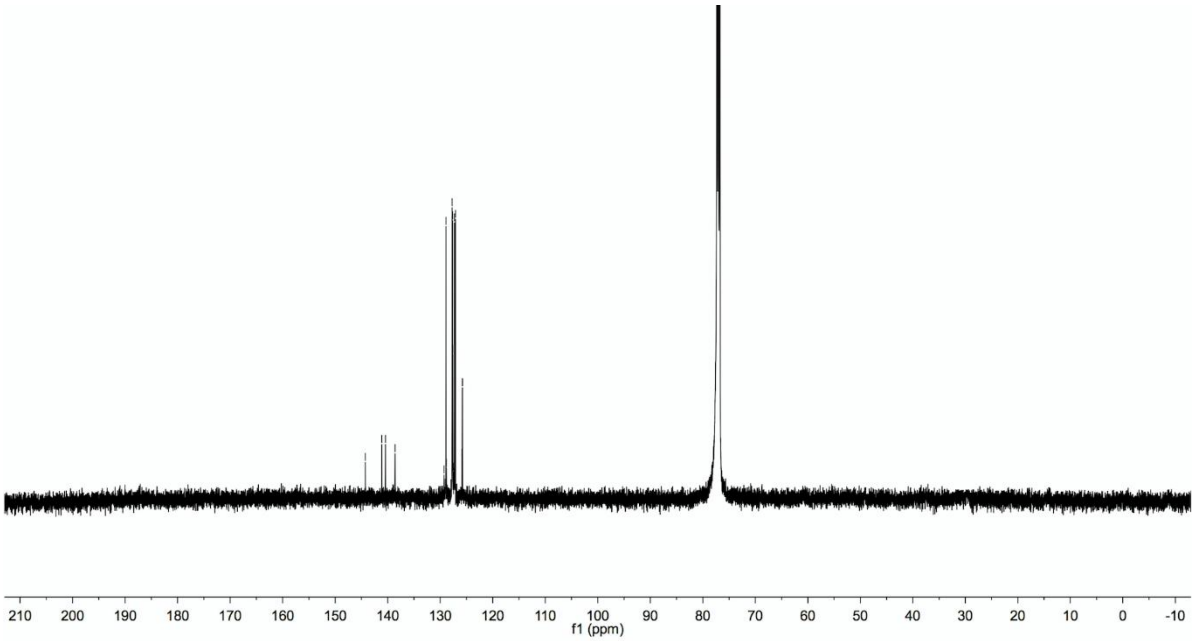

Figure S37. ^{19}F NMR spectrum of **3q**, related to **Figure 3**

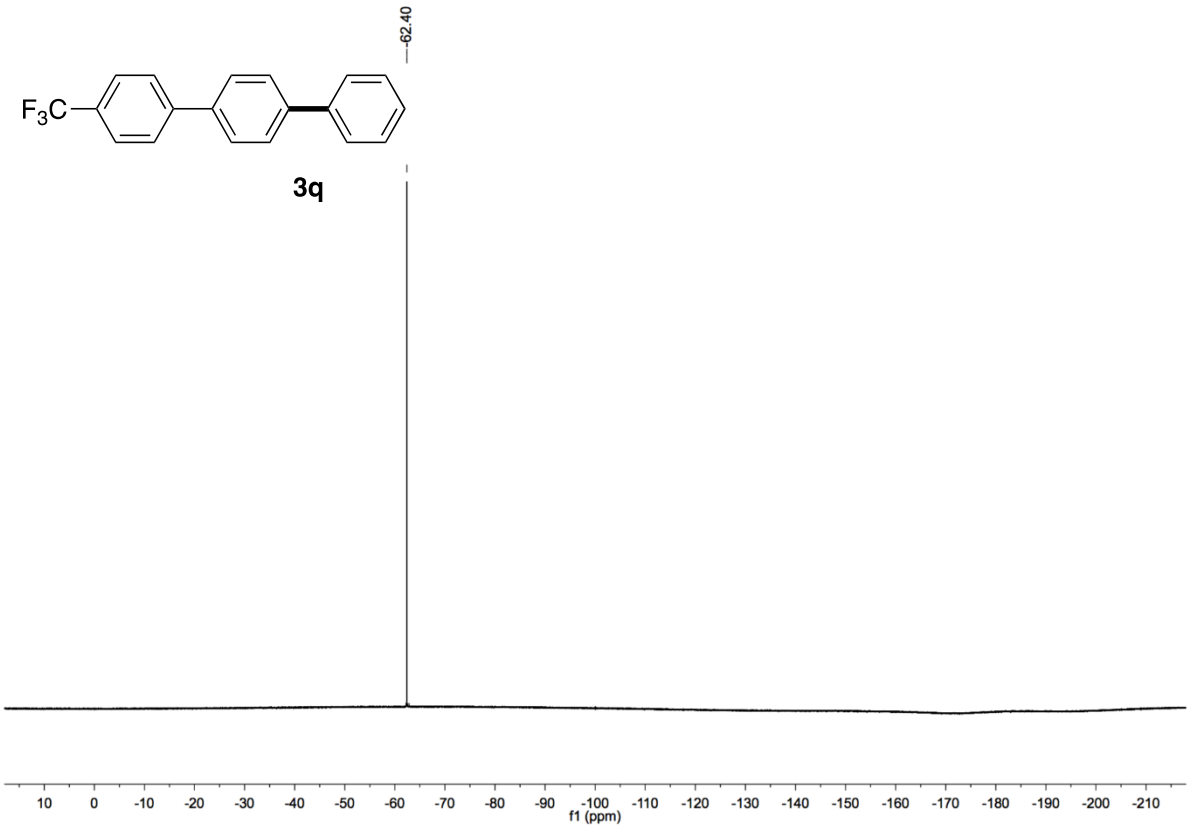

Figure S38. ^{1}H NMR spectrum of **3r**, related to **Figure 3**

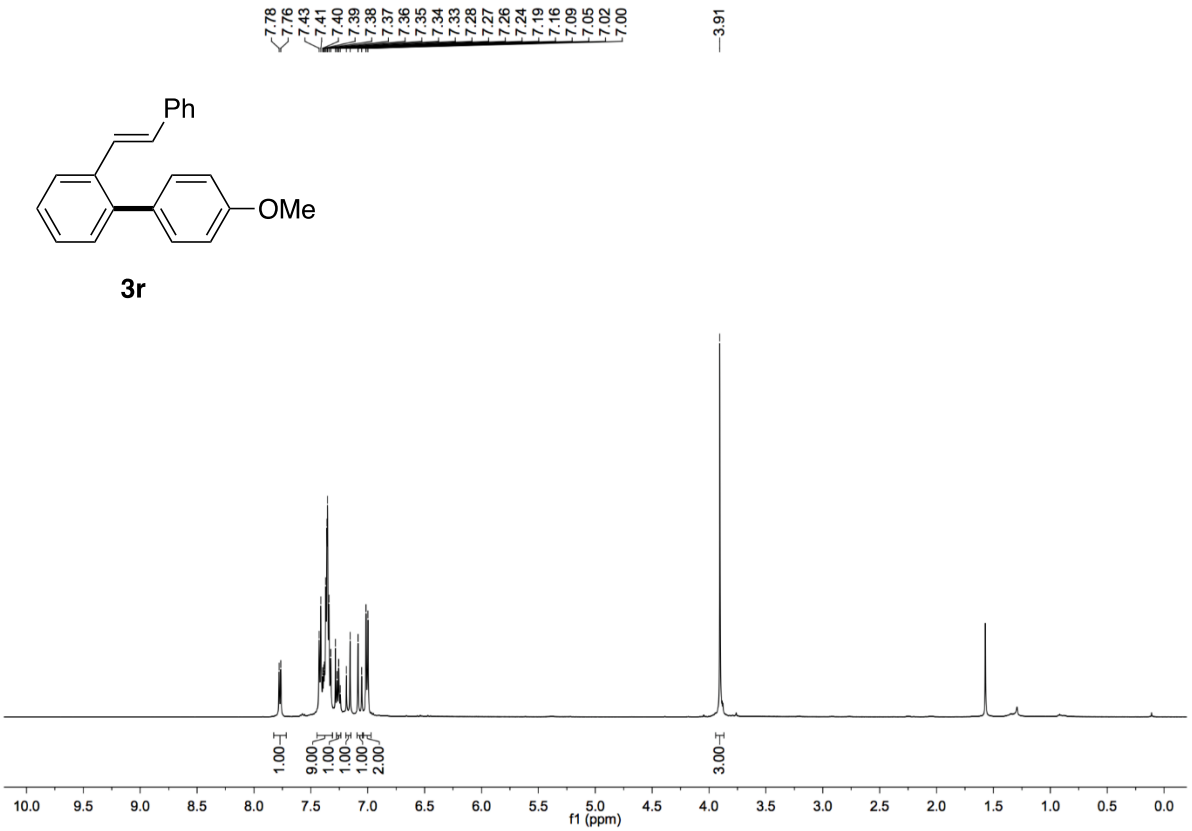

Figure S39. ^{13}C NMR spectrum of **3r**, related to **Figure 3**

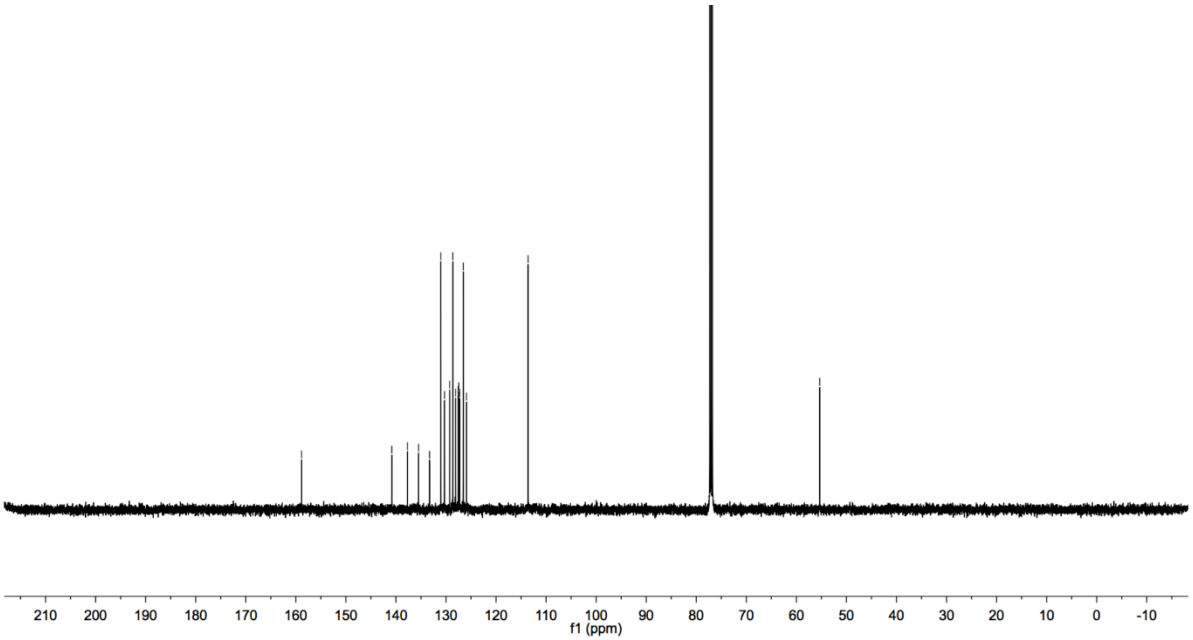

Figure S40. ^{1}H NMR spectrum of **3s**, related to **Figure 3**

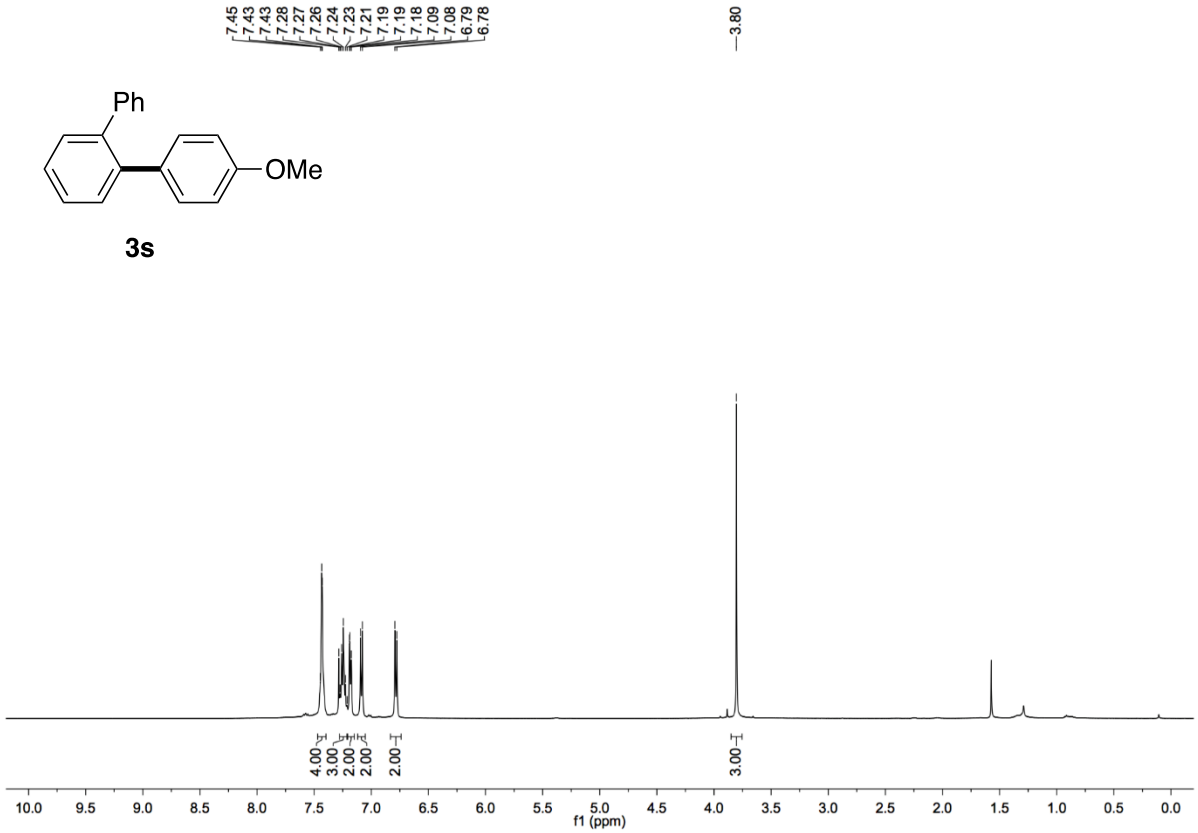

Figure S41. ^{13}C NMR spectrum of **3s**, related to **Figure 3**

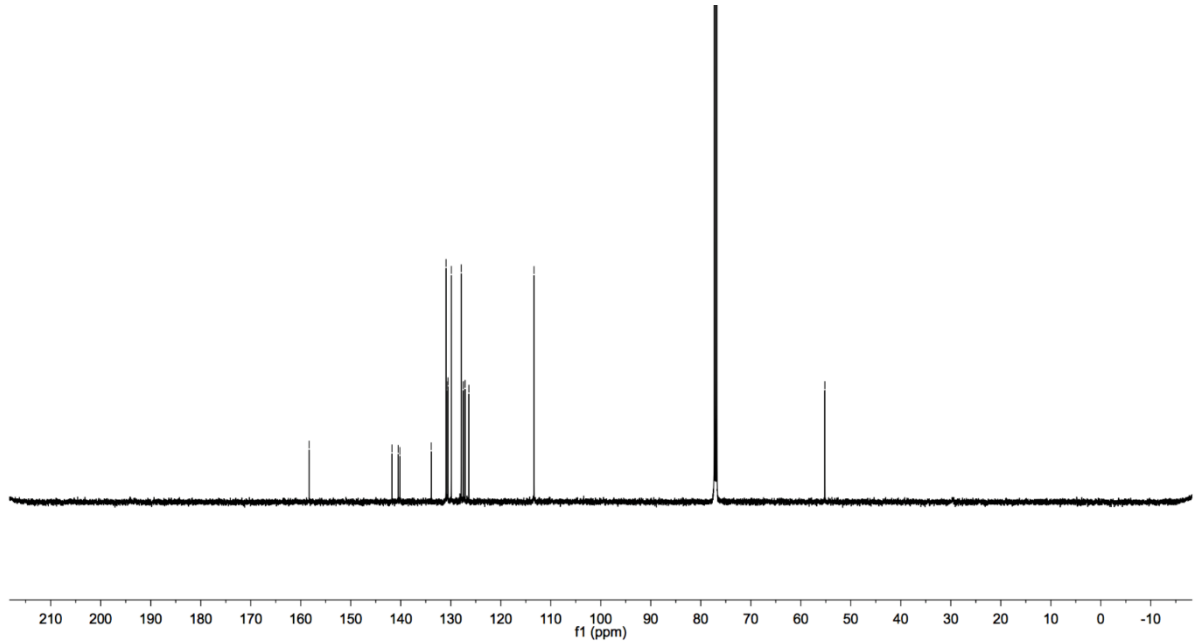

Figure S42. ^{1}H NMR spectrum of **3t**, related to **Figure 3**

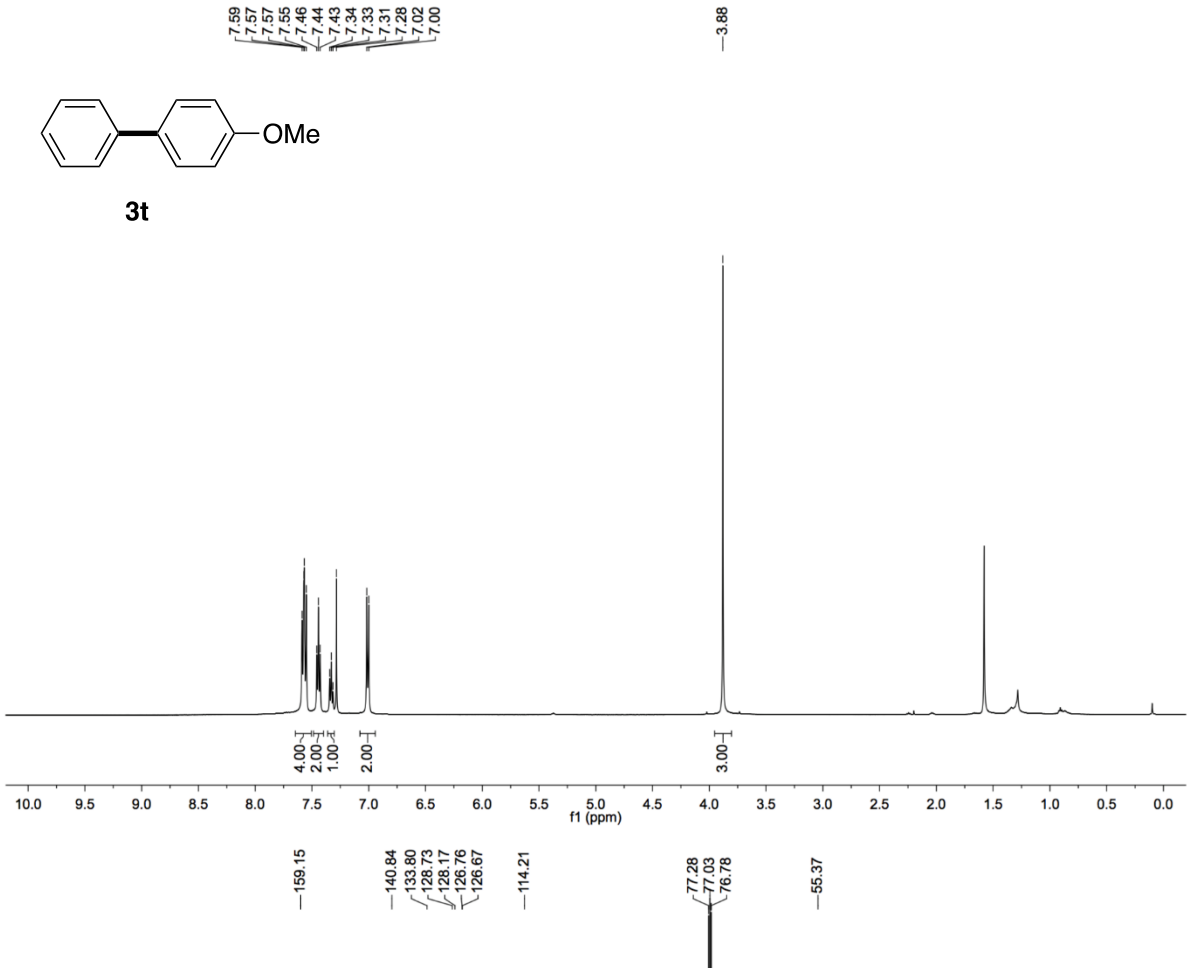

Figure S43. ^{13}C NMR spectrum of **3t**, related to **Figure 3**

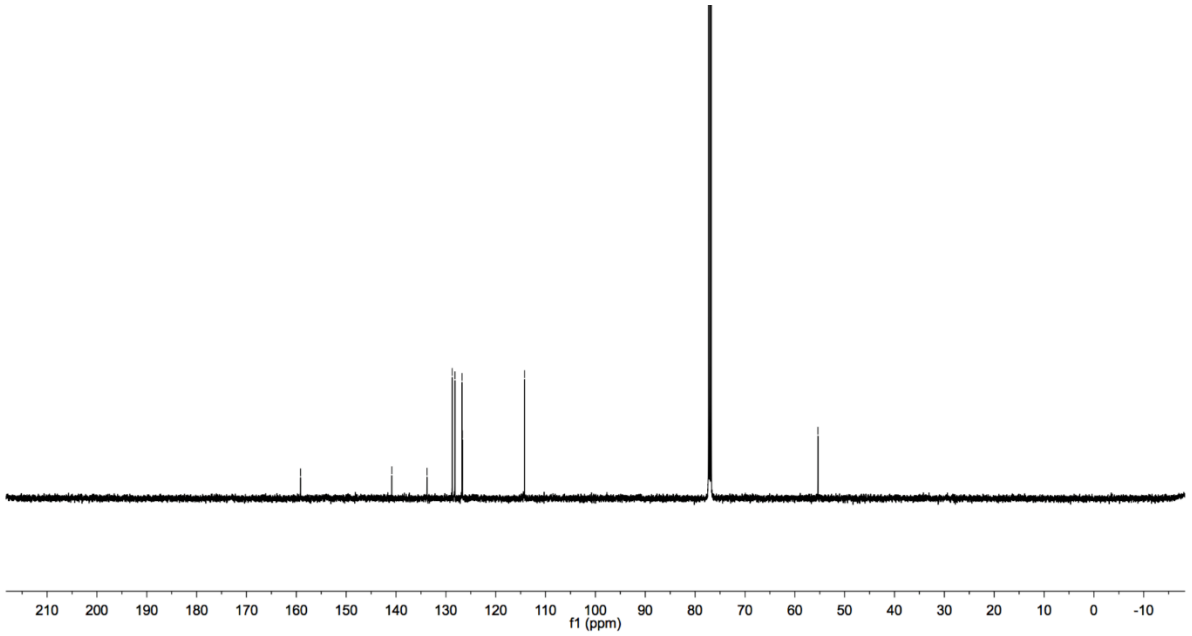

Figure S44. ^{1}H NMR spectrum of **3u**, related to **Figure 3**

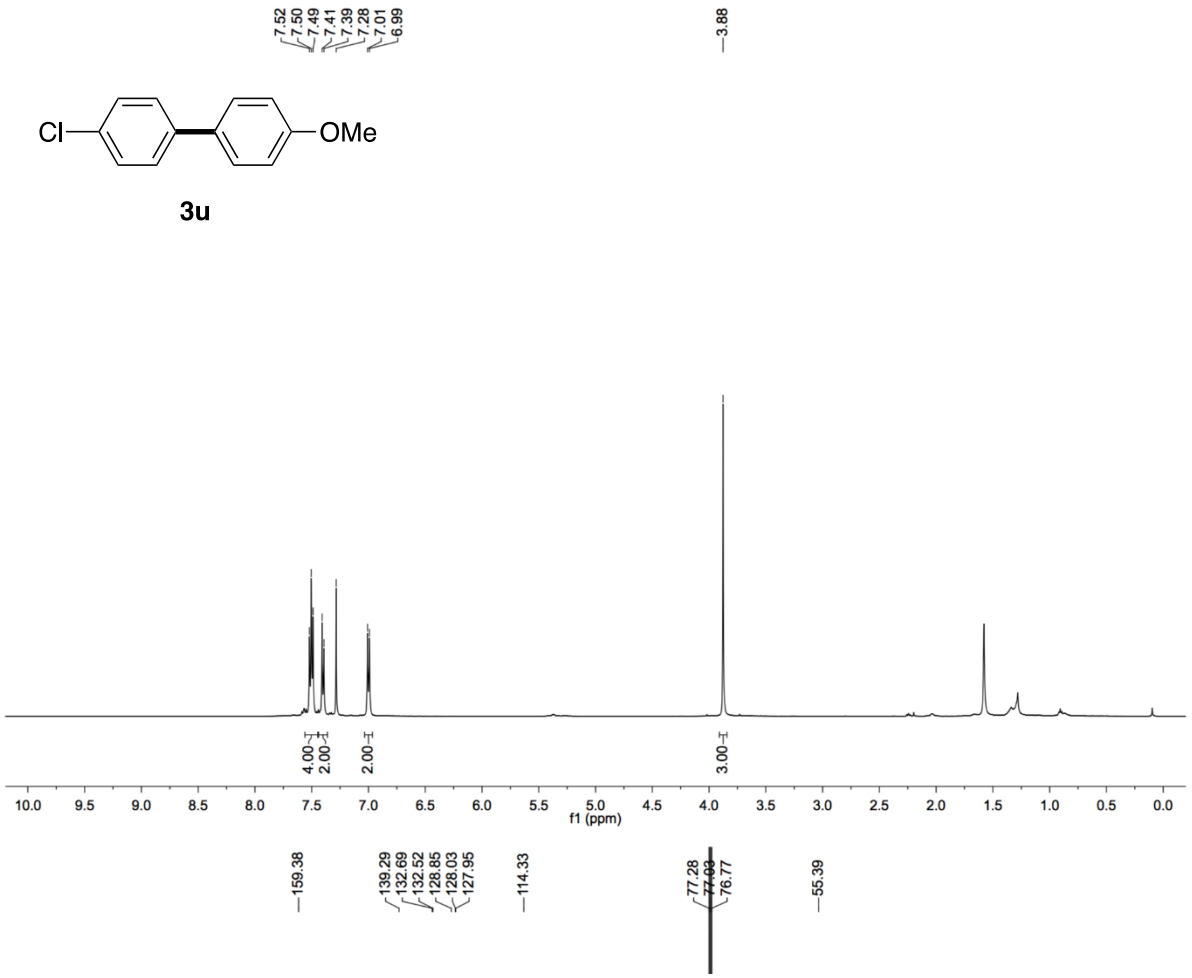

Figure S45. ^{13}C NMR spectrum of **3u**, related to **Figure 3**

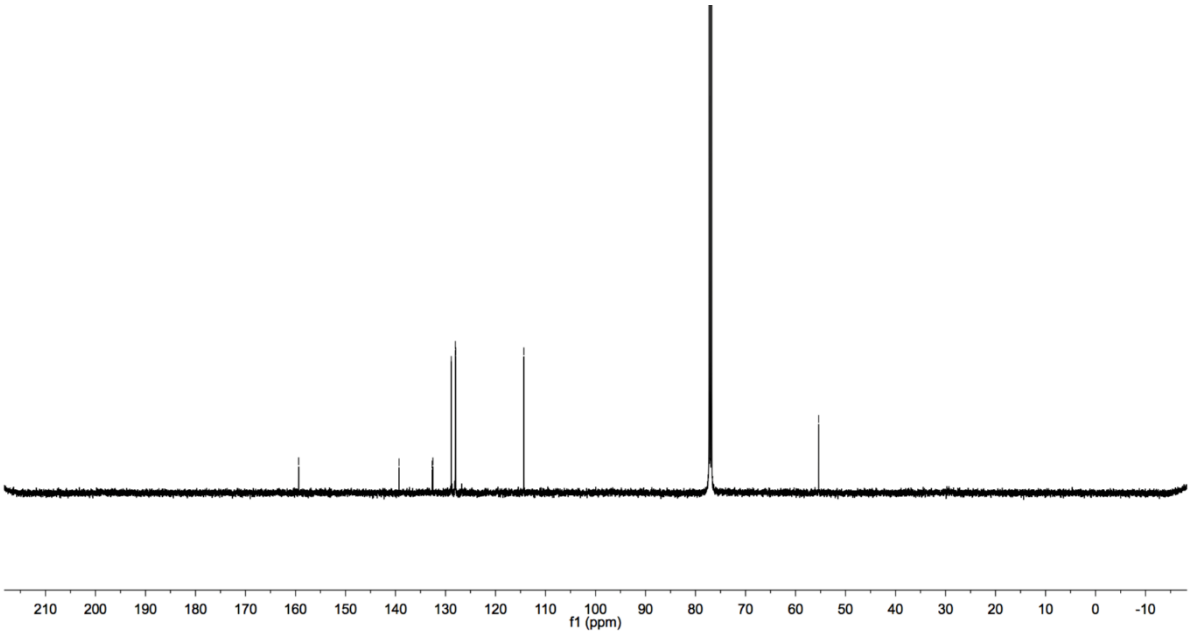

Figure S46. ^{1}H NMR spectrum of **3v**, related to **Figure 3**

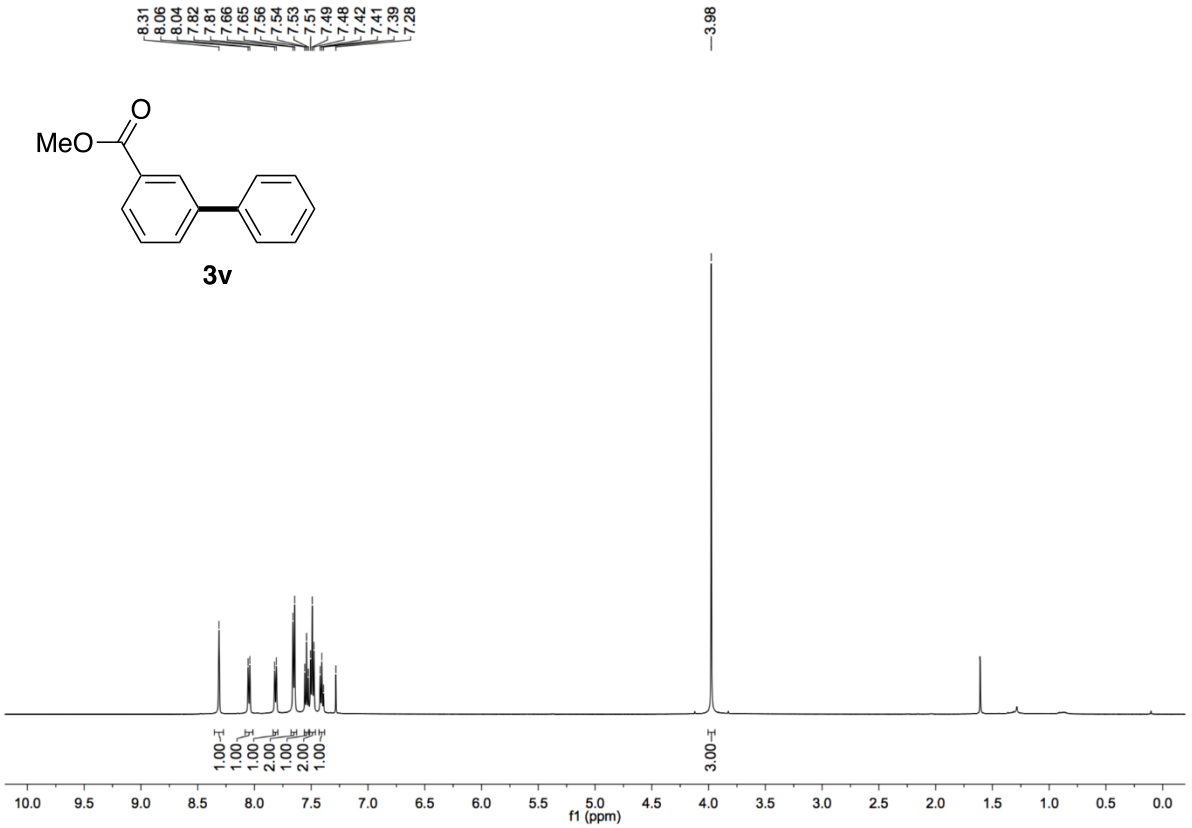

Figure S47. ^{13}C NMR spectrum of **3v**, related to **Figure 3**

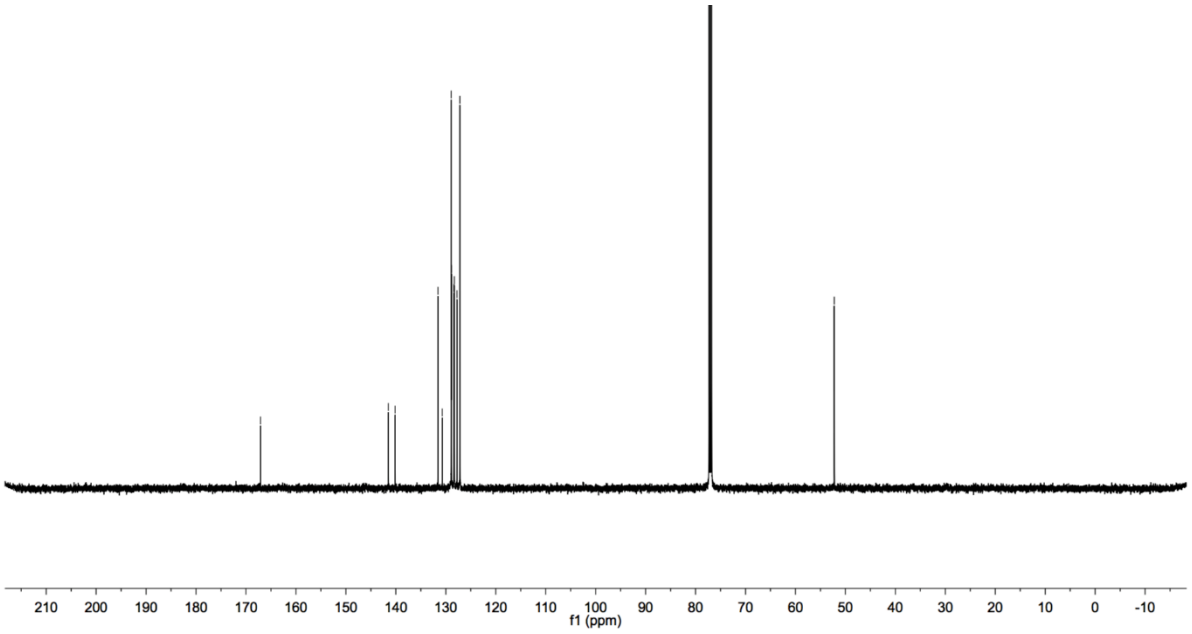

Figure S48. ^{1}H NMR spectrum of **3w**, related to **Figure 3**

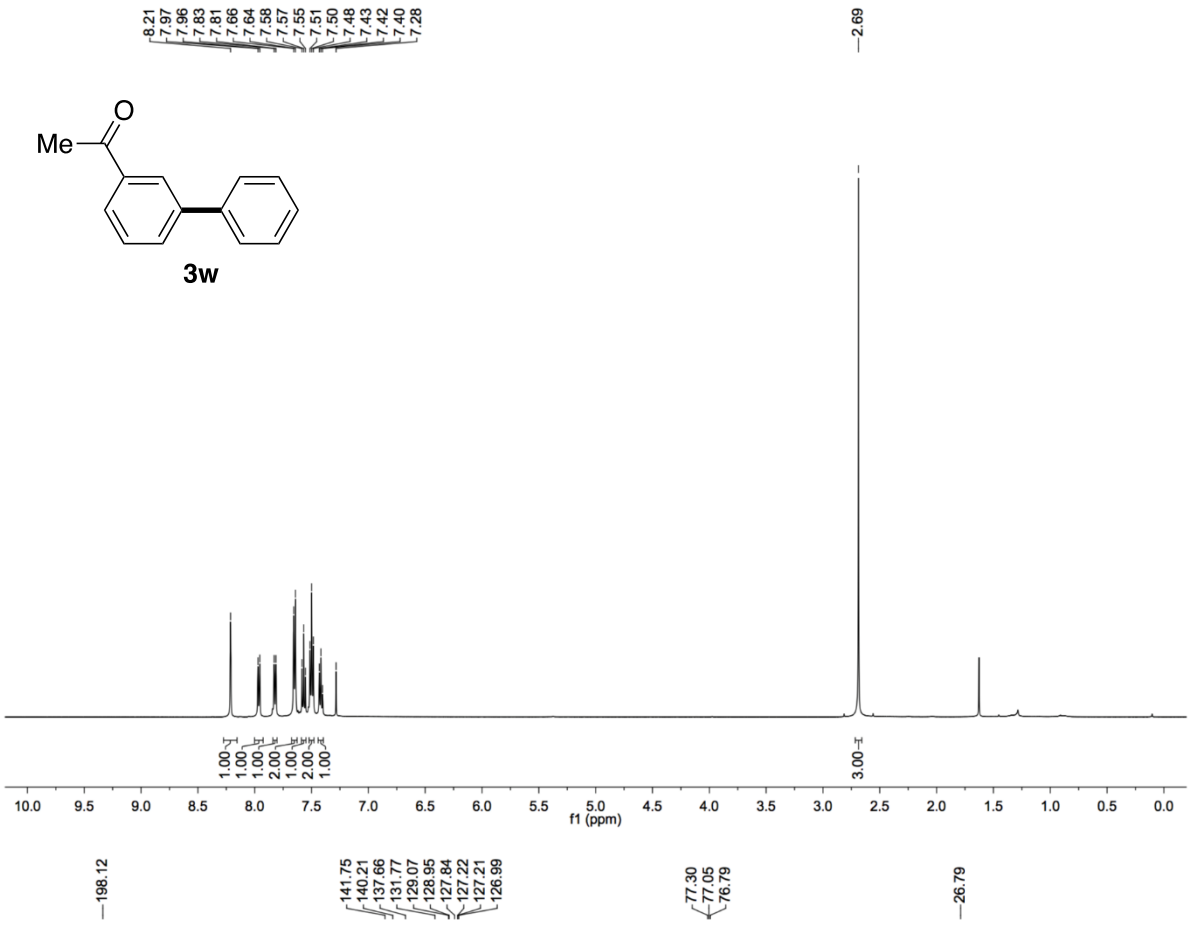

Figure S49. ^{13}C NMR spectrum of **3w**, related to **Figure 3**

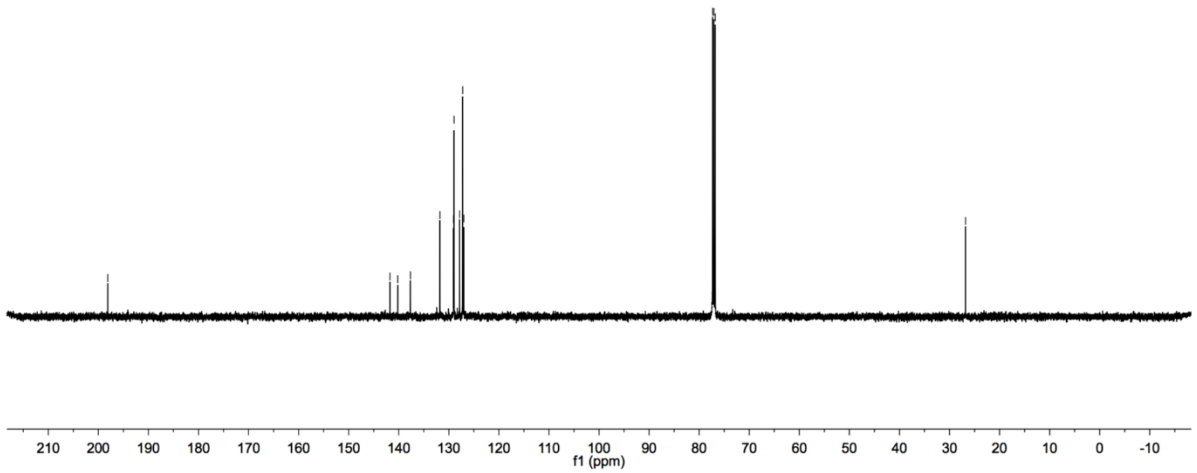

Figure S50. ^{1}H NMR spectrum of **3x**, related to **Figure 3**

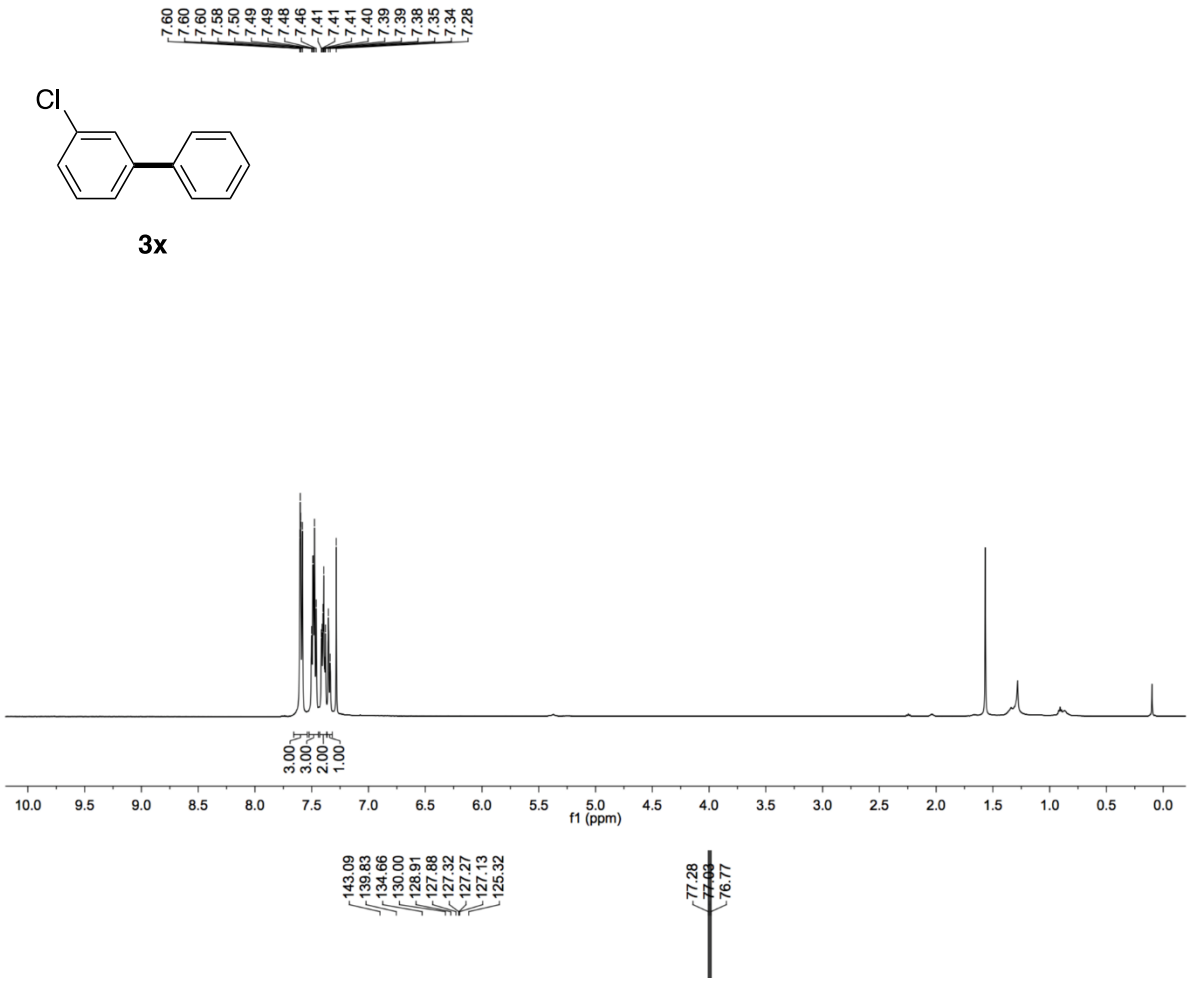

Figure S51. ^{13}C NMR spectrum of **3x**, related to **Figure 3**

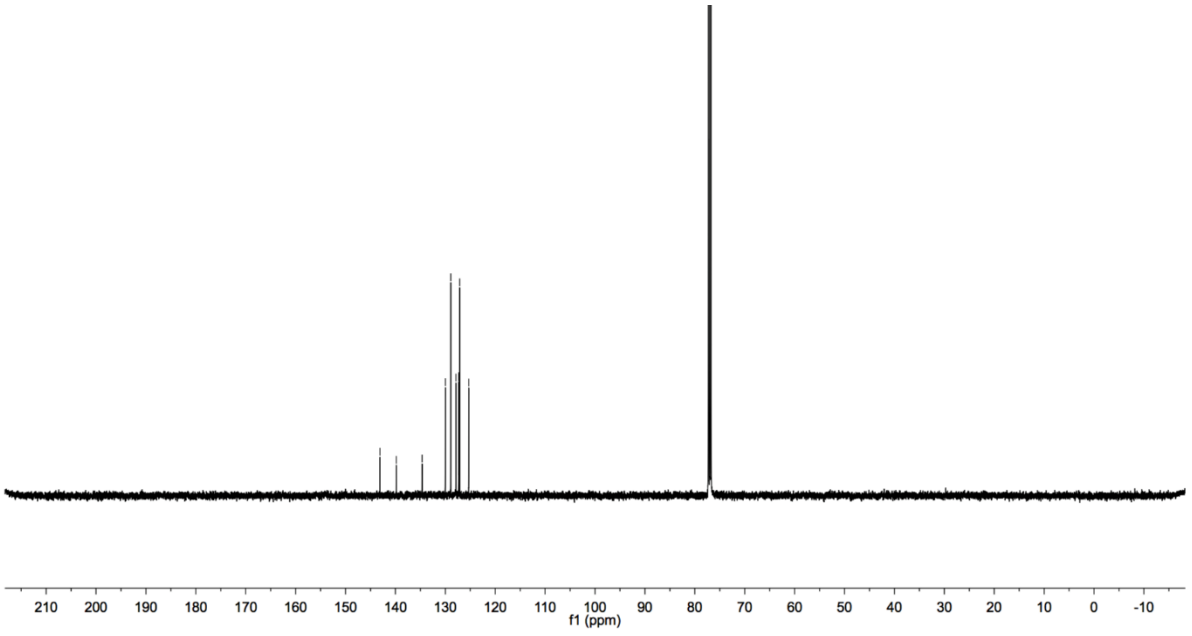

Figure S52. ^{1}H NMR spectrum of **3y**, related to **Figure 3**

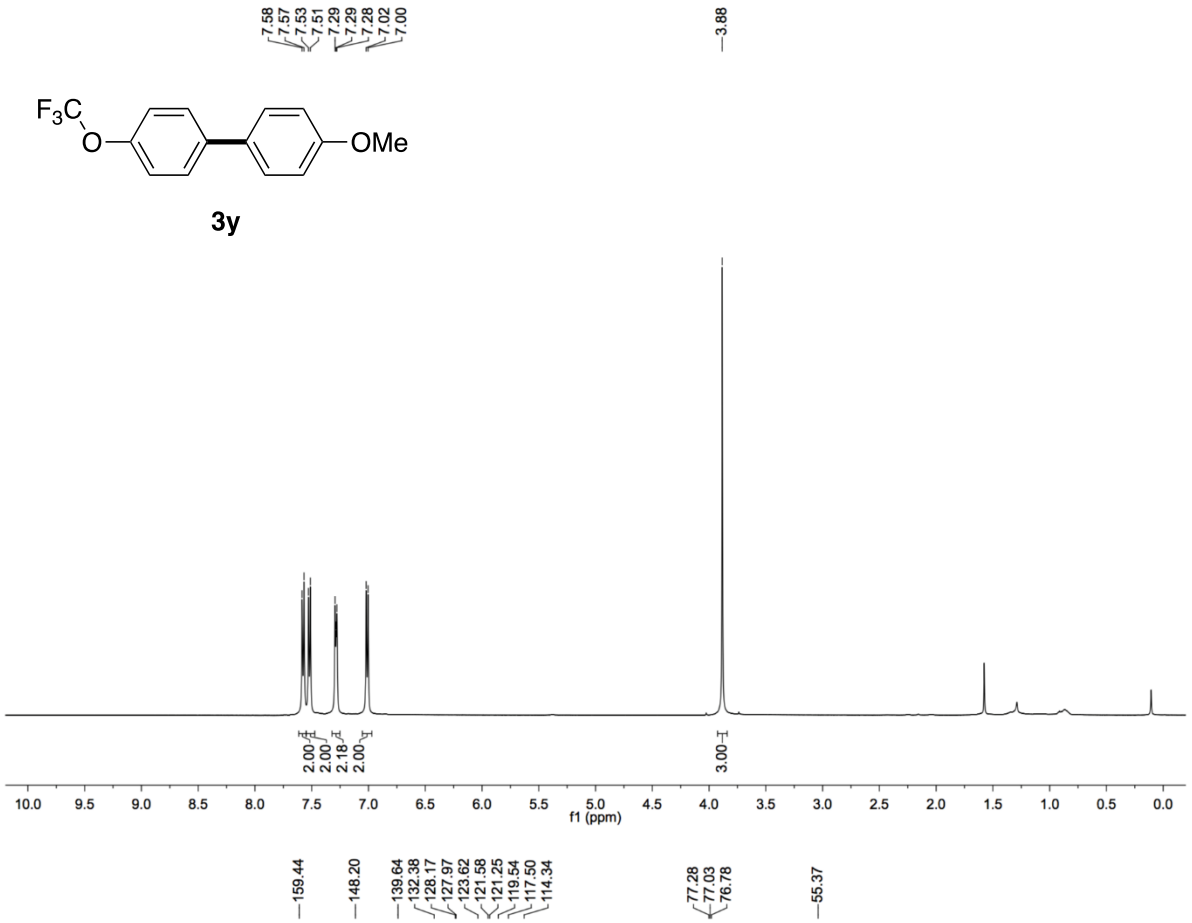

Figure S53. ^{13}C NMR spectrum of **3y**, related to **Figure 3**

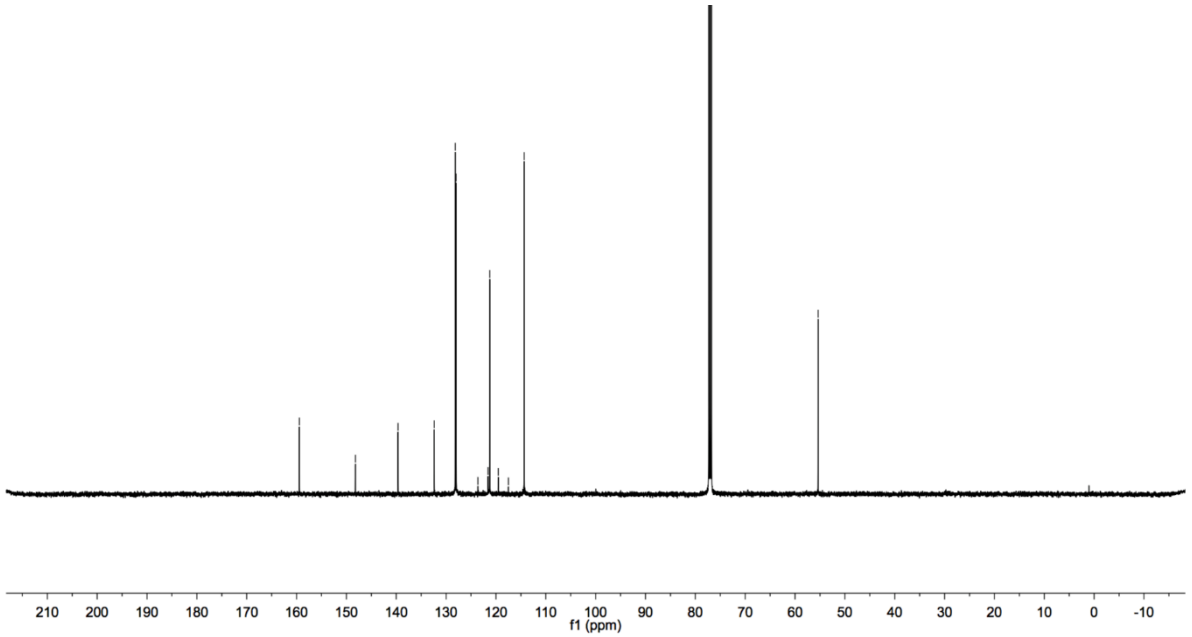

Figure S54. ^{19}F NMR spectrum of **3y**, related to **Figure 3**

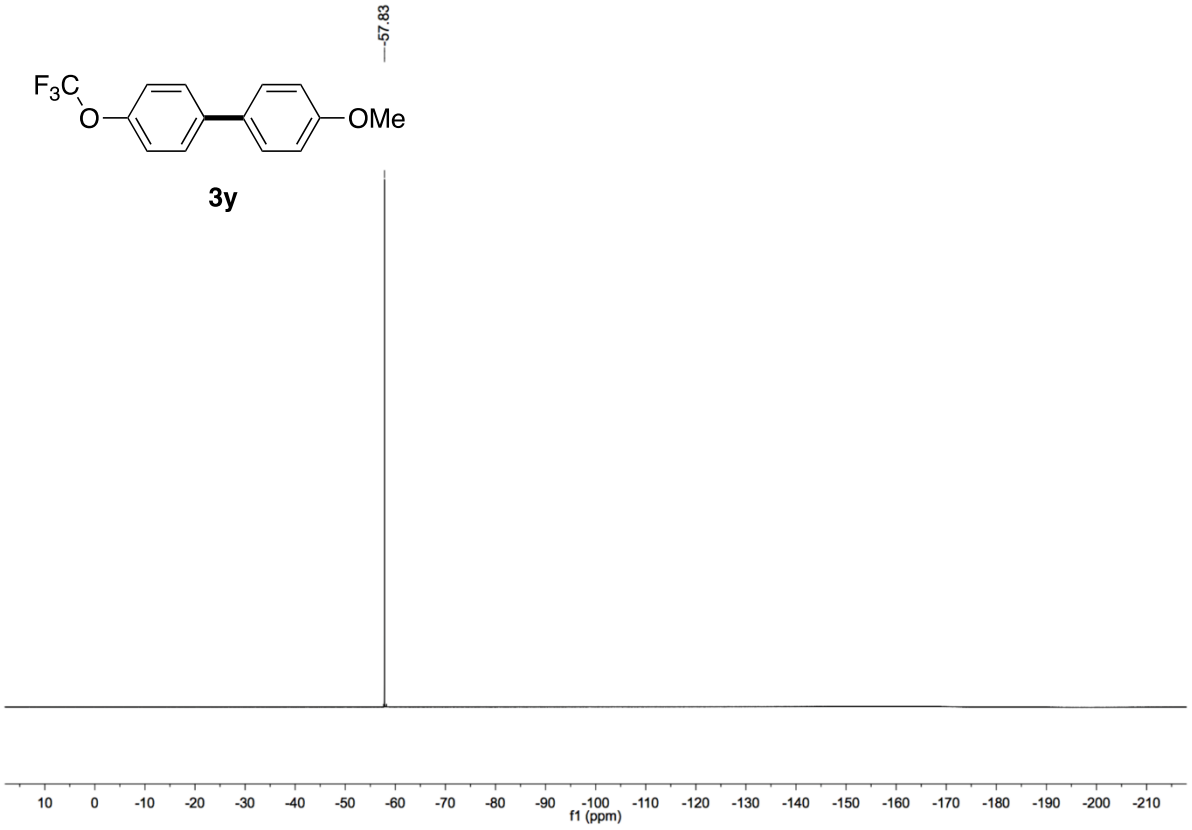

Figure S55. ^{1}H NMR spectrum of **3z**, related to **Figure 3**

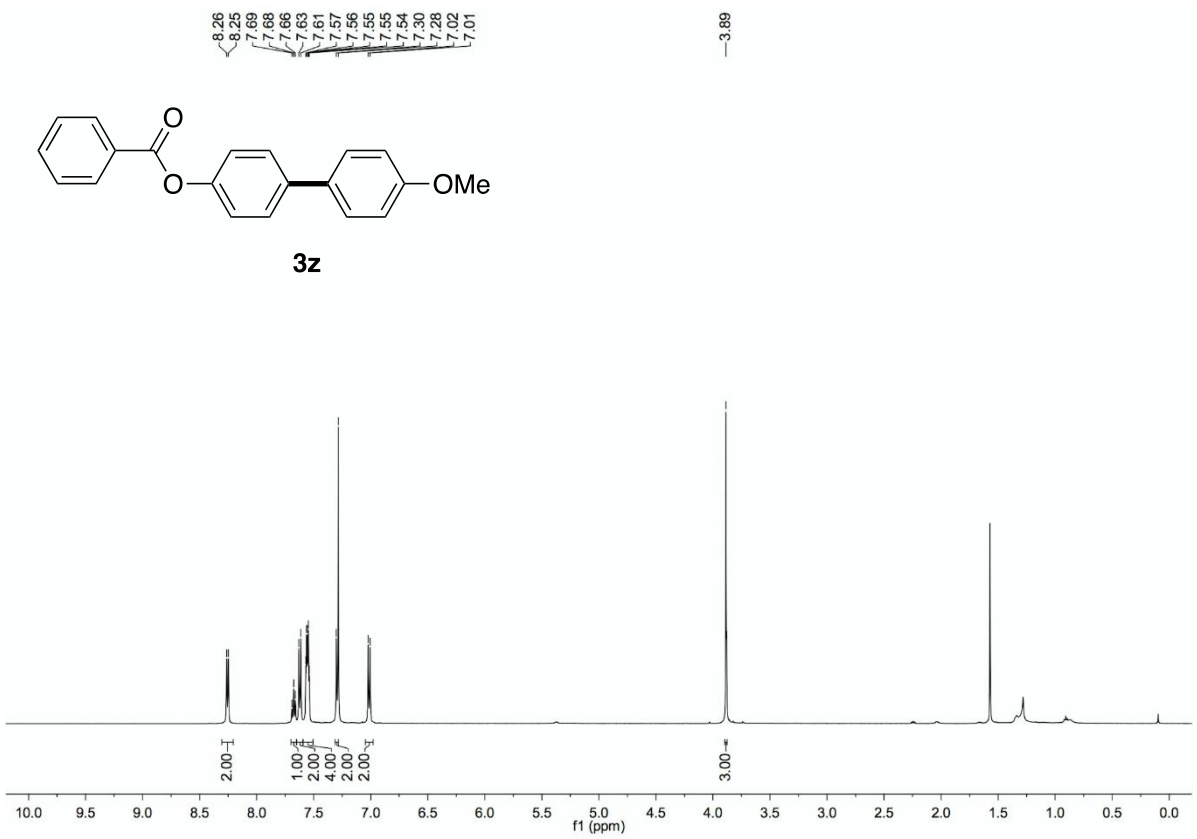

Figure S56. ^{13}C NMR spectrum of **3z**, related to **Figure 3**

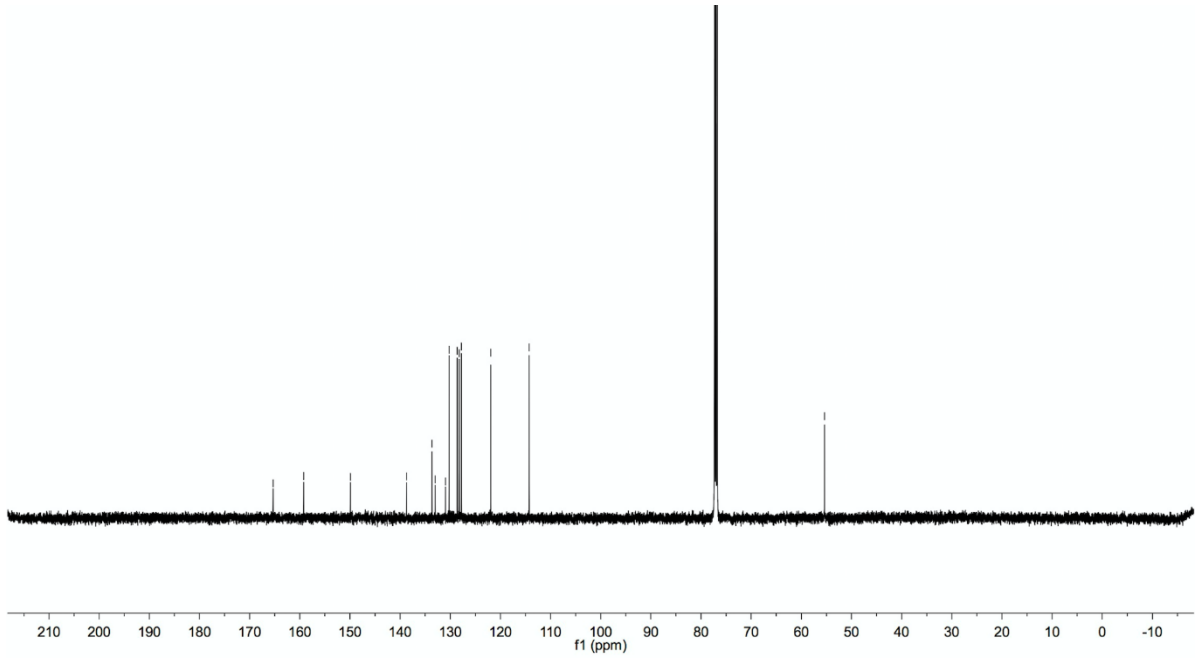

Figure S57. ^{1}H NMR spectrum of **3aa**, related to **Figure 3**

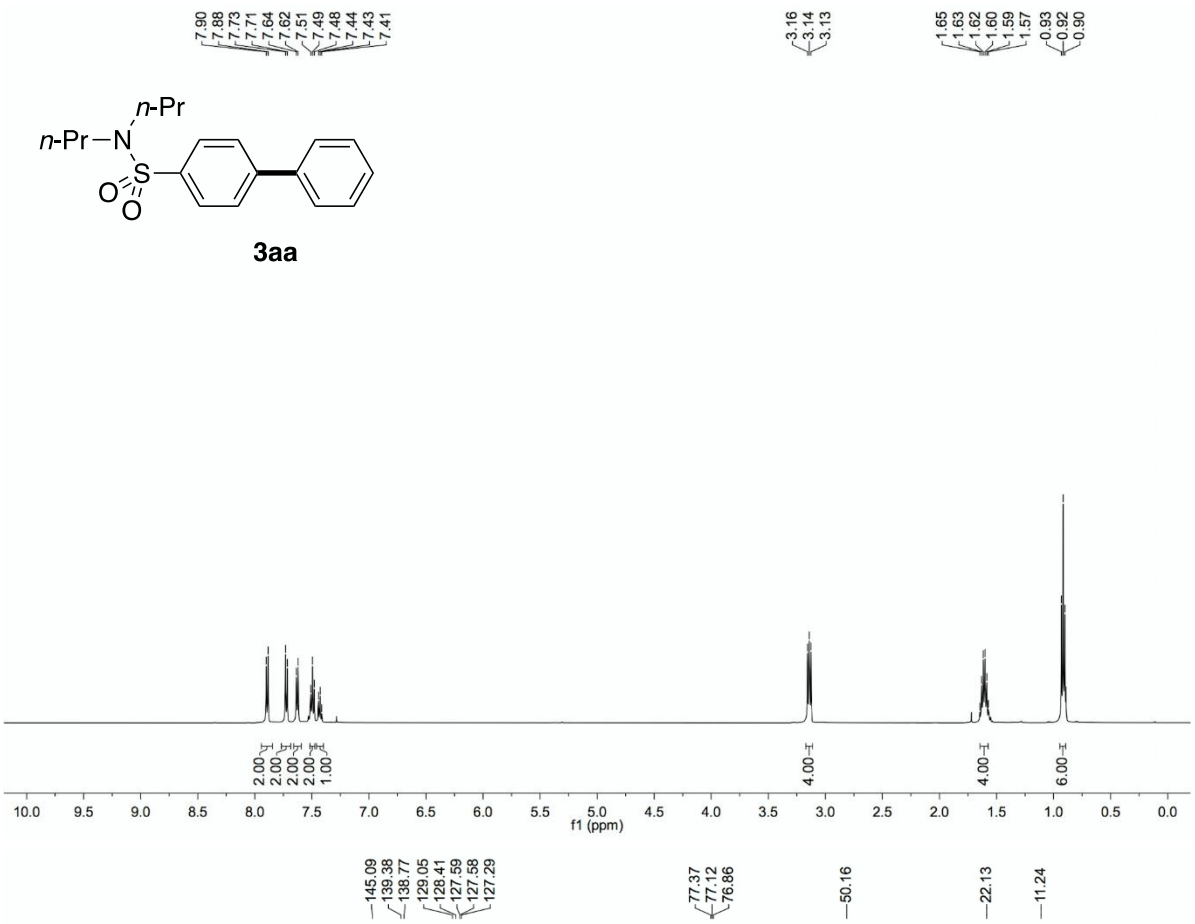

Figure S58. ^{13}C NMR spectrum of **3aa**, related to **Figure 3**

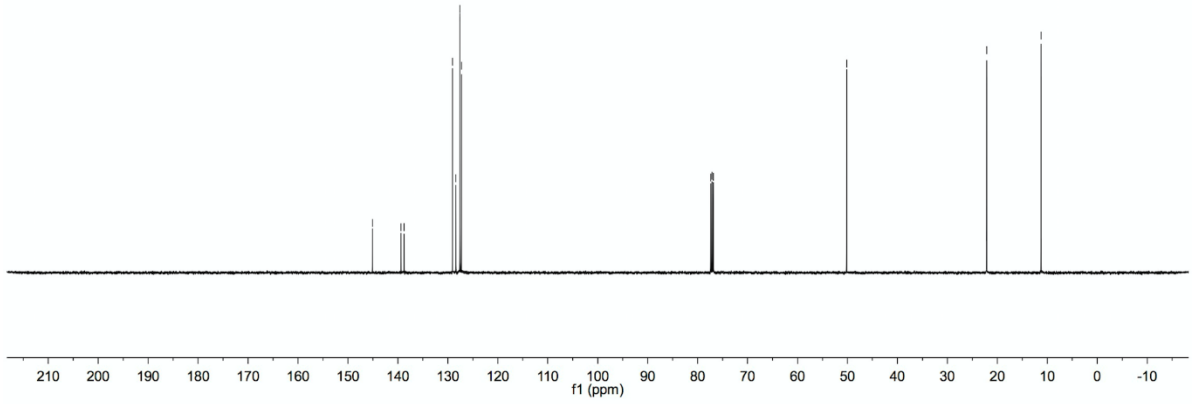

Figure S59. ^{1}H NMR spectrum of **3ab**, related to **Figure 3**

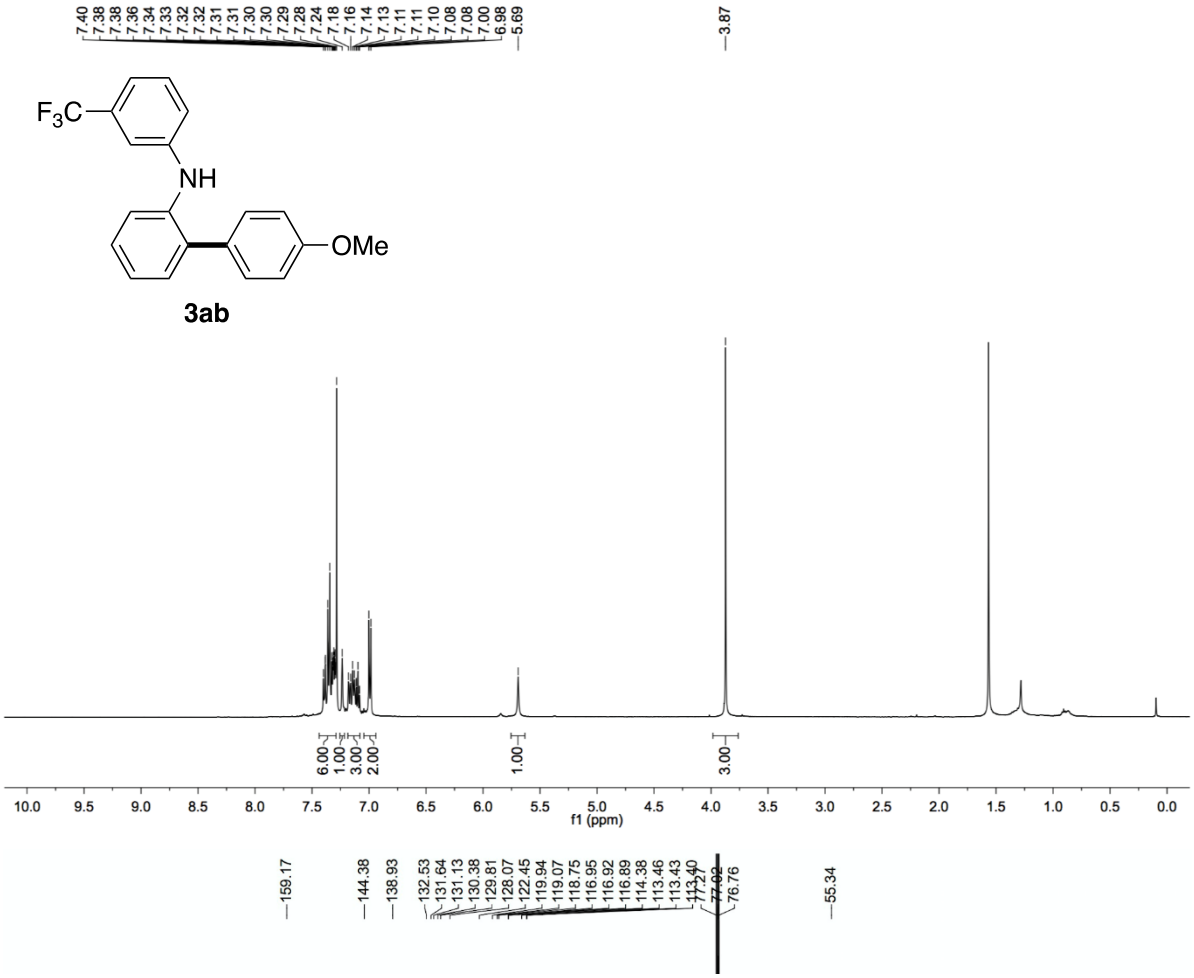

Figure S60. ^{13}C NMR spectrum of **3ab**, related to **Figure 3**

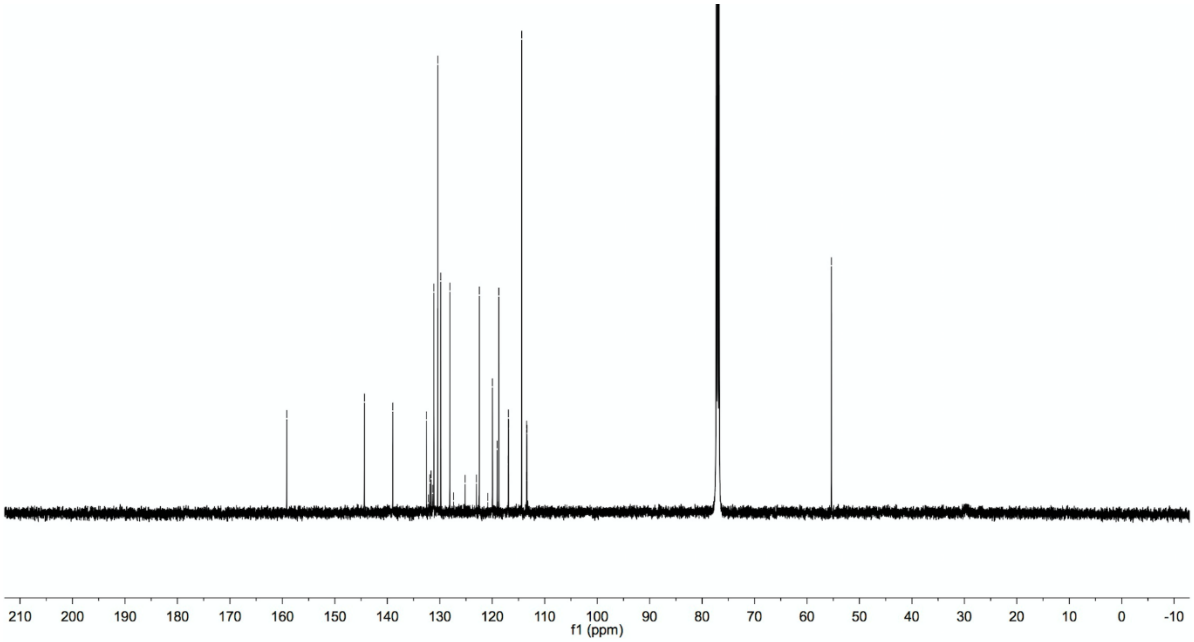

Figure S61. ^{19}F NMR spectrum of **3ab**, related to **Figure 3**

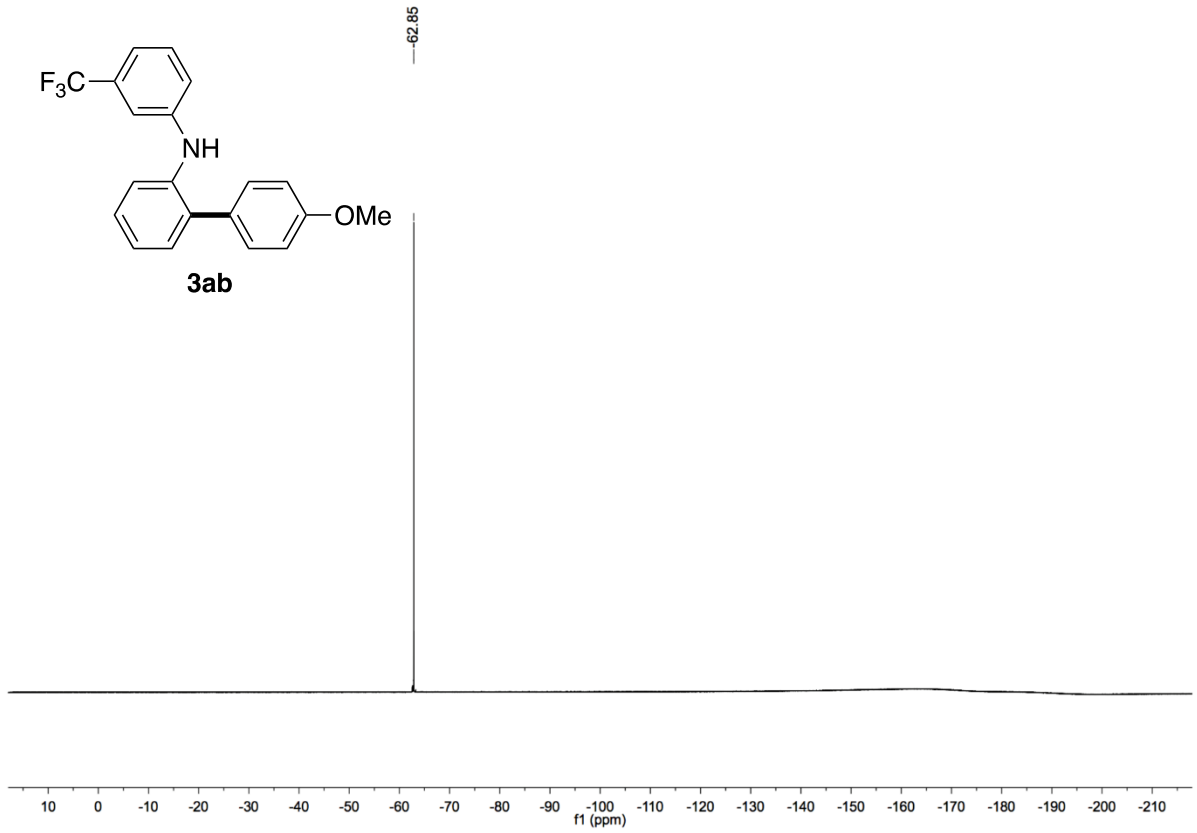

Figure S62. [1]H NMR spectrum of **3ac**, related to **Figure 3**

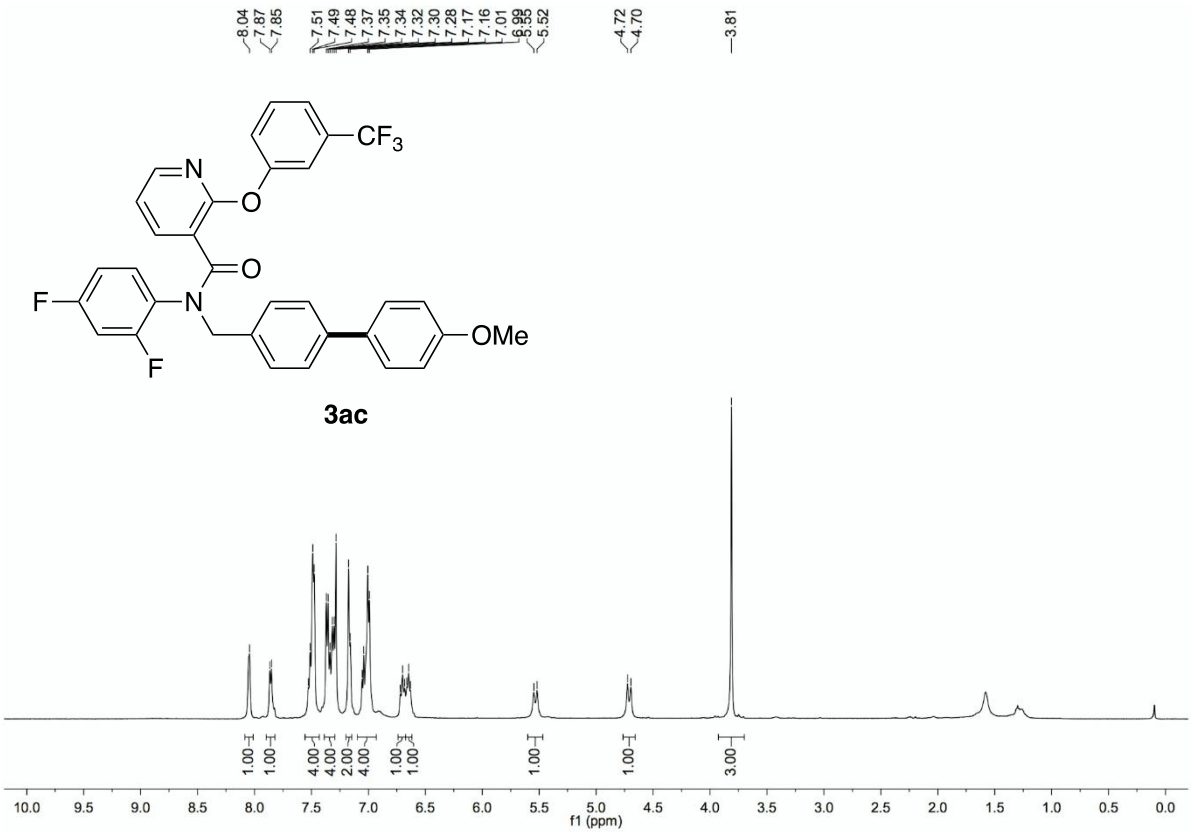

Figure S63. [13]C NMR spectrum of **3ac**, related to **Figure 3**

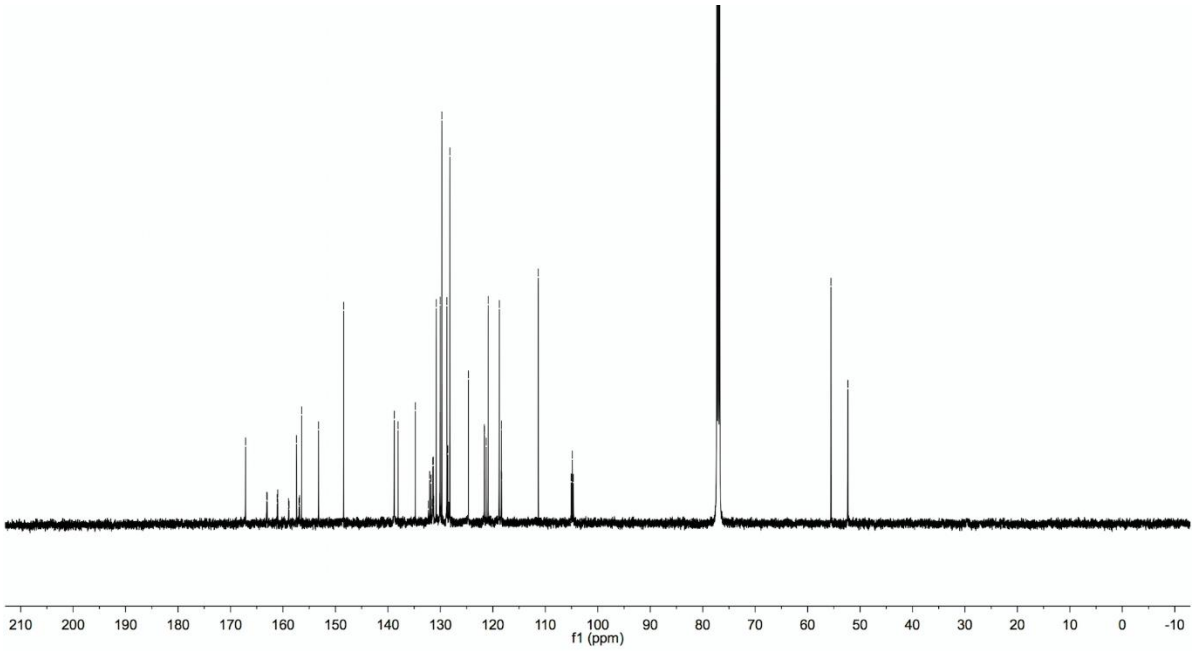

Figure S64. ^{19}F NMR spectrum of **3ac**, related to **Figure 3**

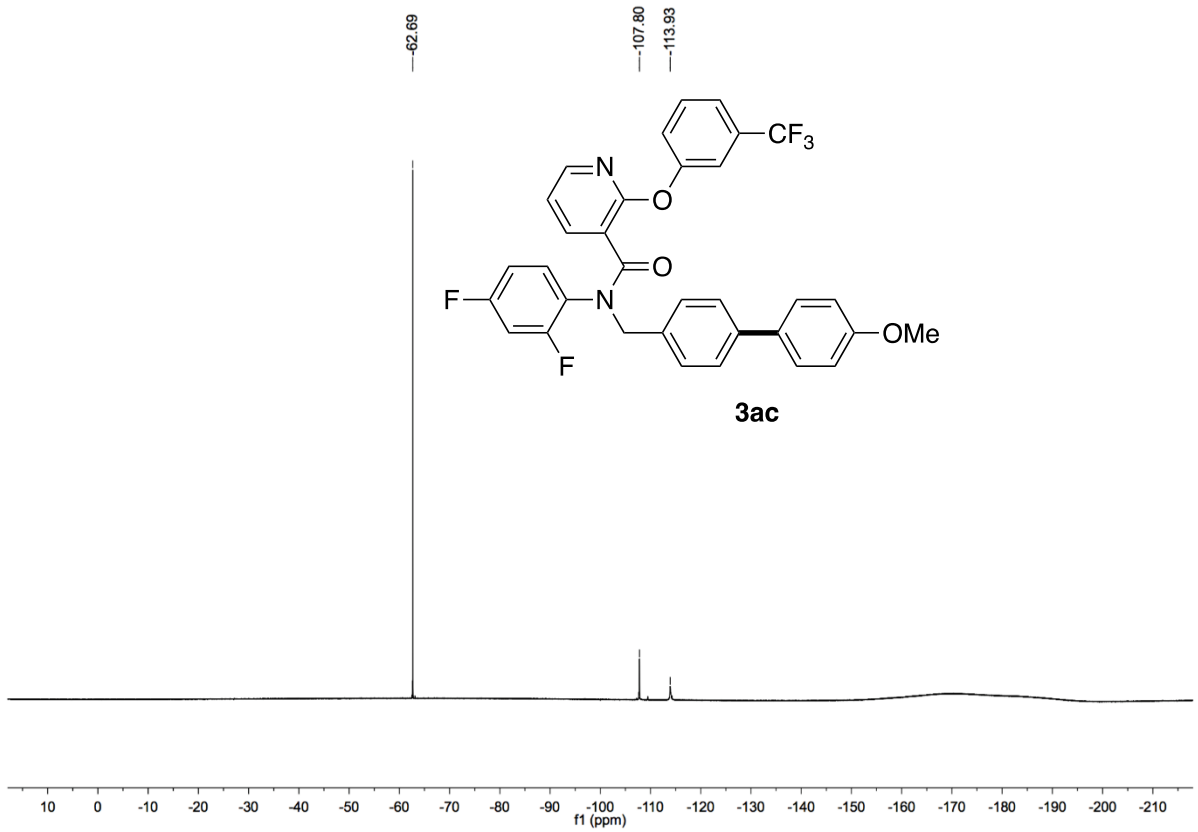

Figure S65. ^{1}H NMR spectrum of **3ad**, related to **Figure 3**

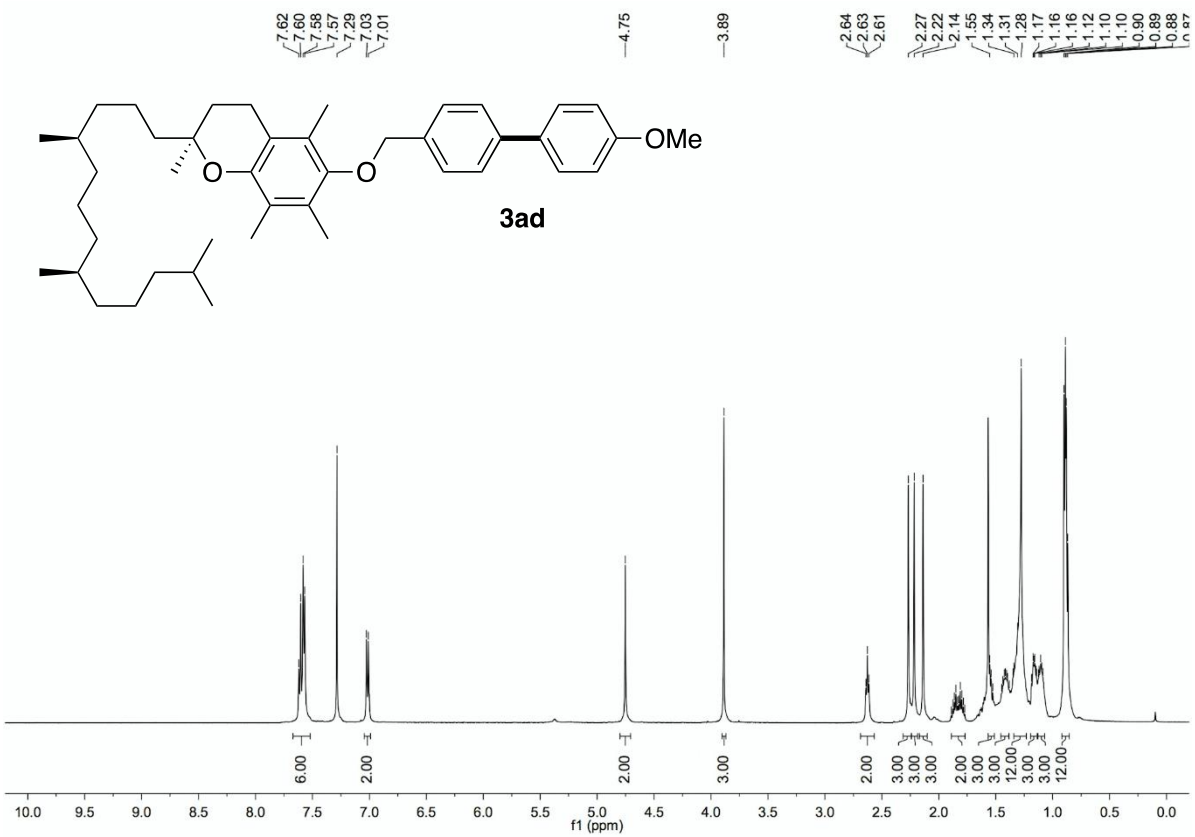

Figure S66. ^{13}C NMR spectrum of **3ad**, related to **Figure 3**

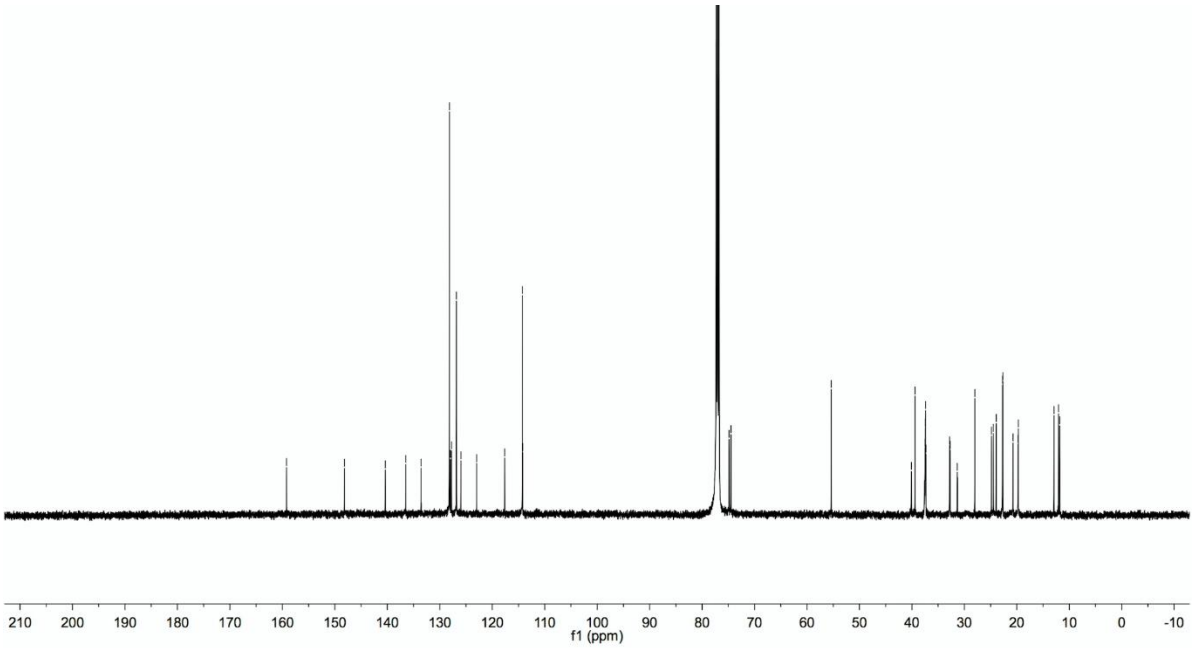

Figure S67. ^{1}H NMR spectrum of **3ae**, related to **Figure 3**

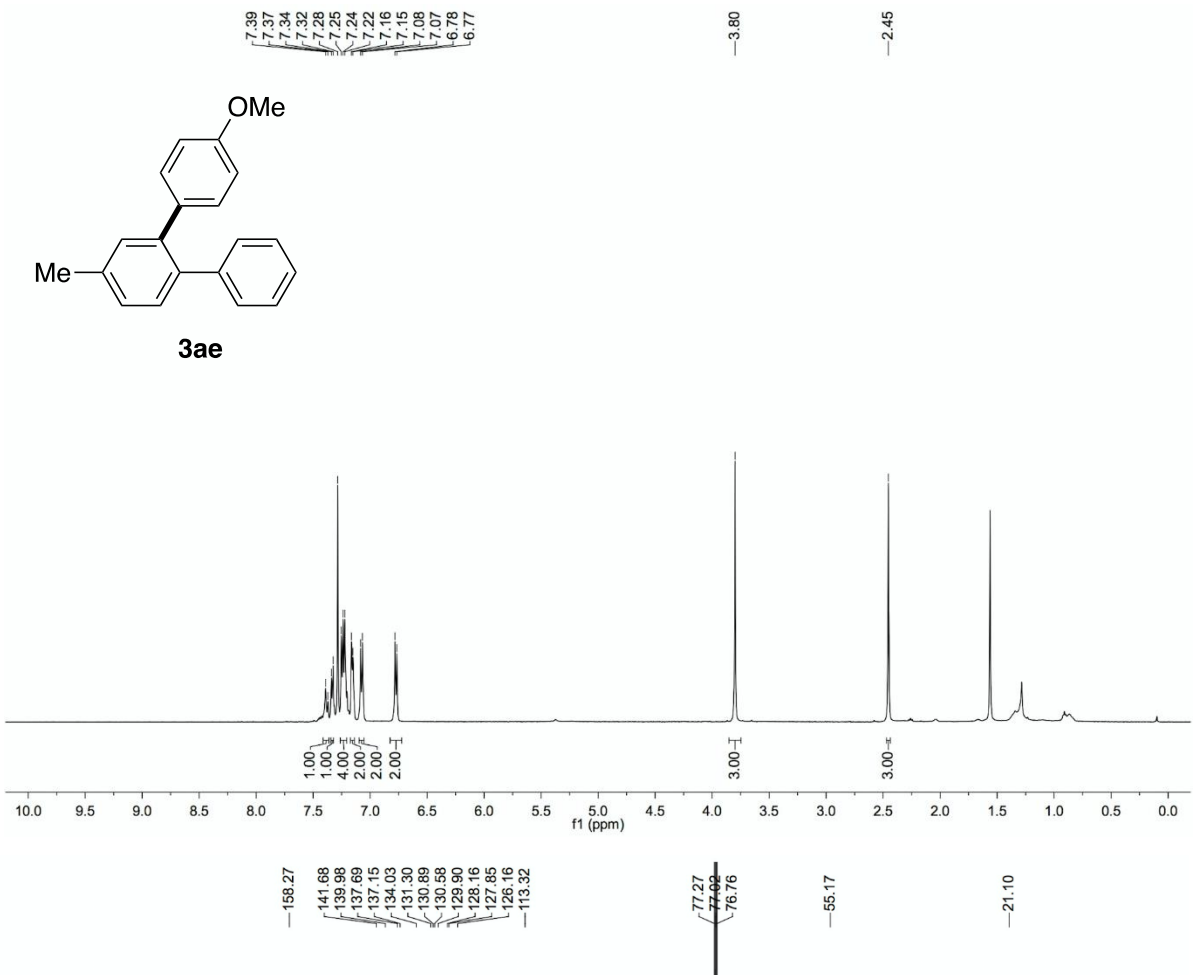

Figure S68. ^{13}C NMR spectrum of **3ae**, related to **Figure 3**

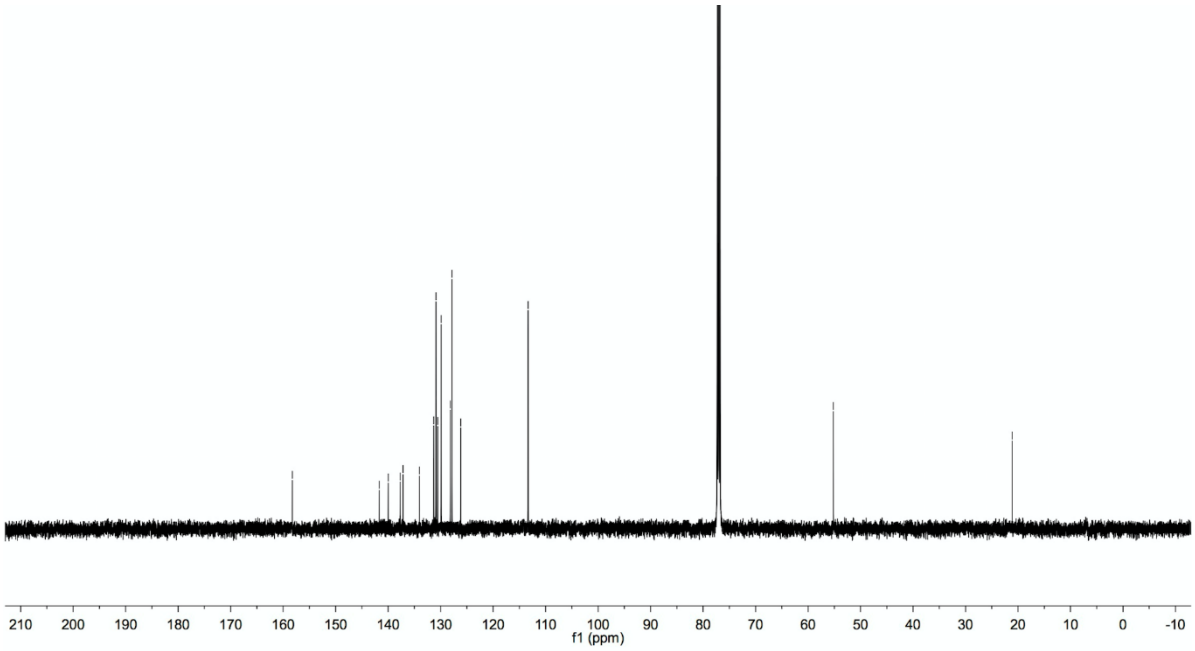

Figure S69. ^{1}H NMR spectrum of **3af**, related to **Figure 3**

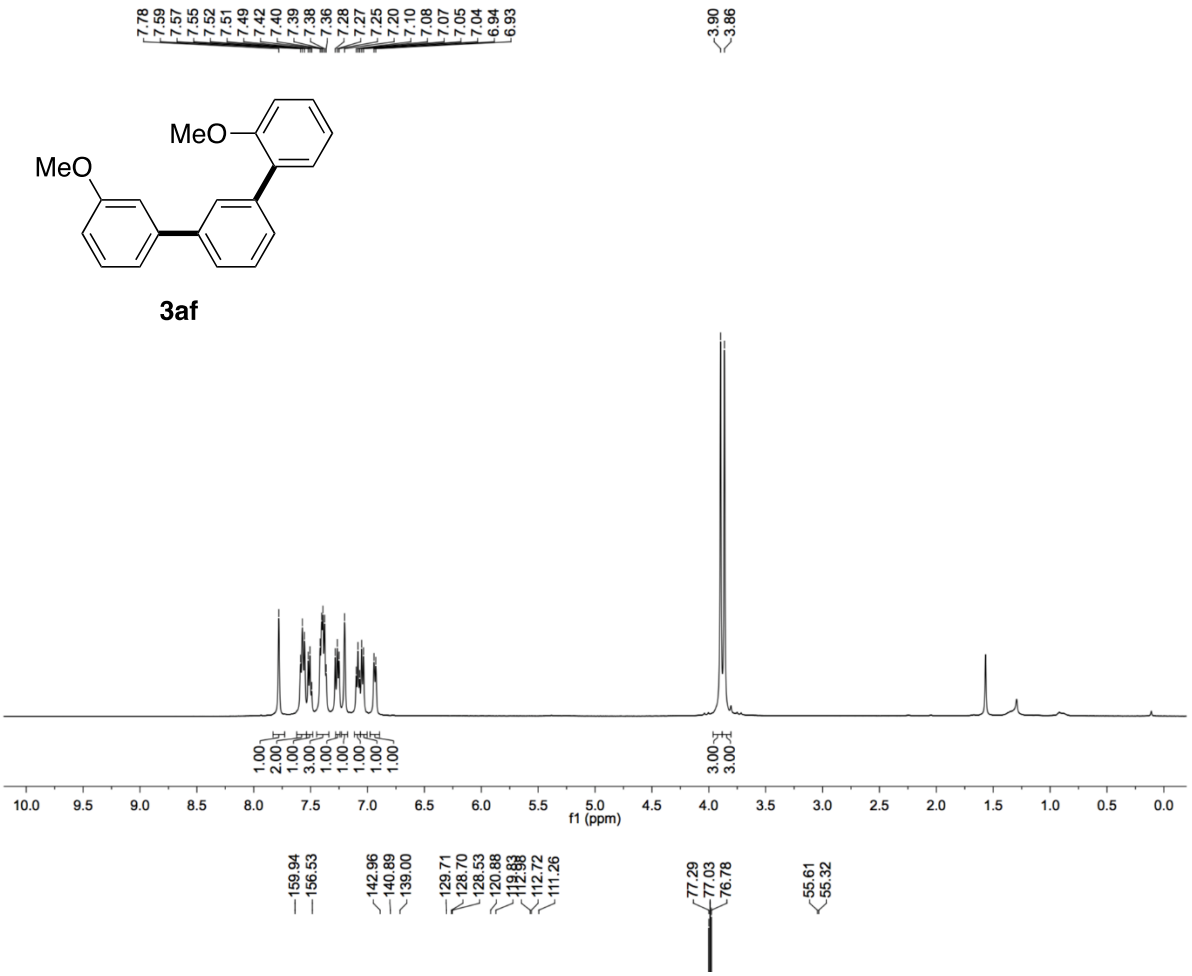

Figure S70. ^{13}C NMR spectrum of **3af**, related to **Figure 3**

Figure S71. [1]H NMR spectrum of **3ag**, related to **Figure 3**

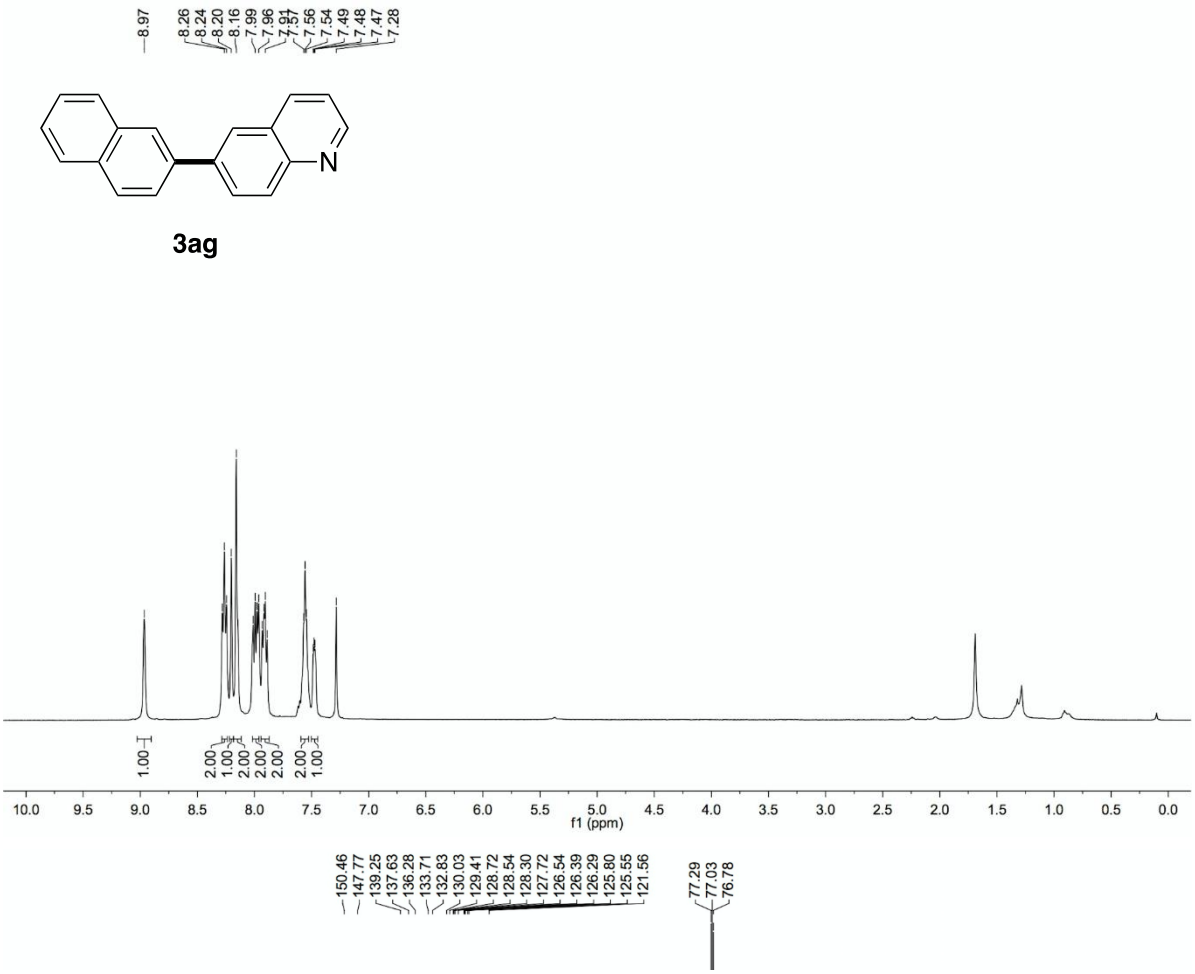

Figure S72. [13]C NMR spectrum of **3ag**, related to **Figure 3**

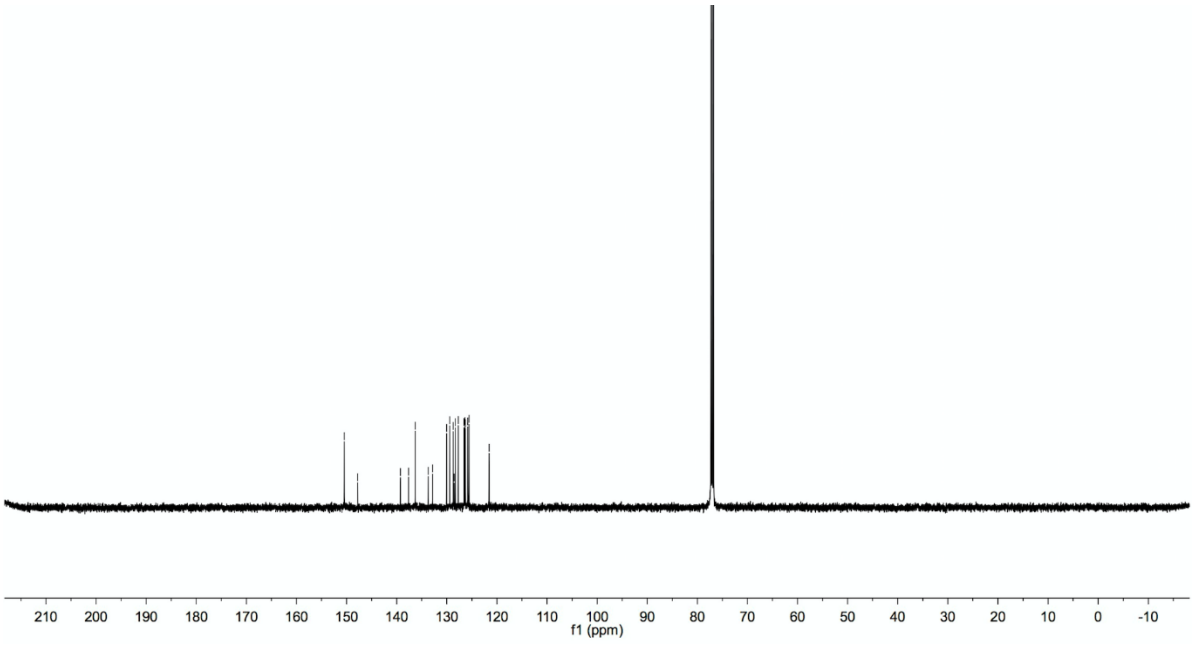

Figure S73. ^{1}H NMR spectrum of **3ah**, related to **Figure 3**

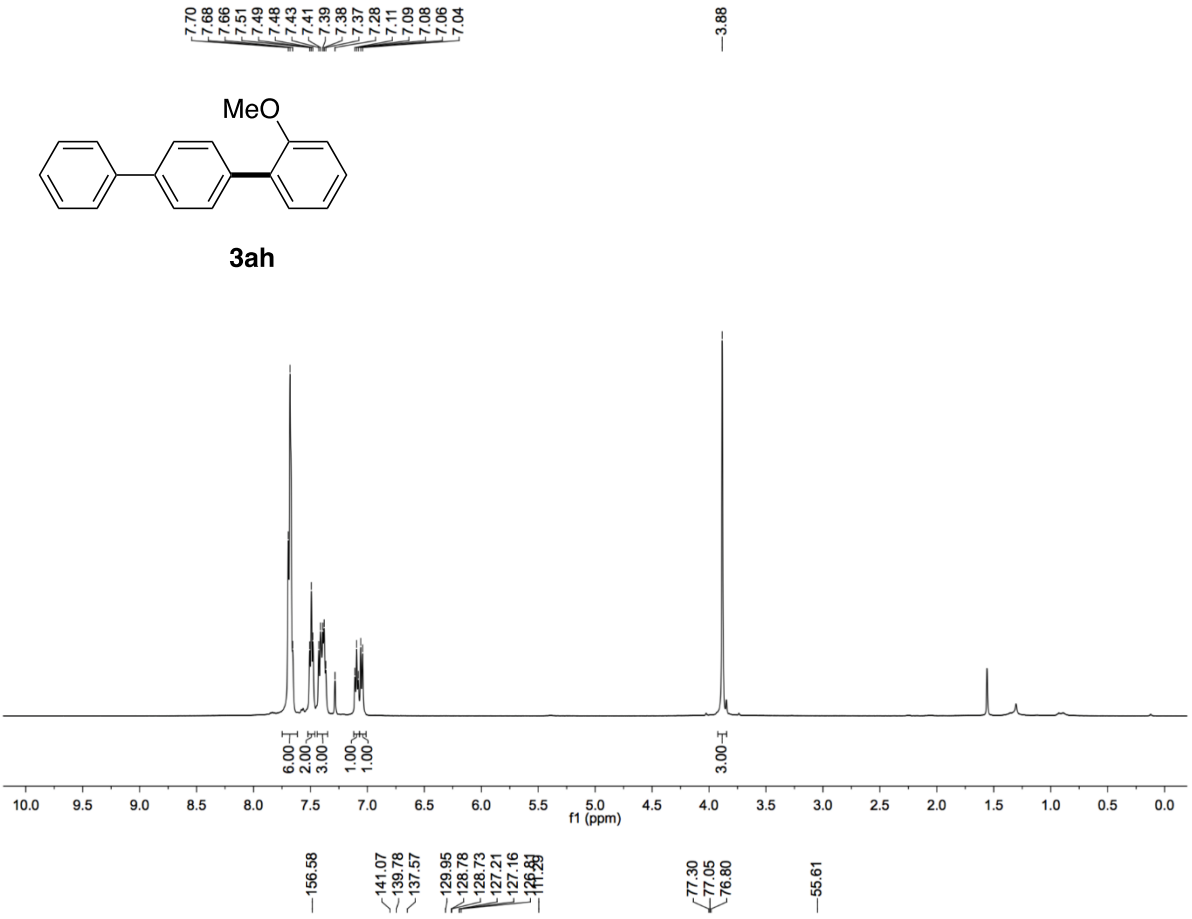

Figure S74. ^{13}C NMR spectrum of **3ah**, related to **Figure 3**

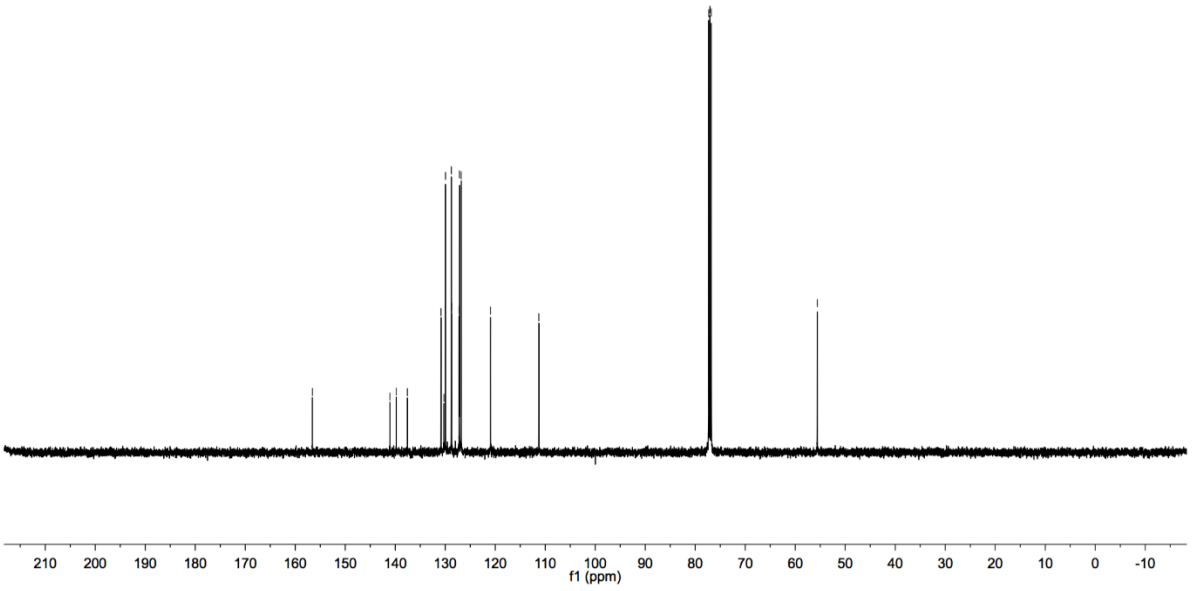

Figure S75. ^{1}H NMR spectrum of **3ai**, related to **Figure 4**

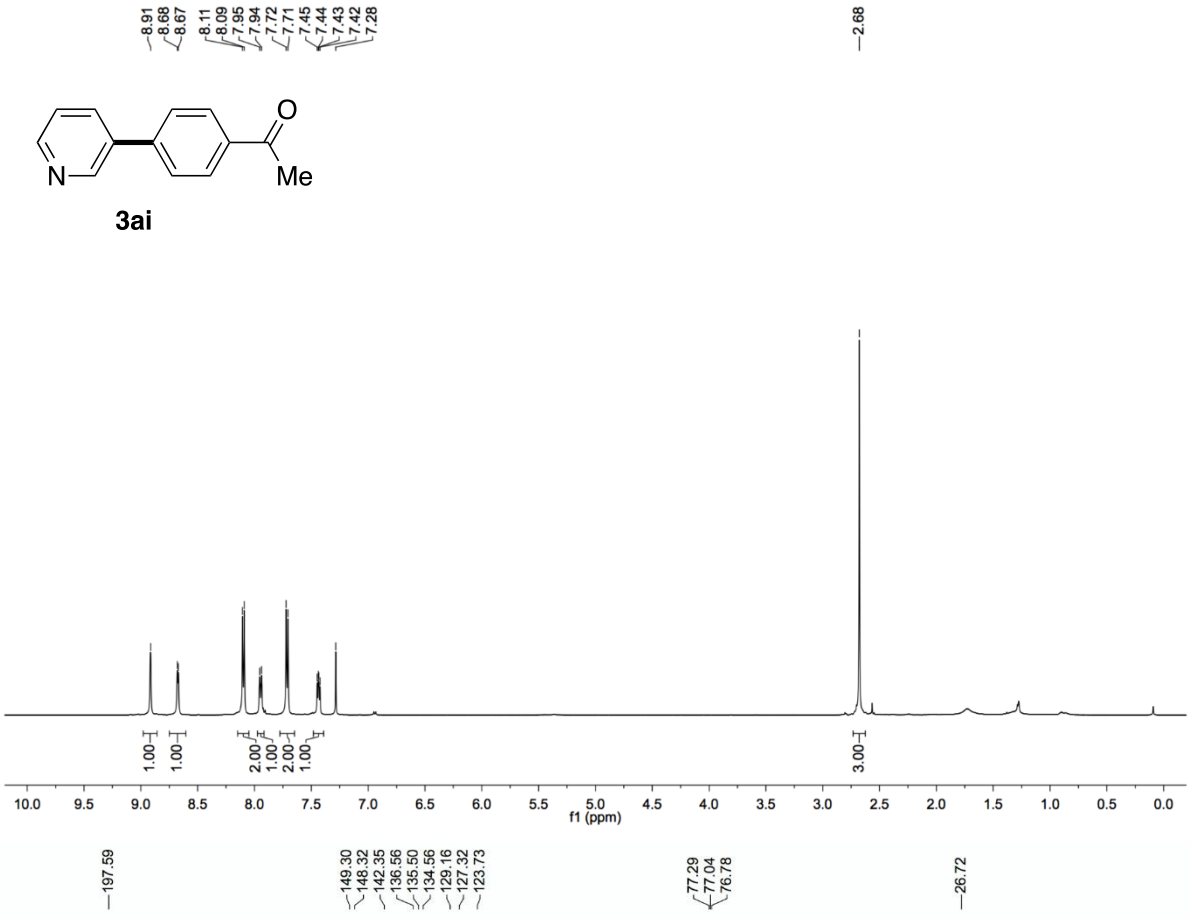

Figure S76. ^{13}C NMR spectrum of **3ai**, related to **Figure 4**

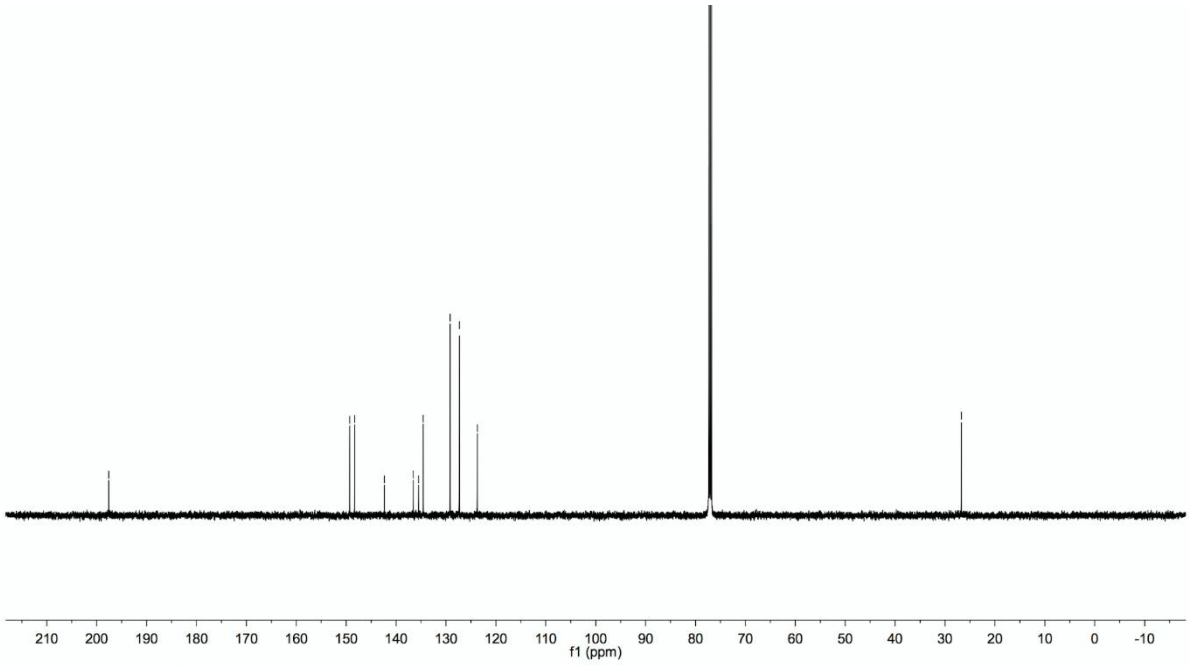

Figure S77. ^{1}H NMR spectrum of **3aj**, related to **Figure 4**

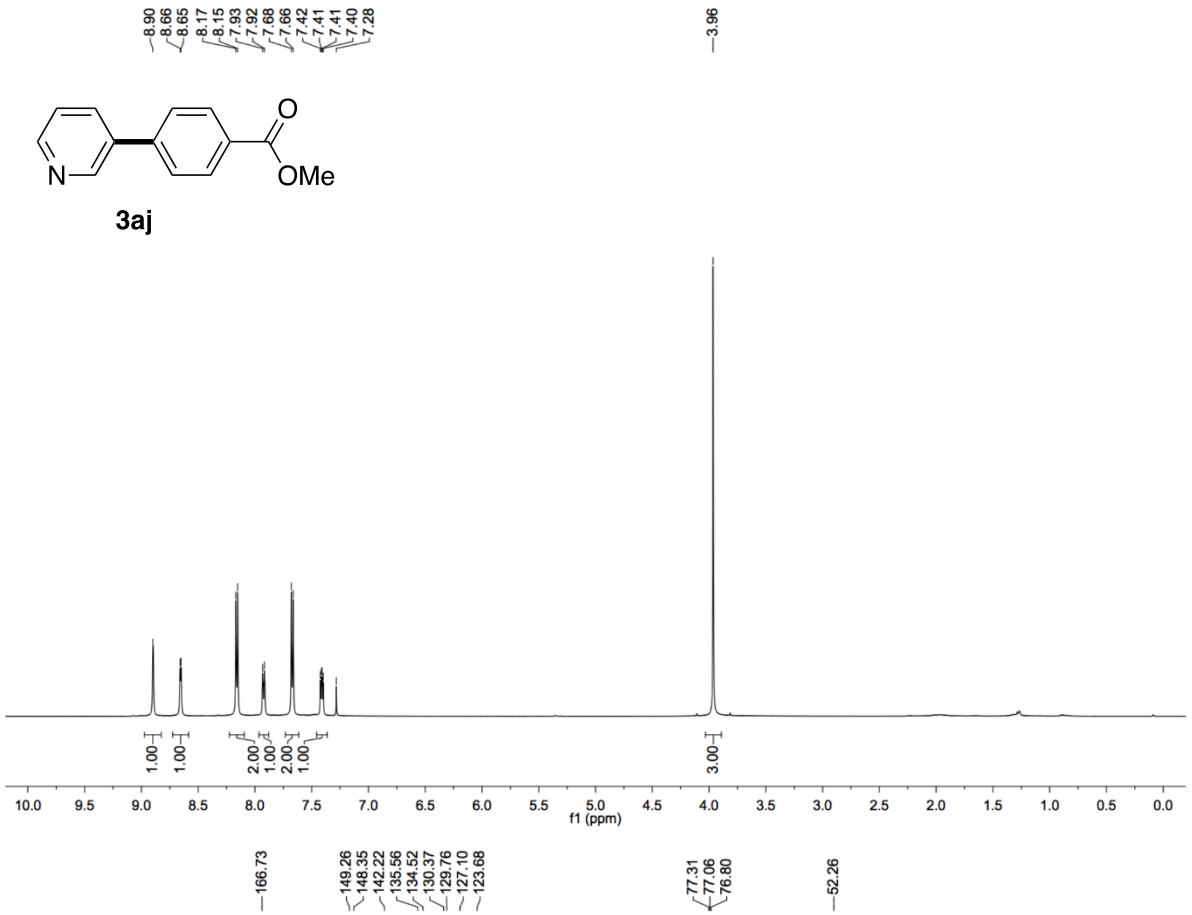

Figure S78. ^{13}C NMR spectrum of **3aj**, related to **Figure 4**

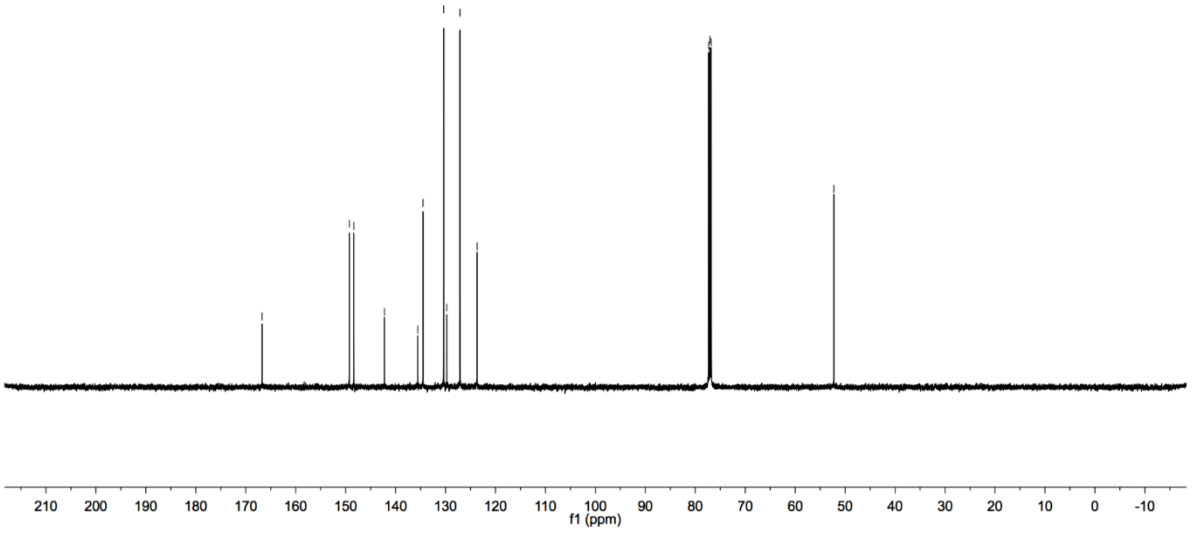

Figure S79. ^{1}H NMR spectrum of **3ak**, related to **Figure 4**

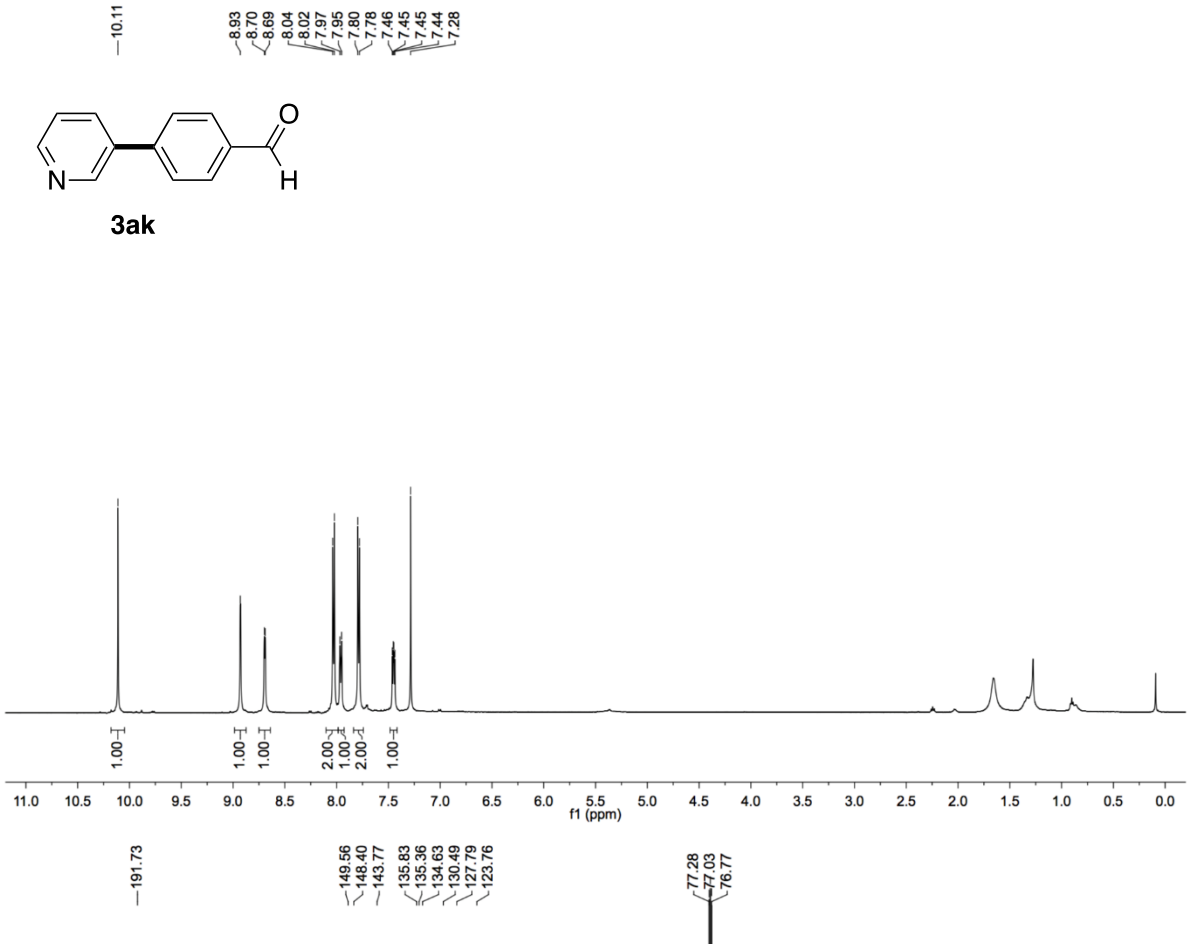

Figure S80. ^{13}C NMR spectrum of **3ak**, related to **Figure 4**

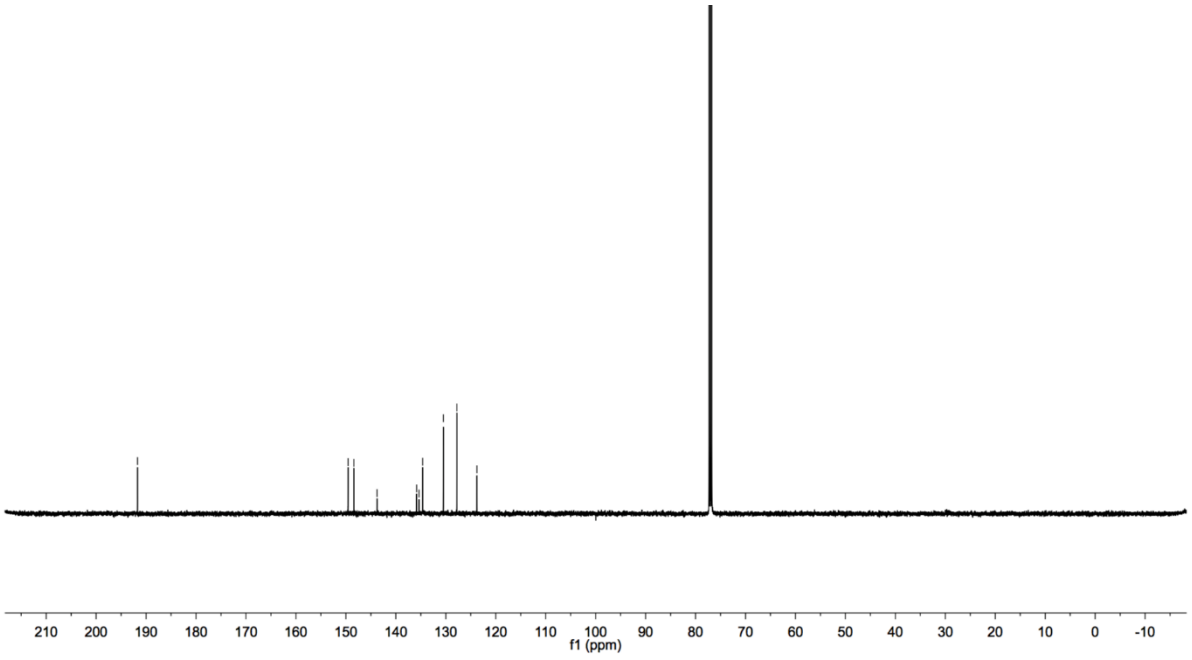

Figure S81. ^{1}H NMR spectrum of **3al**, related to **Figure 4**

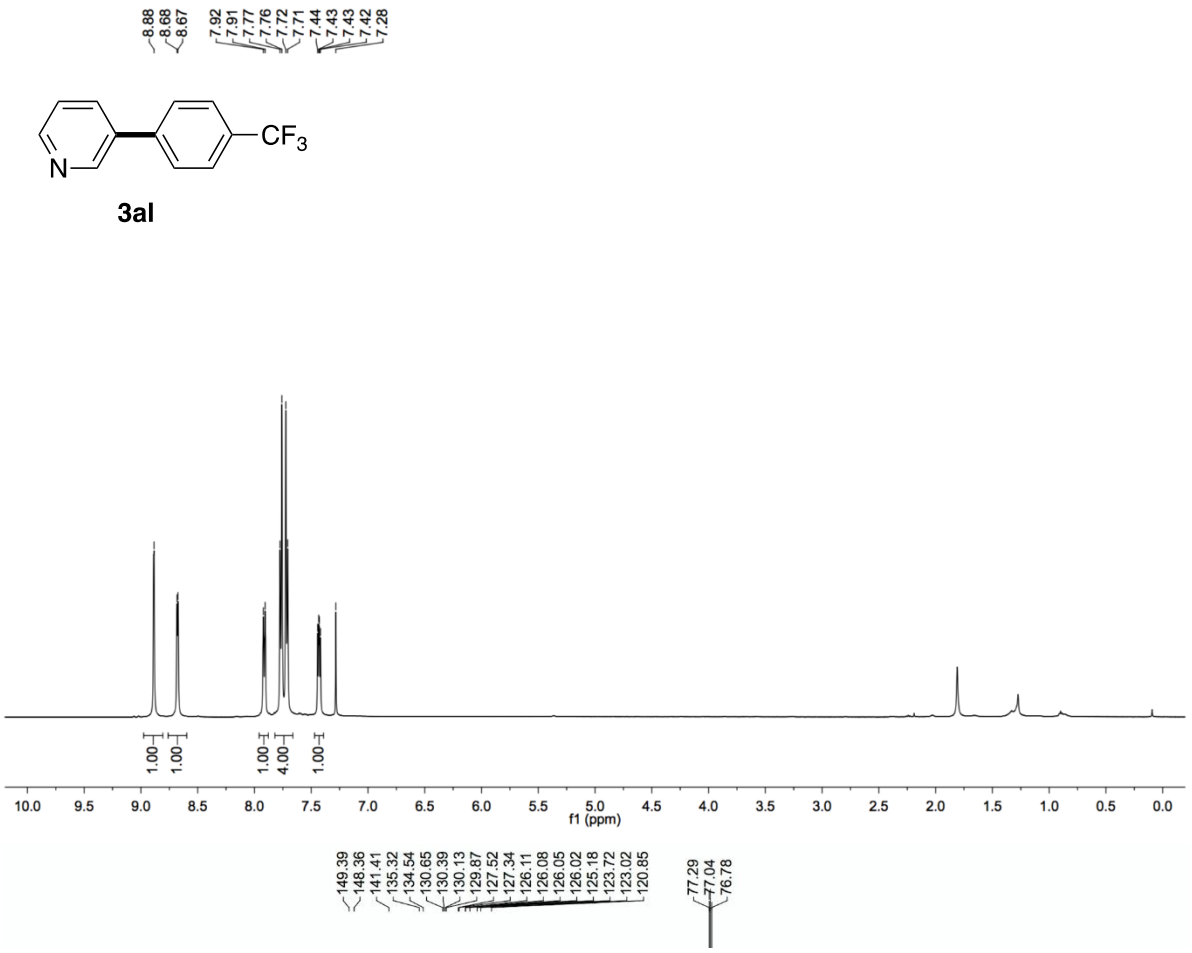

Figure S82. ^{13}C NMR spectrum of **3al**, related to **Figure 4**

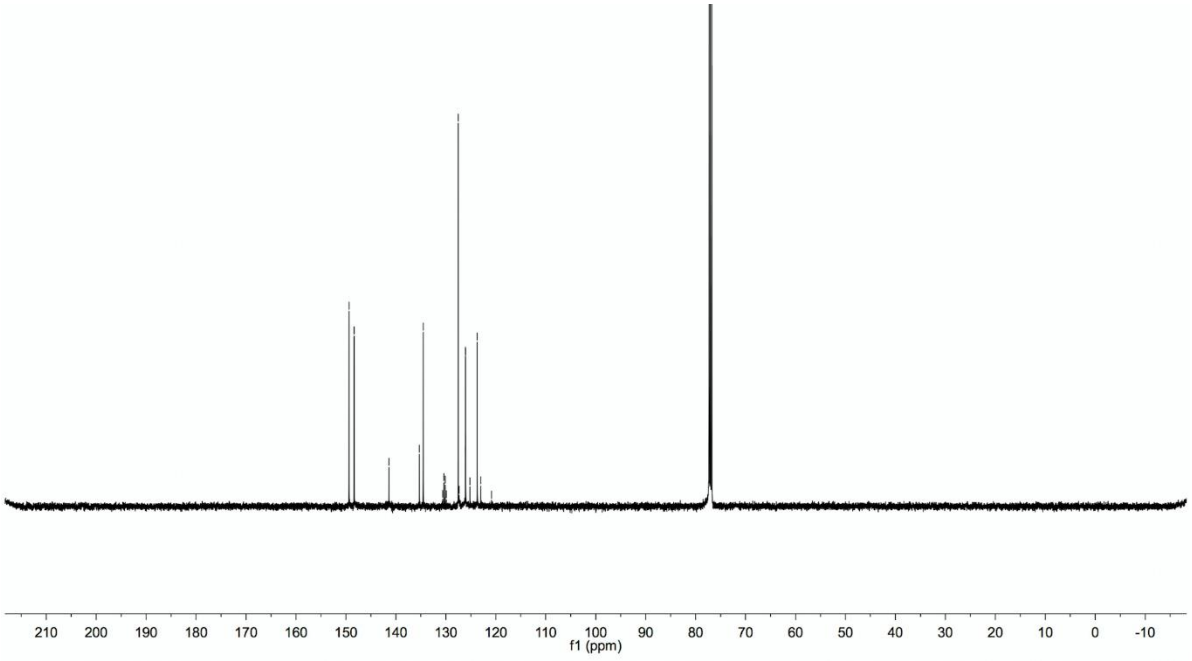

Figure S83. ^{19}F NMR spectrum of **3al**, related to **Figure 4**

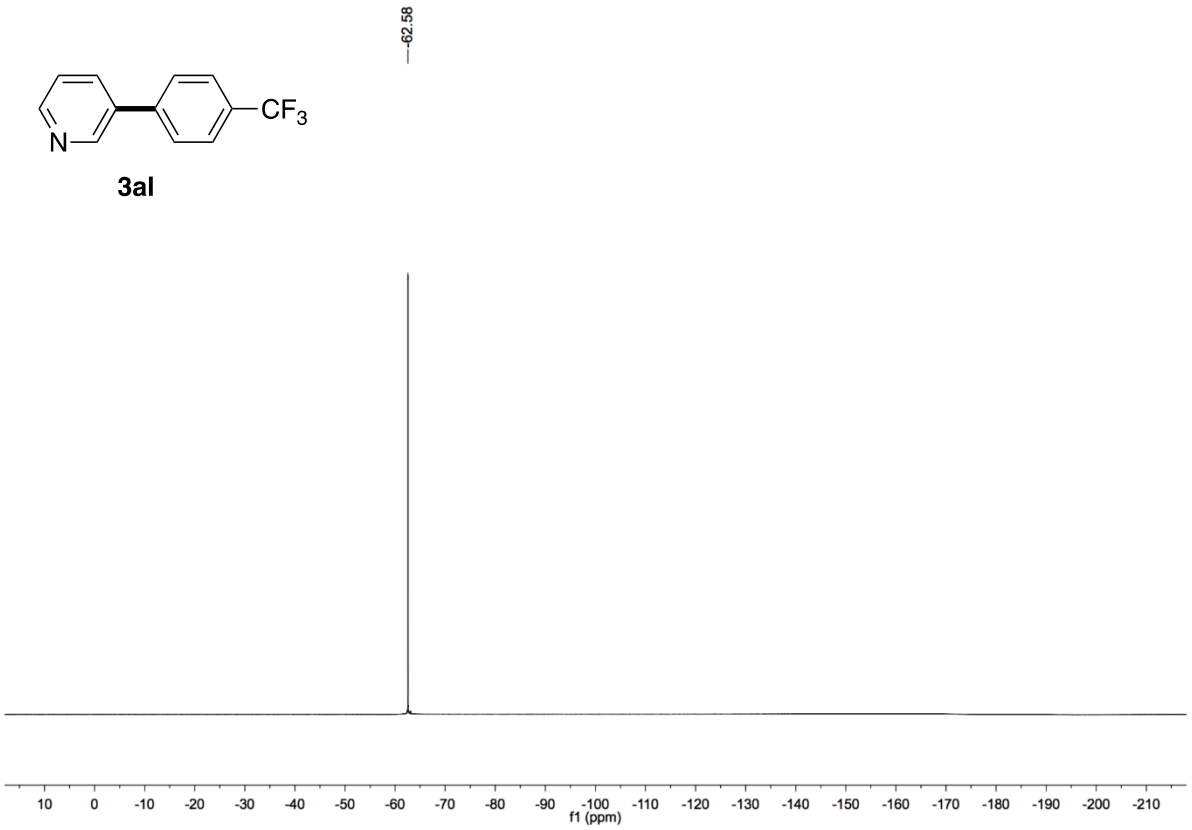

Figure S84. ^{1}H NMR spectrum of **3am**, related to **Figure 4**

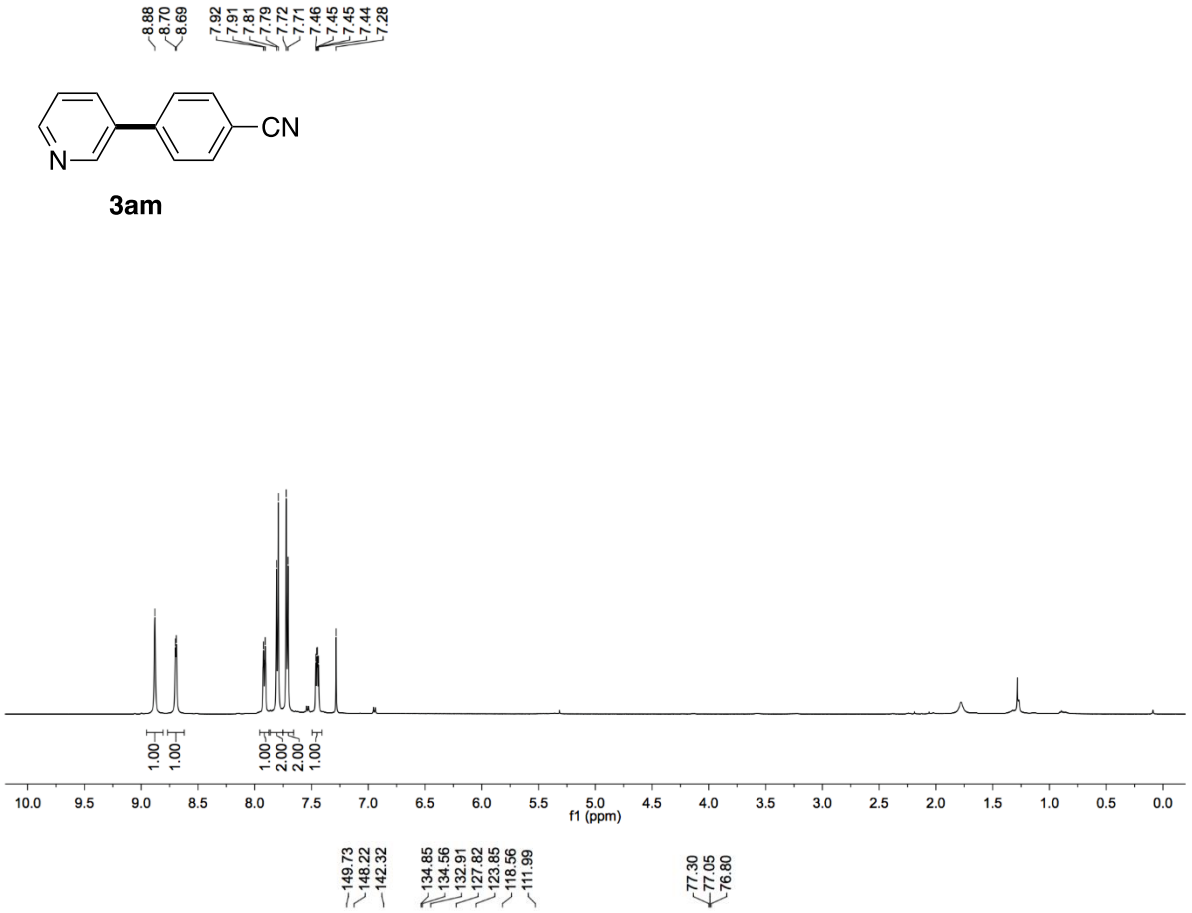

Figure S85. ^{13}C NMR spectrum of **3am**, related to **Figure 4**

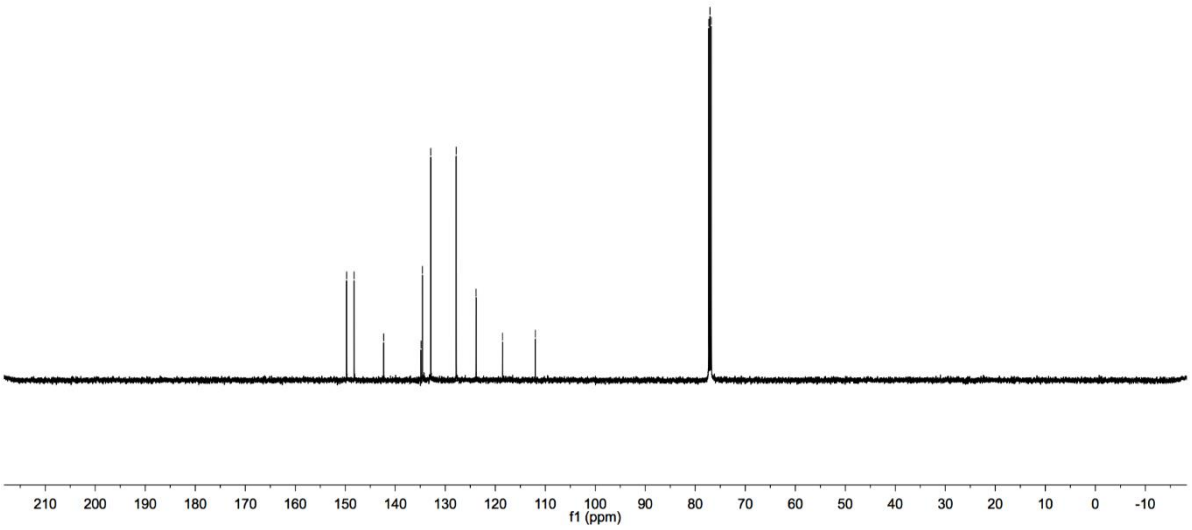

Figure S86. ^{1}H NMR spectrum of **3an**, related to **Figure 4**

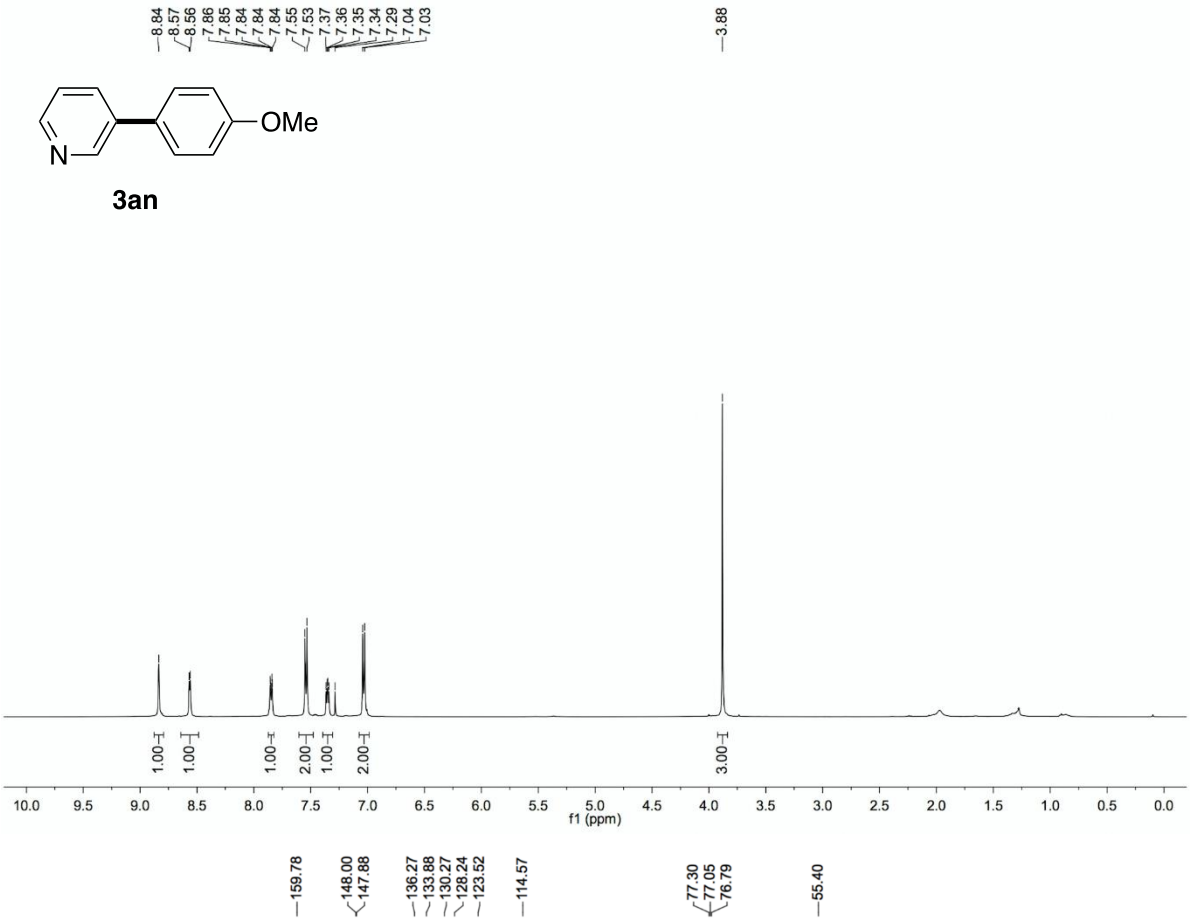

Figure S87. ^{13}C NMR spectrum of **3an**, related to **Figure 4**

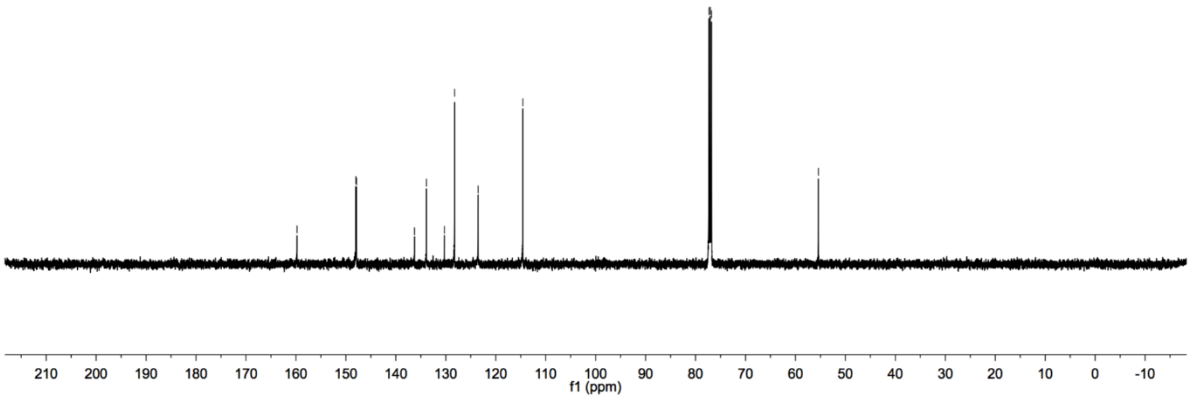

Figure S88. ^{1}H NMR spectrum of **3ao**, related to **Figure 4**

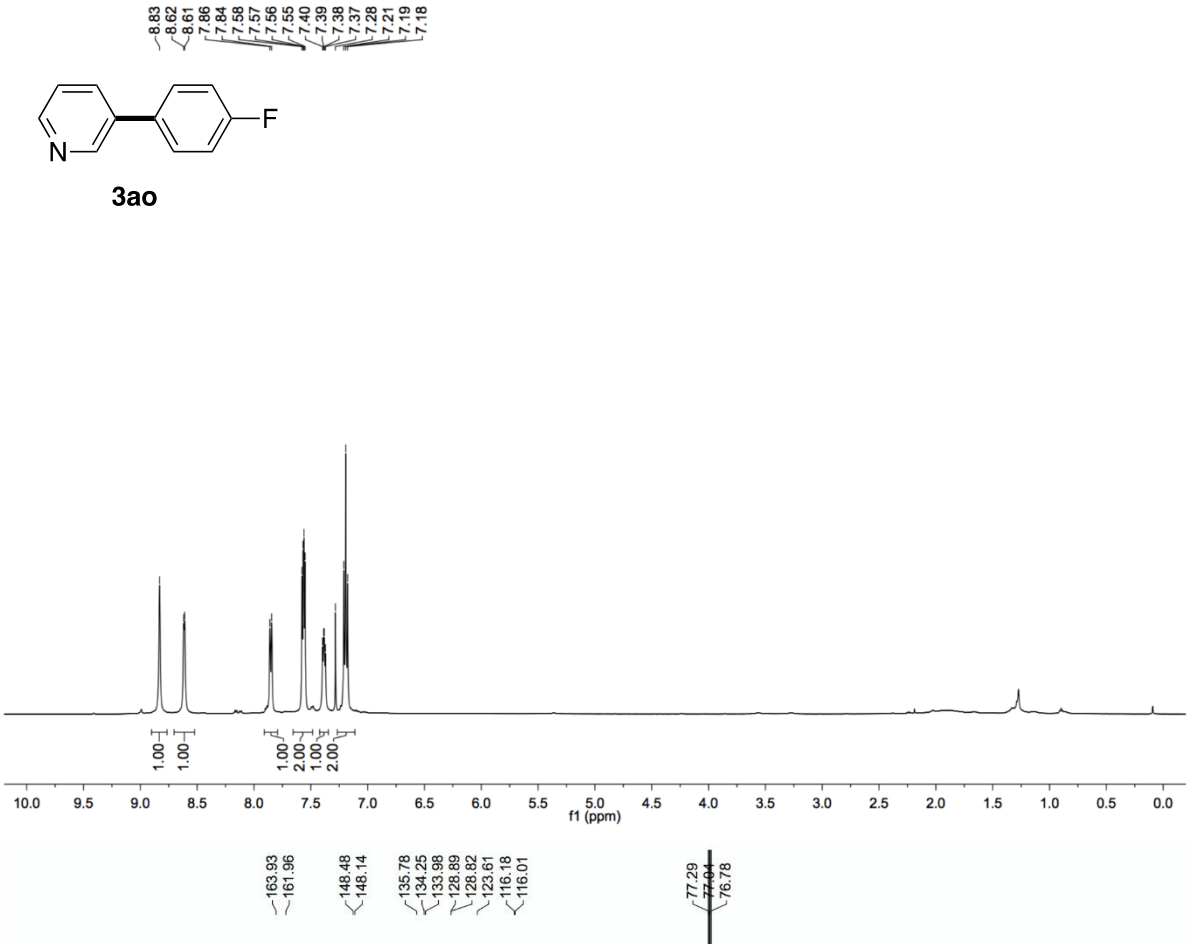

Figure S89. ^{13}C NMR spectrum of **3ao**, related to **Figure 4**

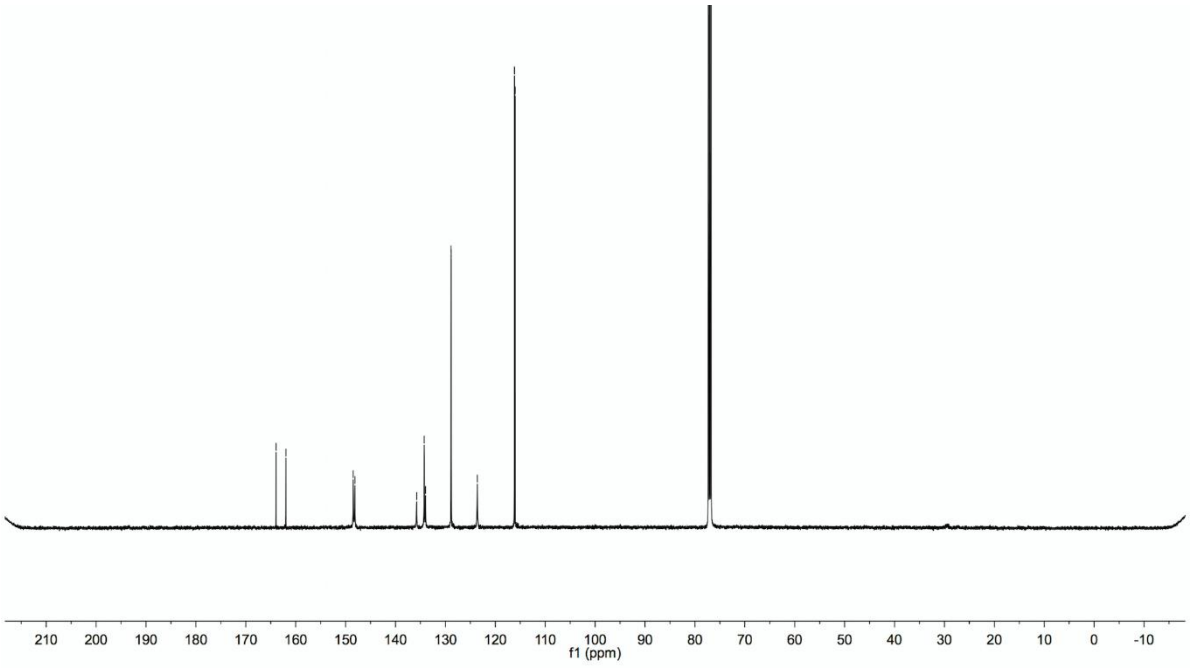

Figure S90. ^{19}F NMR spectrum of **3ao**, related to **Figure 4**

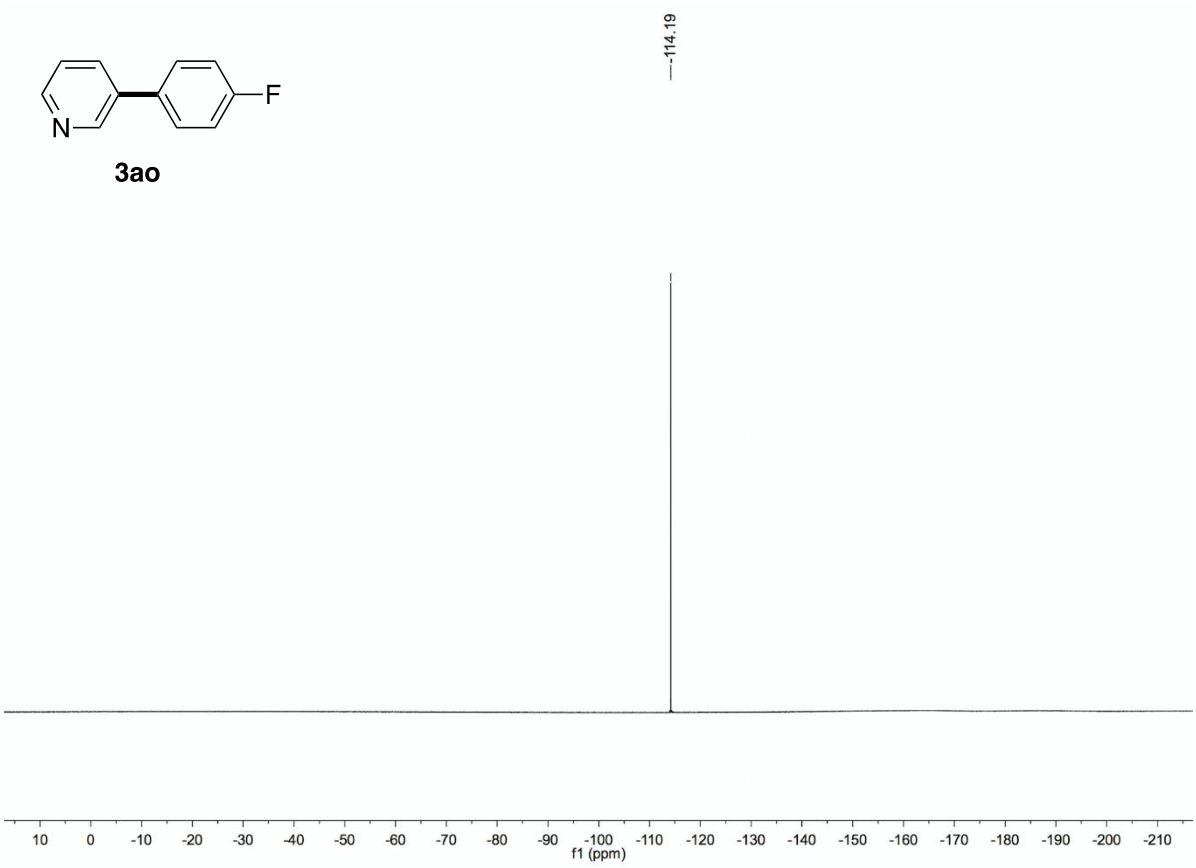

Figure S91. ^{1}H NMR spectrum of **3ap**, related to **Figure 4**

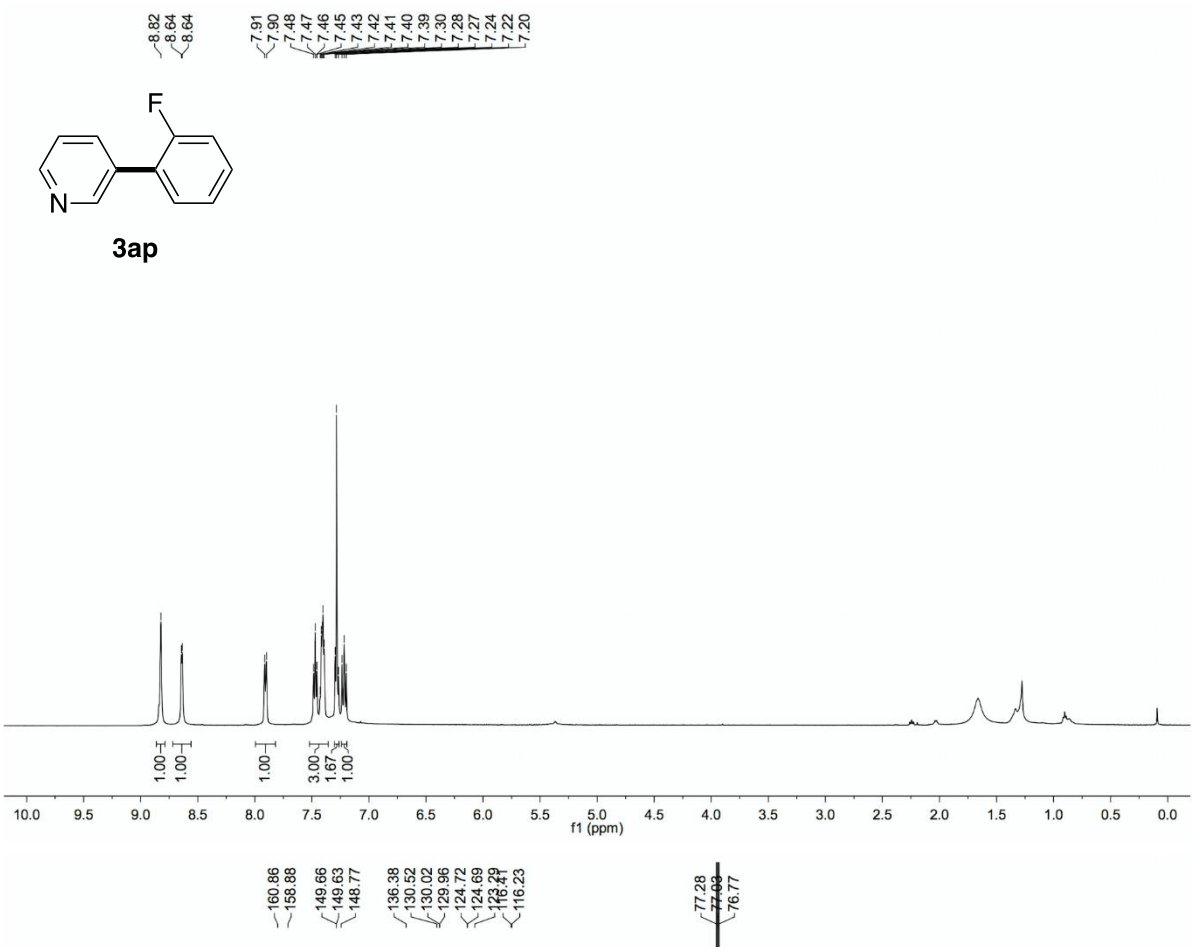

Figure S92. ^{13}C NMR spectrum of **3ap**, related to **Figure 4**

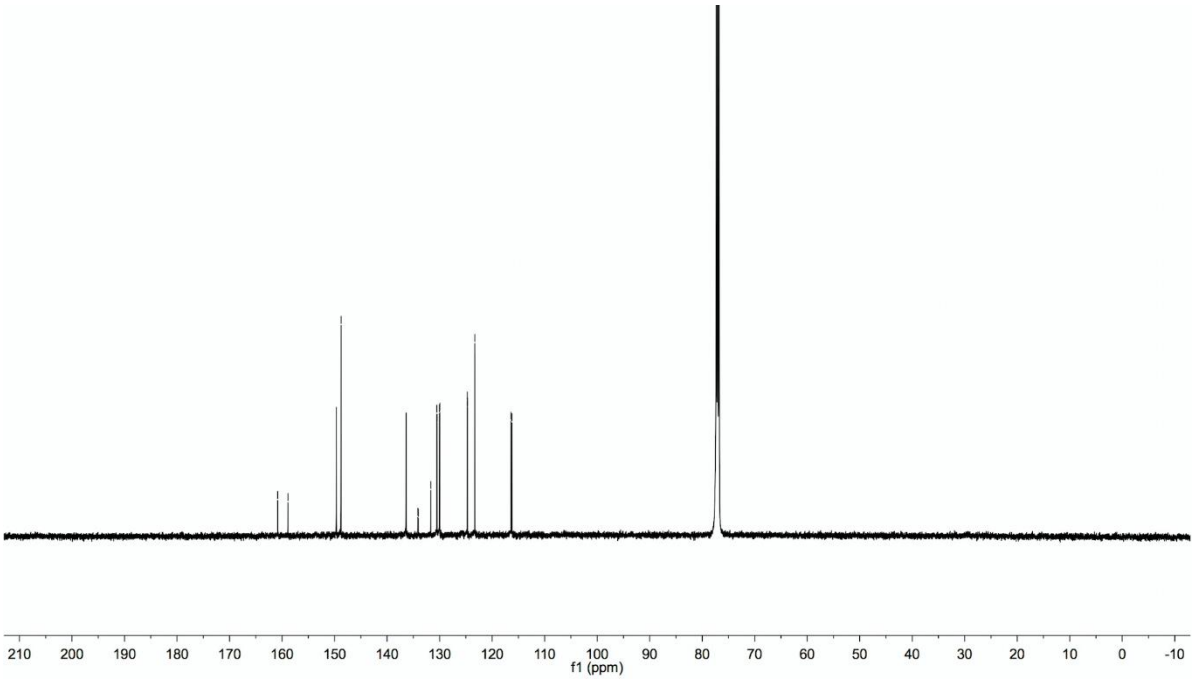

Figure S93. ^{19}F NMR spectrum of **3ap**, related to **Figure 4**

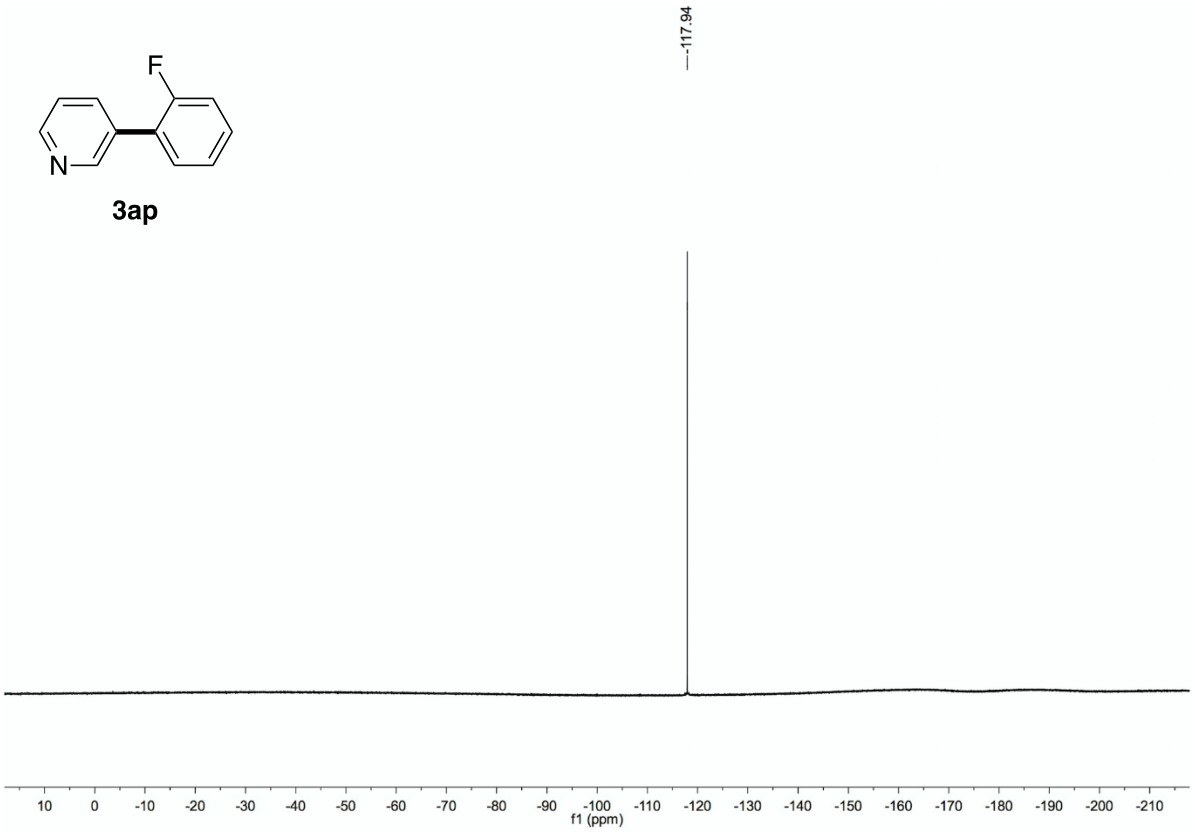

Figure S94. ^{1}H NMR spectrum of **3aq**, related to **Figure 4**

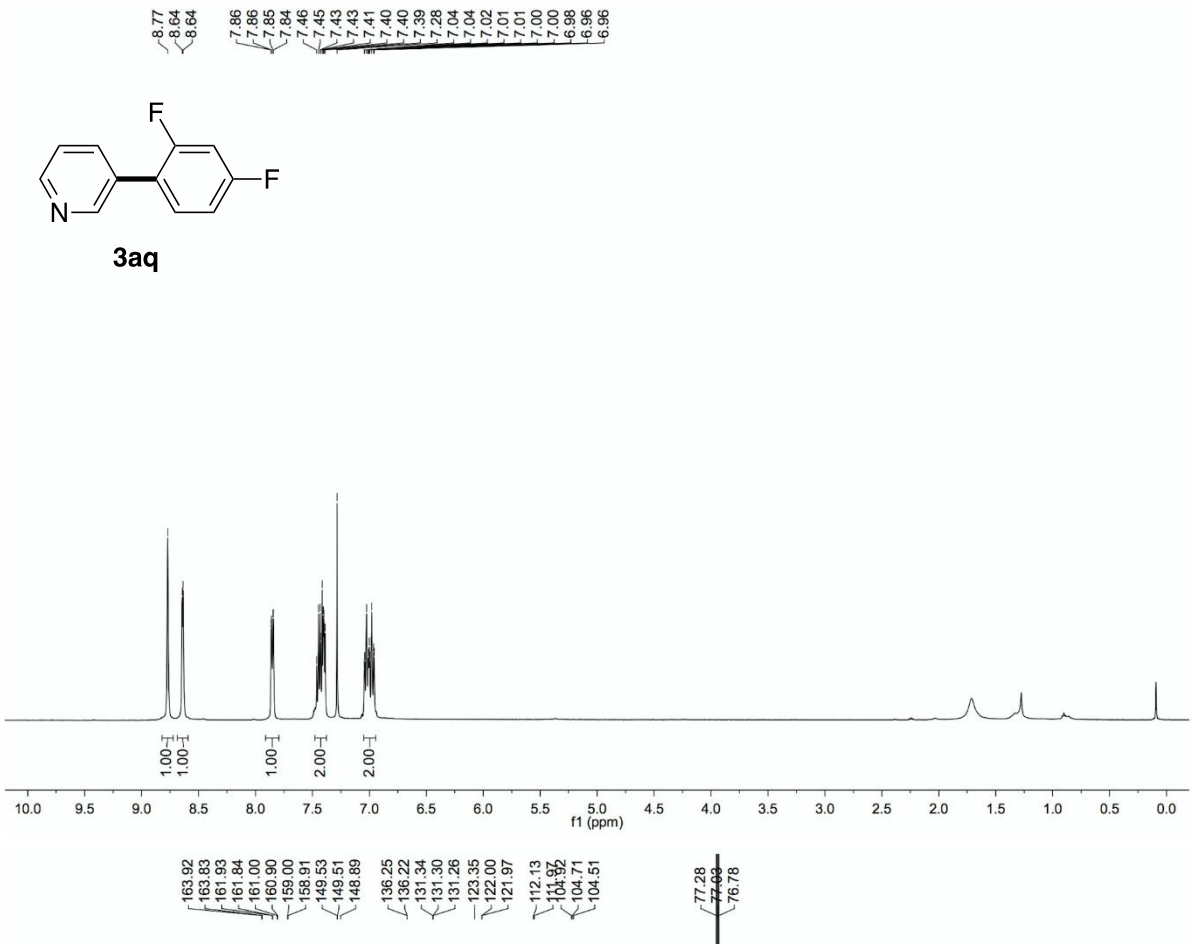

Figure S95. ^{13}C NMR spectrum of **3aq**, related to **Figure 4**

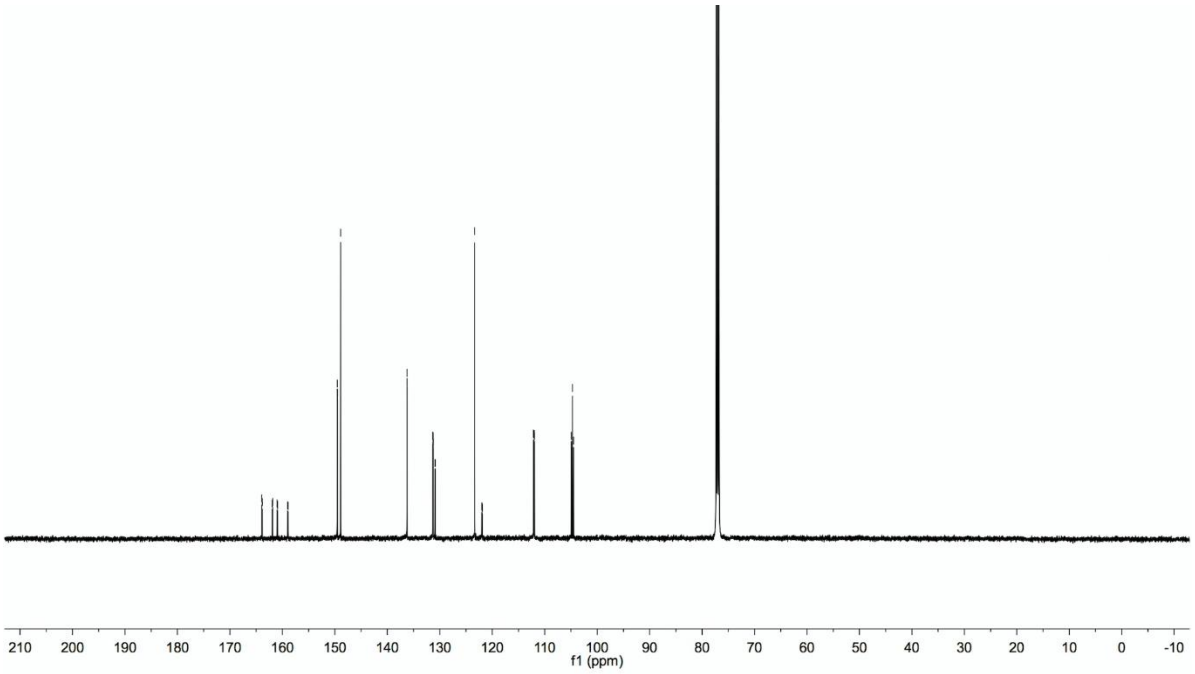

Figure S96. ^{19}F NMR spectrum of **3aq**, related to **Figure 4**

Figure S97. ^{1}H NMR spectrum of **3ar**, related to **Figure 4**

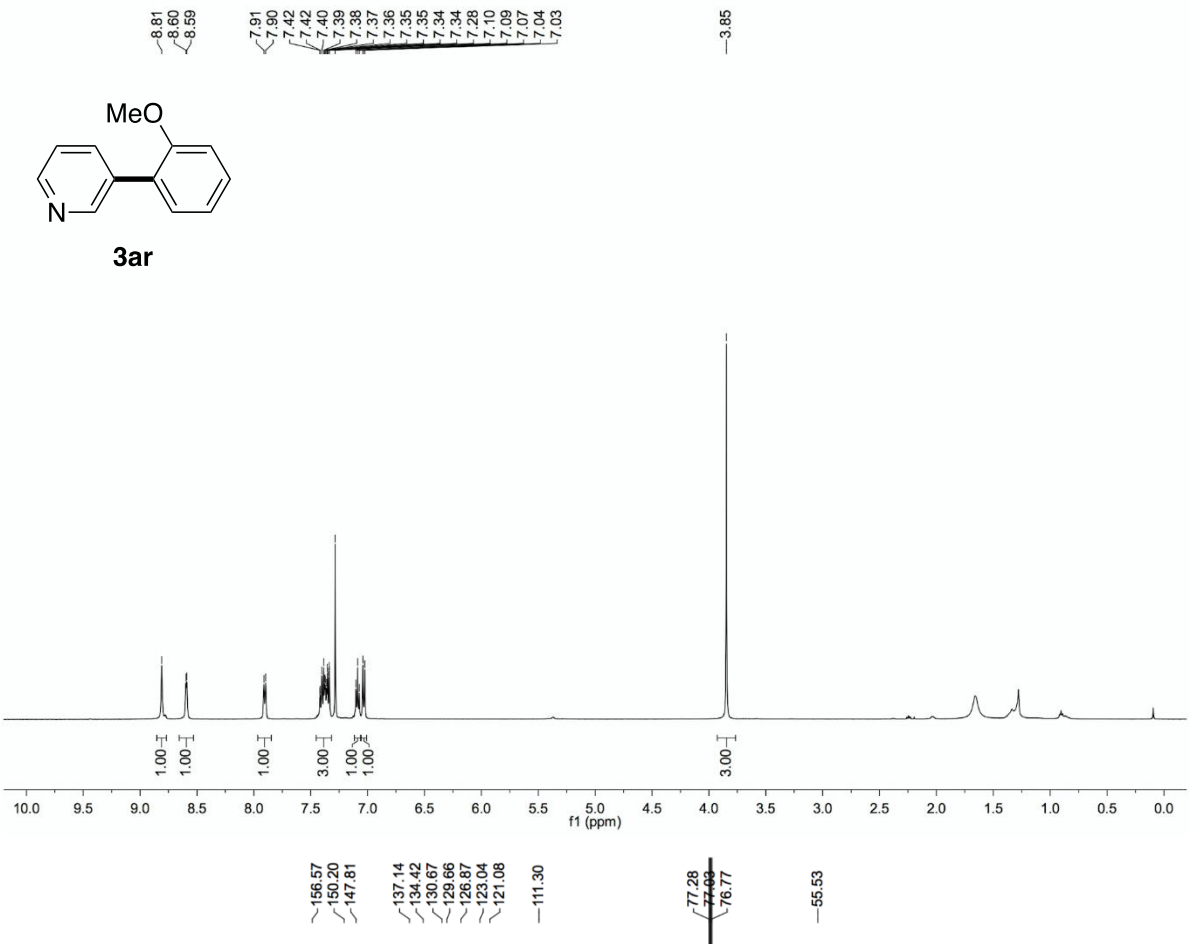

Figure S98. ^{13}C NMR spectrum of **3ar**, related to **Figure 4**

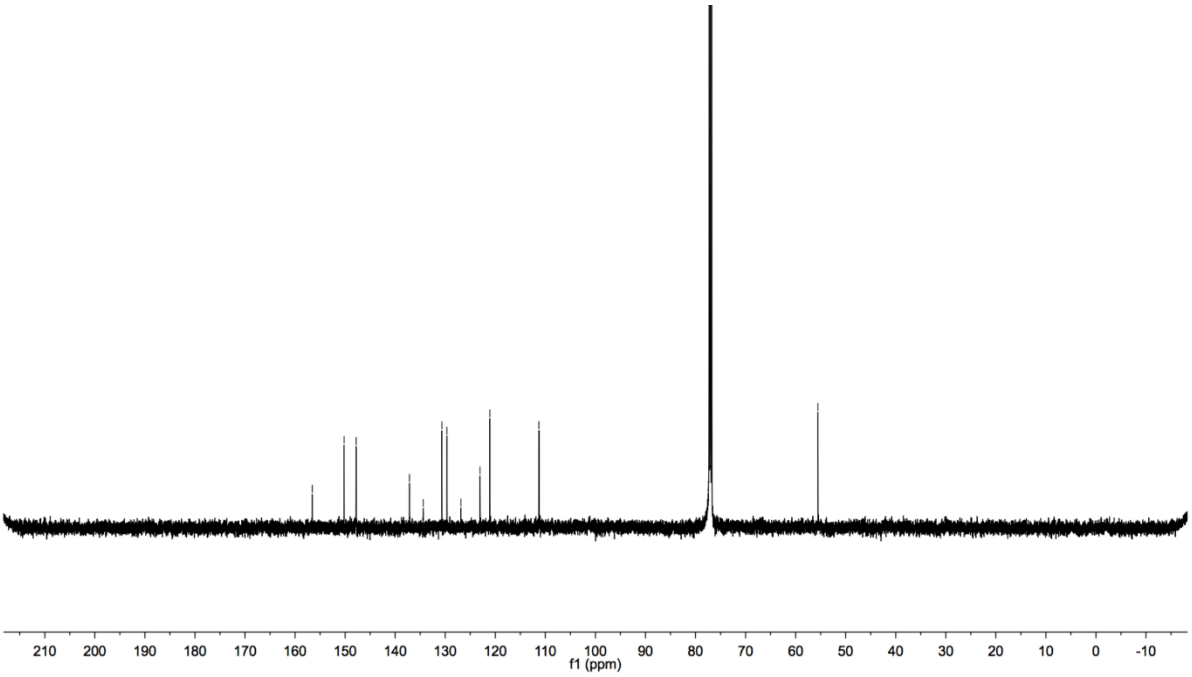

Figure S99. ^{1}H NMR spectrum of **3as**, related to **Figure 4**

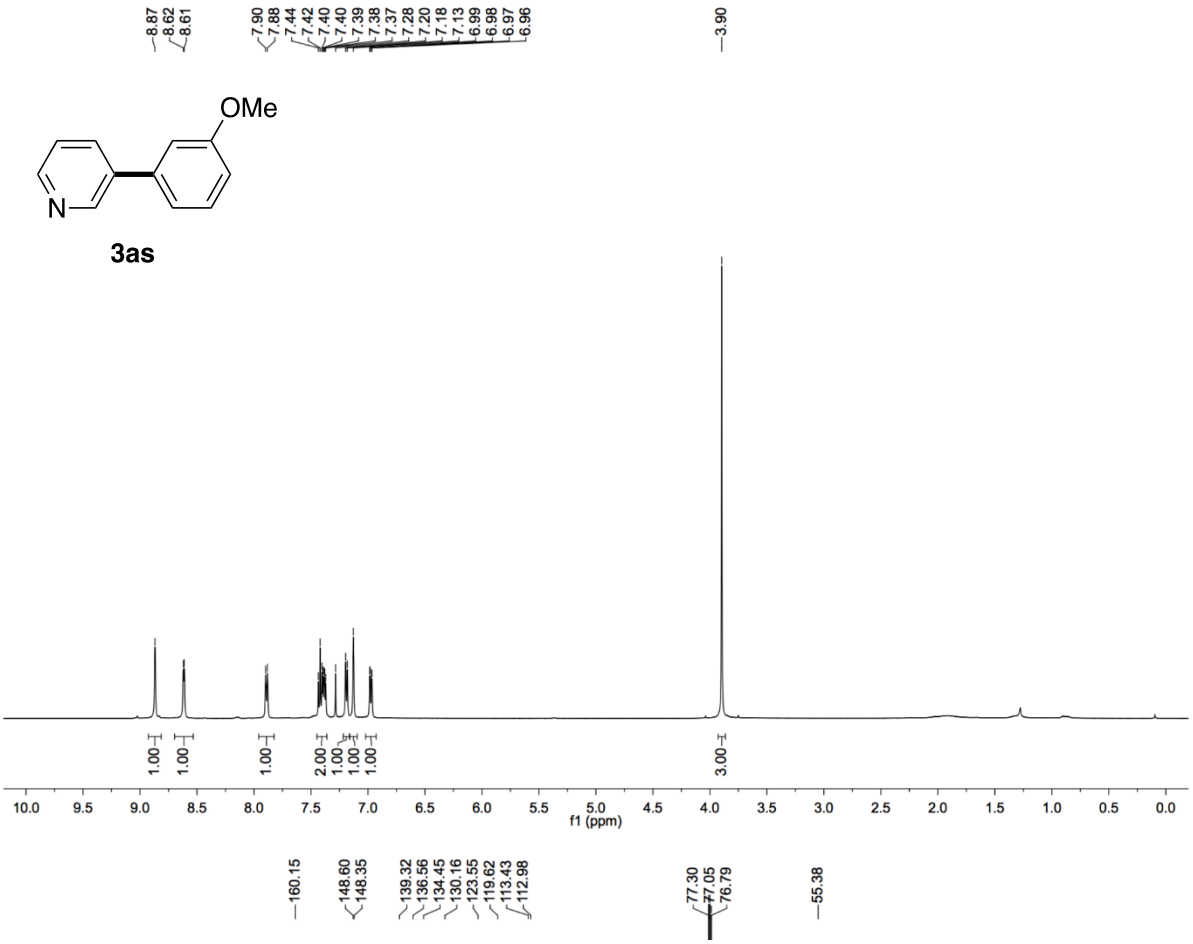

Figure S100. ^{13}C NMR spectrum of **3as**, related to **Figure 4**

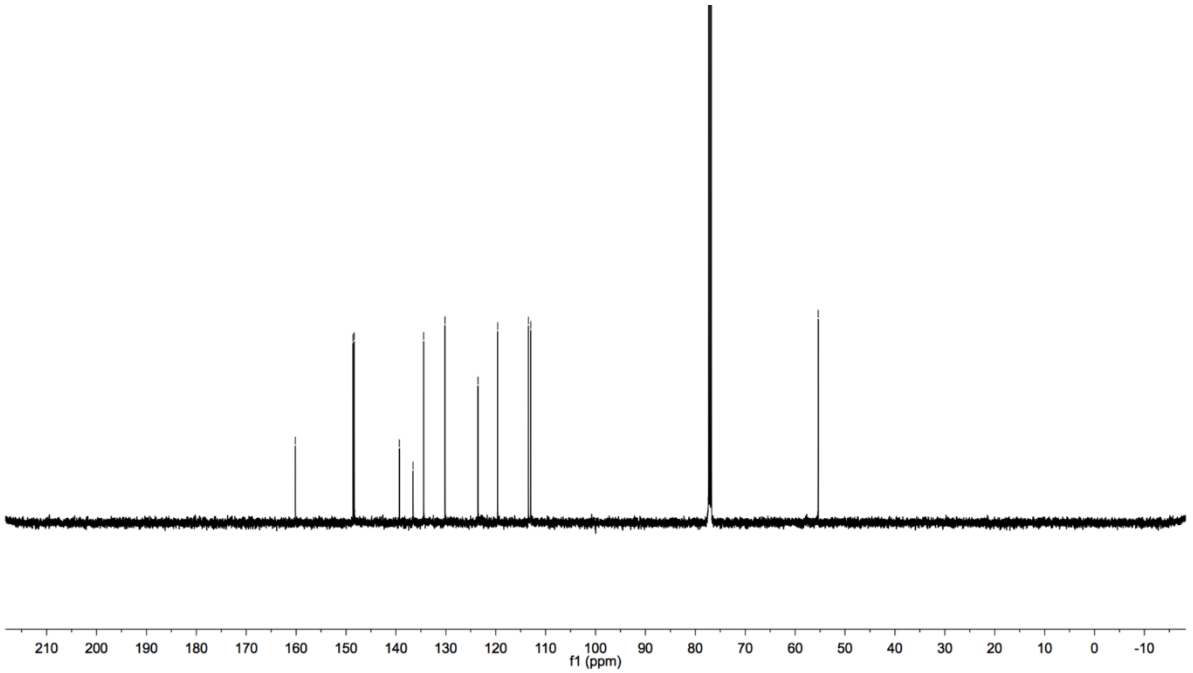

Figure S101. ^{1}H NMR spectrum of **3at**, related to **Figure 4**

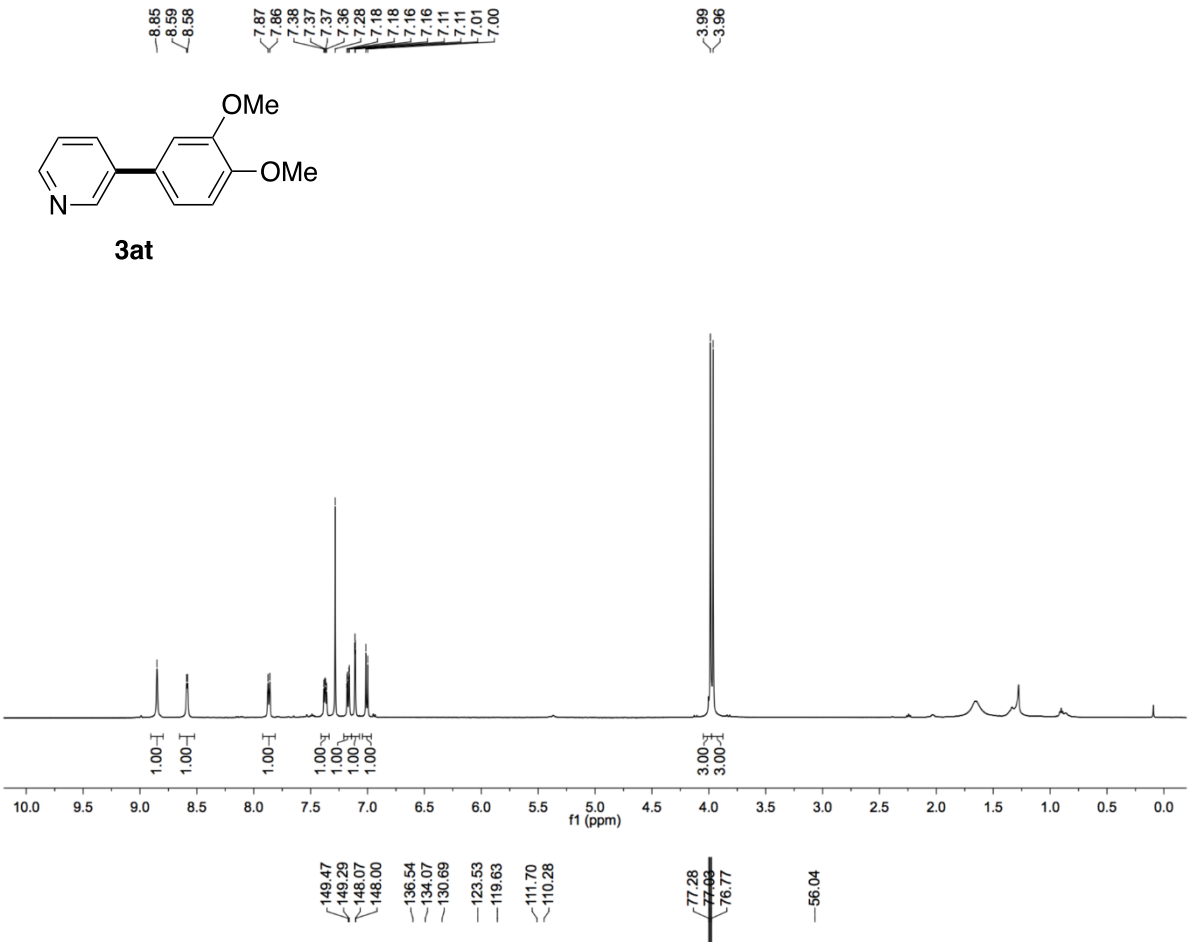

Figure S102. ^{13}C NMR spectrum of **3at**, related to **Figure 4**

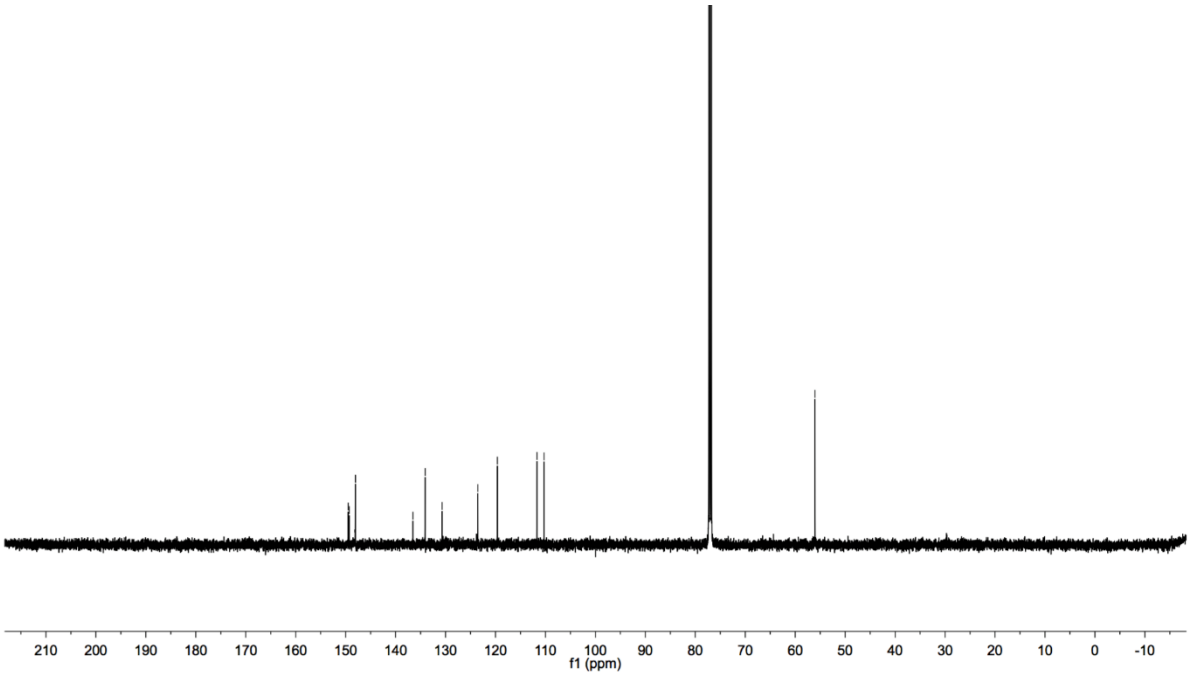

Figure S103. ^{1}H NMR spectrum of **3au**, related to **Figure 4**

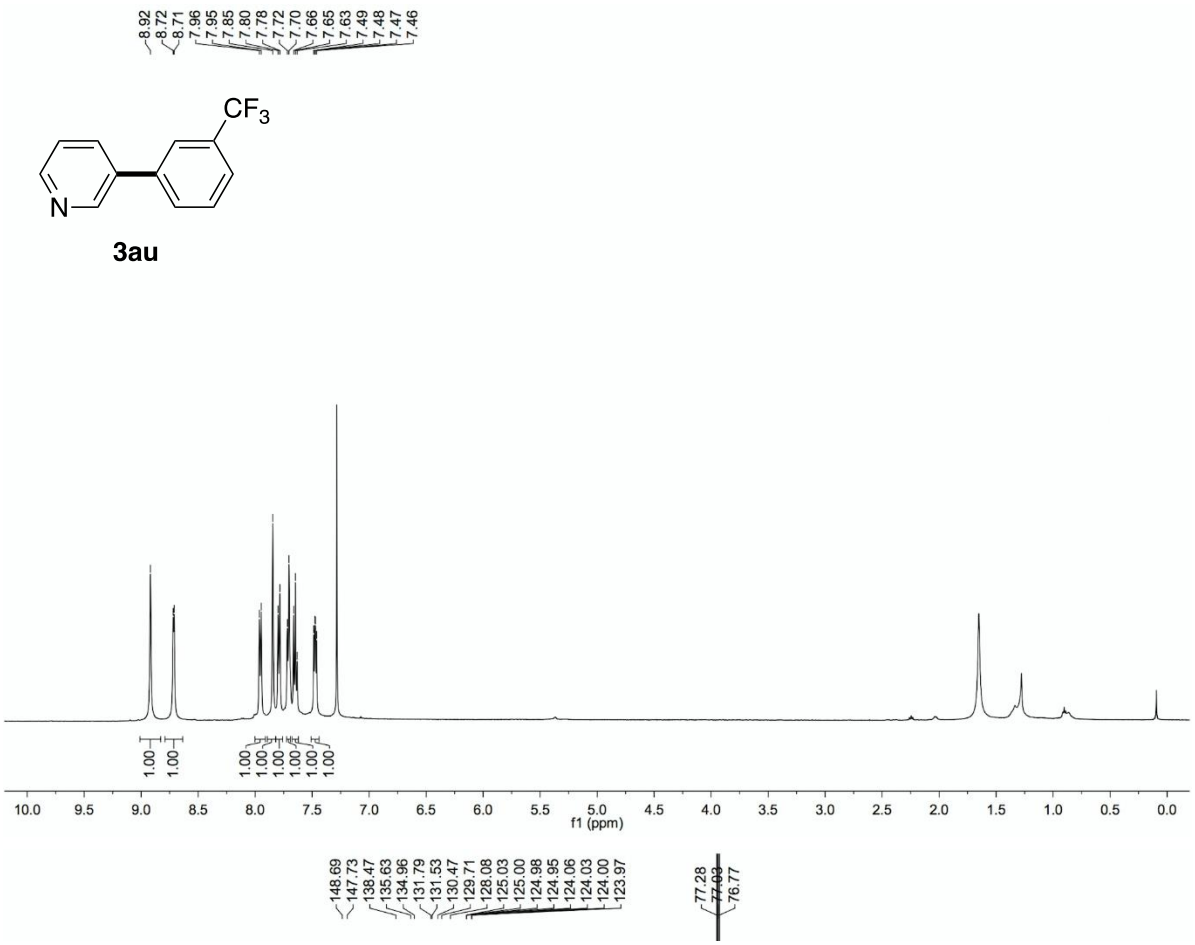

Figure S104. ^{13}C NMR spectrum of **3au**, related to **Figure 4**

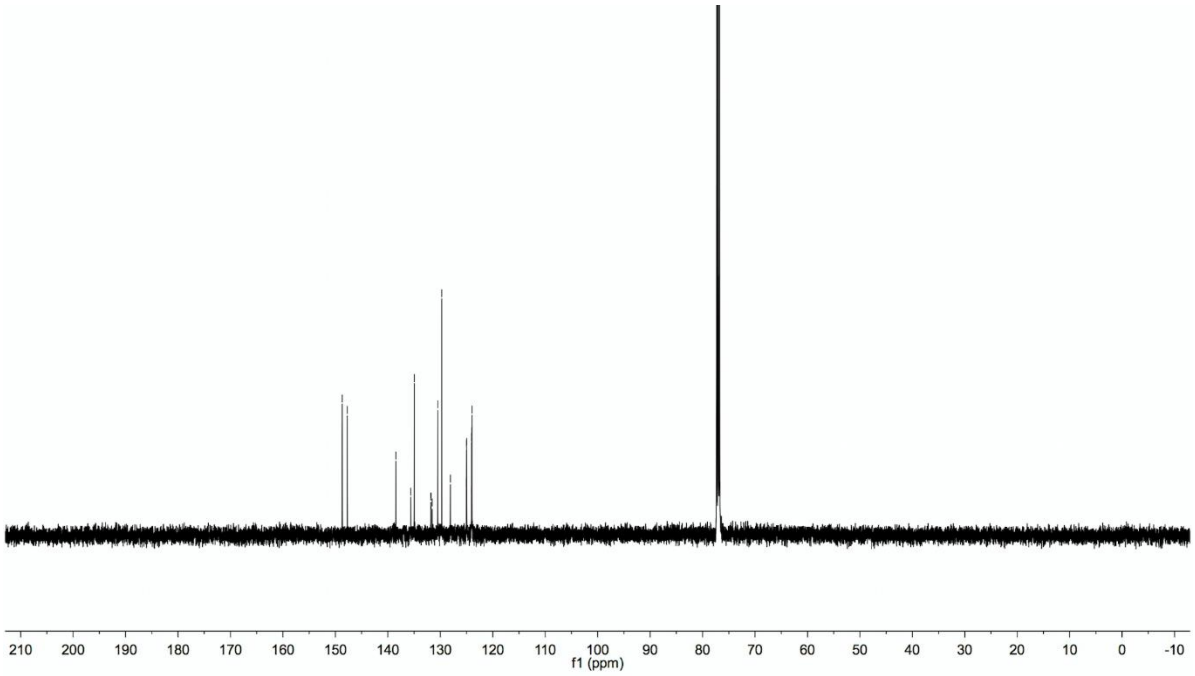

Figure S105. ^{19}F NMR spectrum of **3au**, related to **Figure 4**

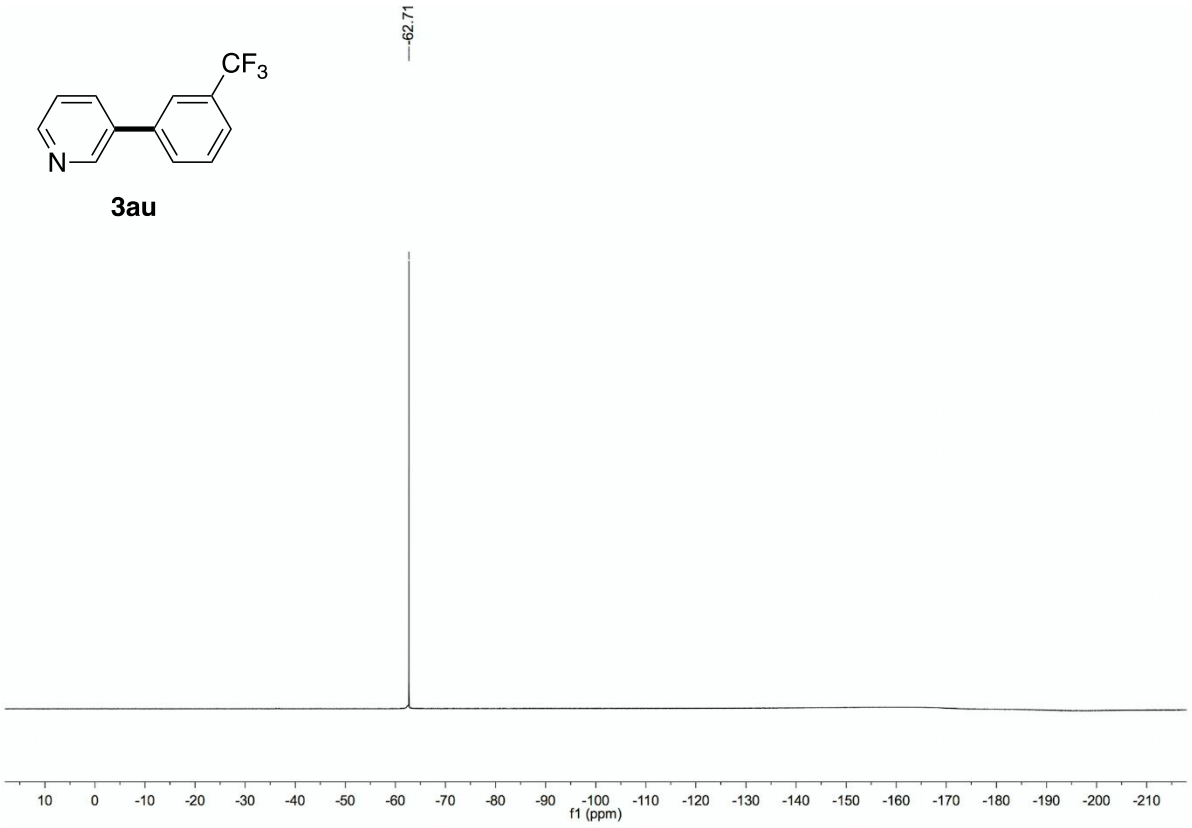

Figure S106. ^{1}H NMR spectrum of **3av**, related to **Figure 4**

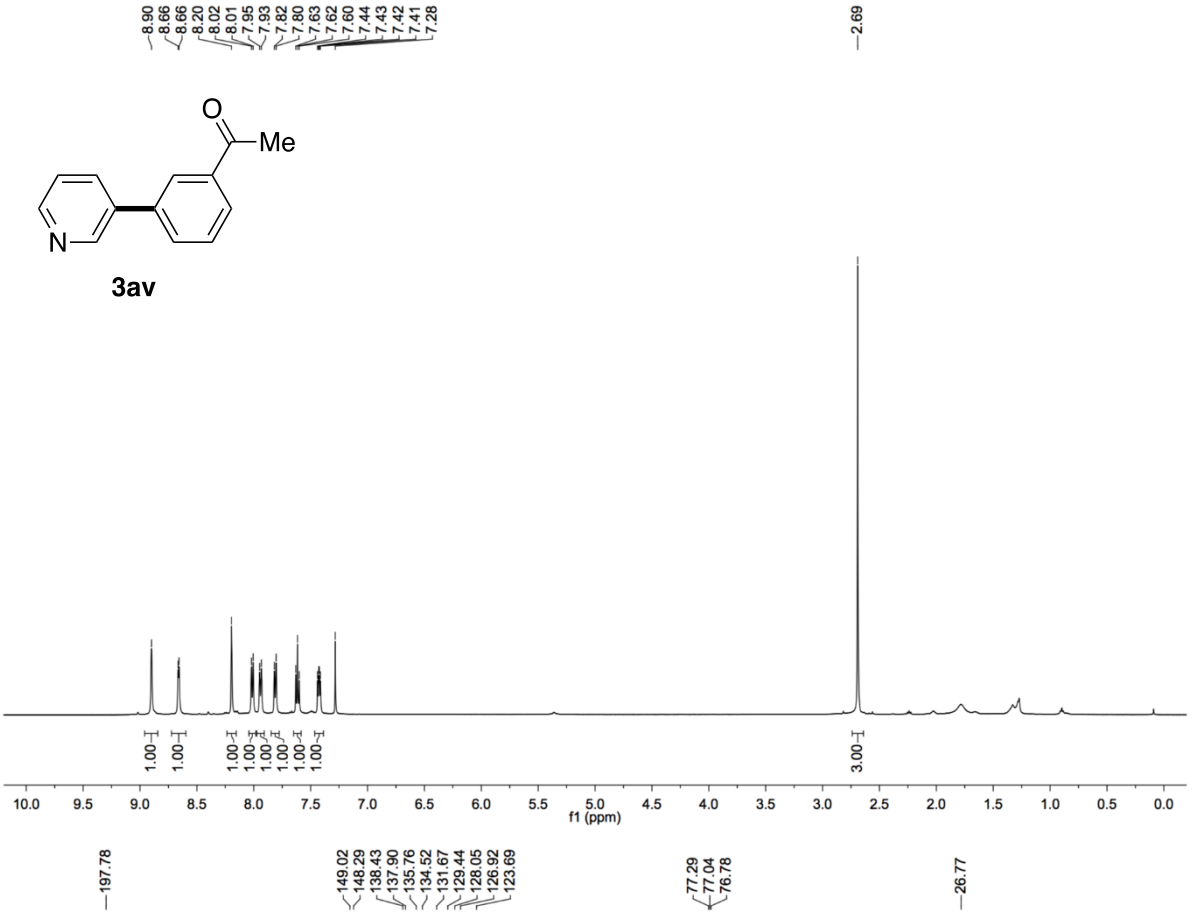

Figure S107. ^{13}C NMR spectrum of **3av**, related to **Figure 4**

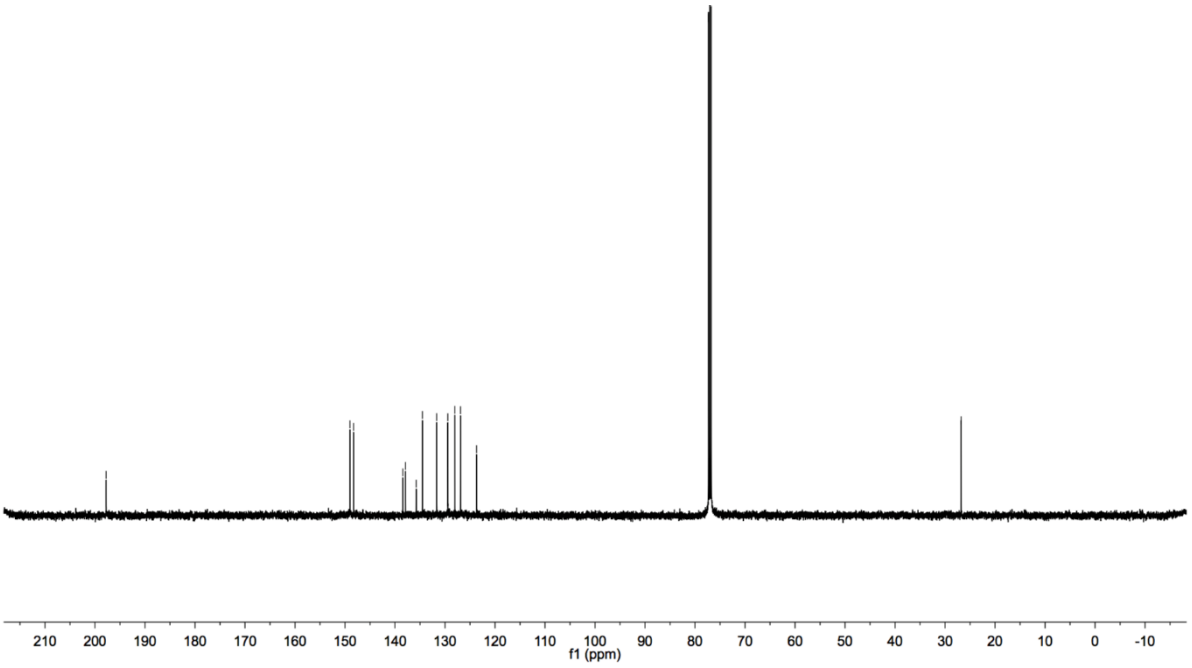

Figure S108. ^{1}H NMR spectrum of **3aw**, related to **Figure 4**

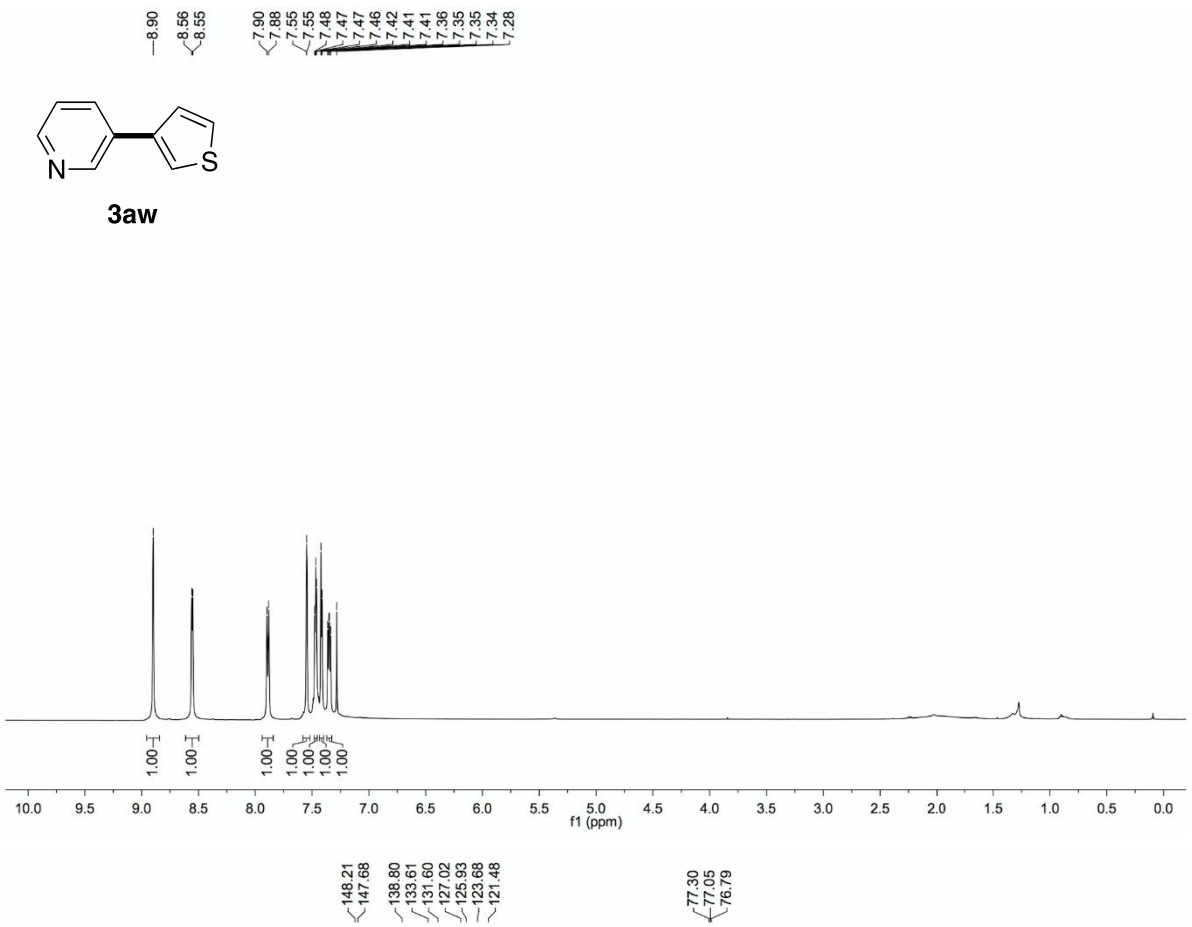

Figure S109. ^{13}C NMR spectrum of **3aw**, related to **Figure 4**

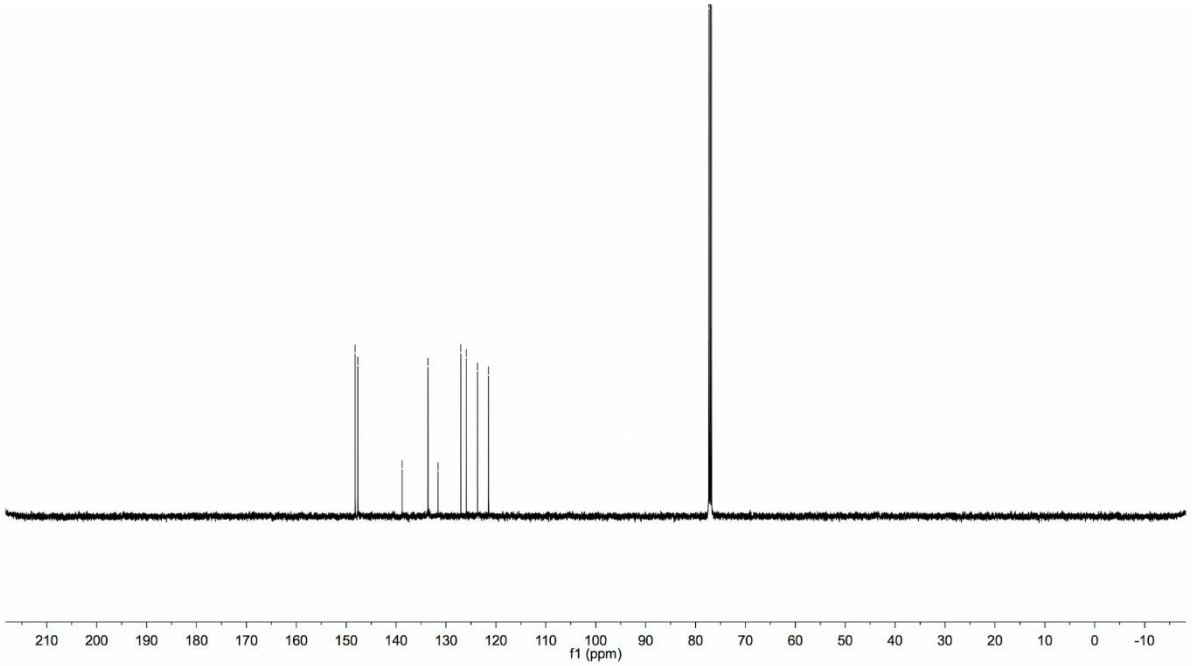

Figure S110. ^{1}H NMR spectrum of **3ax**, related to **Figure 4**

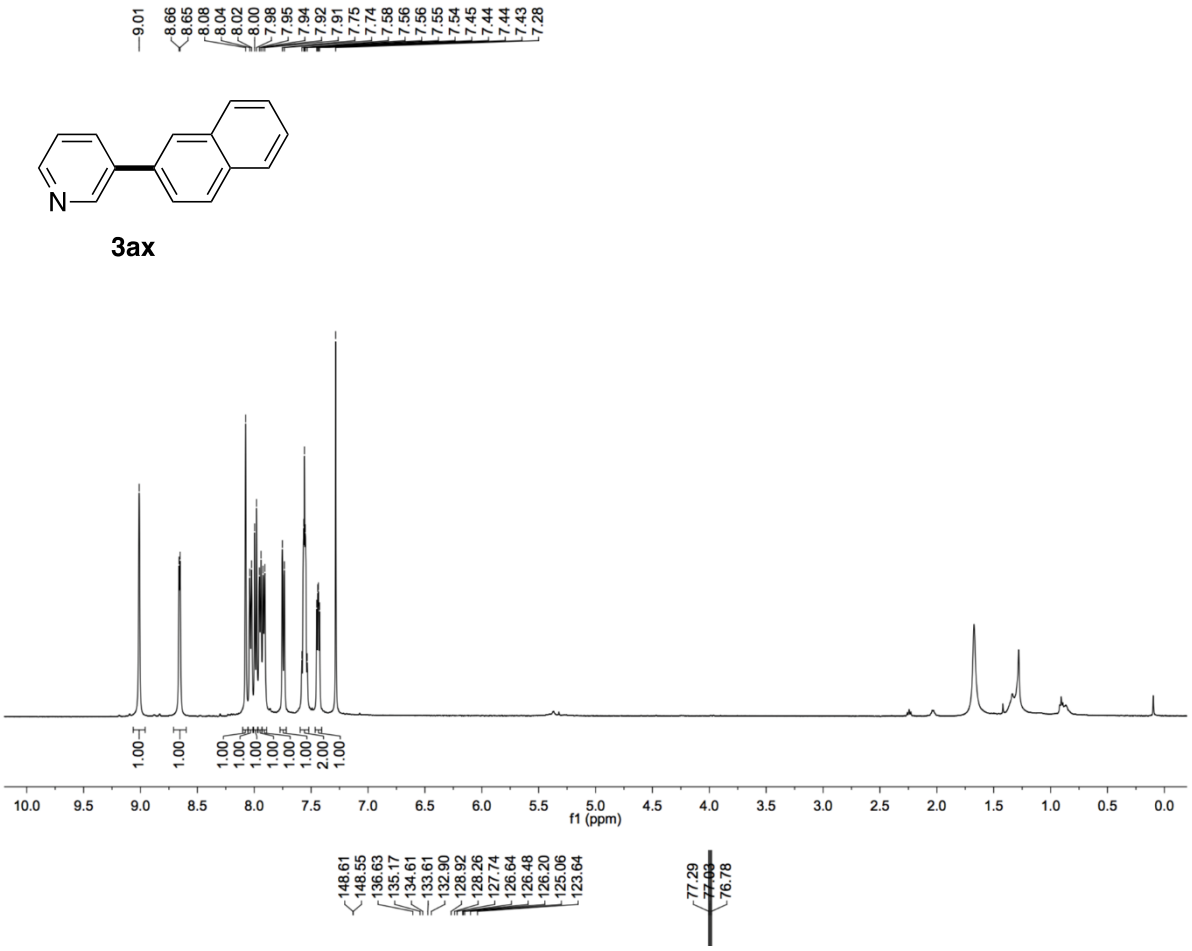

Figure S111. ^{13}C NMR spectrum of **3ax**, related to **Figure 4**

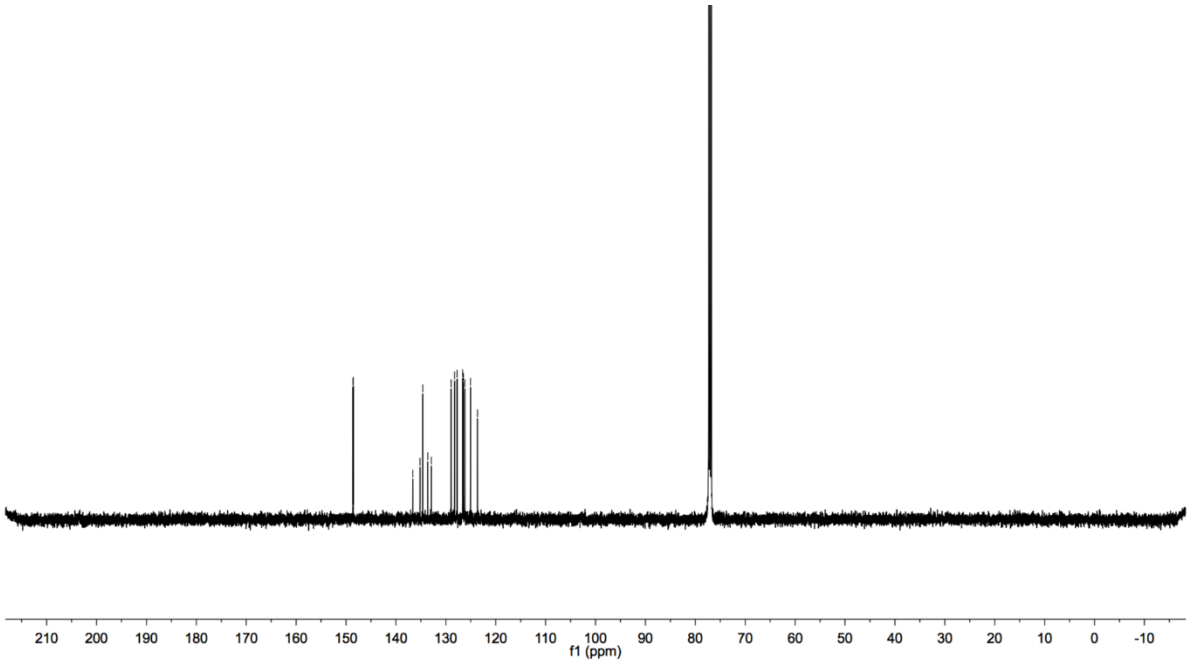

Figure S112. ^{1}H NMR spectrum of **3ay**, related to **Figure 4**

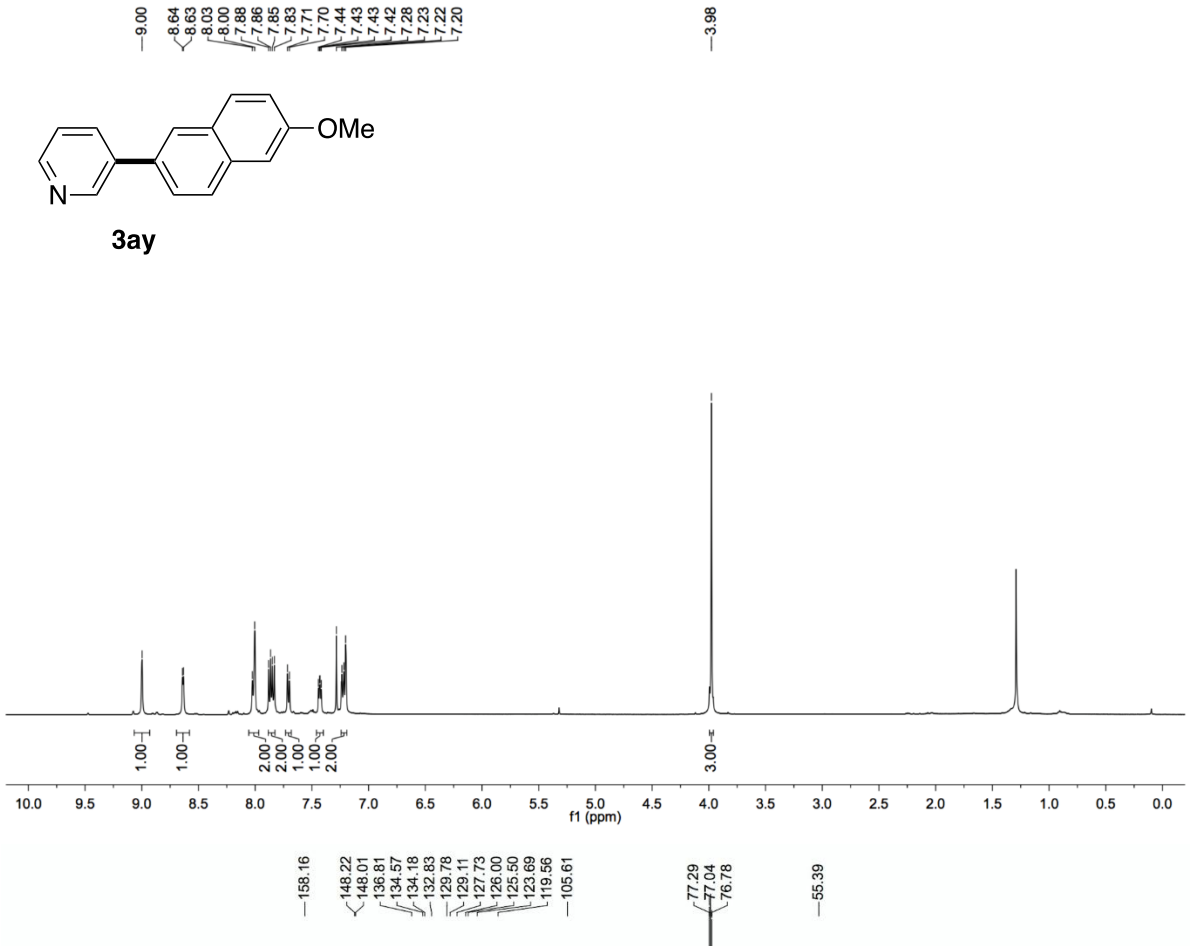

Figure S113. ^{13}C NMR spectrum of **3ay**, related to **Figure 4**

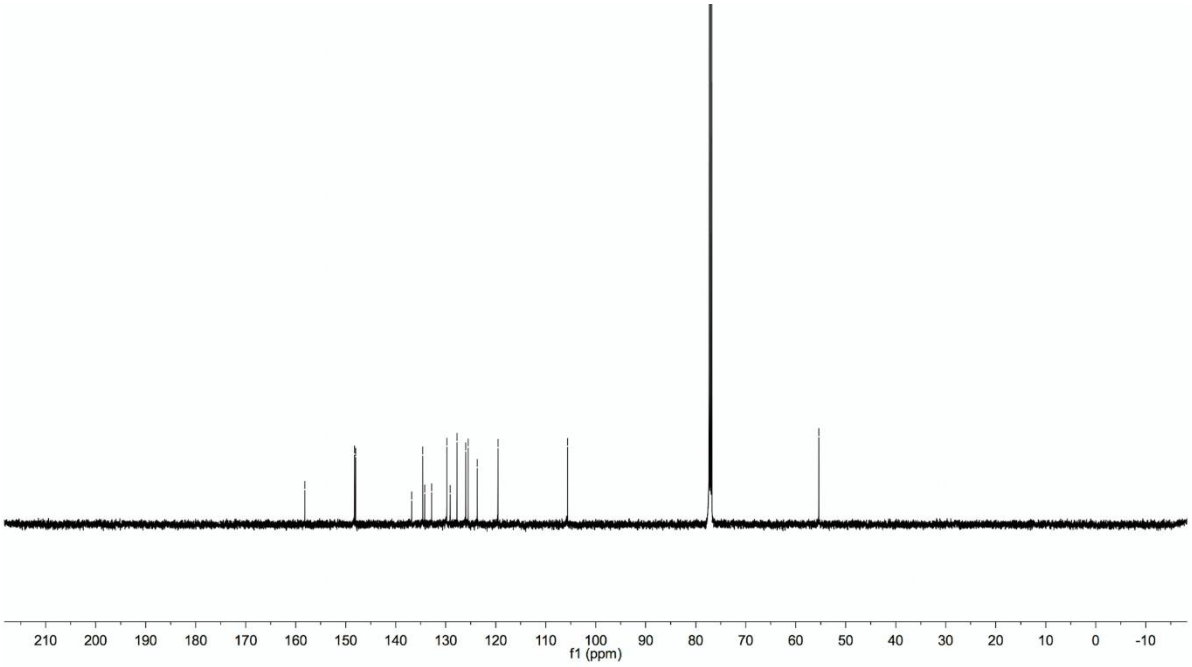

Figure S114. ^{1}H NMR spectrum of **3az**, related to **Figure 4**

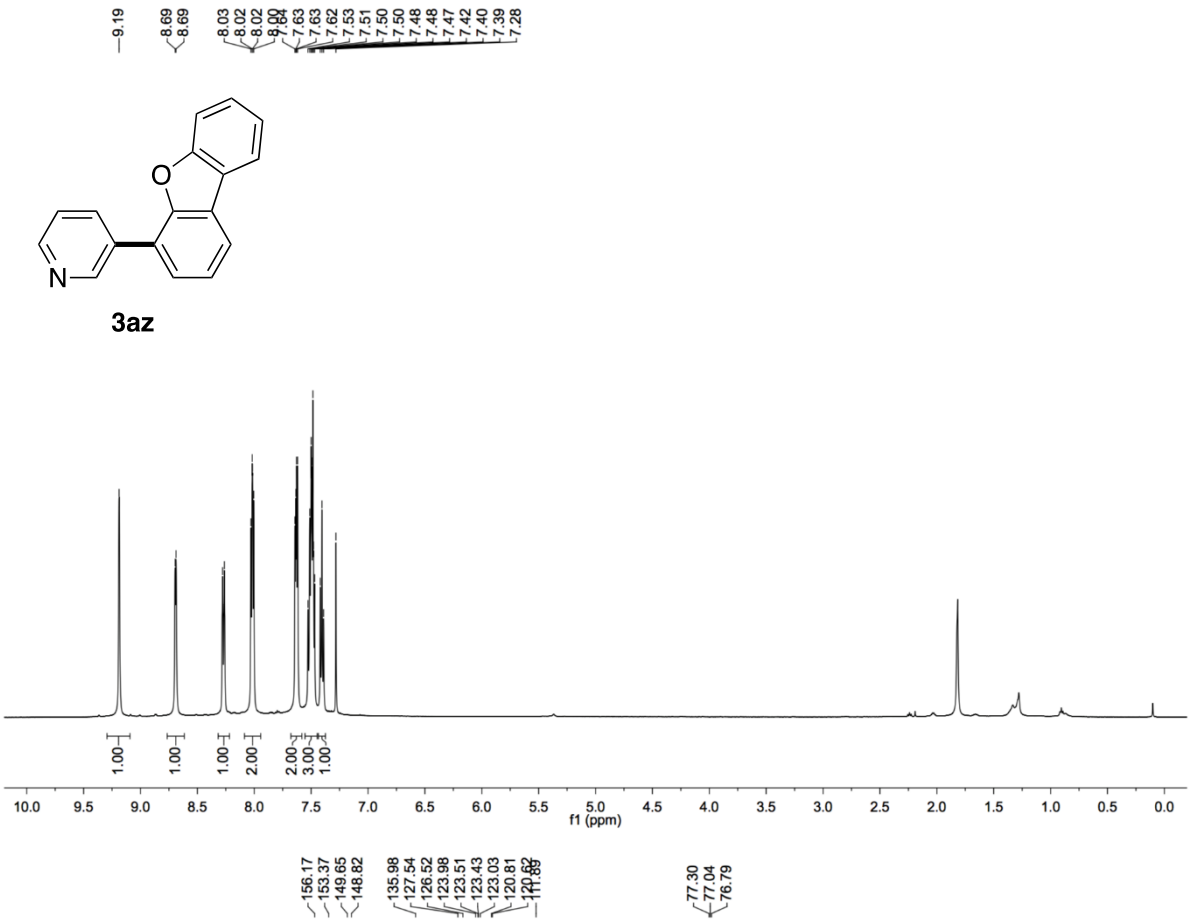

Figure S115. ^{13}C NMR spectrum of **3az**, related to **Figure 4**

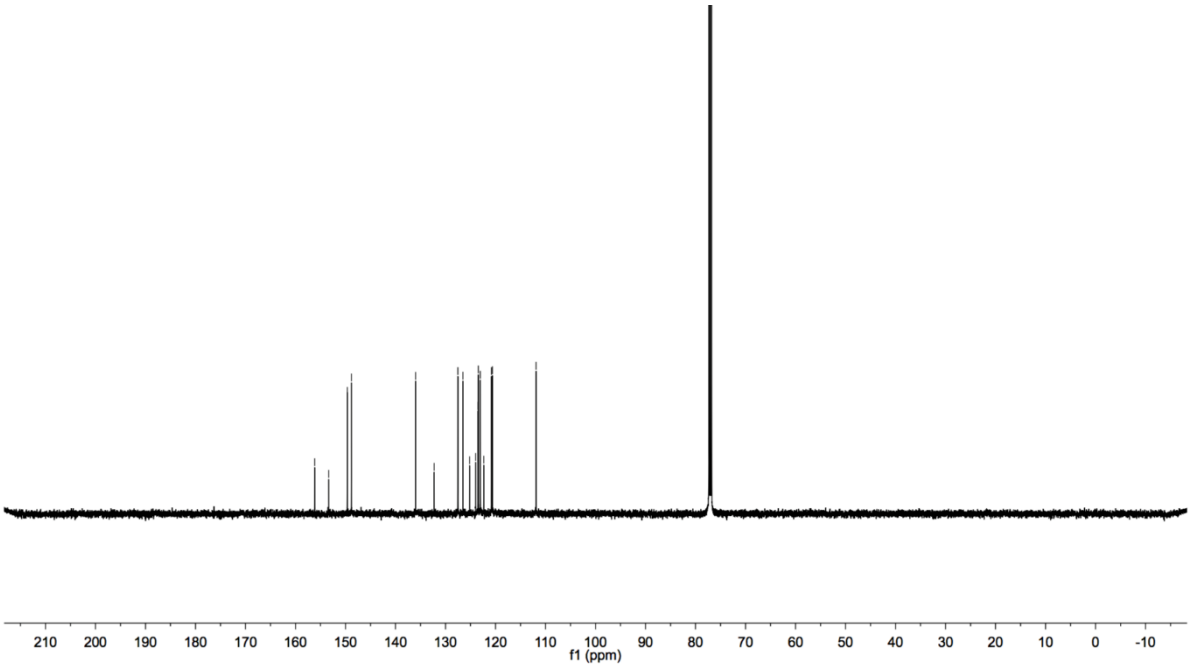

Figure S116. ^{1}H NMR spectrum of **3ba**, related to **Figure 4**

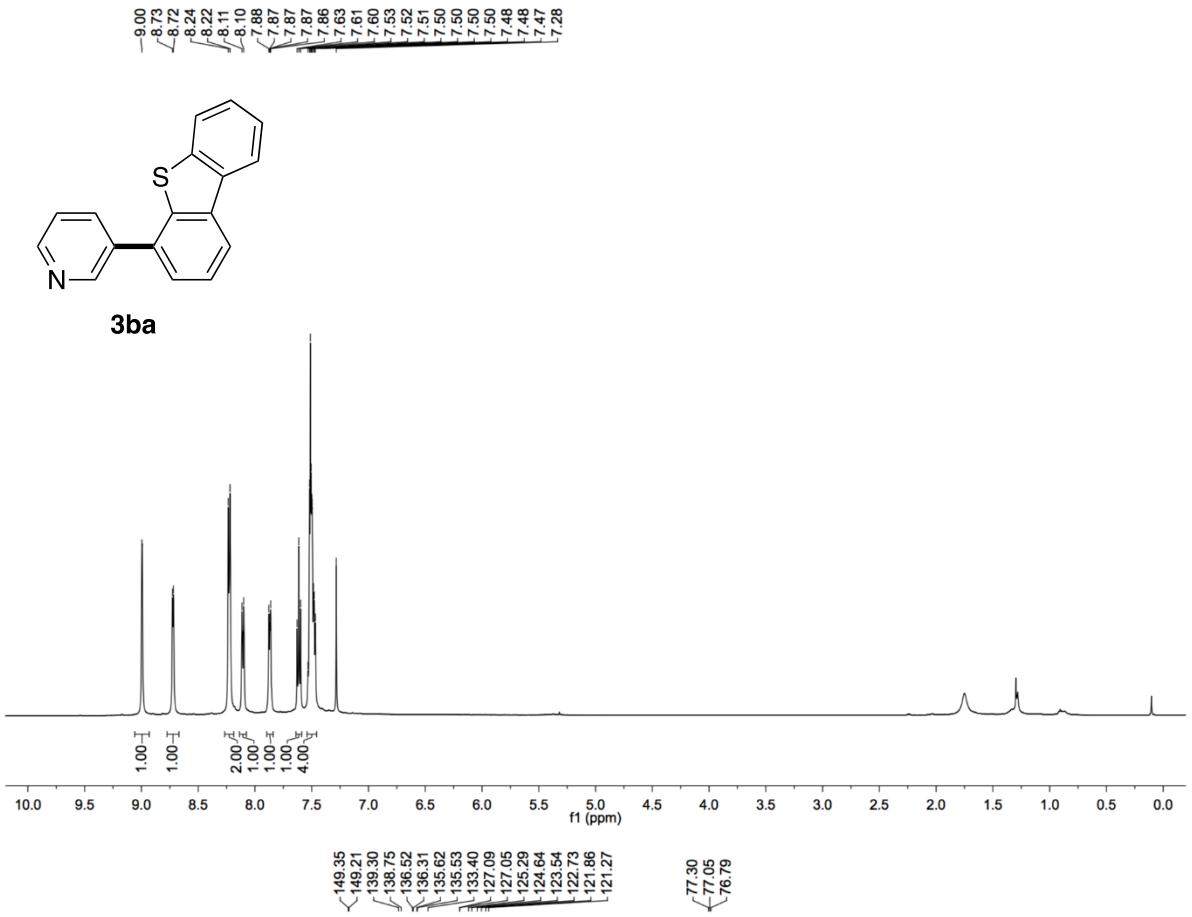

Figure S117. ^{13}C NMR spectrum of **3ba**, related to **Figure 4**

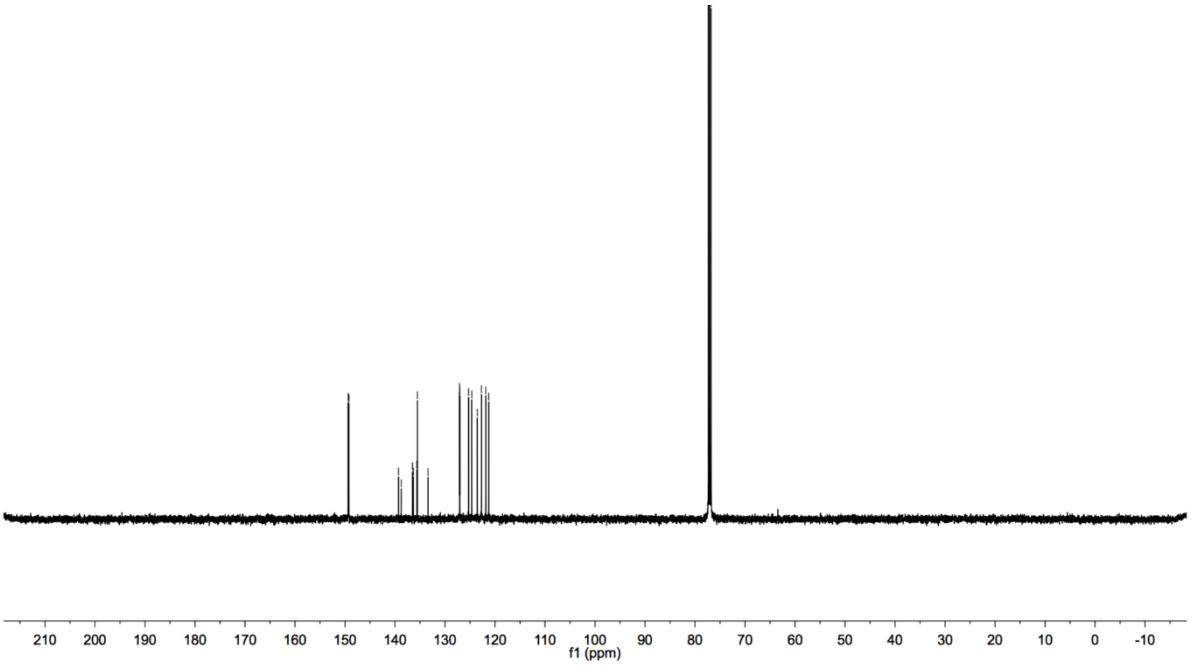

Figure S118. ^{1}H NMR spectrum of **3bb**, related to **Figure 4**

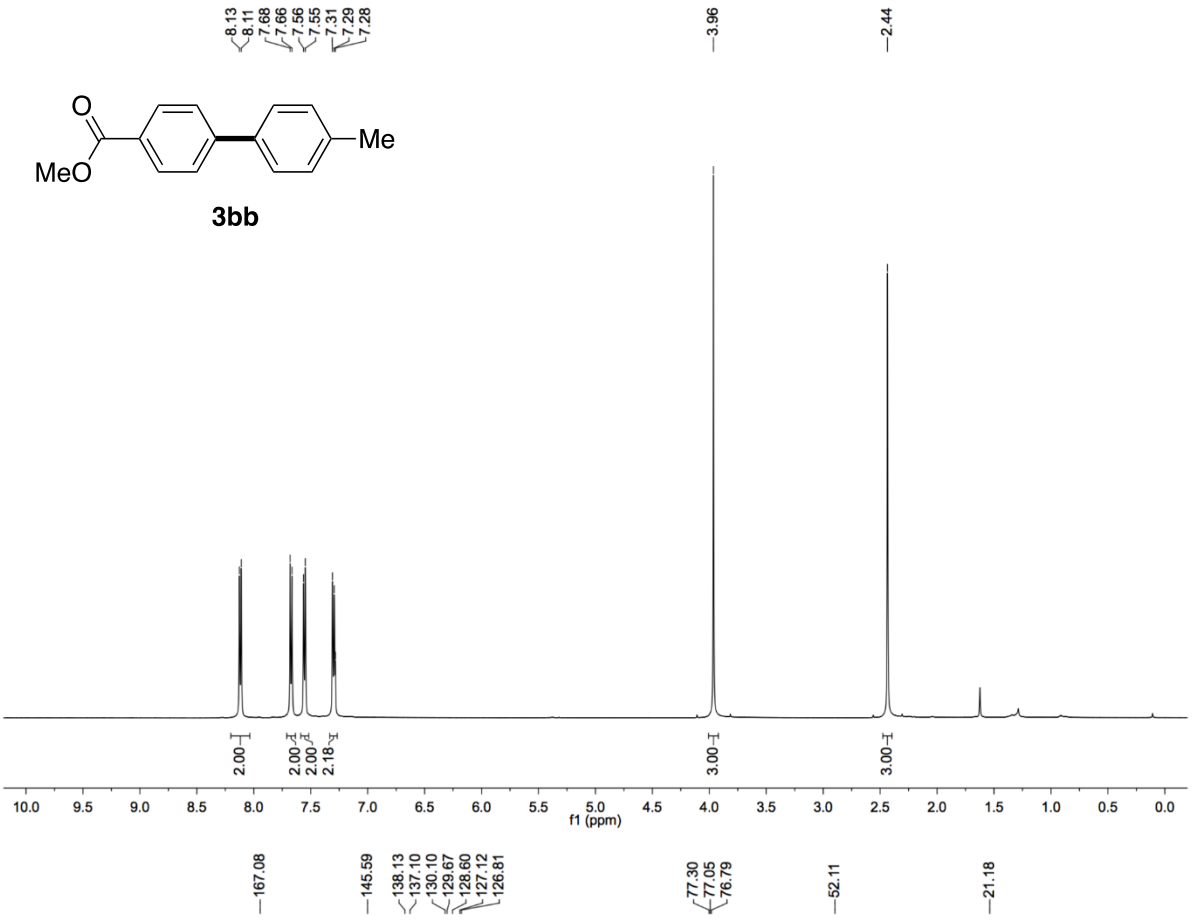

Figure S119. ^{13}C NMR spectrum of **3bb**, related to **Figure 4**

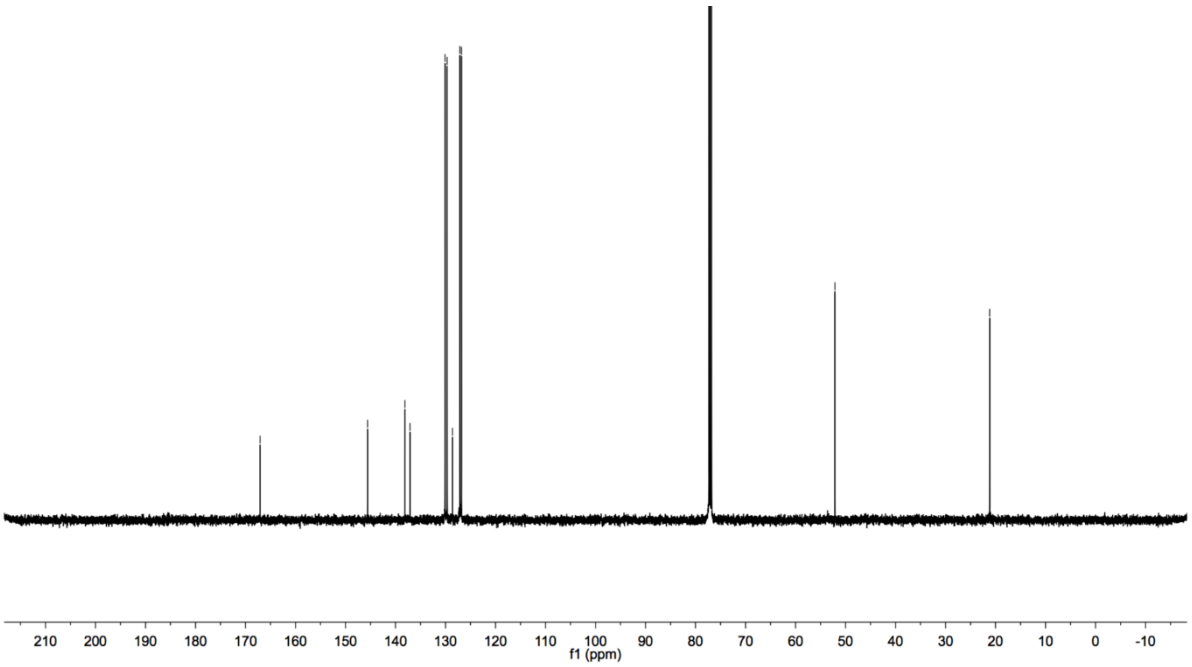

Figure S120. ^{1}H NMR spectrum of **3bc**, related to **Figure 4**

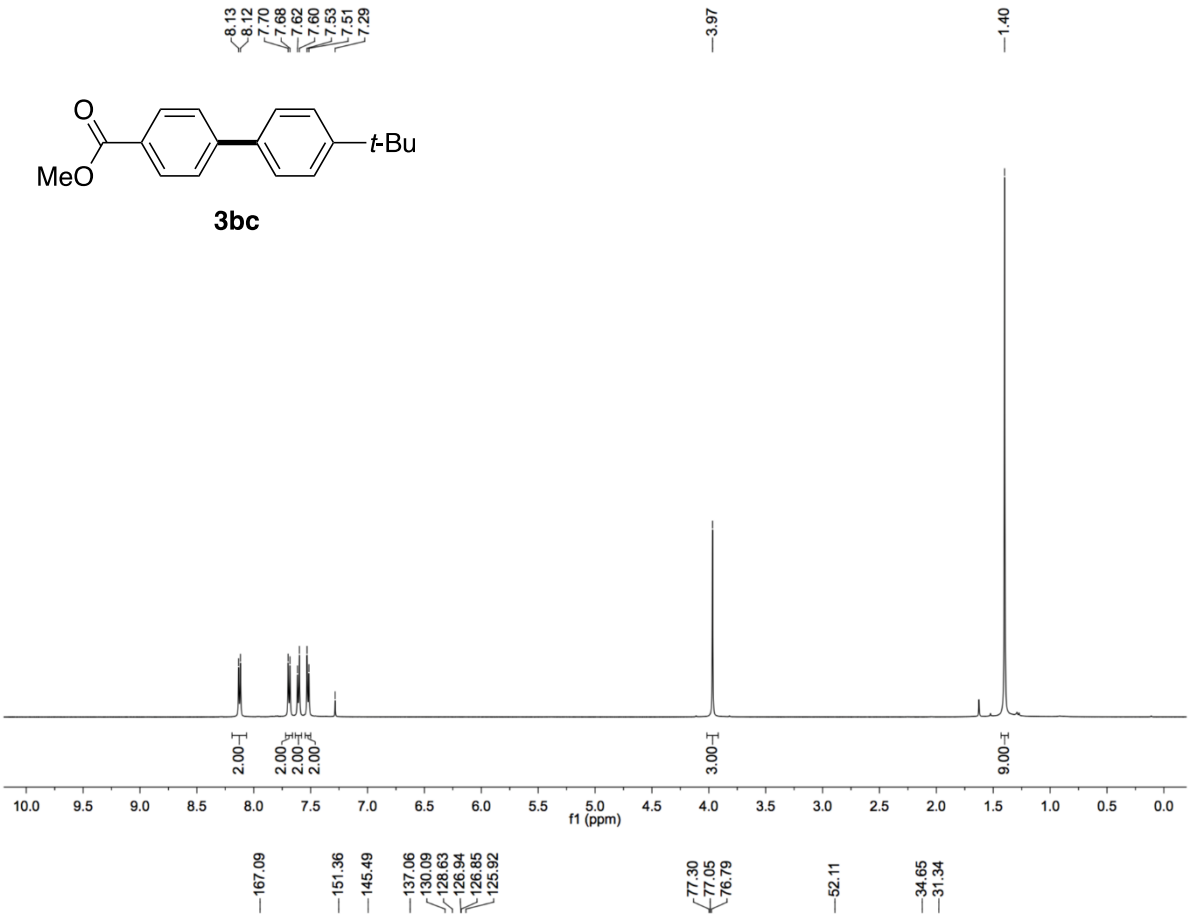

Figure S121. ^{13}C NMR spectrum of **3bc**, related to **Figure 4**

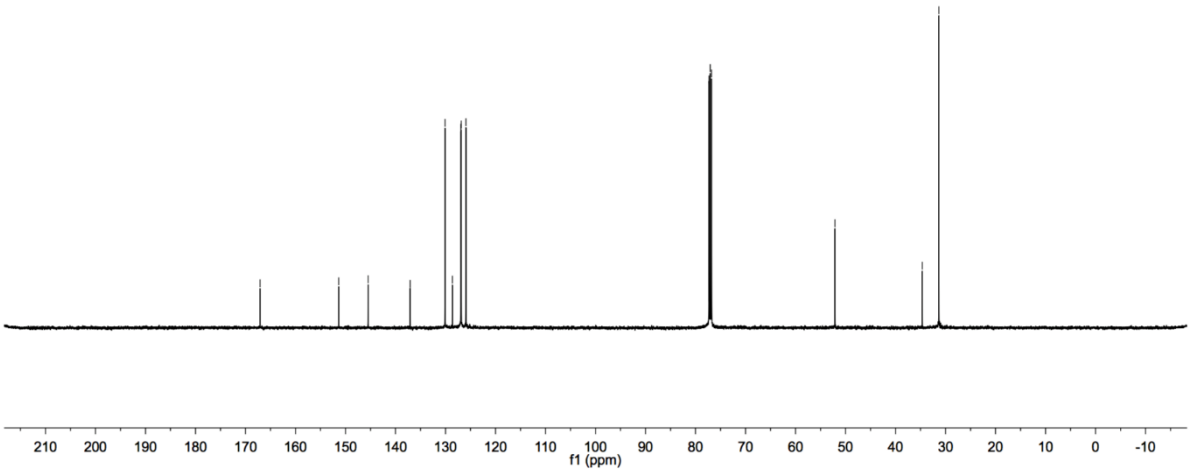

Figure S122. ^{1}H NMR spectrum of **3bd**, related to **Figure 4**

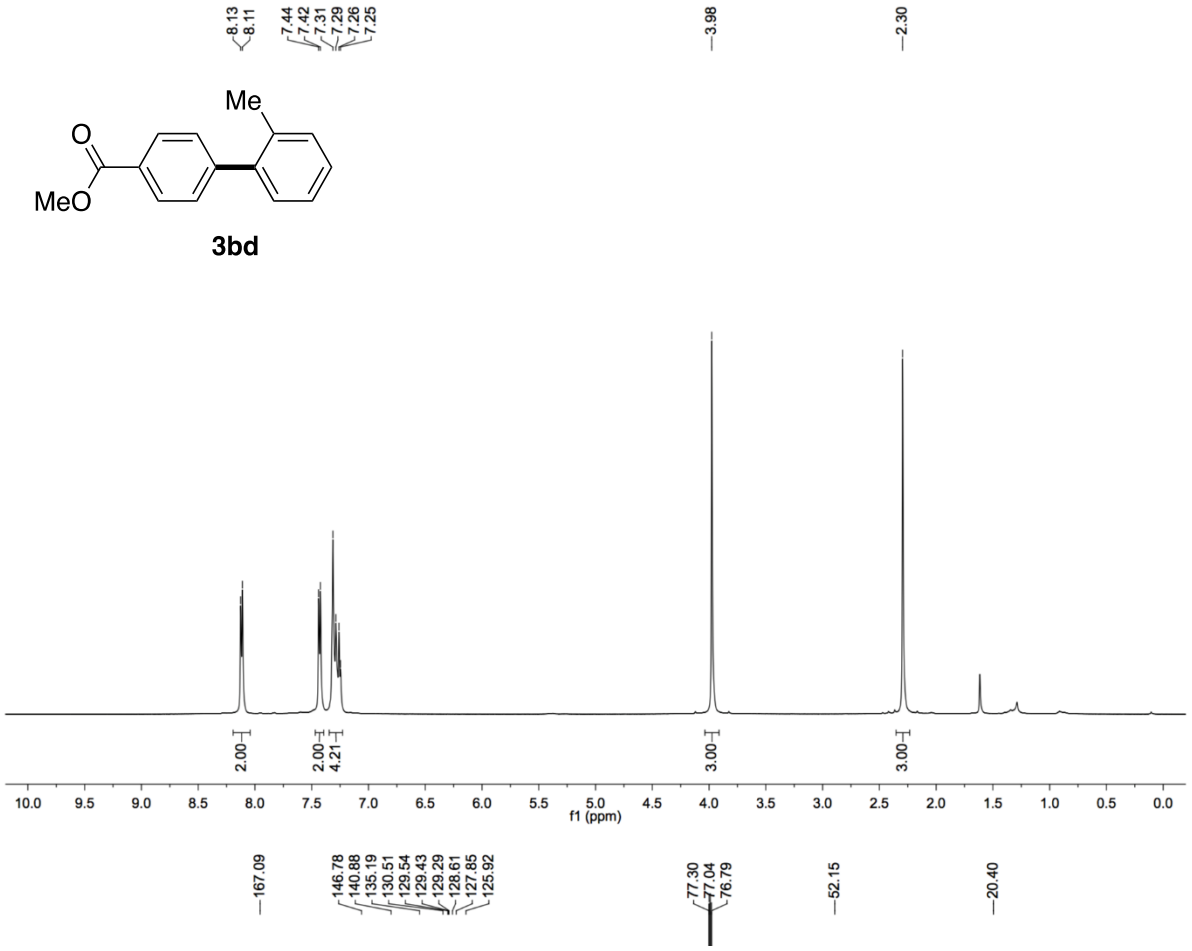

Figure S123. ^{13}C NMR spectrum of **3bd**, related to **Figure 4**

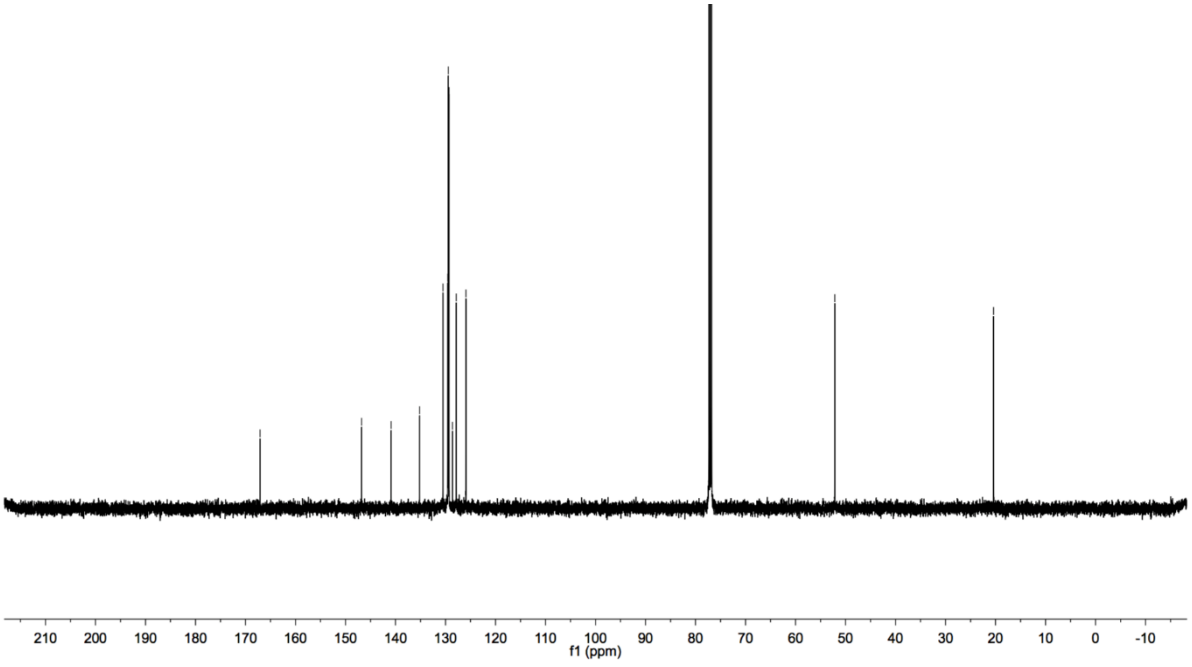

Figure S124. ^{1}H NMR spectrum of **3be**, related to **Figure 4**

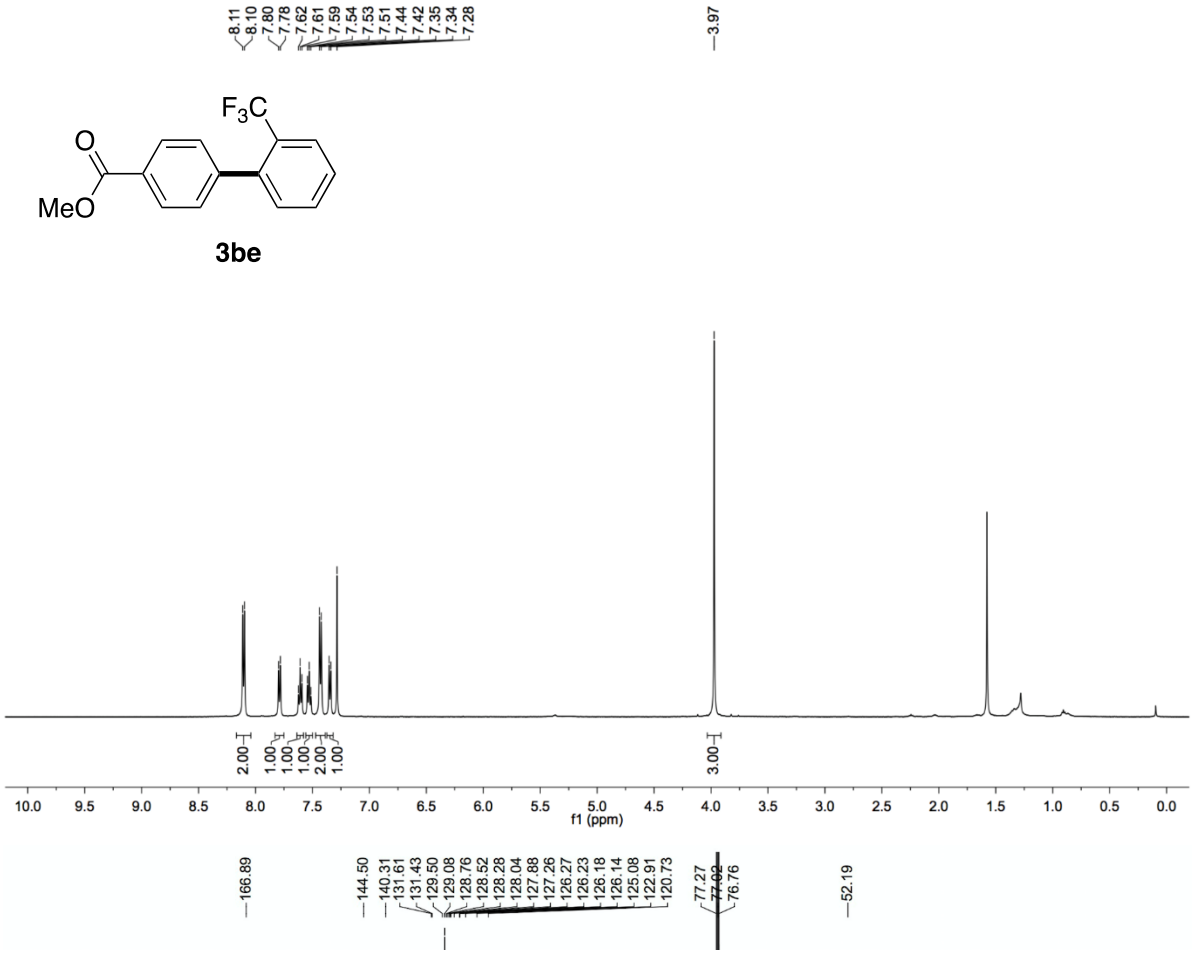

Figure S125. ^{13}C NMR spectrum of **3be**, related to **Figure 4**

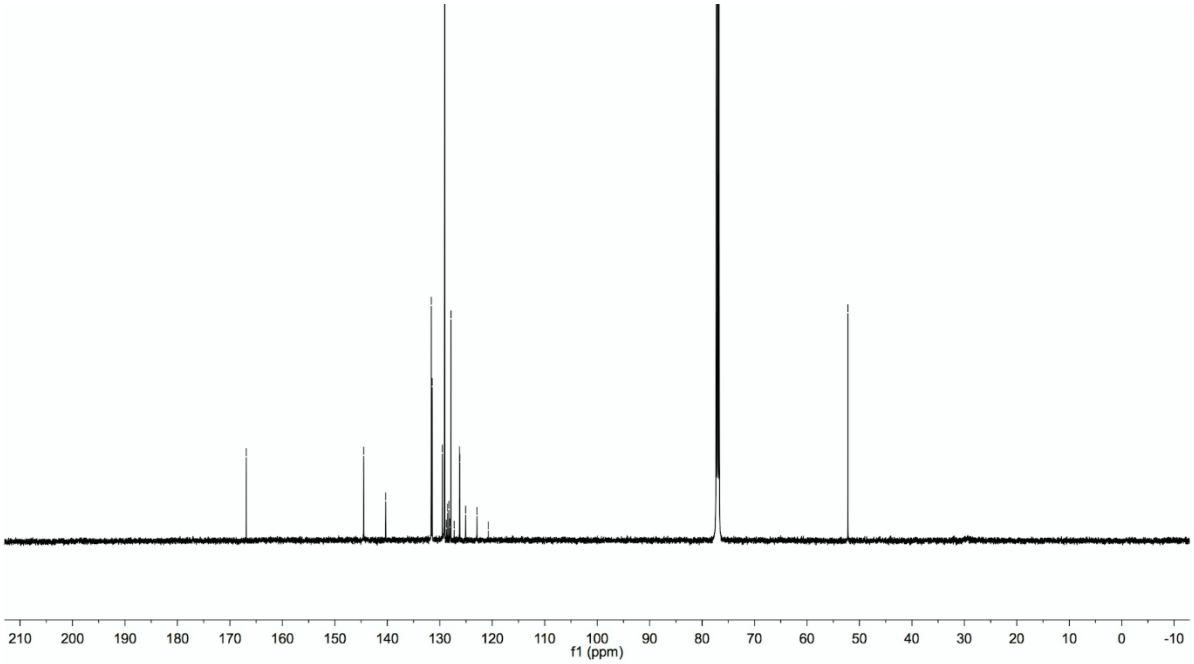

Figure S126. ^{1}H NMR spectrum of **3be**, related to **Figure 4**

Figure S127. ^{1}H NMR spectrum of **3bf**, related to **Figure 4**

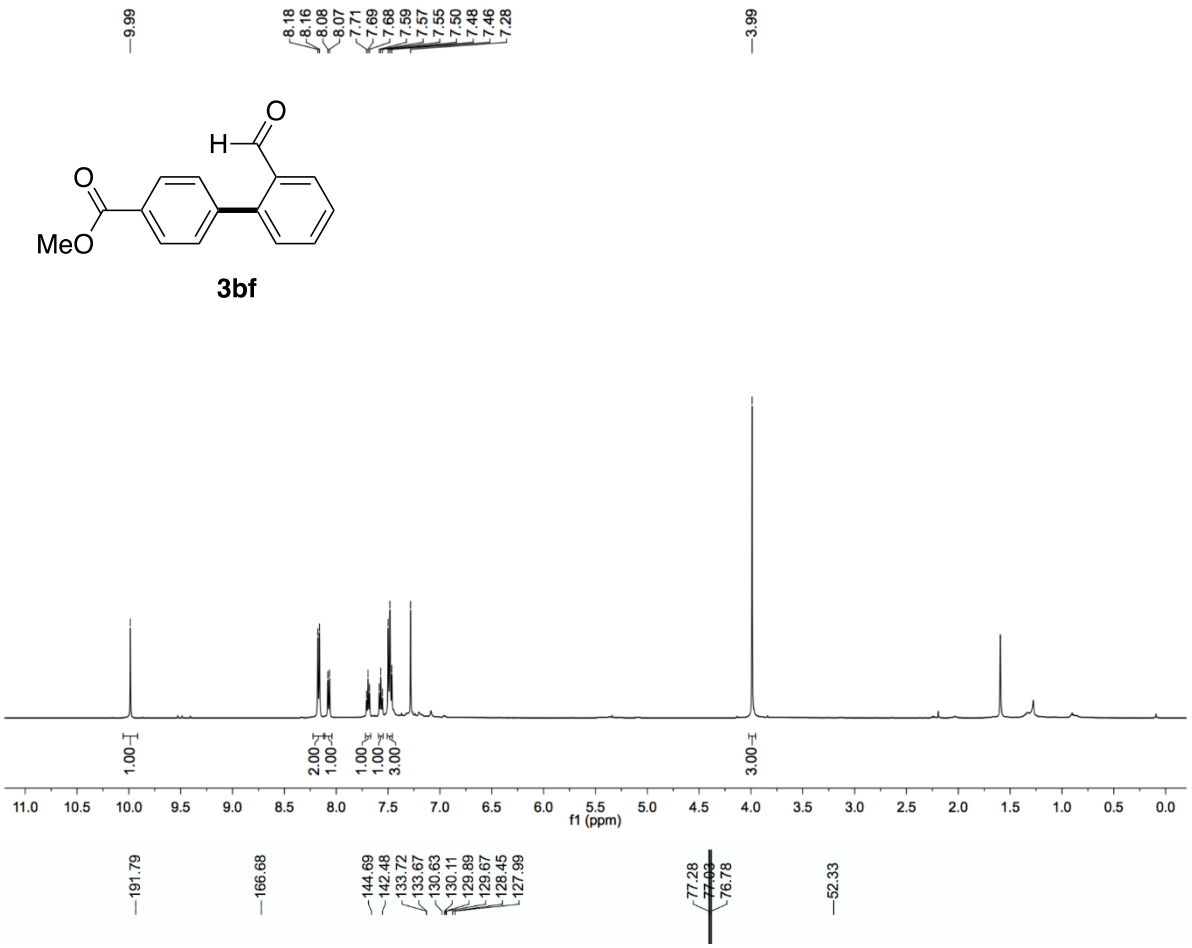

Figure S128. ^{13}C NMR spectrum of **3bf**, related to **Figure 4**

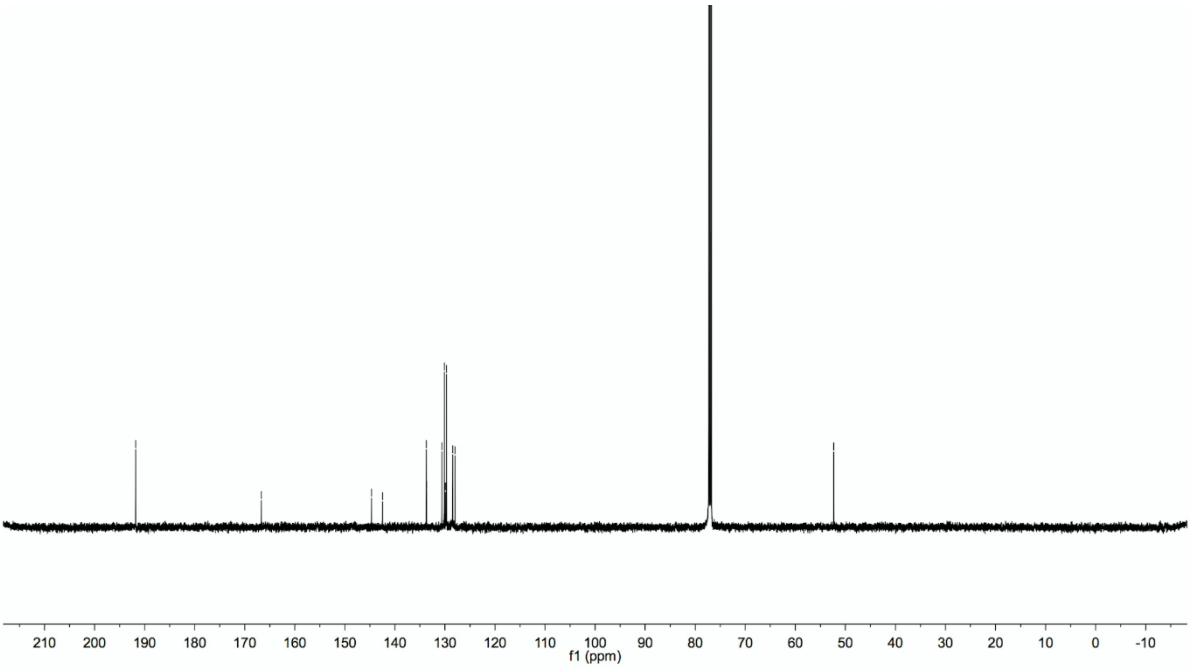

Figure S129. ^{1}H NMR spectrum of **3bg**, related to **Figure 4**

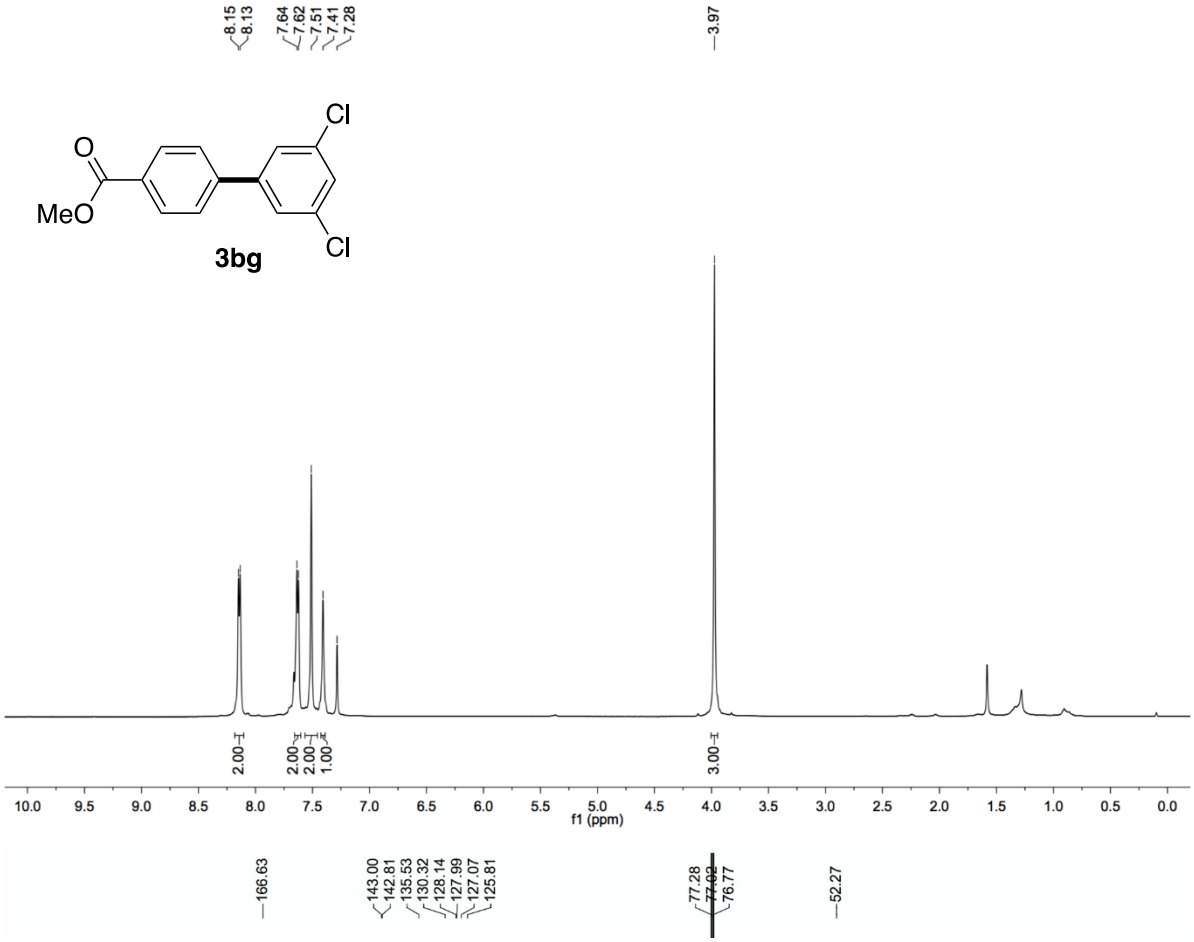

Figure S130. ^{13}C NMR spectrum of **3bg**, related to **Figure 4**

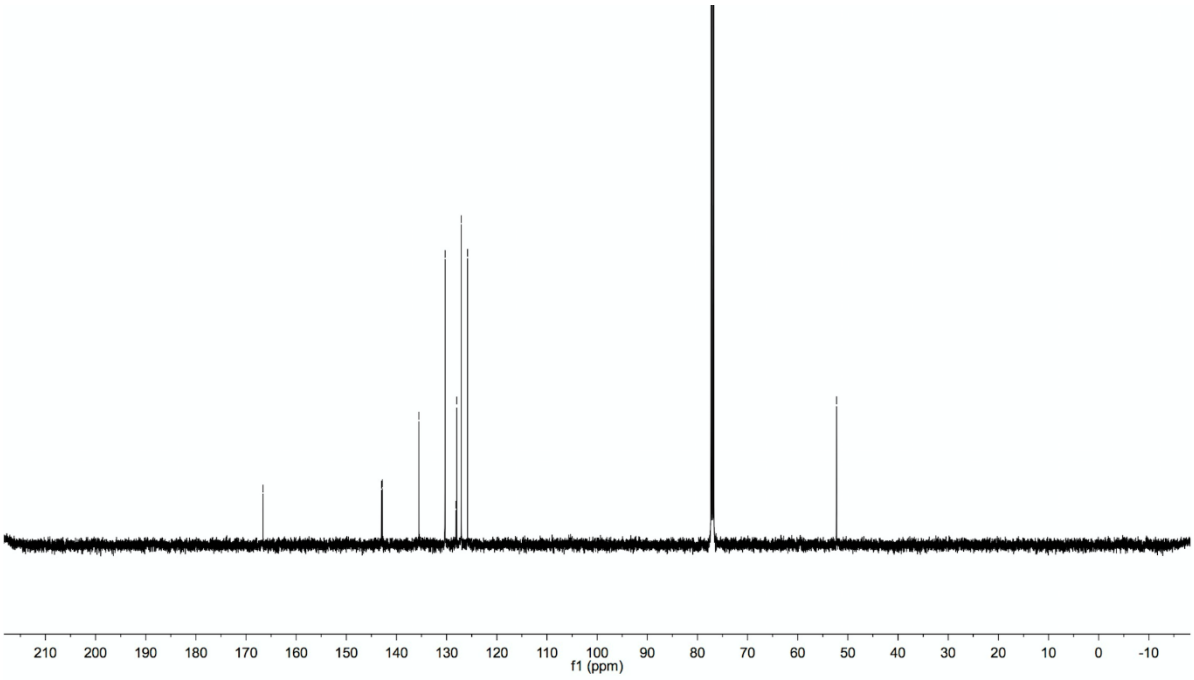

Figure S131. ^{1}H NMR spectrum of **3bh**, related to **Figure 4**

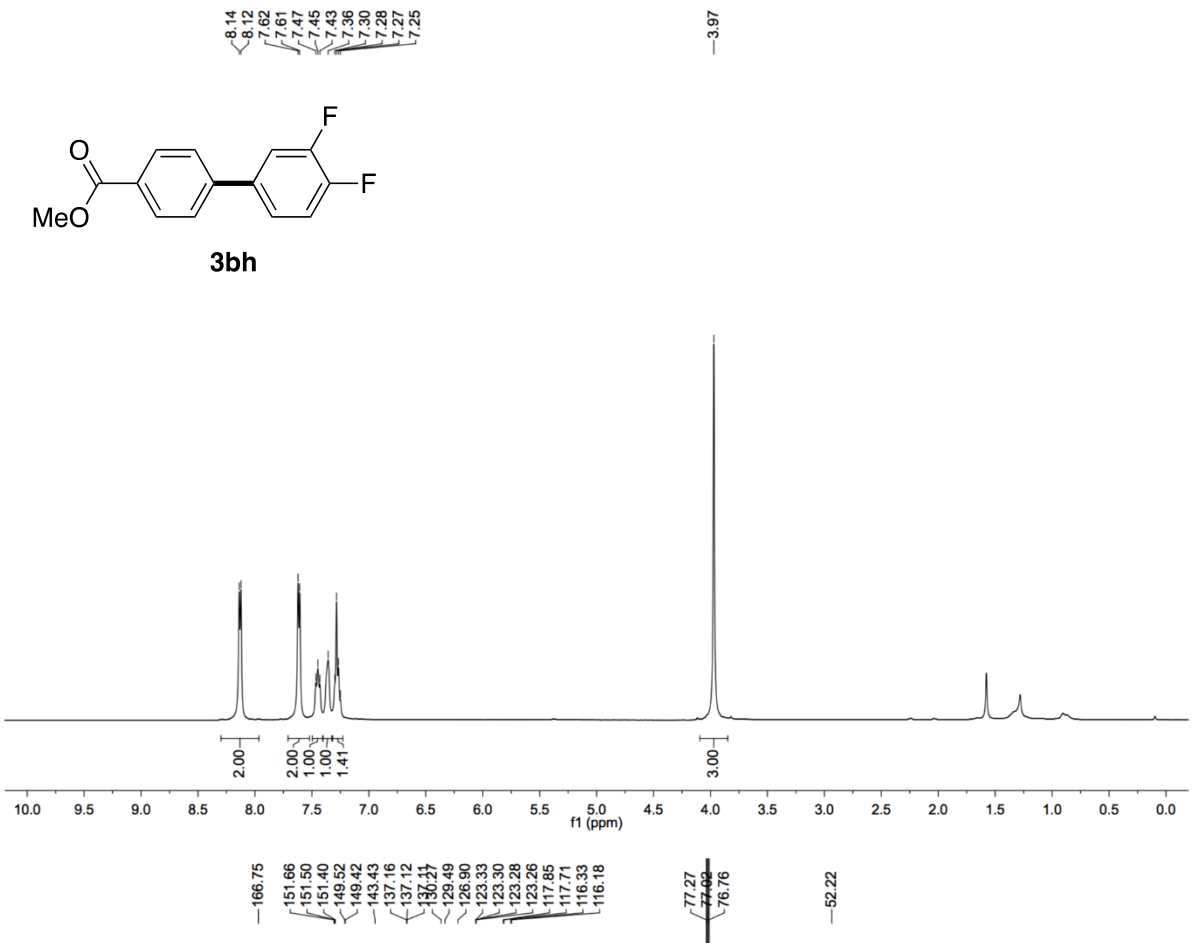

Figure S132. ^{13}C NMR spectrum of **3bh**, related to **Figure 4**

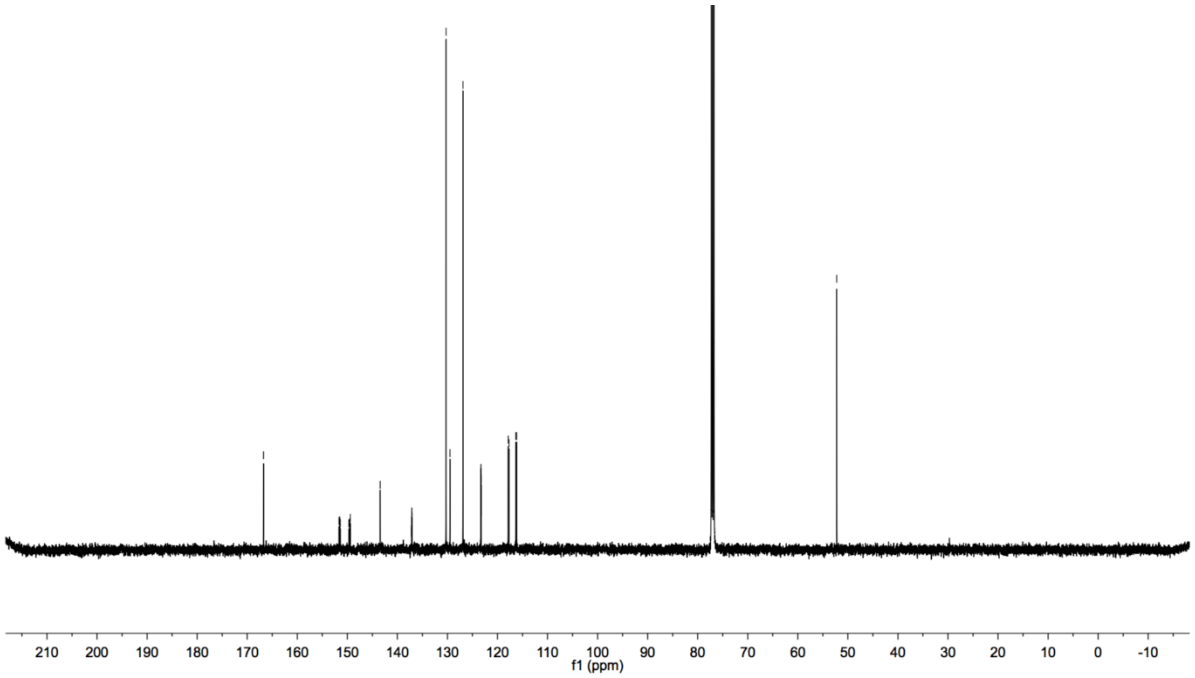

Figure S133. ^{19}F NMR spectrum of **3bh**, related to **Figure 4**

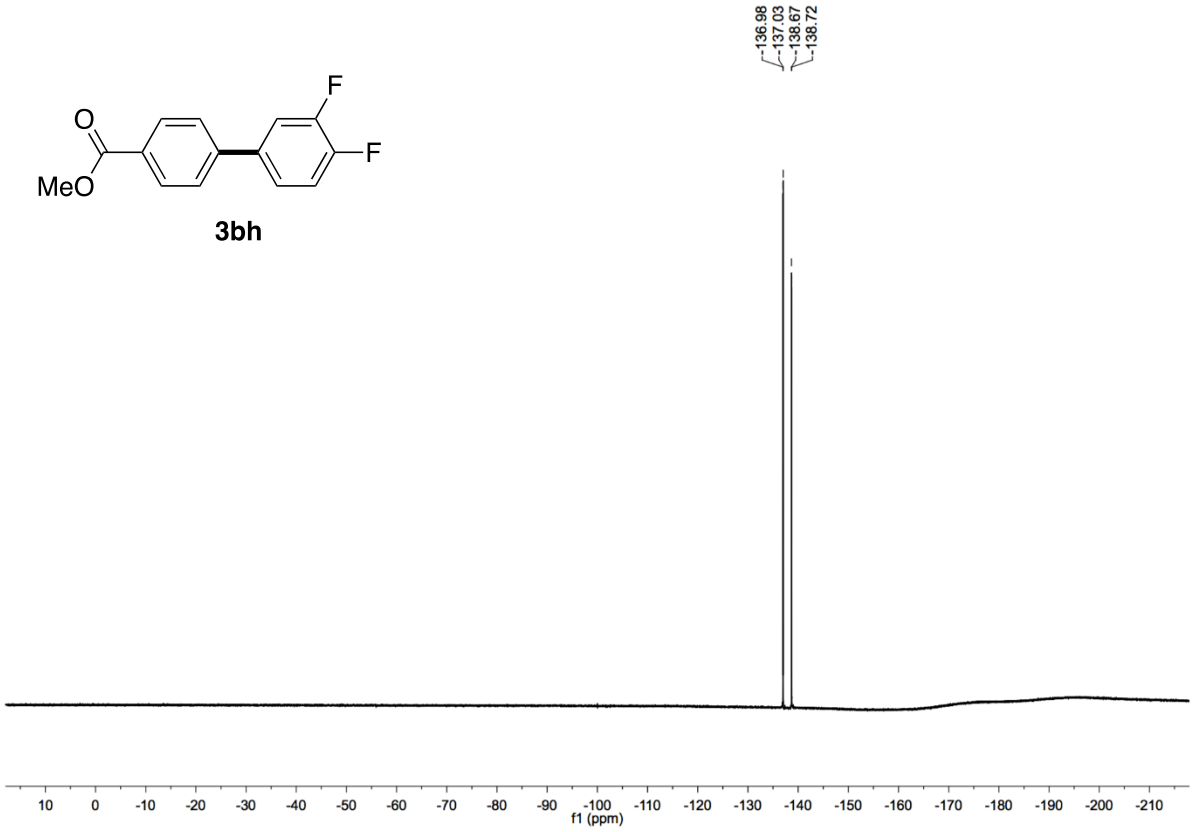

Figure S134. ^{1}H NMR spectrum of **3bi**, related to **Figure 4**

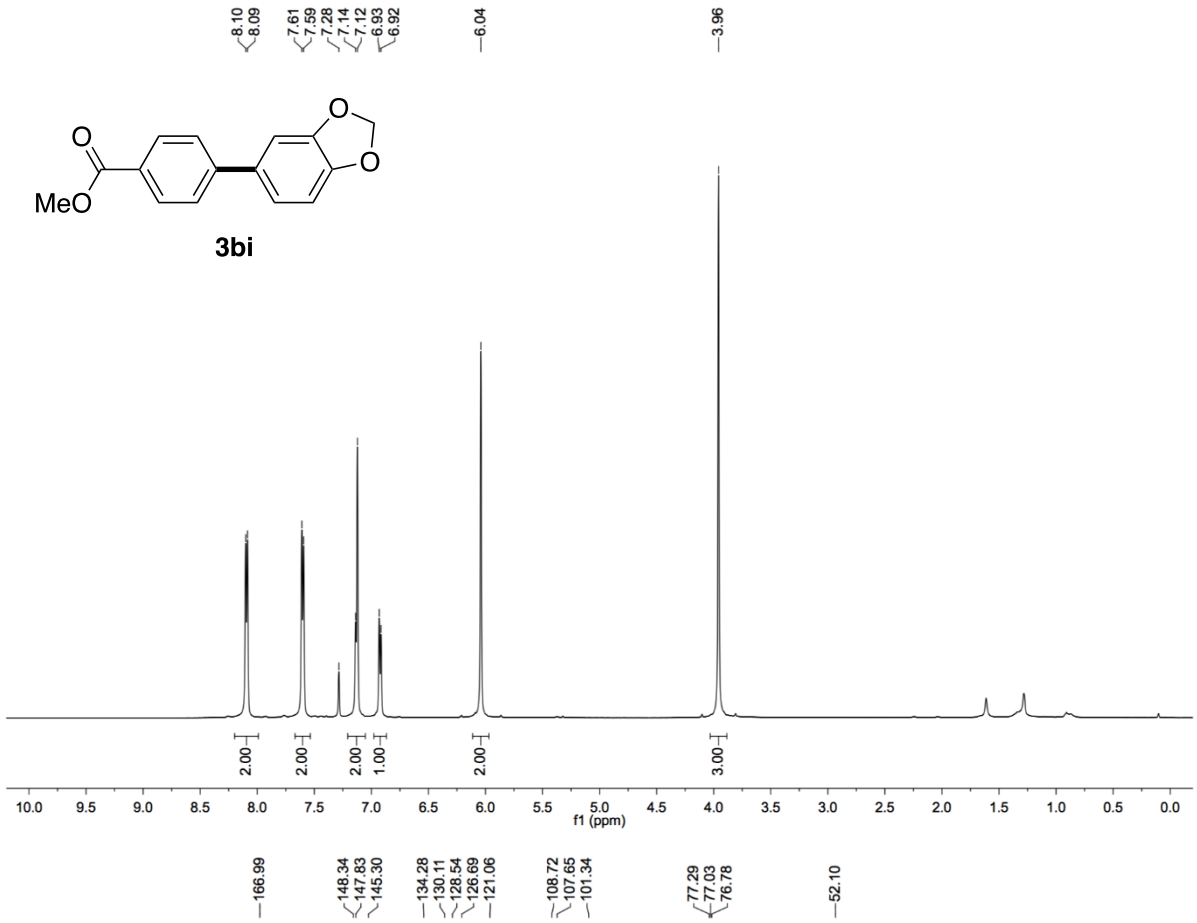

Figure S135. ^{13}C NMR spectrum of **3bi**, related to **Figure 4**

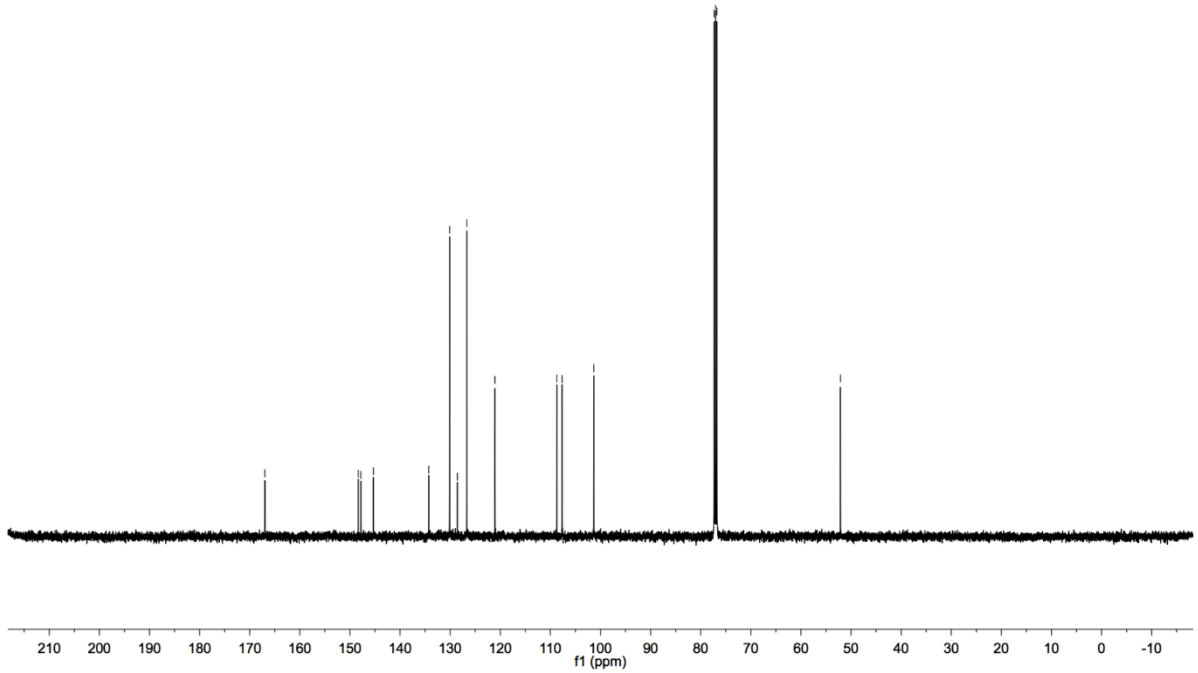

Figure S136. ^{1}H NMR spectrum of **3bj**, related to **Figure 4**

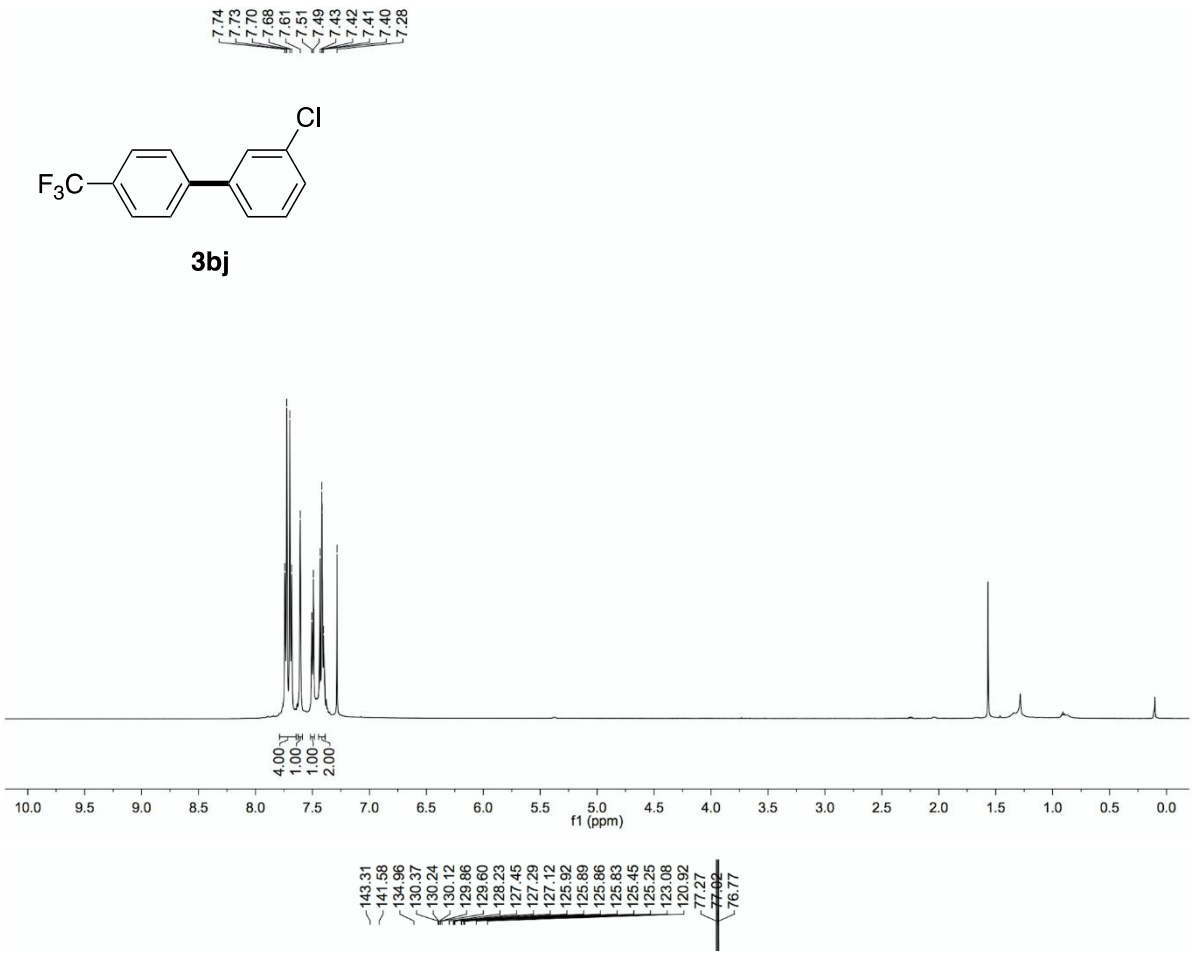

Figure S137. ^{13}C NMR spectrum of **3bj**, related to **Figure 4**

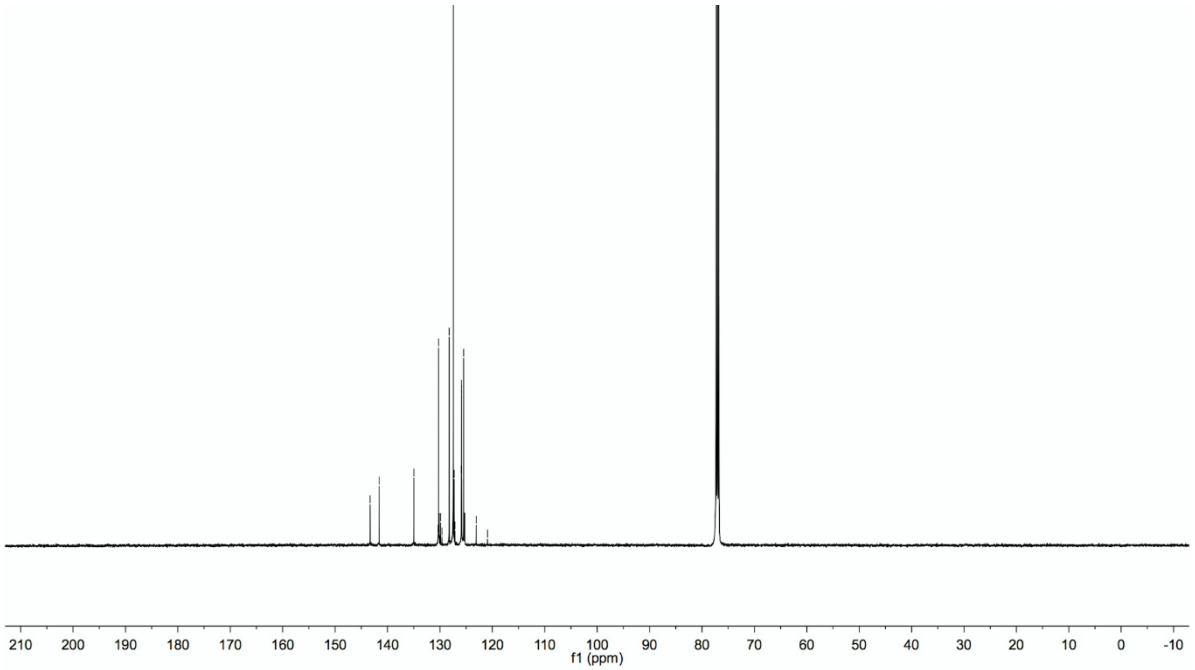

Figure S138. ^{1}H NMR spectrum of **3bj**, related to **Figure 4**

Figure S139. ^{1}H NMR spectrum of **3bk**, related to **Figure 4**

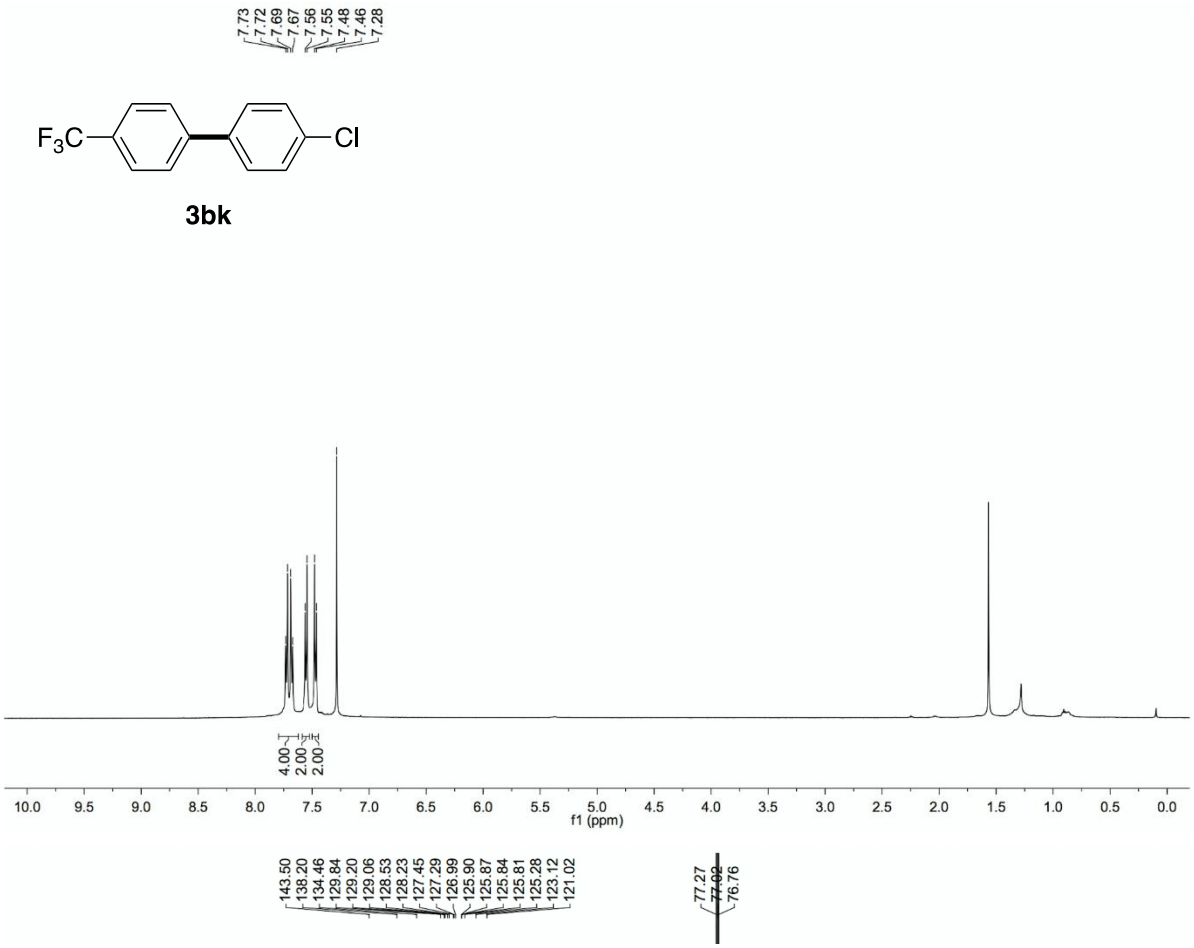

Figure S140. ^{13}C NMR spectrum of **3bk**, related to **Figure 4**

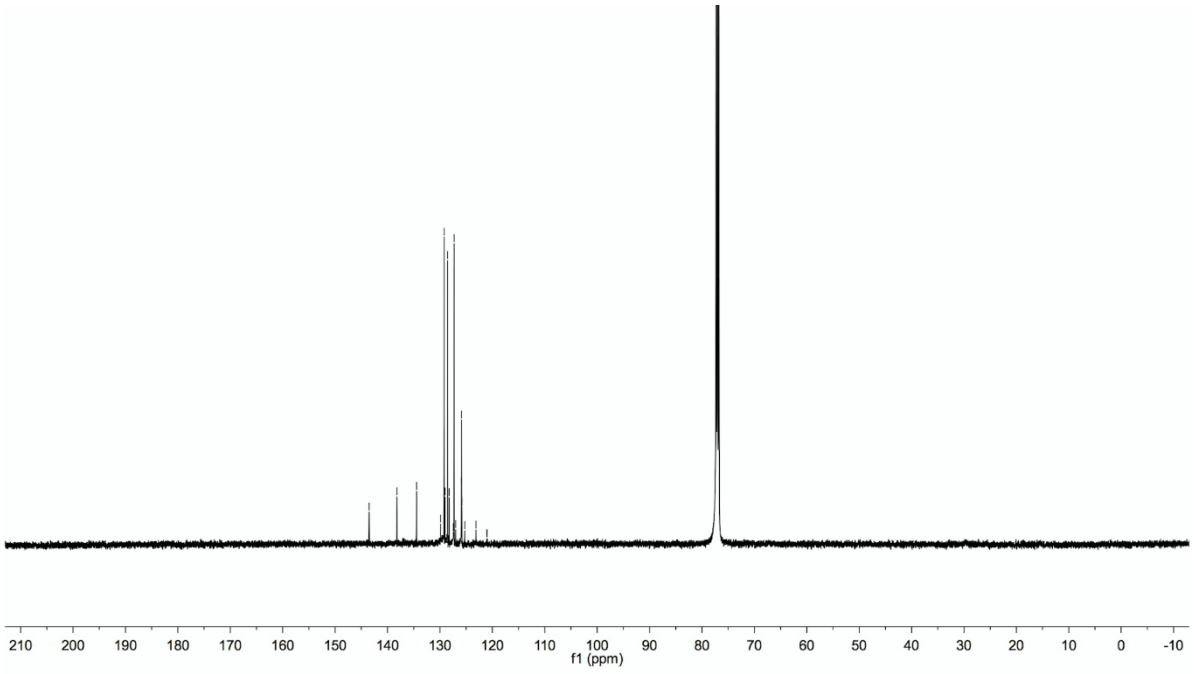

Figure S141. ^{1}H NMR spectrum of **3bk**, related to **Figure 4**

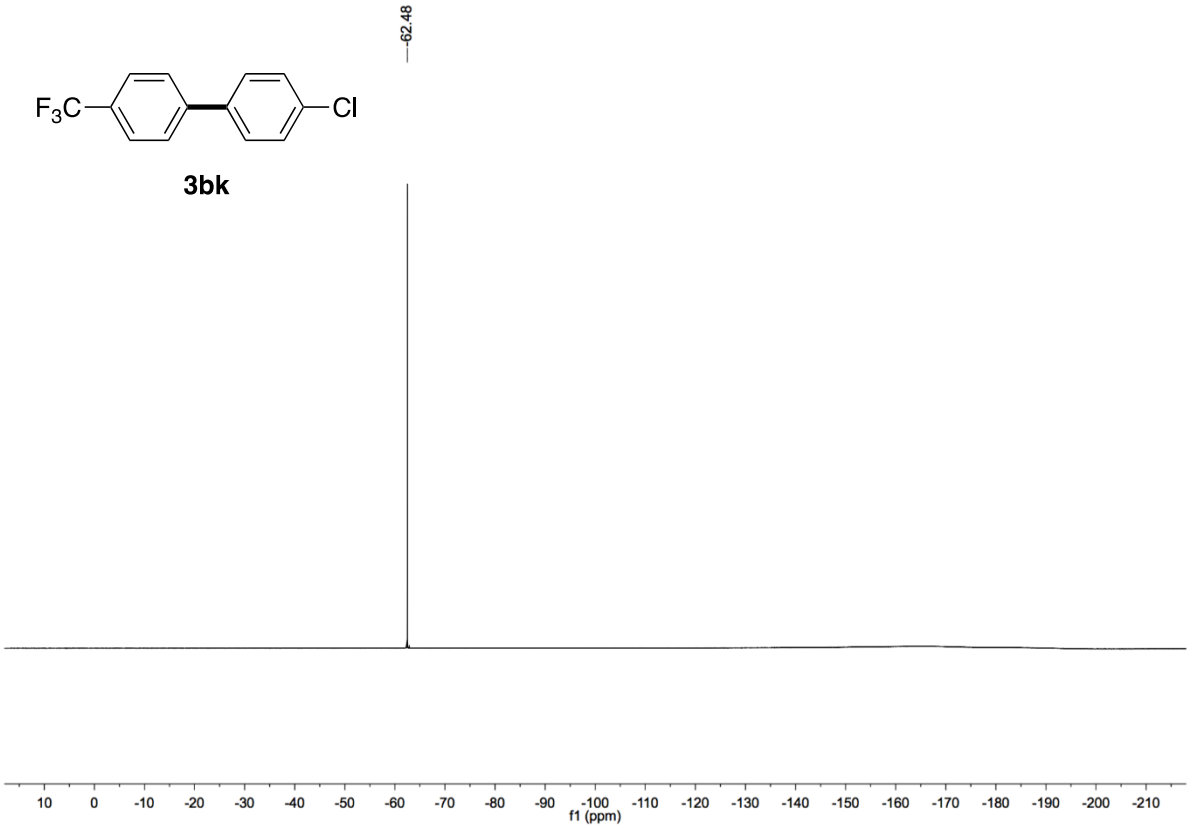

Figure S142. ^{1}H NMR spectrum of **3bl**, related to **Figure 4**

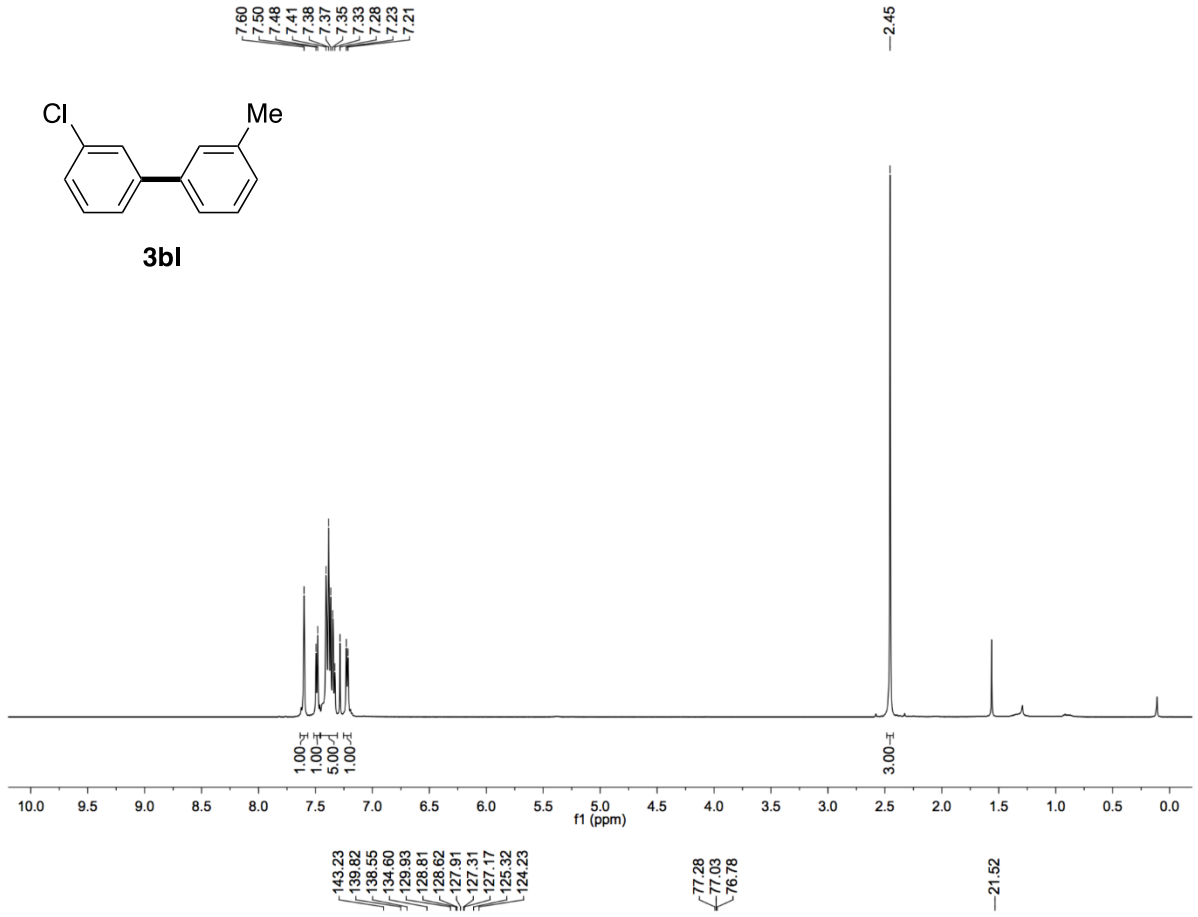

Figure S143. ^{13}C NMR spectrum of **3bl**, related to **Figure 4**

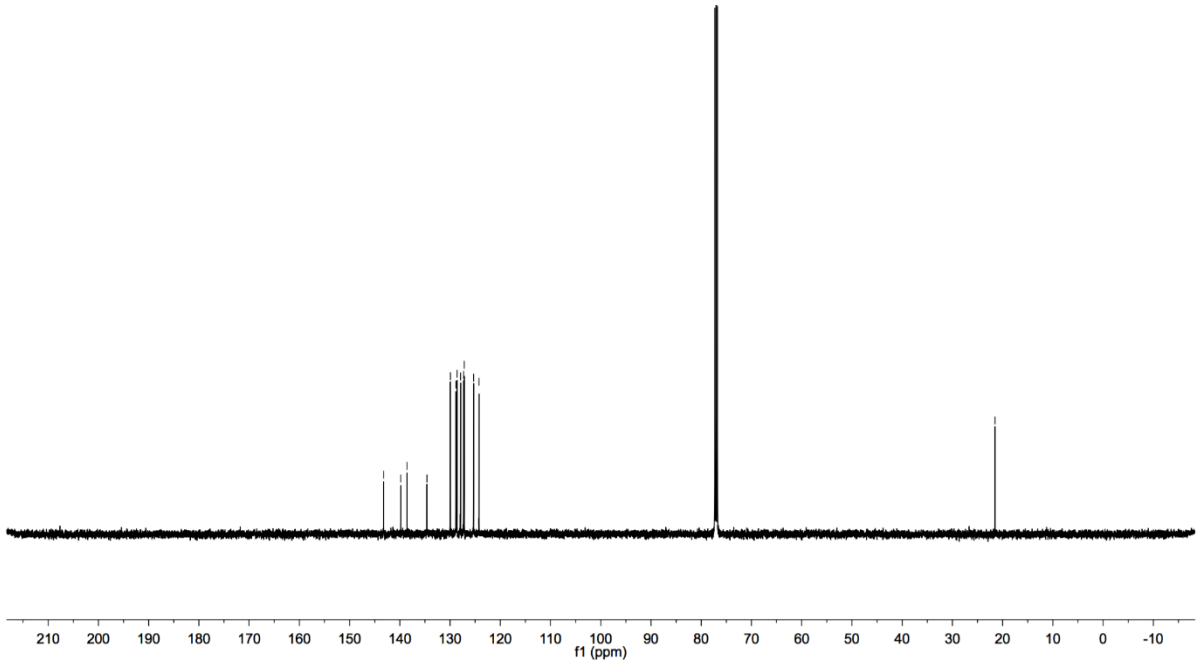

Figure S144. ^{1}H NMR spectrum of **3bm**, related to **Figure 4**

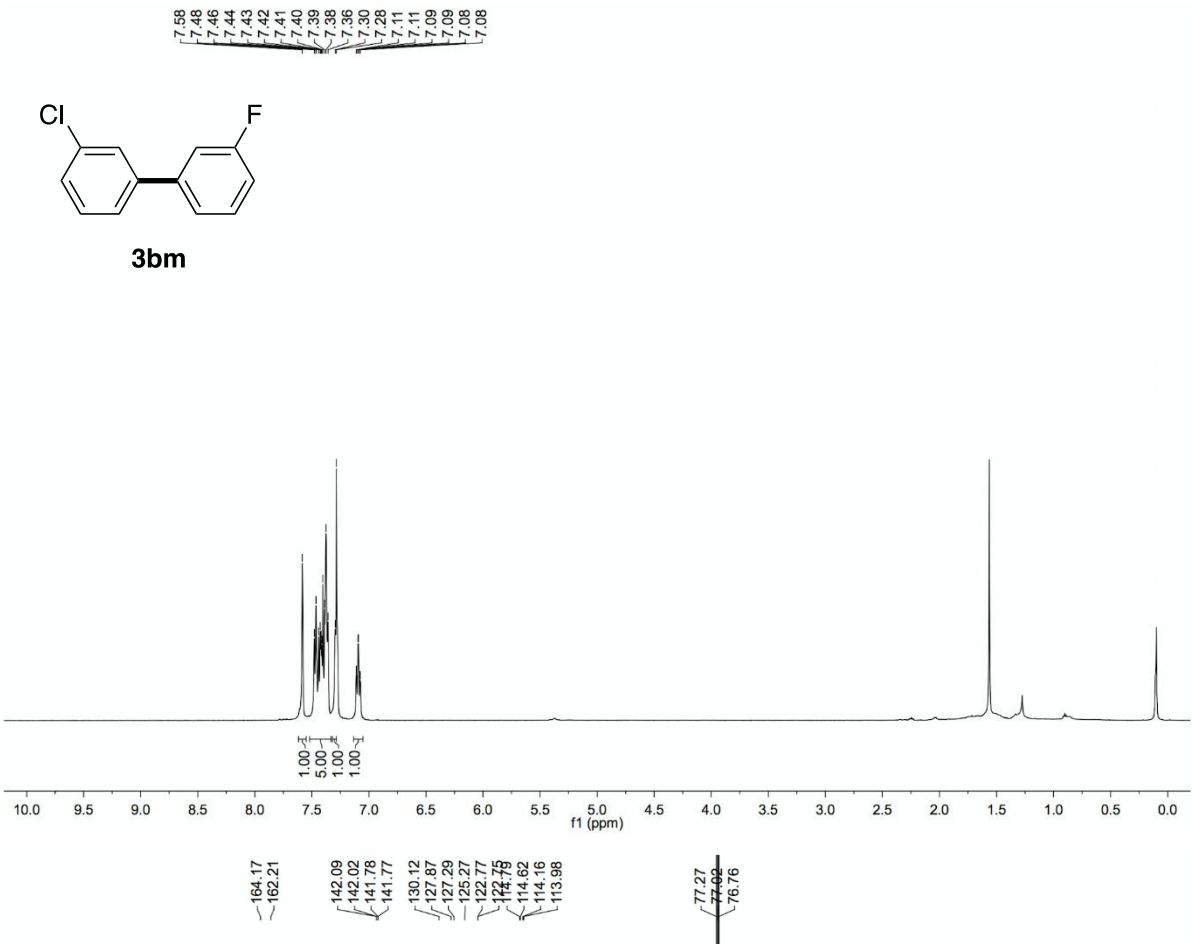

Figure S145. ^{13}C NMR spectrum of **3bm**, related to **Figure 4**

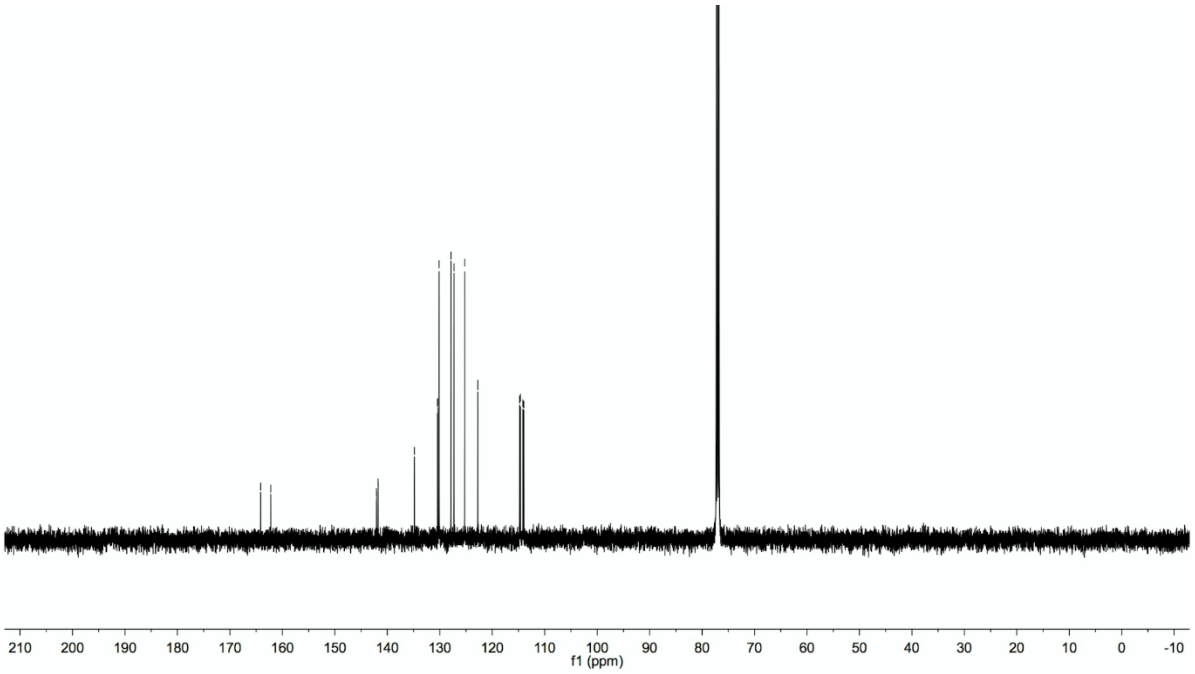

Figure S146. ^{19}F NMR spectrum of **3bm**, related to **Figure 4**

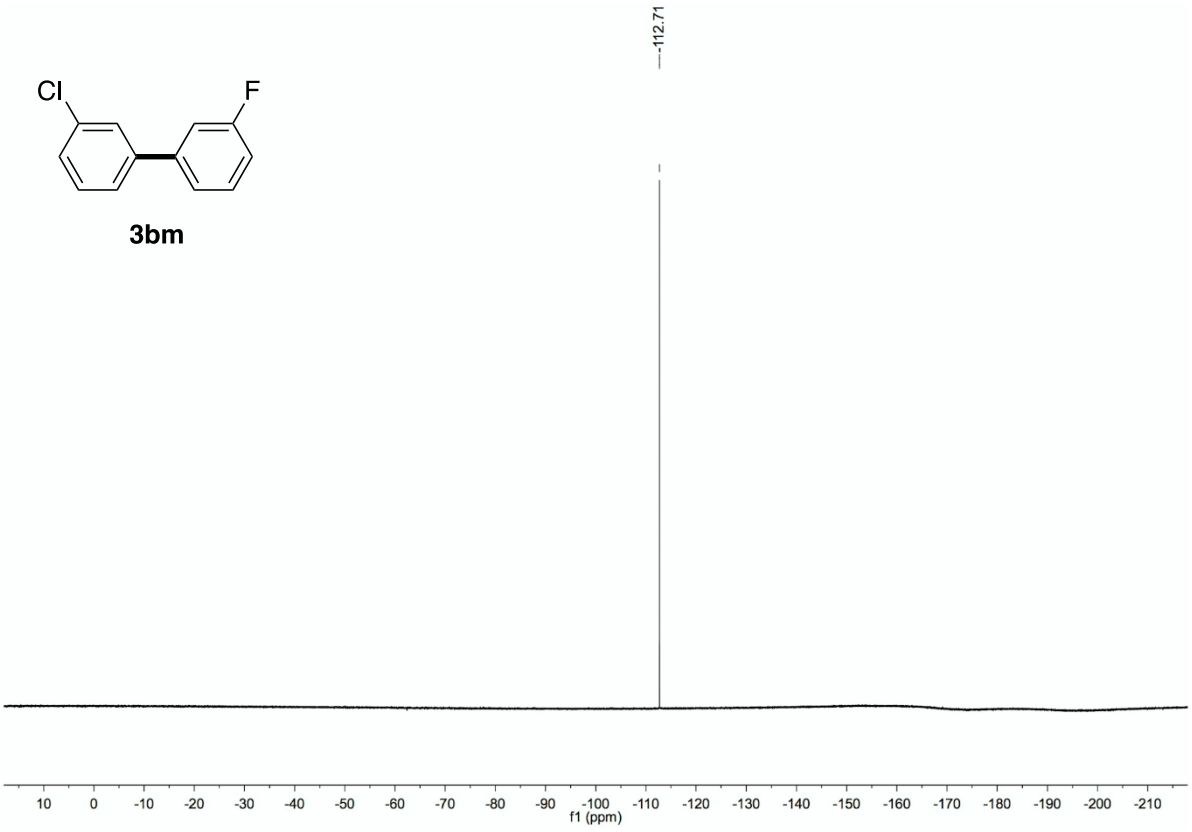

Figure S147. ^{1}H NMR spectrum of **3bn**, related to **Figure 4**

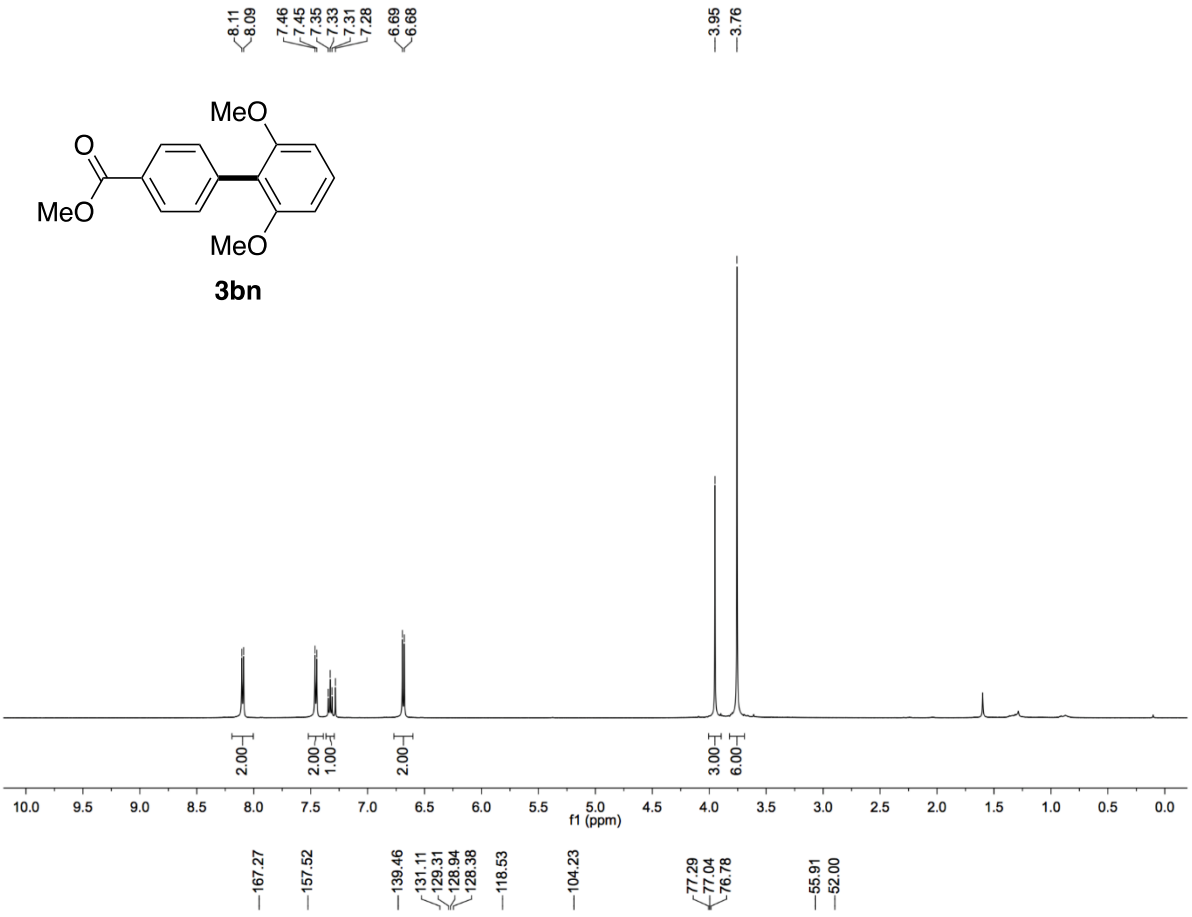

Figure S148. ^{13}C NMR spectrum of **3bn**, related to **Figure 4**

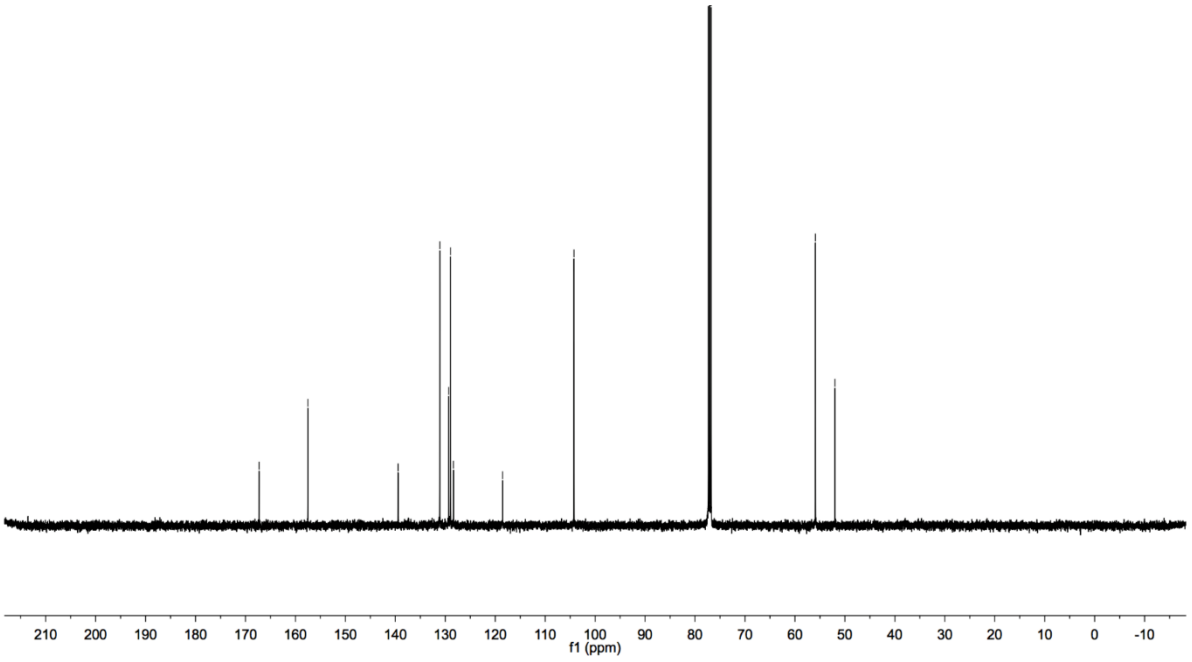

Figure S149. ^{1}H NMR spectrum of **3bo**, related to **Figure 4**

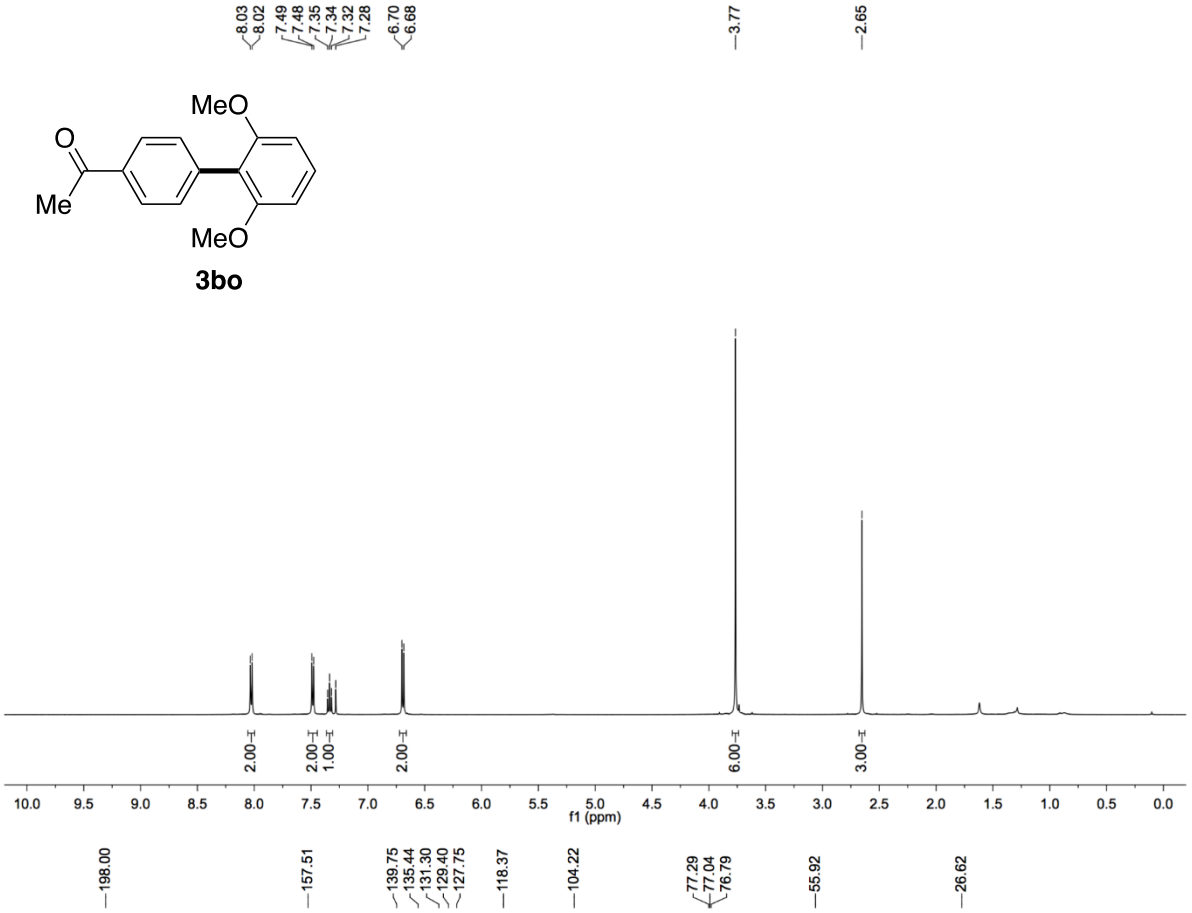

Figure S150. ^{13}C NMR spectrum of **3bo**, related to **Figure 4**

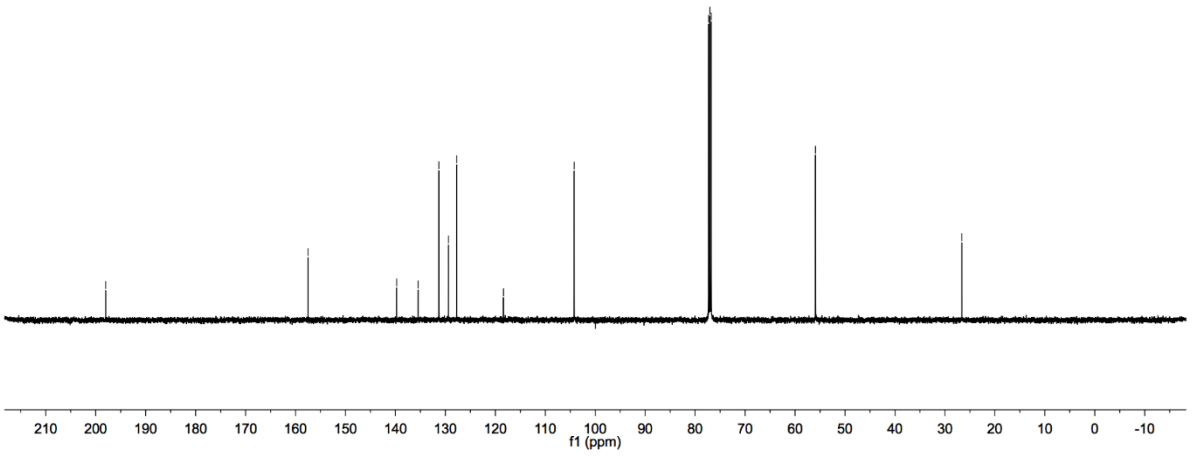

Figure S151. ^{1}H NMR spectrum of **3bp**, related to **Figure 4**

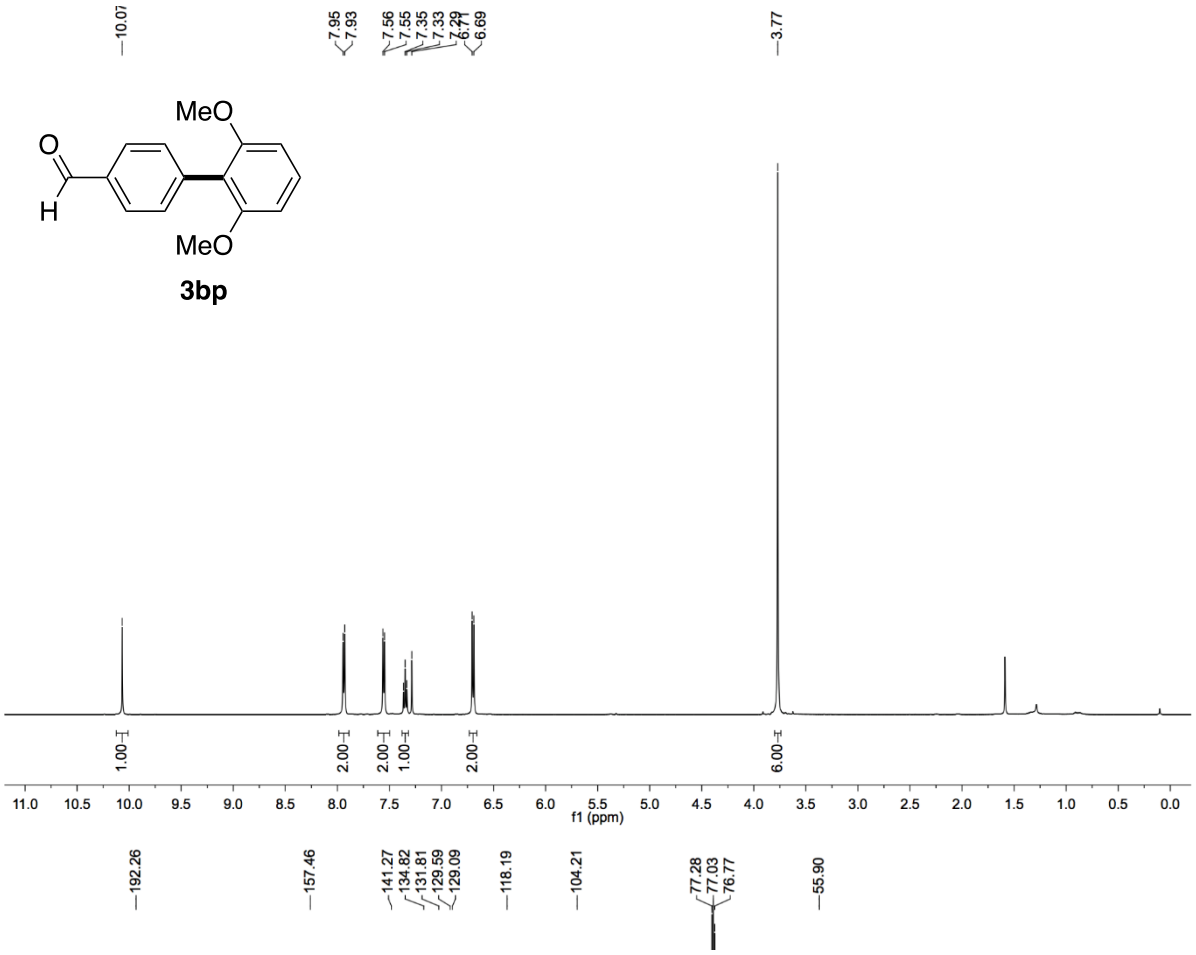

Figure S152. ^{13}C NMR spectrum of **3bp**, related to **Figure 4**

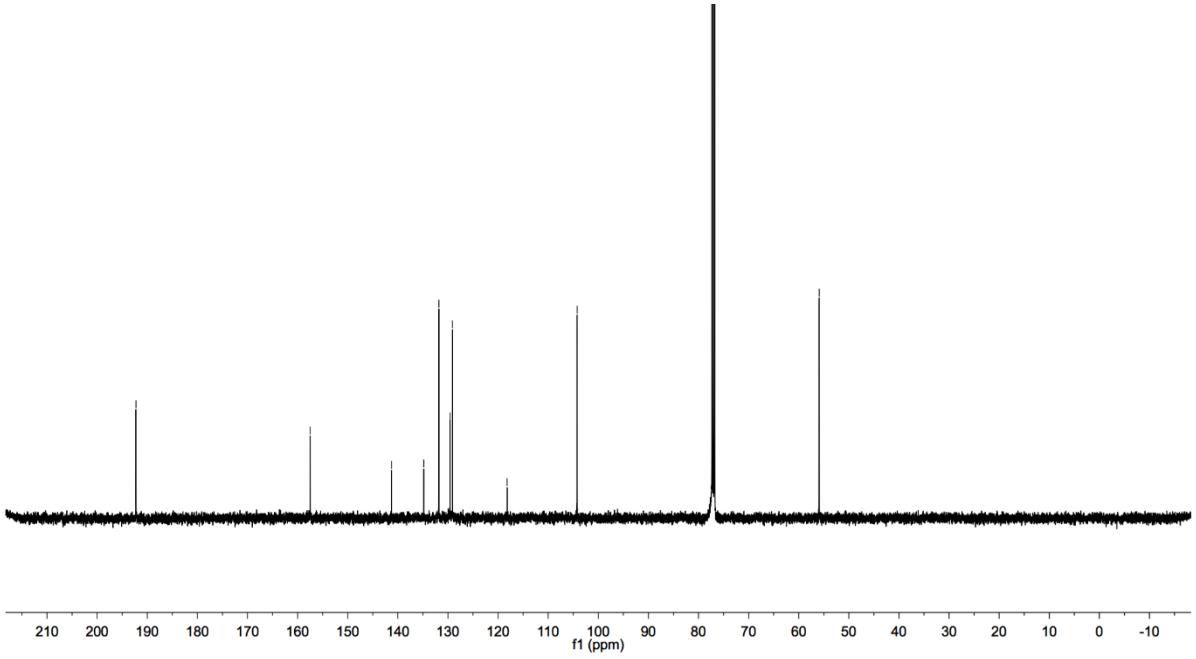

Figure S153. ^{1}H NMR spectrum of **3bq**, related to **Figure 4**

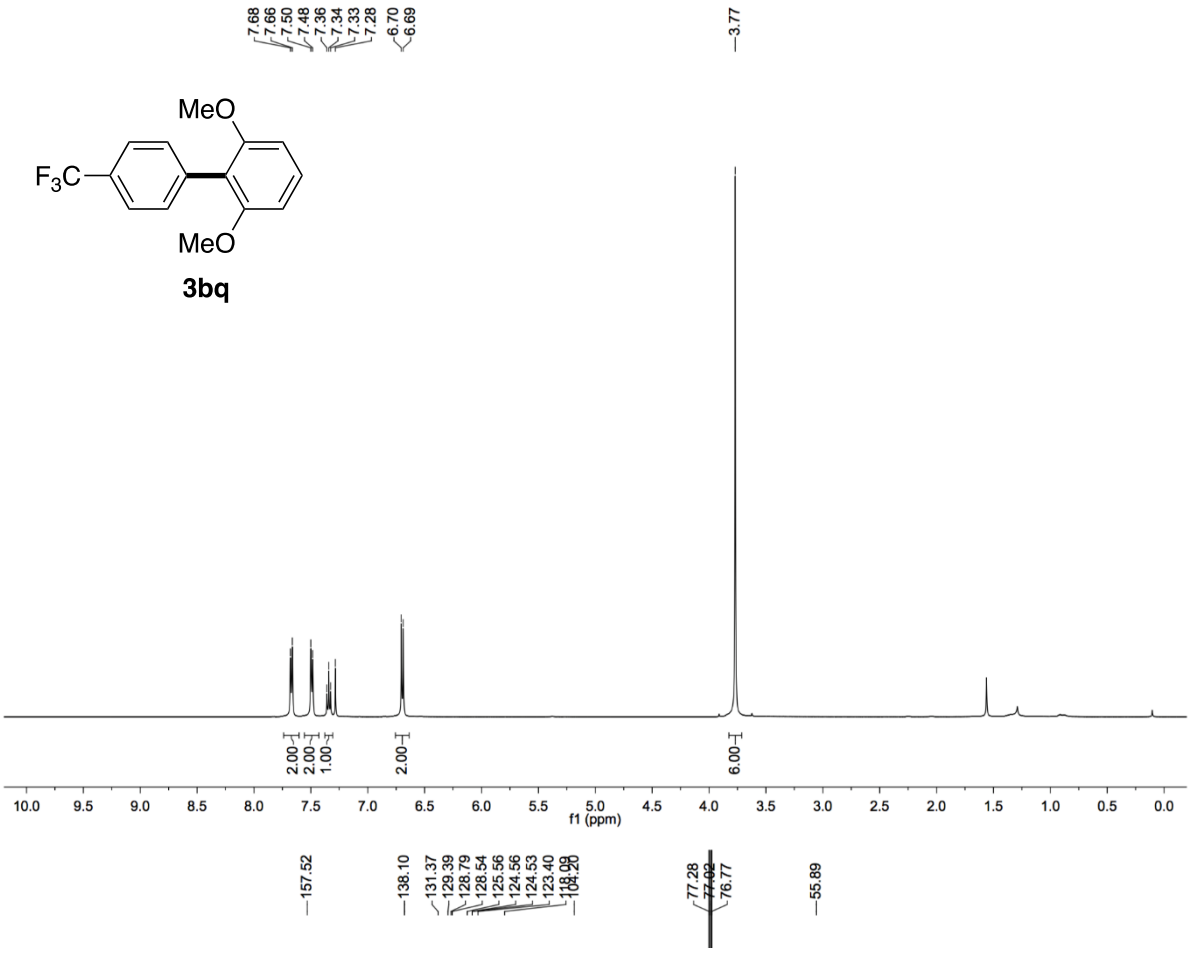

Figure S154. ^{13}C NMR spectrum of **3bq**, related to **Figure 4**

Figure S155. ^{19}F NMR spectrum of **3bq**, related to **Figure 4**

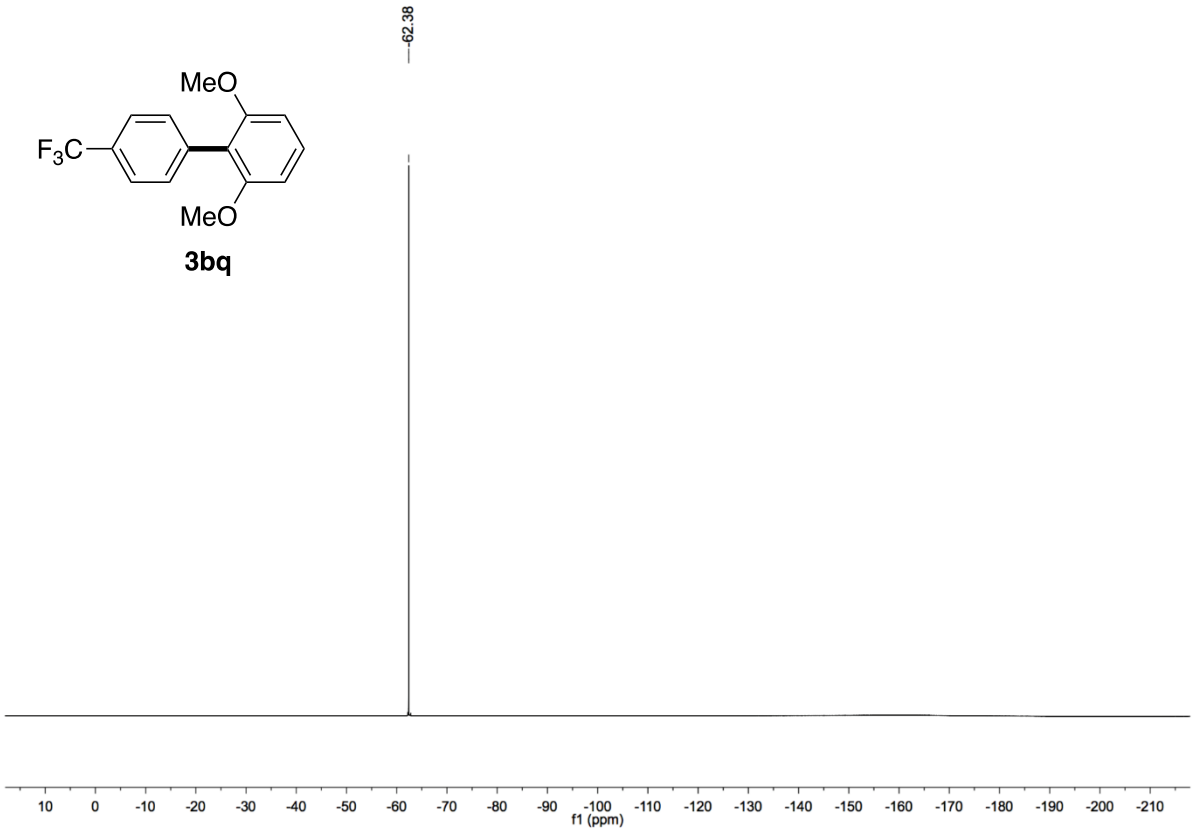

Figure S156. ^{1}H NMR spectrum of **3br**, related to **Figure 4**

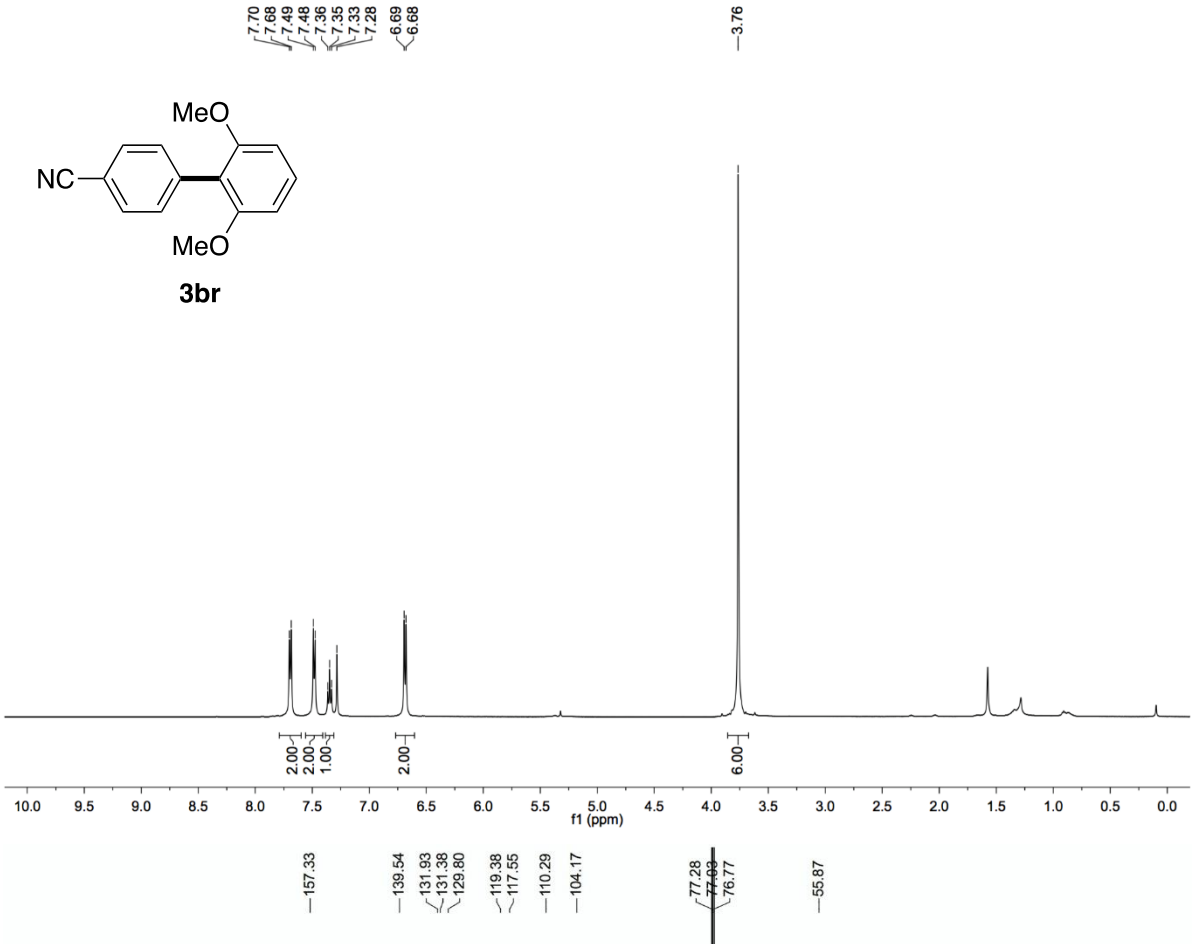

Figure S157. ^{13}C NMR spectrum of **3br**, related to **Figure 4**

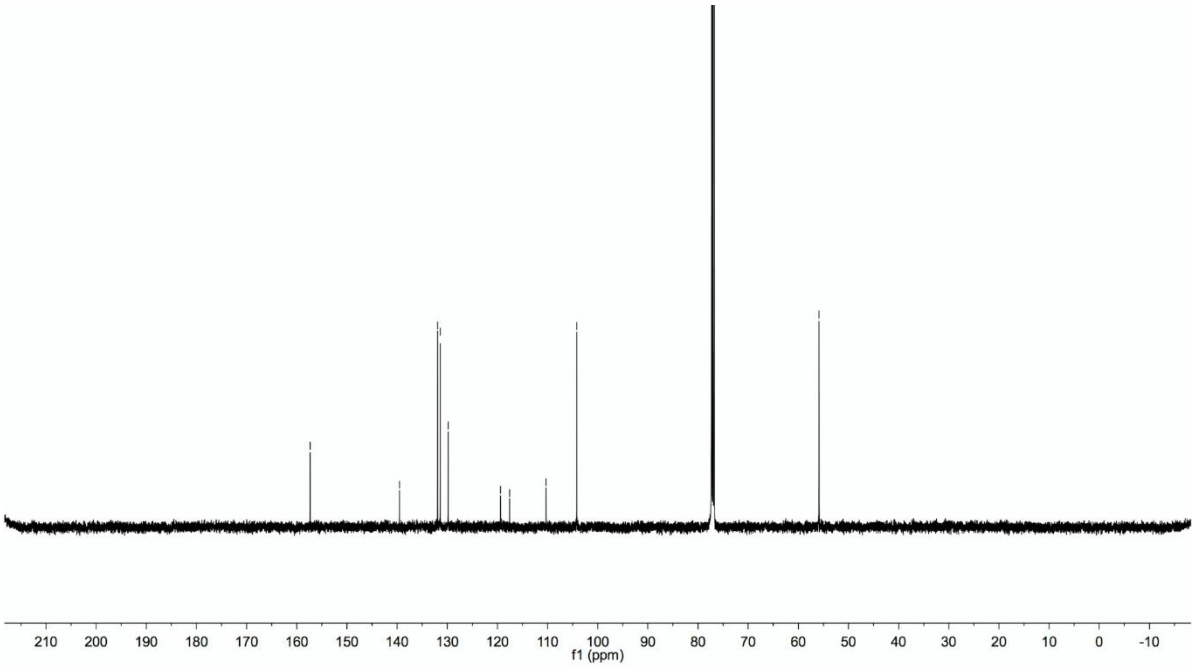

Figure S158. ^{1}H NMR spectrum of **3bs**, related to **Figure 4**

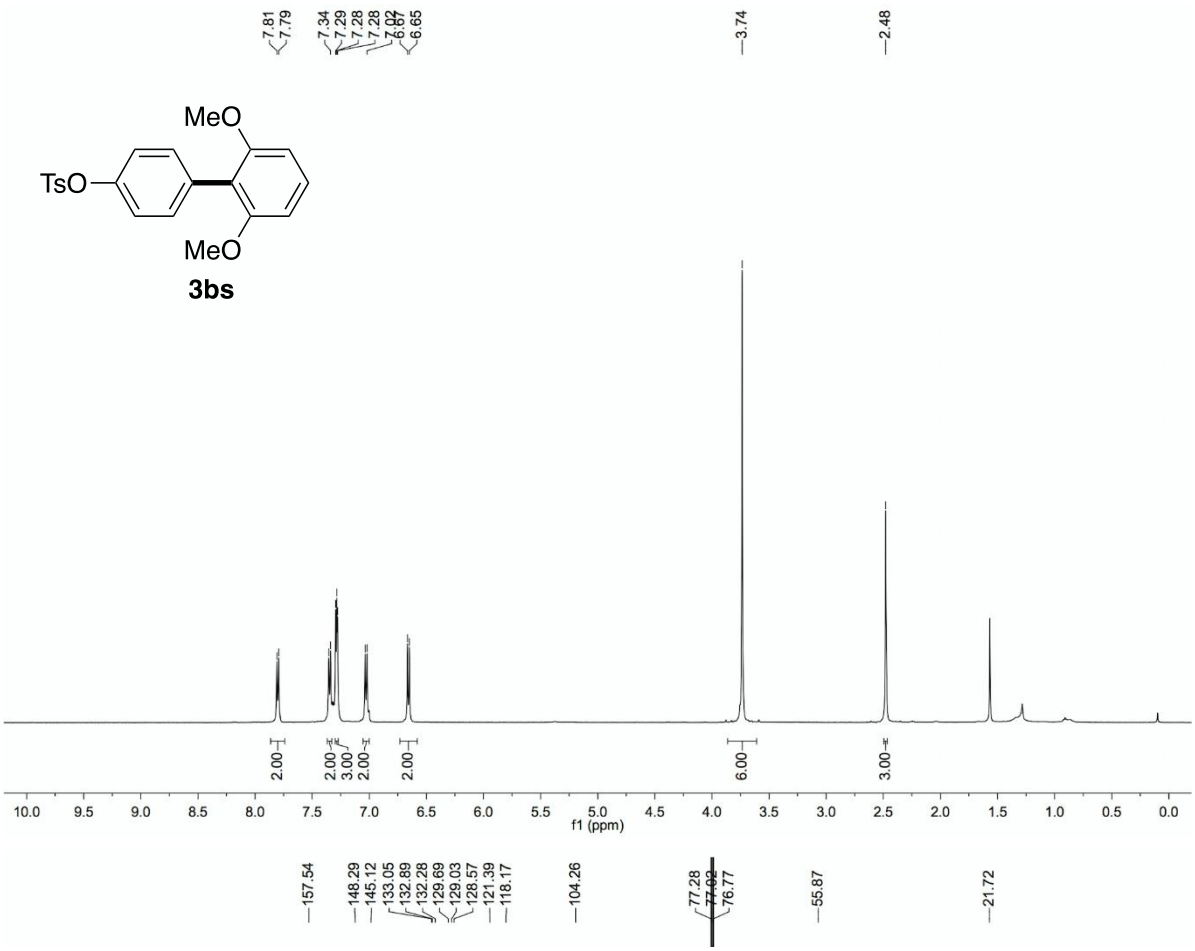

Figure S159. ^{13}C NMR spectrum of **3bs**, related to **Figure 4**

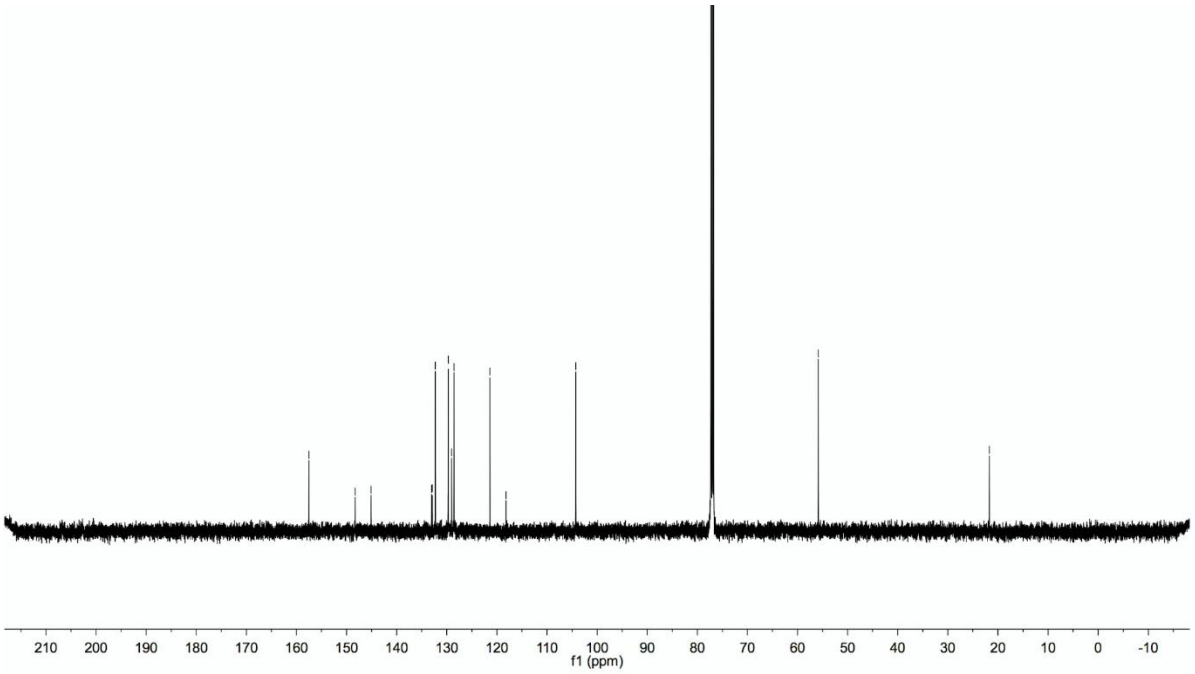

Figure S160. ^{1}H NMR spectrum of **3bt**, related to **Figure 4**

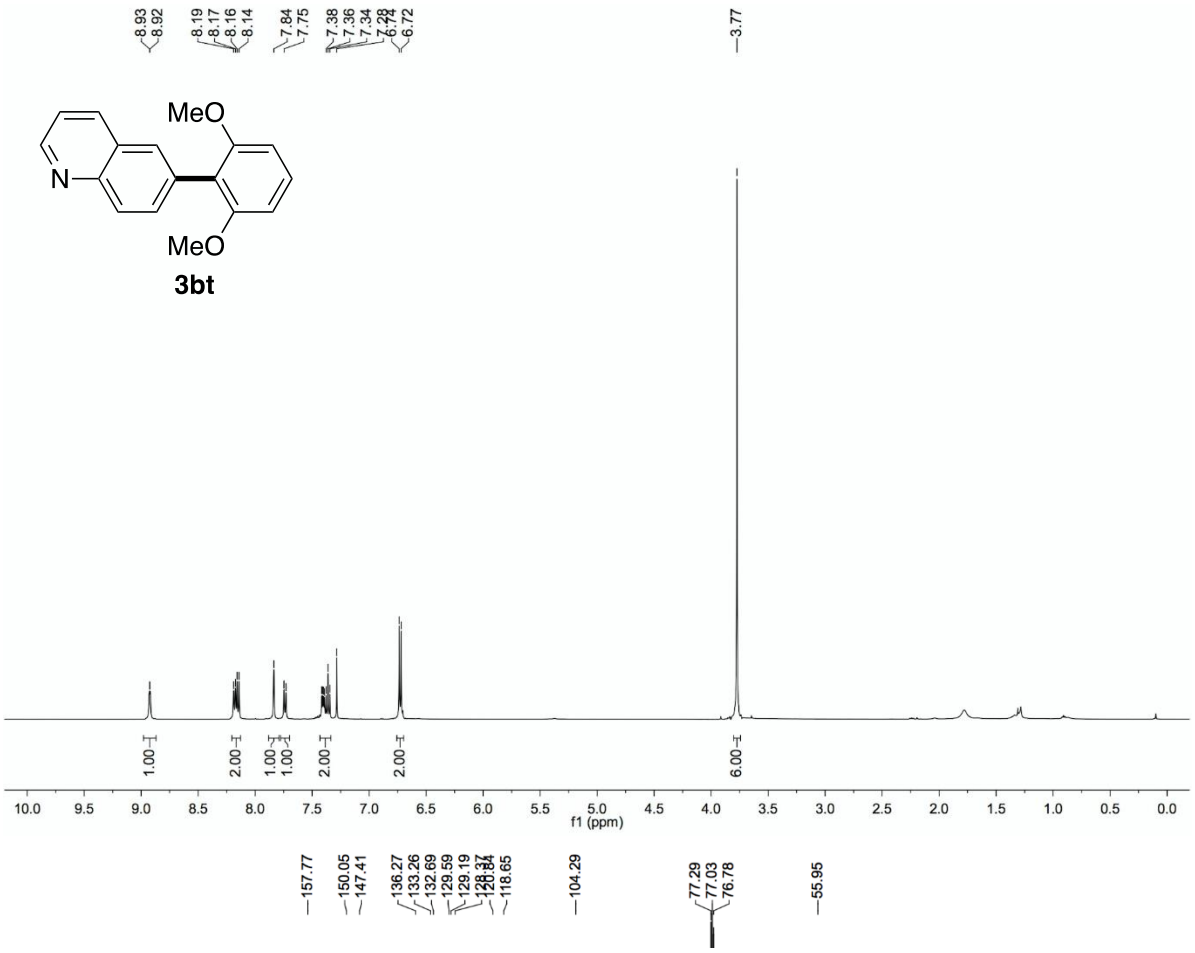

Figure S161. ^{13}C NMR spectrum of **3bt**, related to **Figure 4**

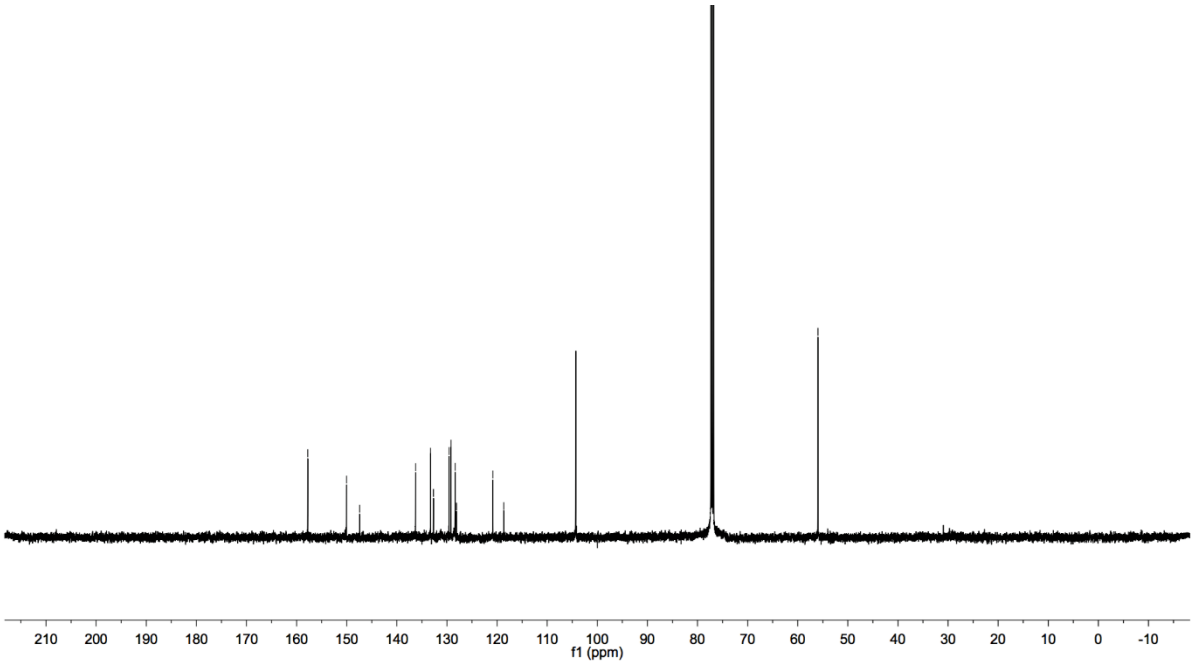

Figure S162. ^{1}H NMR spectrum of **3bu**, related to **Figure 4**

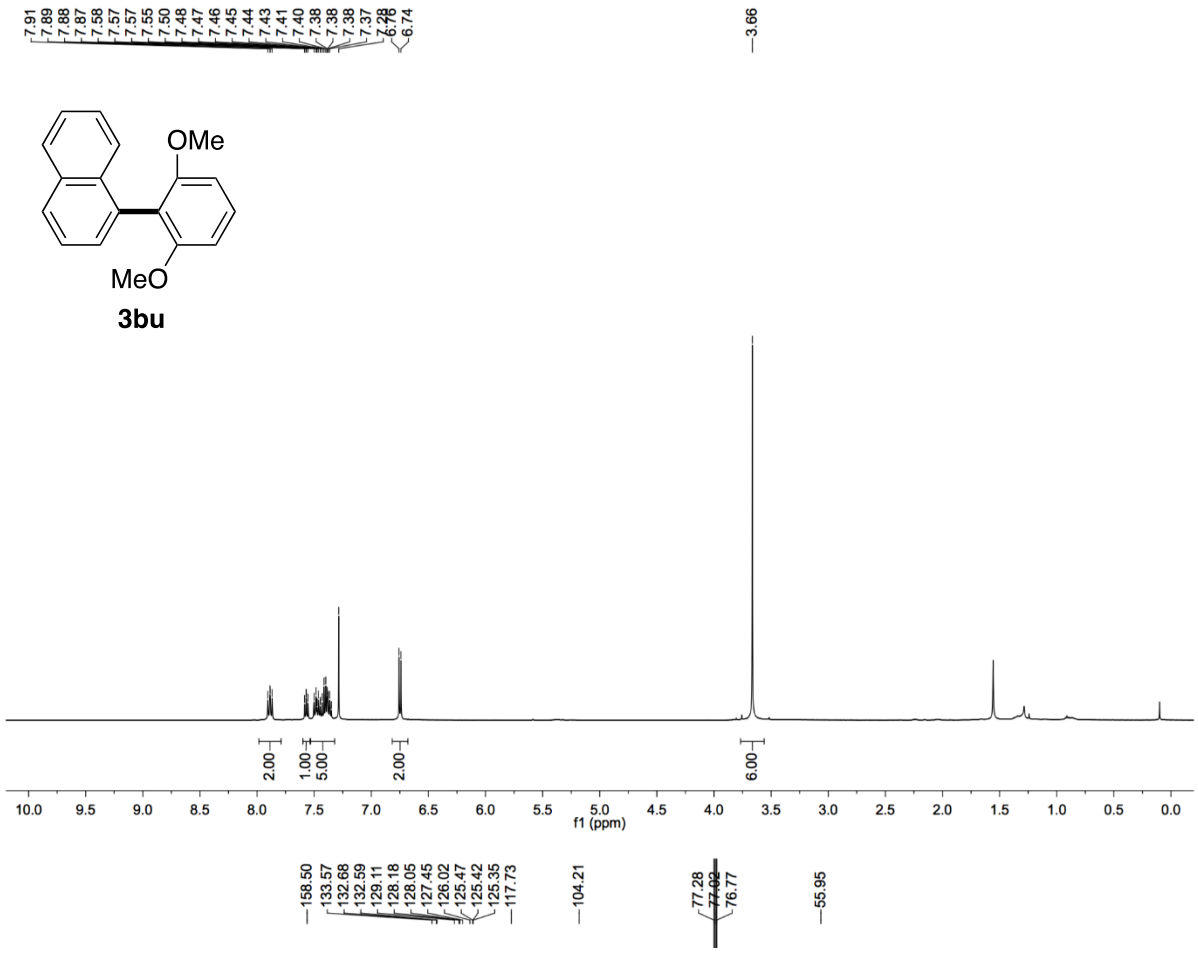

Figure S163. ^{13}C NMR spectrum of **3bu**, related to **Figure 4**

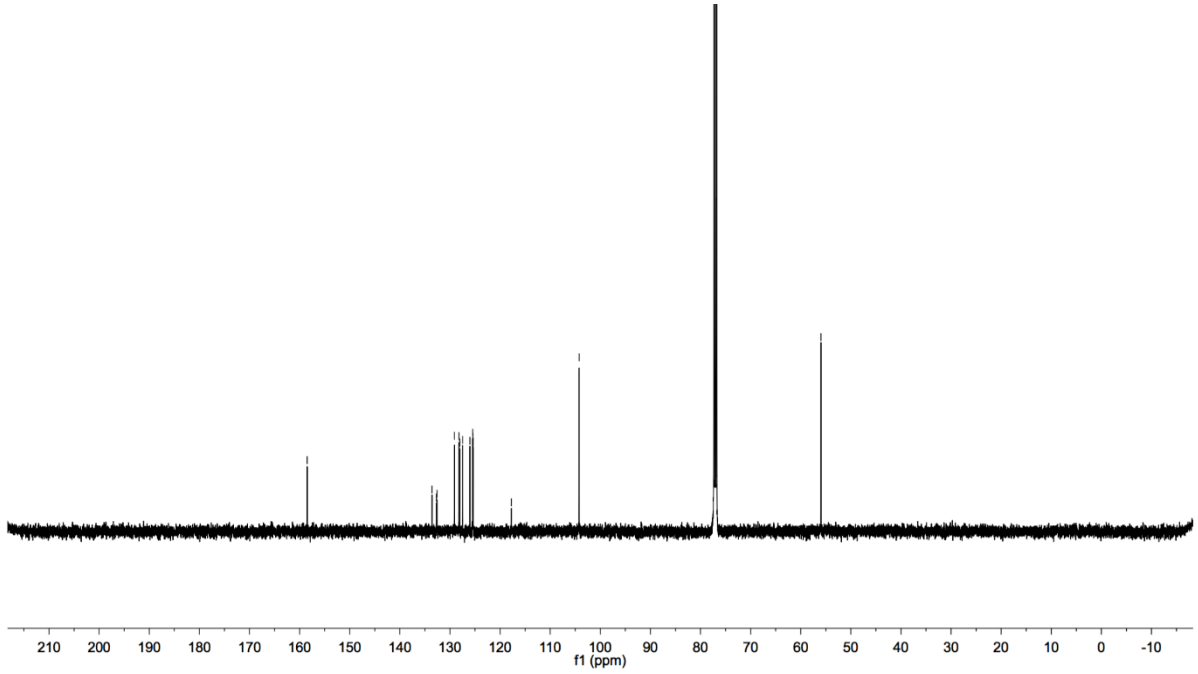

Figure S164. ^{1}H NMR spectrum of **3bv**, related to **Figure 4**

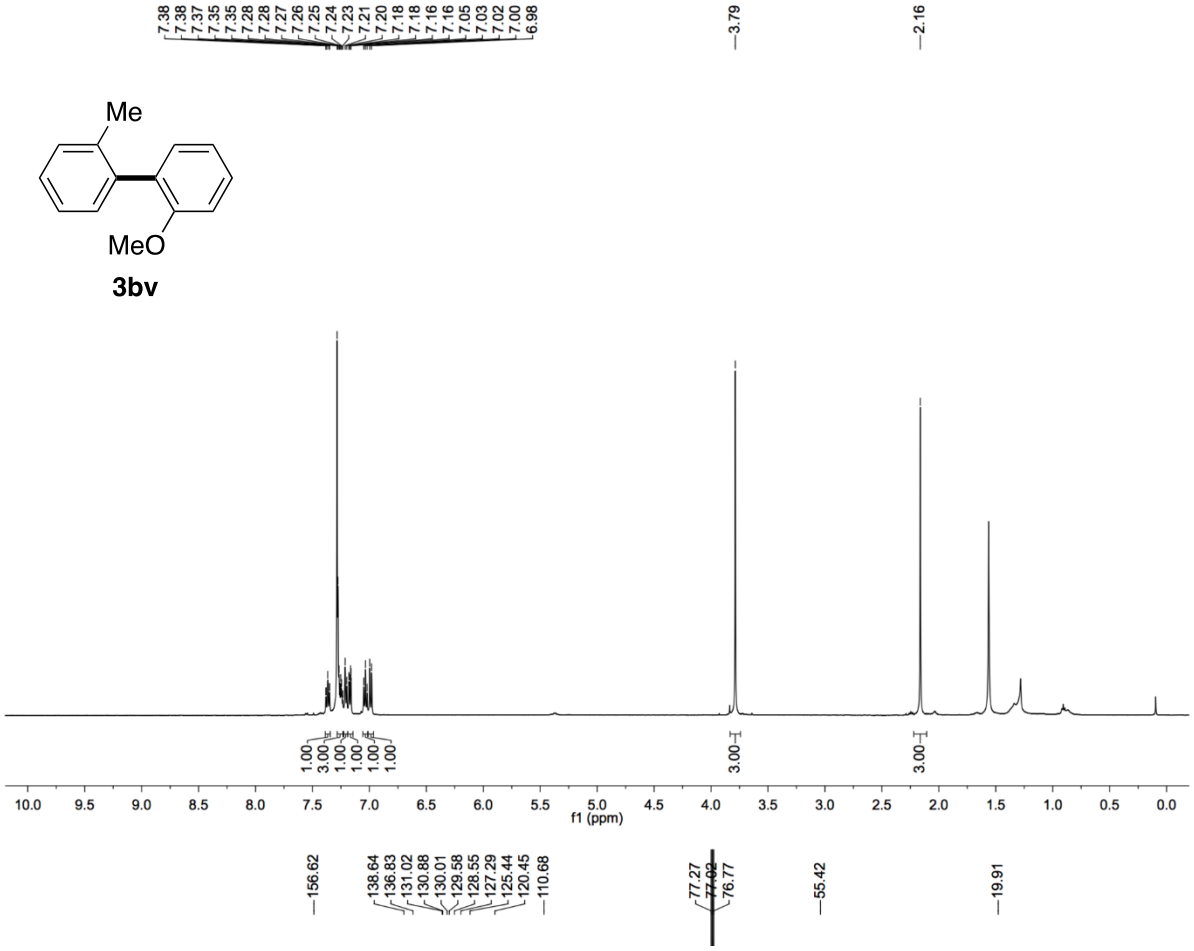

Figure S165. ^{13}C NMR spectrum of **3bv**, related to **Figure 4**

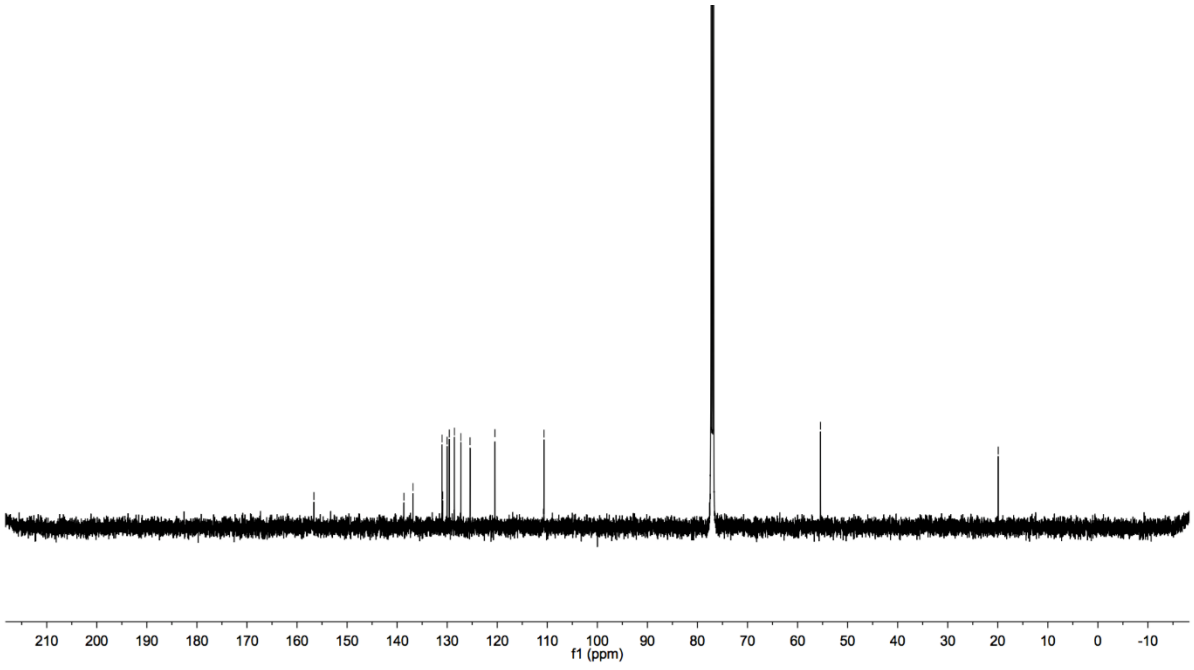

Figure S166. ^{1}H NMR spectrum of **3bw**, related to **Figure 4**

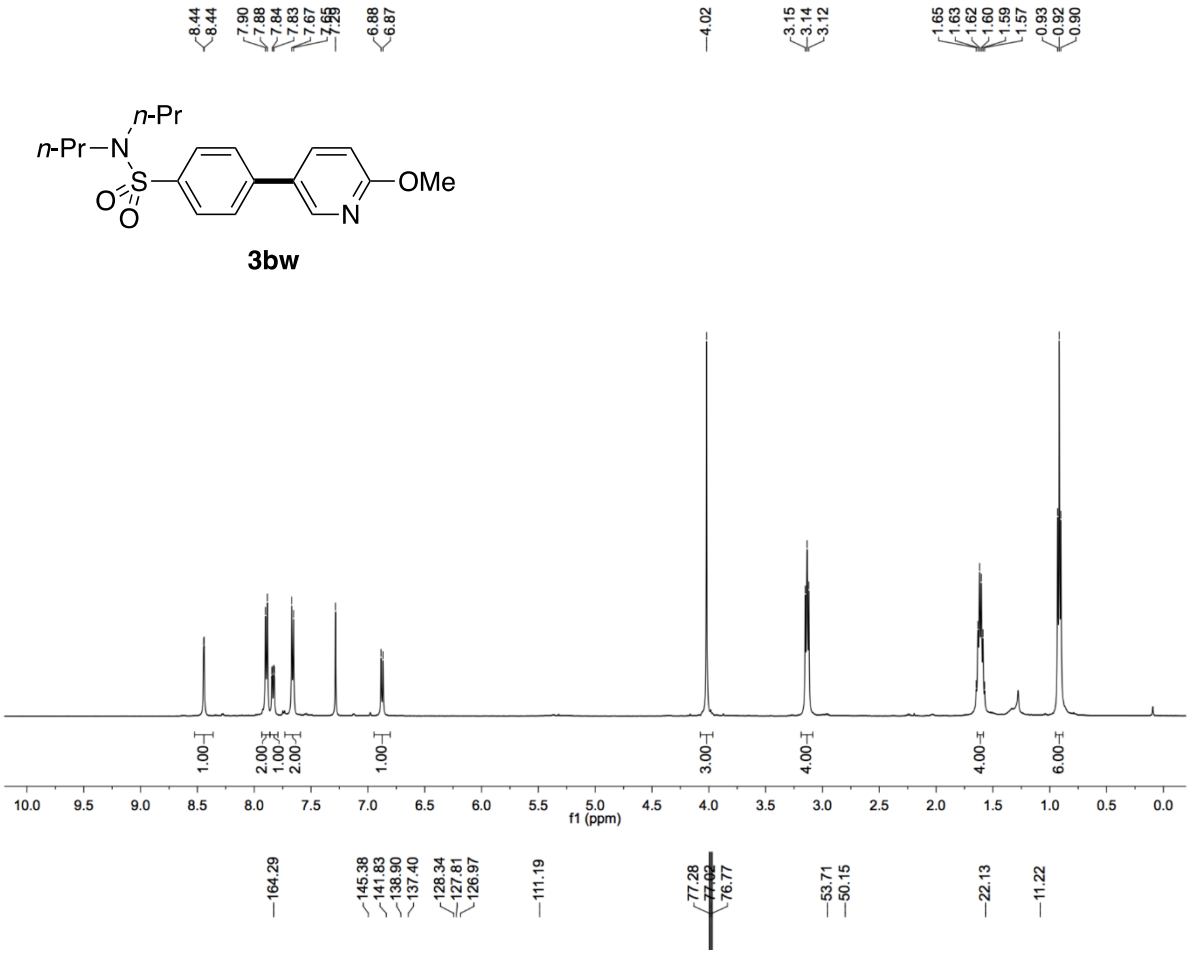

Figure S167. ^{13}C NMR spectrum of **3bw**, related to **Figure 4**

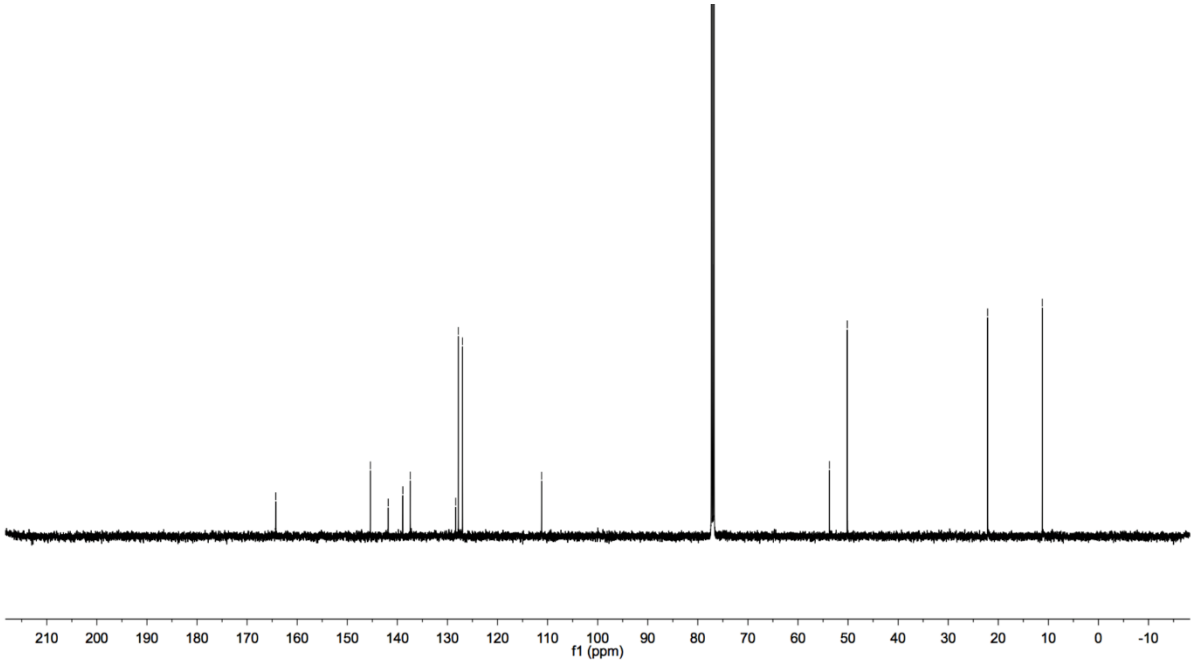

Figure S168. ^{1}H NMR spectrum of **3bx**, related to **Figure 4**

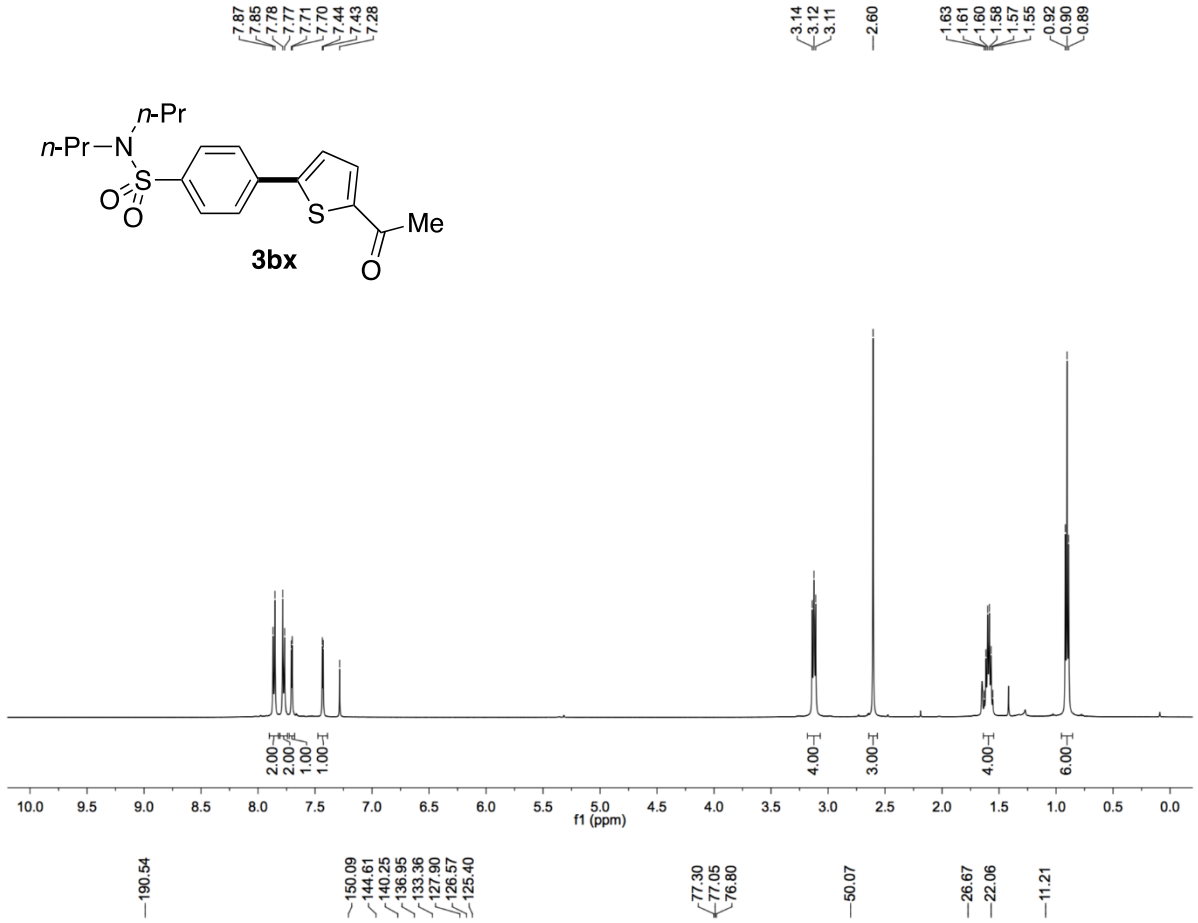

Figure S169. ^{13}C NMR spectrum of **3bx**, related to **Figure 4**

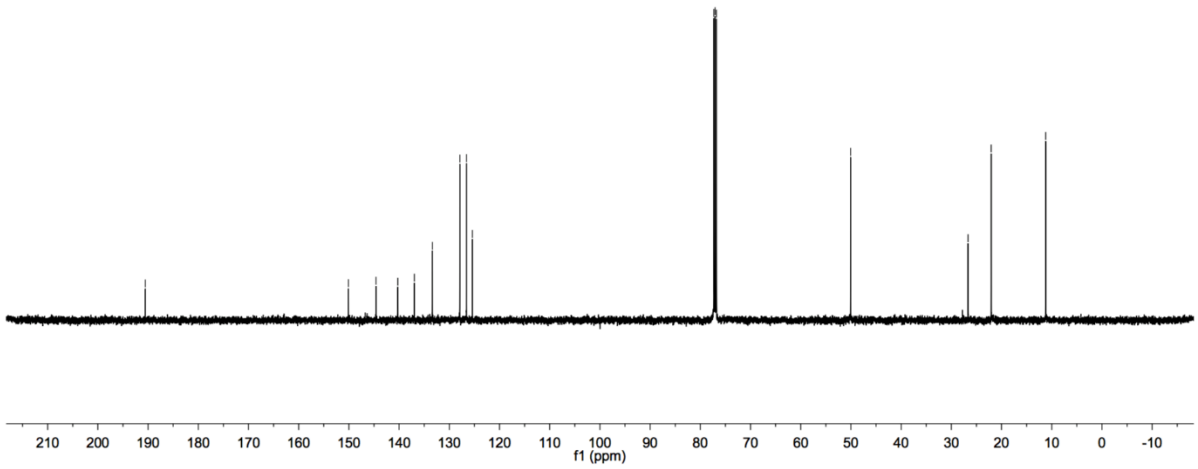

Figure S170. ^{1}H NMR spectrum of **3by**, related to **Figure 4**

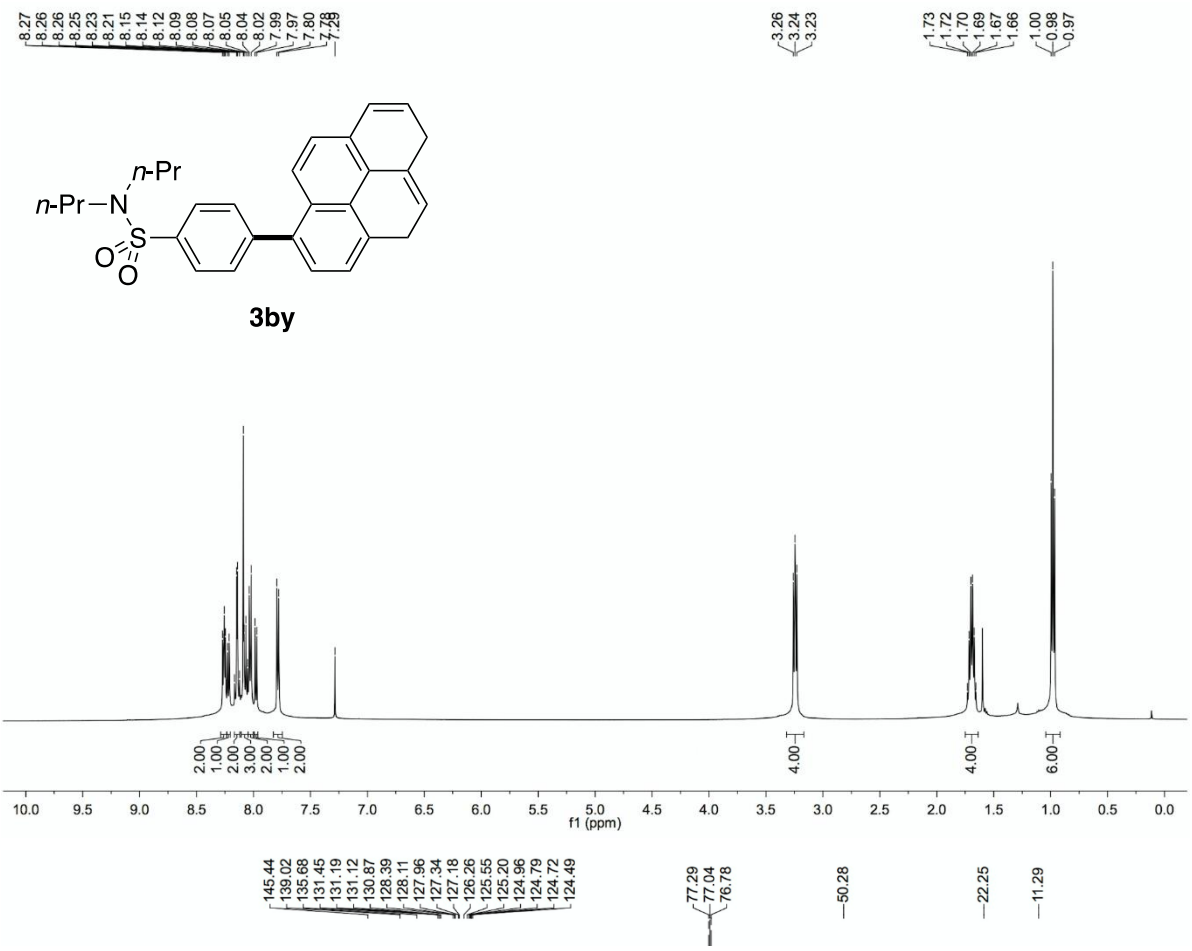

Figure S171. ^{13}C NMR spectrum of **3by**, related to **Figure 4**

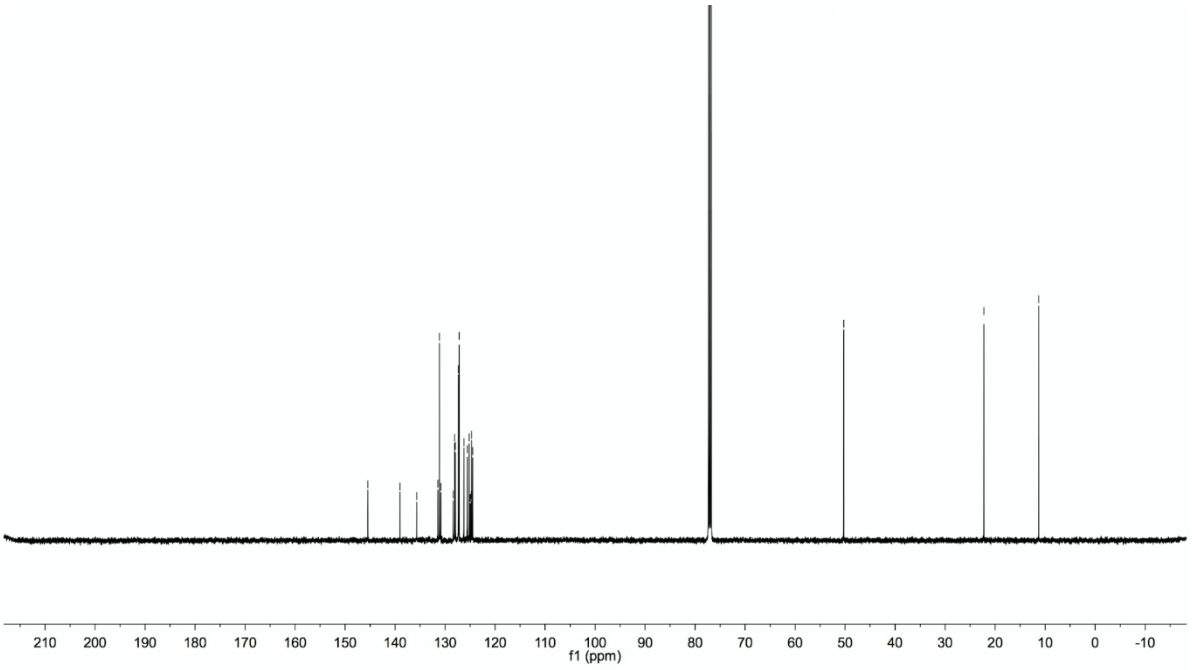

Figure S172. ^{1}H NMR spectrum of **3bz**, related to **Figure 4**

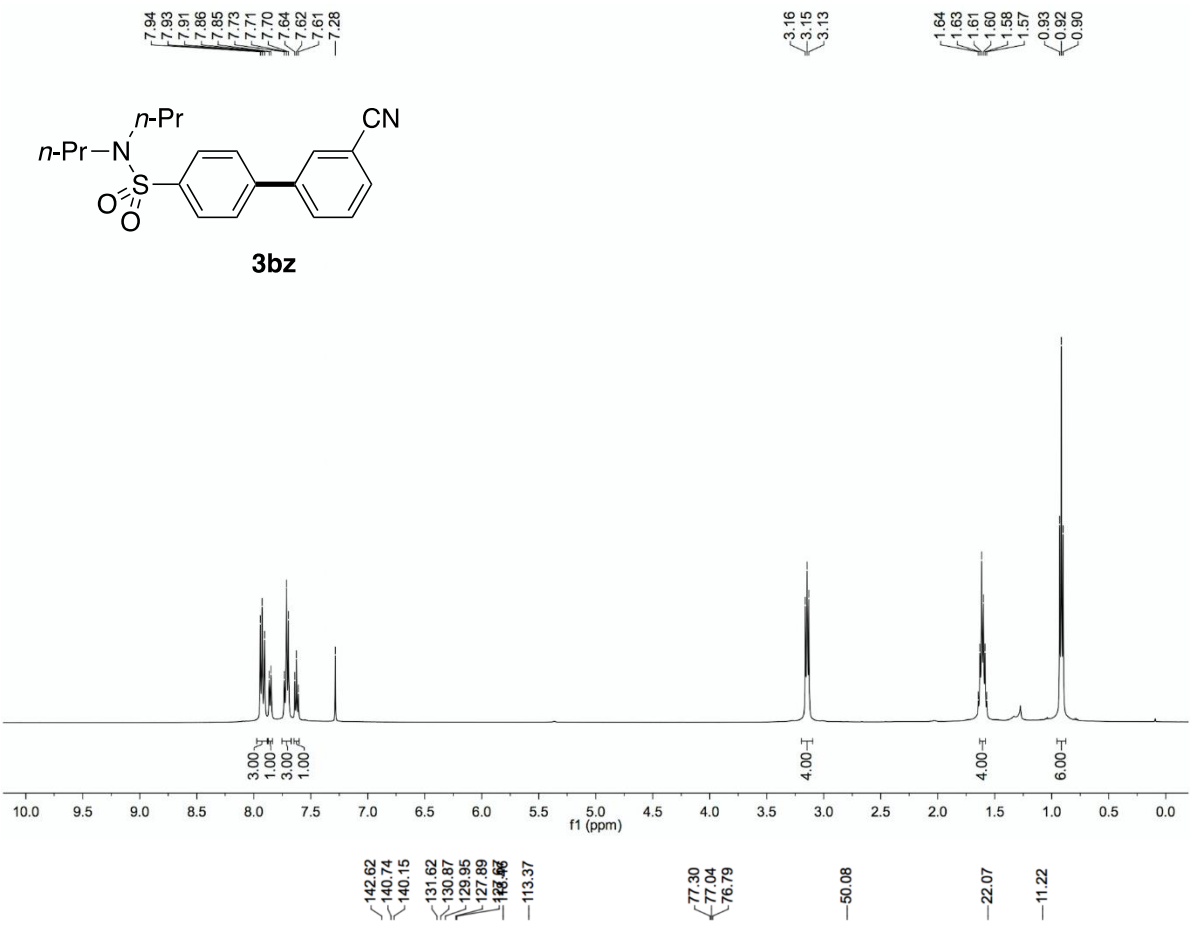

Figure S173. ^{13}C NMR spectrum of **3bz**, related to **Figure 4**

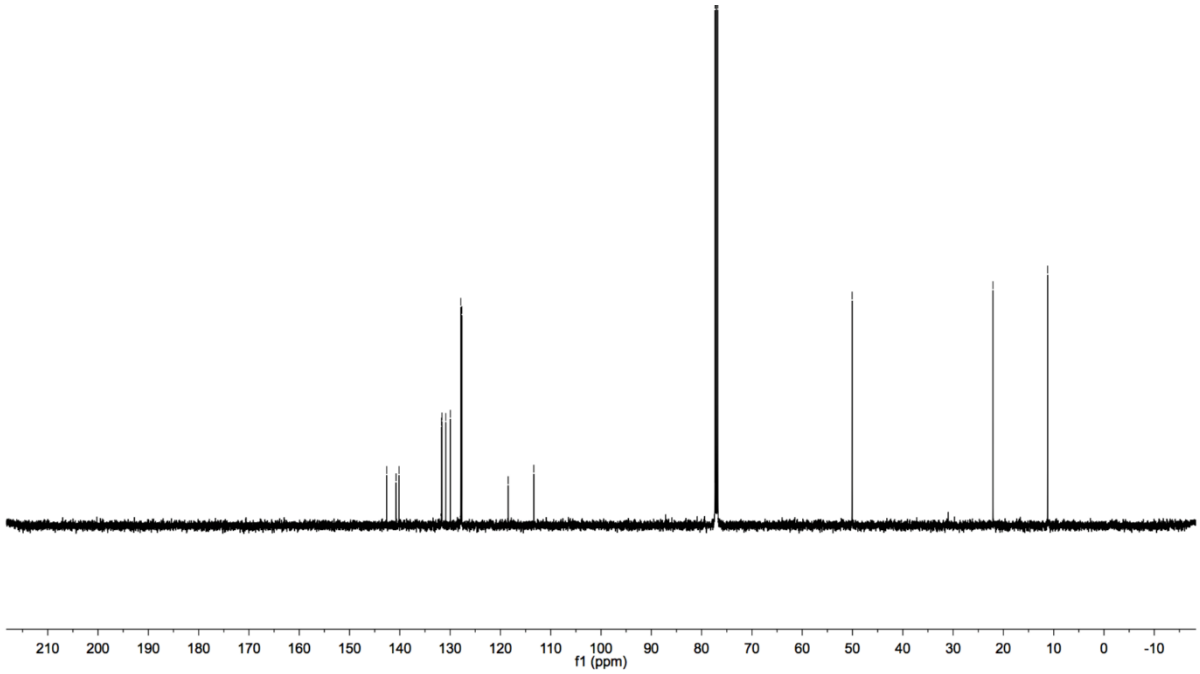

Figure S174. ^{1}H NMR spectrum of **3ca**, related to **Figure 4**

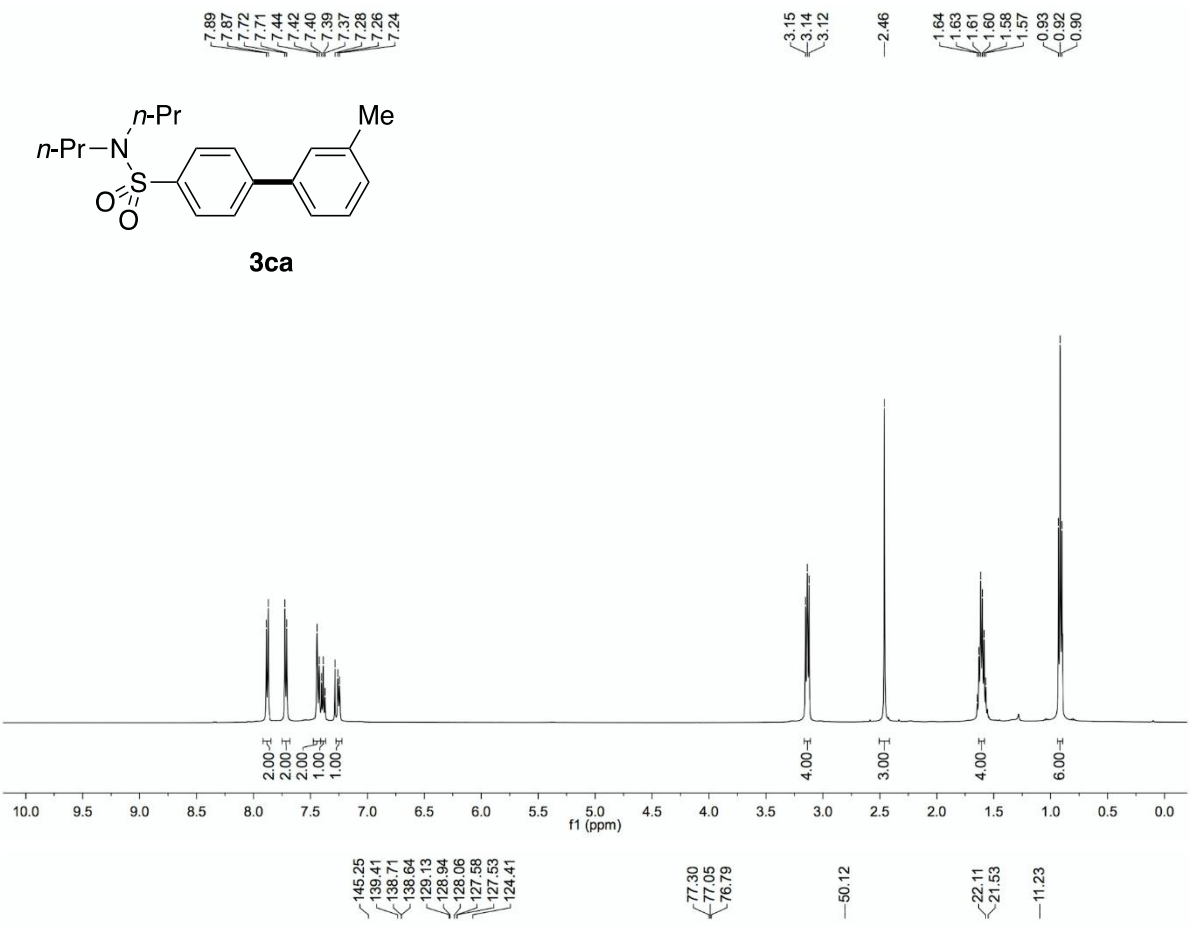

Figure S175. ^{13}C NMR spectrum of **3ca**, related to **Figure 4**

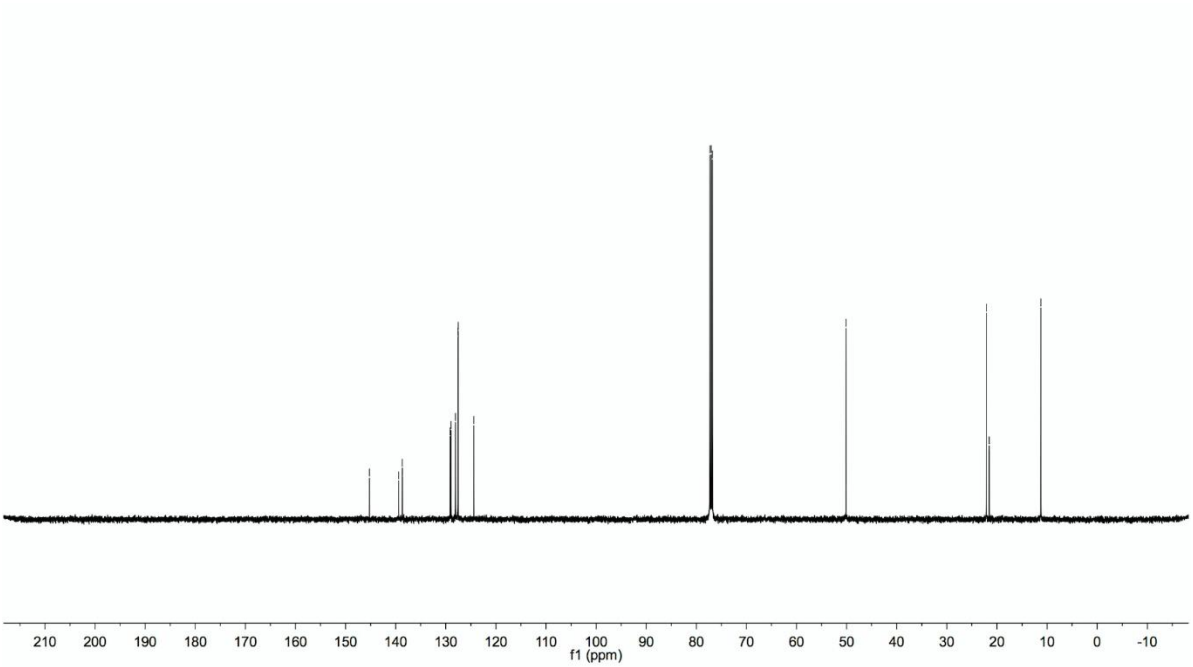

Figure S176. ^{1}H NMR spectrum of **3cb**, related to **Figure 4**

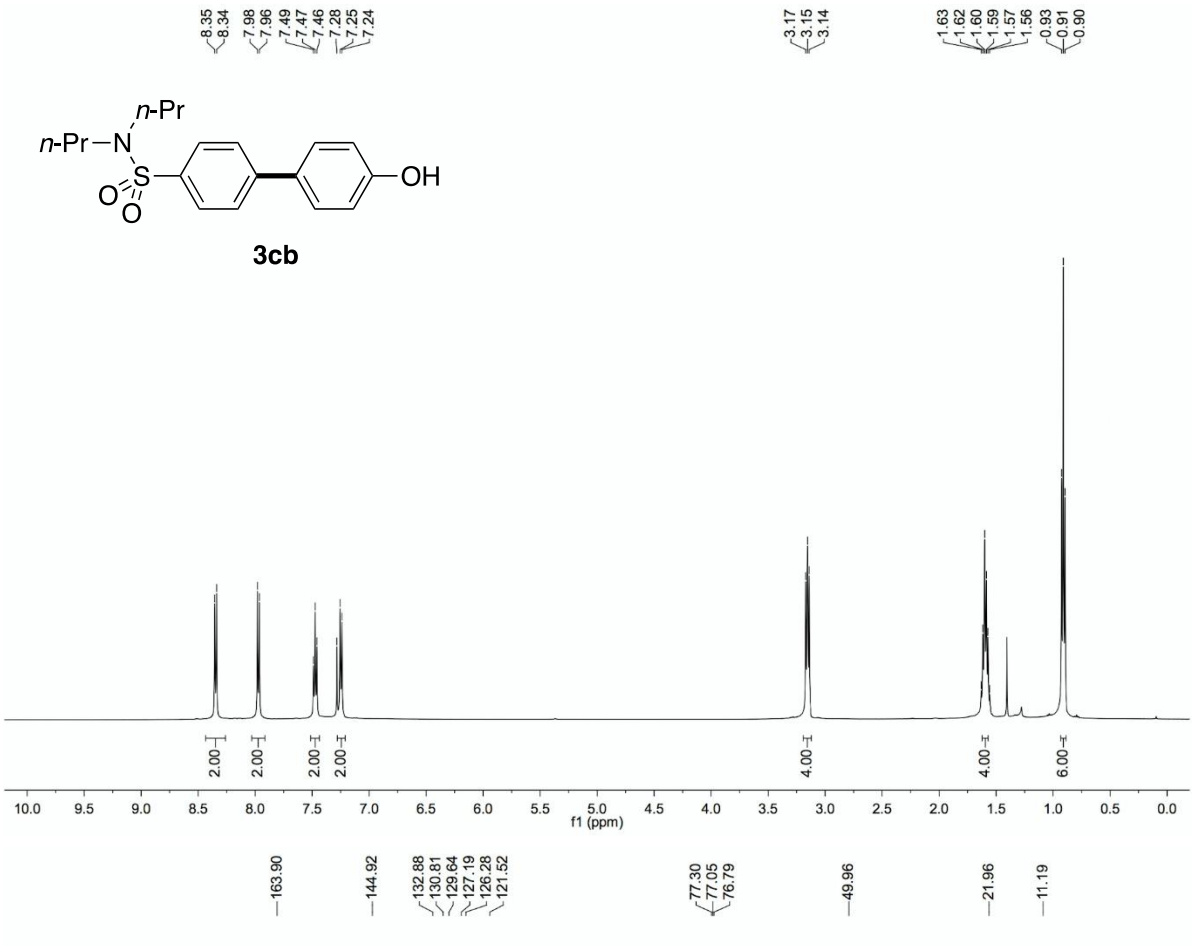

Figure S177. ^{13}C NMR spectrum of **3cb**, related to **Figure 4**

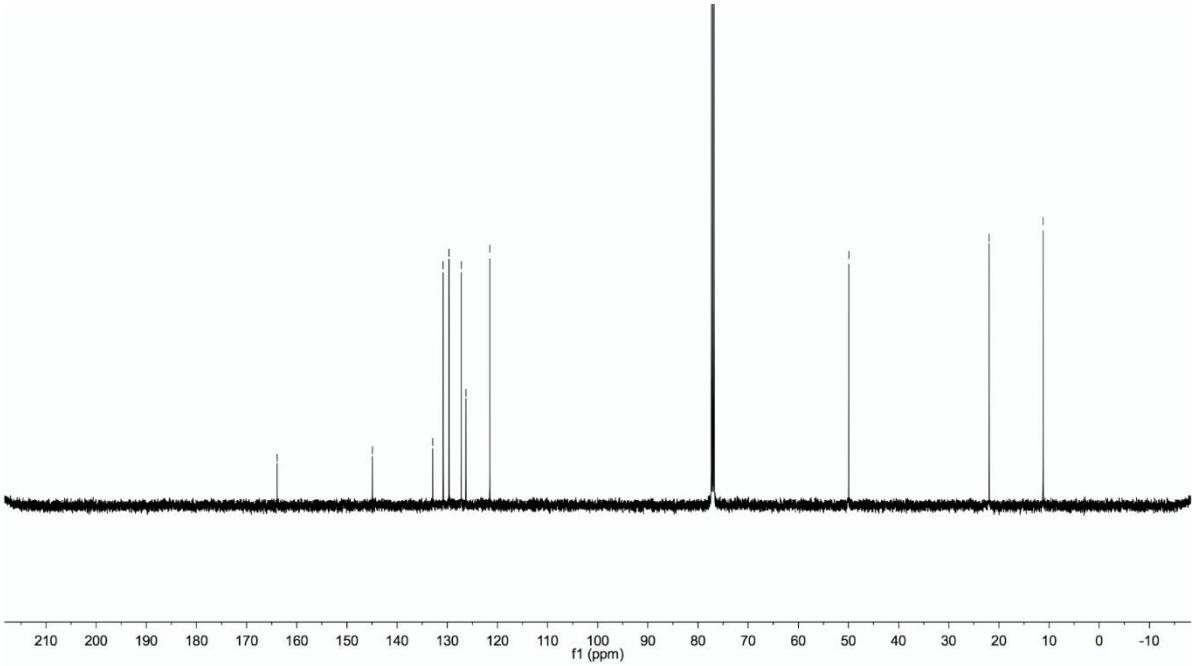

Figure S178. ^{1}H NMR spectrum of **3cc**, related to **Figure 4**

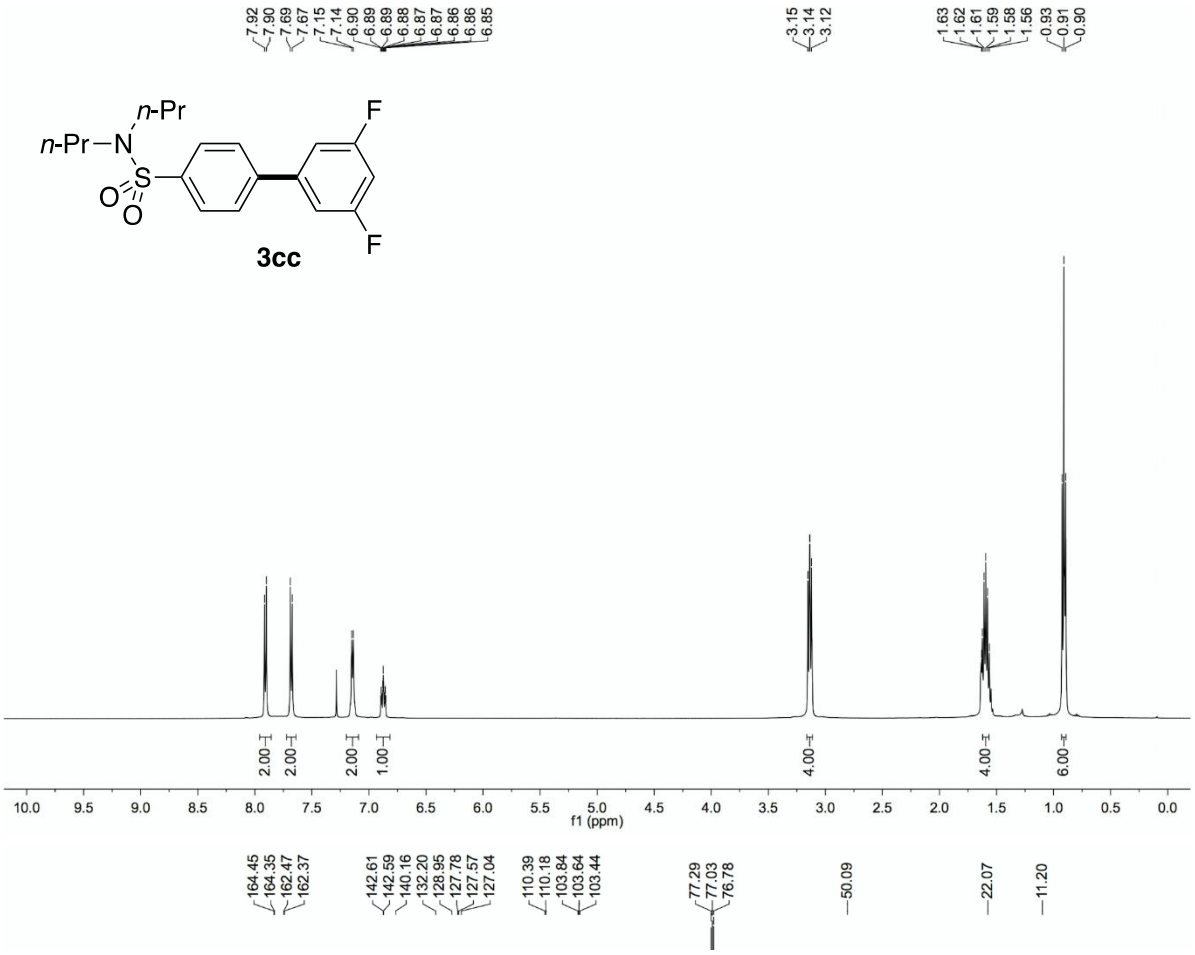

Figure S179. ^{13}C NMR spectrum of **3cc**, related to **Figure 4**

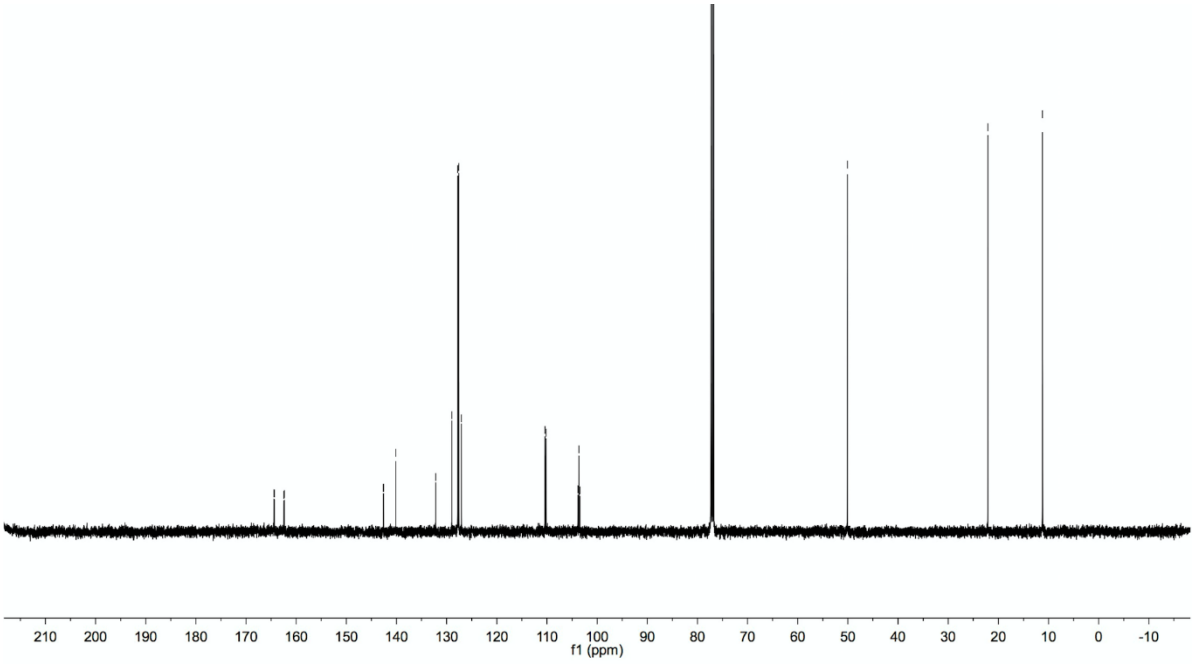

Figure S180. ^{19}F NMR spectrum of **3cc**, related to **Figure 4**

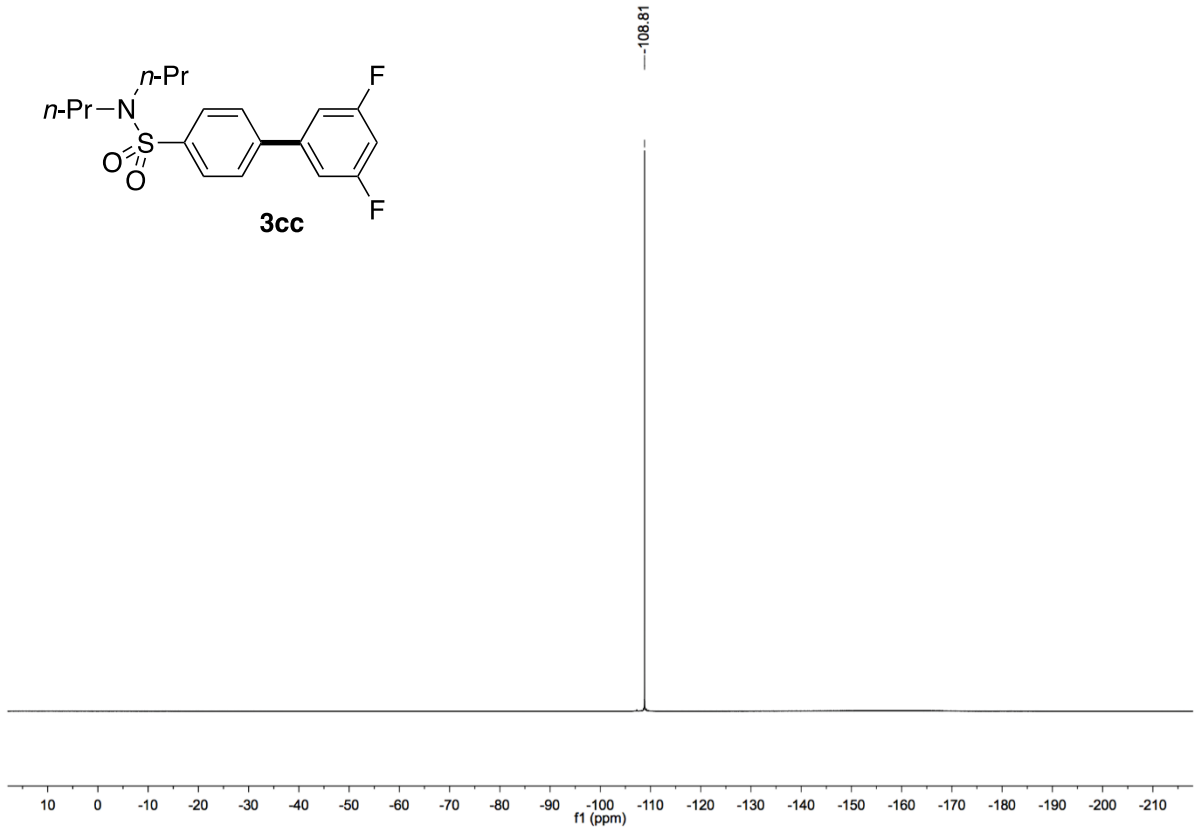

Figure S181. ^{1}H NMR spectrum of **3cd**, related to **Figure 4**

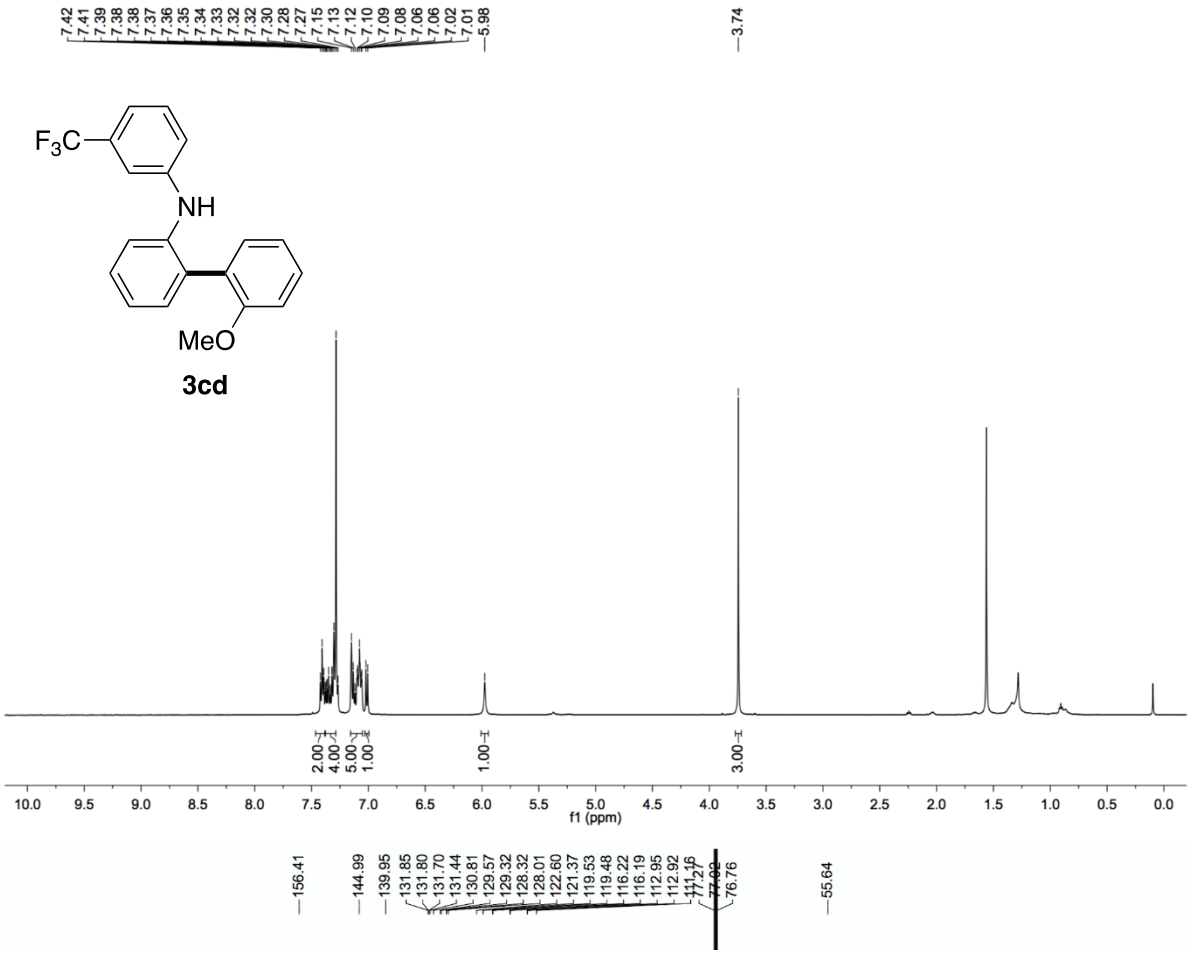

Figure S182. ^{13}C NMR spectrum of **3cd**, related to **Figure 4**

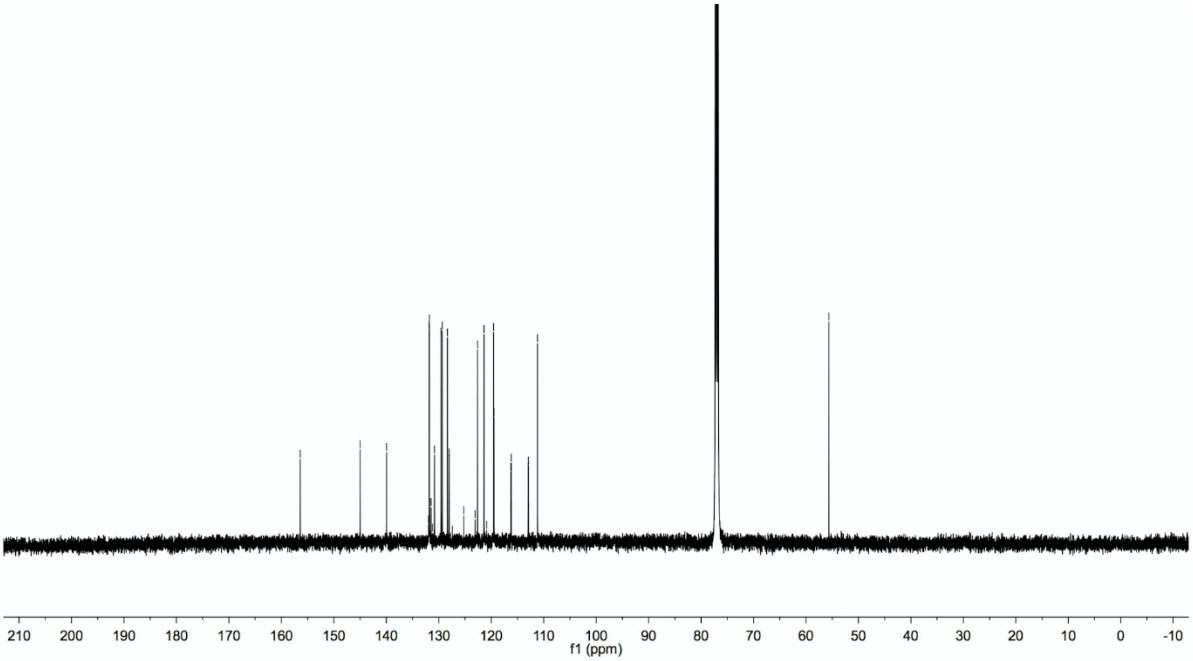

Figure S183. ^{19}F NMR spectrum of **3cd**, related to **Figure 4**

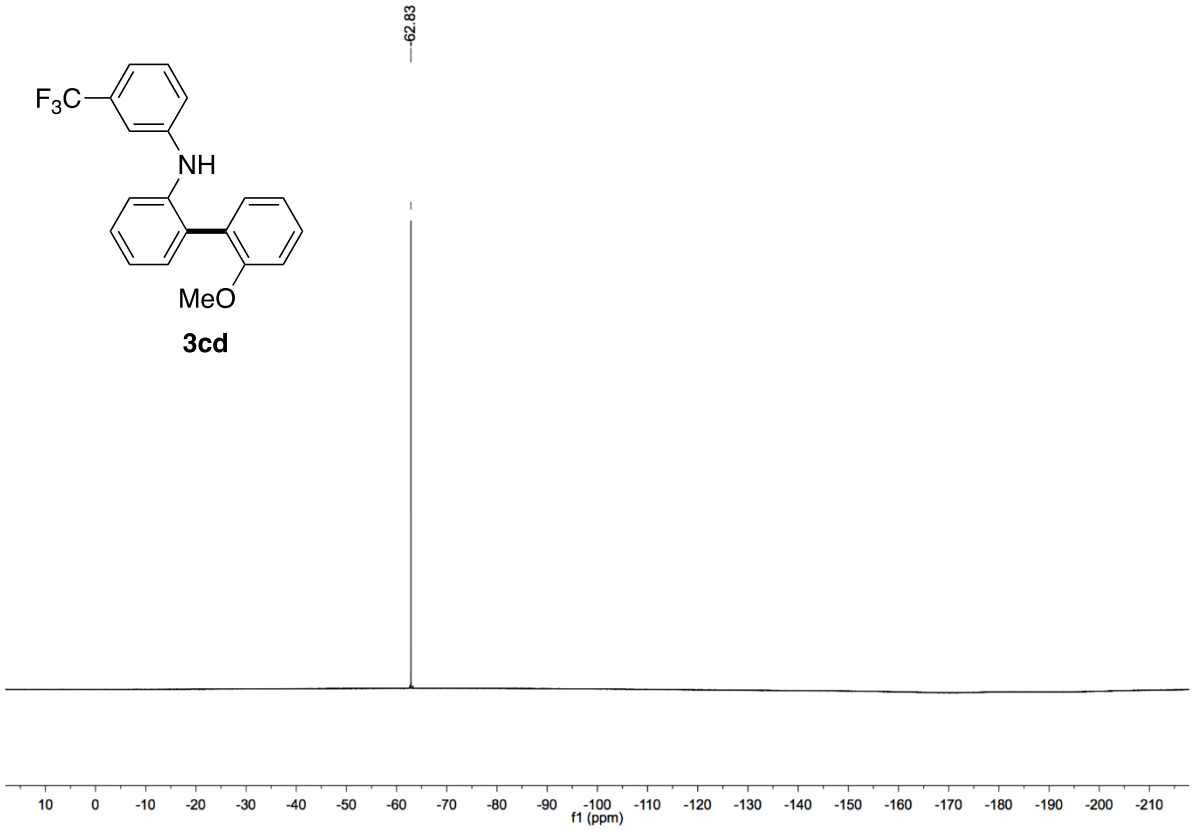

Figure S184. ^{1}H NMR spectrum of **3ce**, related to **Figure 4**

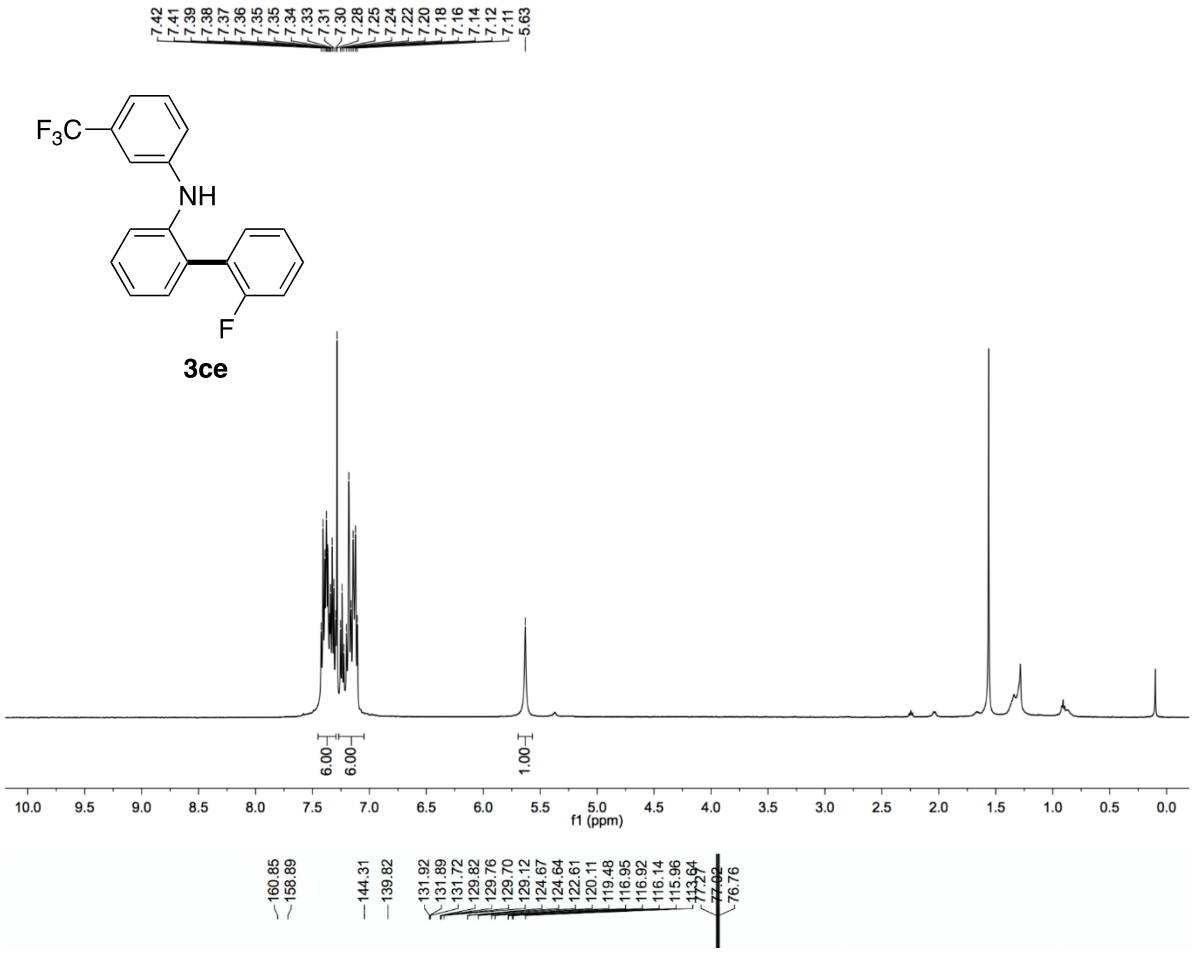

Figure S185. ^{13}C NMR spectrum of **3ce**, related to **Figure 4**

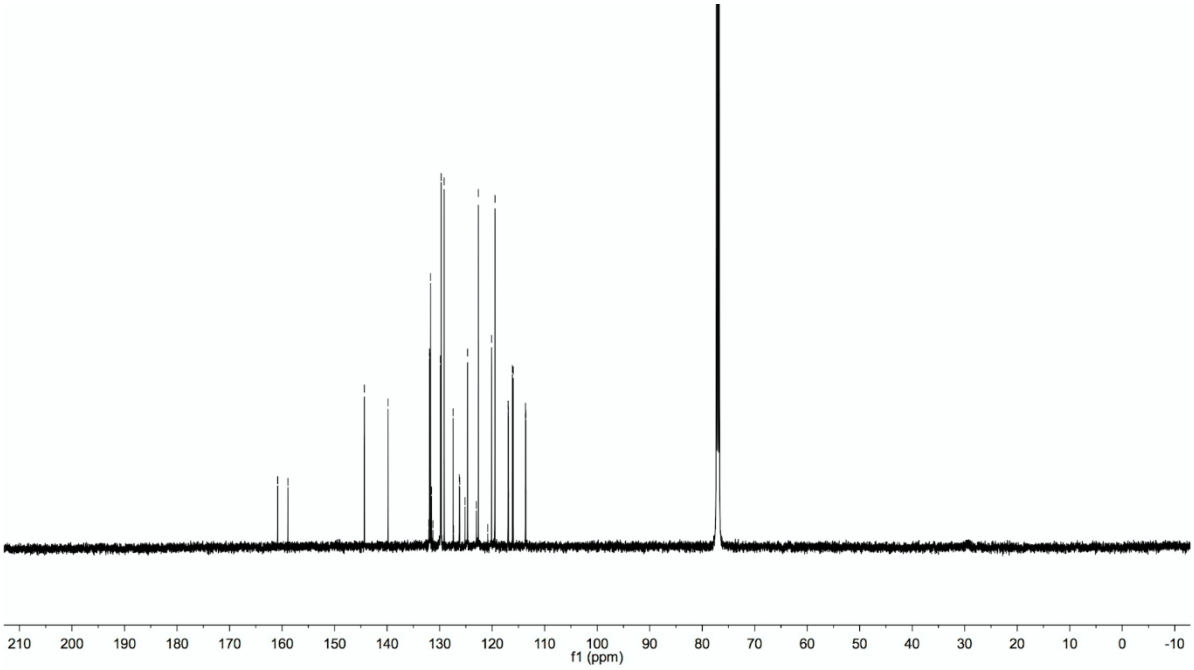

Figure S186. ^{19}F NMR spectrum of **3ce**, related to **Figure 4**

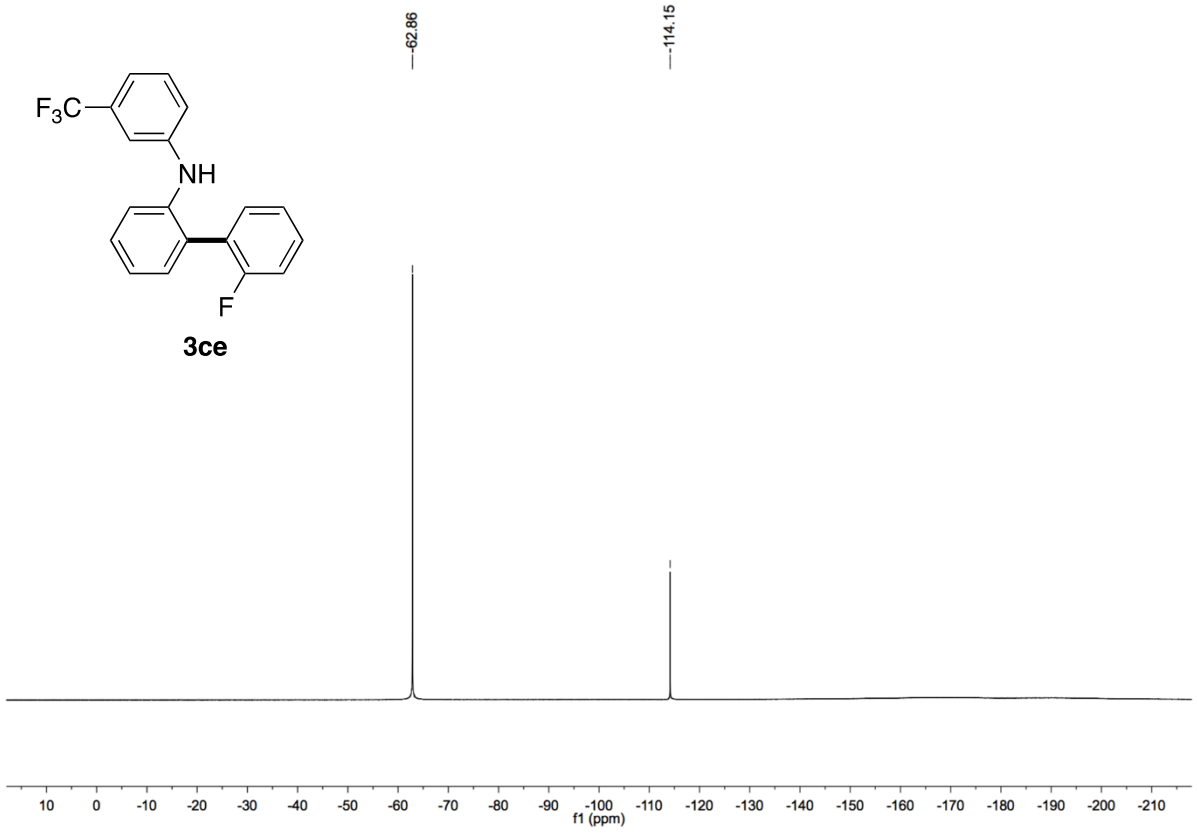

Supplemental Tables

Table S1. Table of energies, related to **Figure 2**.[a]

Structures	*ZPE*	*tcH*	*tcG*	*E*	*H*	*G*	Imaginary Frequency
4	0.720759	0.768242	0.631103	-2585.076110	-2584.307868	-2584.445007	
TS5	0.719659	0.766234	0.634892	-2585.056356	-2584.290122	-2584.421464	219.5i
6	0.721010	0.768049	0.634402	-2585.084588	-2584.316539	-2584.450186	
TS7	0.718489	0.765785	0.633776	-2585.045331	-2584.279546	-2584.411555	265.6i
8	0.718602	0.766500	0.633911	-2585.057358	-2584.290858	-2584.423447	
9	0.711880	0.756666	0.630785	-2471.763250	-2471.006584	-2471.132465	
10	0.837748	0.892049	0.737099	-2879.871451	-2878.979402	-2879.134352	
TS11	0.835418	0.889795	0.736457	-2879.856567	-2878.966772	-2879.120110	272.2i
12	0.836135	0.891635	0.733007	-2879.877414	-2878.985779	-2879.144407	
13	0.664032	0.705341	0.586658	-2356.942849	-2356.237508	-2356.356191	
TS14	0.662757	0.703609	0.585497	-2356.928693	-2356.225084	-2356.343196	316.6i
15	0.665036	0.706460	0.582992	-2356.982031	-2356.275571	-2356.399039	
16	0.182078	0.191889	0.147524	-463.048132	-462.856243	-462.900608	
TS17	0.845338	0.901703	0.742053	-2993.180885	-2992.279182	-2992.438832	274.8i
18	0.192113	0.203769	0.154571	-576.351077	-576.147308	-576.196506	
19	0.725325	0.764631	0.648919	-1865.903522	-1865.138891	-1865.254603	
20	0.725188	0.764422	0.650581	-1865.912683	-1865.148261	-1865.262102	
TS21	0.722477	0.761875	0.648158	-1865.879980	-1865.118105	-1865.231822	258.6i
TS22	0.850548	0.898210	0.767258	-2274.031585	-2273.133375	-2273.264327	275.7i
TS-S1	0.724397	0.762829	0.652398	-1865.890644	-1865.127815	-1865.238246	39.5i
S2	0.852963	0.900590	0.767260	-2274.046953	-2273.146363	-2273.279693	
S3	0.851908	0.900421	0.764789	-2274.053930	-2273.153509	-2273.289141	
S4	0.677439	0.713181	0.605797	-1751.077163	-1750.363982	-1750.471366	
TS-S5	0.677117	0.712121	0.607739	-1751.072247	-1750.360126	-1750.464508	230.5i
S6	0.679487	0.714702	0.609314	-1751.114793	-1750.400091	-1750.505479	
S7	0.722884	0.762930	0.647756	-1865.890254	-1865.127324	-1865.242498	
S8	0.715378	0.752583	0.642984	-1752.586757	-1751.834174	-1751.943773	
CO	0.005036	0.008341	-0.014102	-113.285648	-113.277307	-113.299750	
$PhB(OH)_2$	0.125189	0.134020	0.091304	-408.123464	-407.989444	-408.032160	
PhCOOPiv	0.237711	0.253481	0.194092	-691.139846	-690.886365	-690.945754	
$PivOB(OH)_2$	0.171429	0.184212	0.132914	-522.945261	-522.761049	-522.812347	

[a]Zero-point correction (*ZPE*), thermal correction to enthalpy (*TCH*), thermal correction to Gibbs free energy (*TCG*), energies (*E*), enthalpies (*H*), and Gibbs free energies (*G*) (in Hartree) of the structures calculated at the M06/6-311+G(d,p)-SDD-SMD(1,4-dioxane)//B3LYP/6-31G(d)-LANL2DZ level of theory.

Table S2. Selected optimization in decarbonylative Suzuki-Miyaura coupling of carboxylic acids, related to **Table 1**.[a]

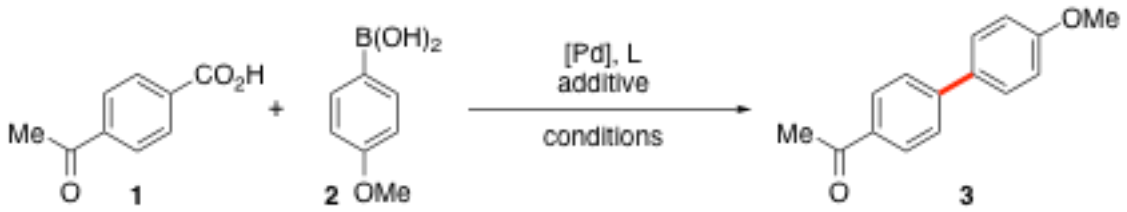

entry	[Pd]	ligand	base	additive	**1**:**2**:base:additive: piv_2O (equiv)	Yield[b] (**3**:**3'**) (%)
1	5% $Pd(OAc)_2$	10% dppb	--	--	1 : 2.0 : 2.0 : 0 : 2.0	14 : 3
2	5% $Pd(OAc)_2$	10% dppb	Et_3N	--	1 : 1.5 : 1.5 : 0 : 1.5	70 : 7
3	5% $Pd(OAc)_2$	10% dppb	Et_3N	--	1 : 2.0 : 2.0 : 0 : 2.0	67 : 8
4	5% $Pd(OAc)_2$	10% dppb	Et_3N	--	1 : 3.0 : 3.0 : 0 : 2.0	60 : 25
5	5% $Pd(OAc)_2$	10% dppb	Et_3N	--	1 : 4.0 : 4.0 : 0 : 2.0	58 : 11
6	5% $Pd(OAc)_2$	6% dppb	Et_3N	--	1 : 2.0 : 2.0 : 0 : 2.0	42 : 6
7	2.5% $Pd(OAc)_2$	5% dppb	Et_3N	--	1 : 2.0 : 2.0 : 0 : 2.0	76 : 3
8[c]	5% $Pd(OAc)_2$	10% dppb	Et_3N	--	1 : 2.0 : 2.0 : 0 : 2.0	49: 9
9	5% $Pd(OAc)_2$	10% dppb	Na_2CO_3	--	1 : 2.0 : 2.0 : 0 : 2.0	52 : 15
10	5% $Pd(OAc)_2$	10% dppb	K_2CO_3	--	1 : 2.0 : 2.0 : 0 : 2.0	51 : 23
11	5% $Pd(OAc)_2$	10% dppb	K_3PO_4	--	1 : 2.0 : 2.0 : 0 : 2.0	<2 : <2
12	5% $Pd(OAc)_2$	10% dppb	Et_3N	Na_2CO_3	1 : 2.0 : 2.0 : 2.0 : 2.0	59 : 12
13	5% $Pd(OAc)_2$	10% dppb	Et_3N	K_2CO_3	1 : 2.0 : 2.0 : 2.0 : 2.0	39 : 19
14	5% $Pd(OAc)_2$	10% dppb	Et_3N	K_3PO_4	1 : 2.0 : 2.0 : 2.0 : 2.0	3 : 5
15	5% $Pd(OAc)_2$	10% dppb	Et_3N	H_3BO_3	1 : 2.0 : 2.0 : 2.0 : 2.0	82 : 15
16	5% $Pd(OAc)_2$	10% dppb	Et_3N	$AdCO_2H$	1 : 2.0 : 2.0 : 2.0 : 2.0	<2 : 0
17	5% $Pd(OAc)_2$	10% dppb	Et_3N	PivOH	1 : 2.0 : 2.0 : 2.0 : 2.0	73 : 4
18	2.5% $Pd(OAc)_2$	5% dppb	Et_3N	PivOH	1 : 1.2 : 1.2 : 1.2 : 1.2	56 : <2
19	5% $Pd(OAc)_2$	10% dppb	Et_3N	H_2O	1 : 2.0 : 2.0 : 2.0 : 2.0	64 : 25
20	5% $Pd(OAc)_2$	10% dppb	Na_2CO_3	H_3BO_3	1 : 2.0 : 2.0 : 2.0 : 2.0	54 : 8
21	5% $Pd(OAc)_2$	10% dppb	K_2CO_3	H_3BO_3	1 : 2.0 : 2.0 : 2.0 : 2.0	59 : 9
22	5% $Pd(OAc)_2$	10% dppb	Et_3N	Na_2CO_3, H_3BO_3	1 : 2.0 : 2.0 : 2.0 : 2.0 :2.0	80 : 12
23	5% $Pd(OAc)_2$	10% dppb	Et_3N	K_2CO_3, H_3BO_3	1 : 2.0 : 2.0 : 2.0 : 2.0 :2.0	71 : 13
24	5% $Pd(OAc)_2$	10% dppb	DIPEA	H_3BO_3	1 : 2.0 : 2.0 : 2.0 : 2.0	69 : 14
25	5% $Pd(OAc)_2$	10% dppb	Bu_3N	H_3BO_3	1 : 2.0 : 2.0 : 2.0 : 2.0	60 : 4
26	5% $Pd(OAc)_2$	10% dppb	DMAP	H_3BO_3	1 : 2.0 : 2.0 : 2.0 : 2.0	43 : <2
27	5% $Pd(OAc)_2$	10% dppb	Pyridine	H_3BO_3	1 : 2.0 : 2.0 : 2.0 : 2.0	43 : 6
28	5% $Pd(OAc)_2$	10% dppb	NMM	H_3BO_3	1 : 2.0 : 2.0 : 2.0 : 2.0	53 : 13

29	5% $Pd(OAc)_2$	10% dppb	Et_2NH	H_3BO_3	1 : 2.0 : 2.0 : 2.0 : 2.0	21 : 3
30[d]	5% $Pd(OAc)_2$	10% dppb	Et_3N	H_3BO_3	1 : 2.0 : 2.0 : 2.0 : 2.0	44 : 9
31[e]	5% $Pd(OAc)_2$	10% dppb	Et_3N	H_3BO_3	1 : 2.0 : 2.0 : 2.0 : 2.0	80 : 7
32[f]	5% $Pd(OAc)_2$	10% dppb	Et_3N	H_3BO_3	1 : 2.0 : 2.0 : 2.0 : 2.0	50 : 14
33[g]	5% $Pd(OAc)_2$	10% dppb	Et_3N	H_3BO_3	1 : 2.0 : 2.0 : 2.0 : 2.0	73 : 12
34	5% $PdCl_2$	10% dppb	Et_3N	H_3BO_3	1 : 2.0 : 2.0 : 2.0 : 2.0	55 : 4
35	10% $Pd_2(dba)_3$	20% dppb	Et_3N	H_3BO_3	1 : 2.0 : 2.0 : 2.0 : 2.0	79 : 9
36	5% $Pd_2(dba)_3$	10% dppb	Et_3N	H_3BO_3	1 : 2.0 : 2.0 : 2.0 : 2.0	70 : 10
37	2.5% $Pd_2(dba)_3$	5% dppb	Et_3N	H_3BO_3	1 : 2.0 : 2.0 : 2.0 : 2.0	80 : 10
38	10% $Pd_2(dba)_3$	40% dppb	Et_3N	H_3BO_3	1 : 2.0 : 2.0 : 2.0 : 2.0	31 : 2
39	5% $Pd_2(dba)_3$	20% dppb	Et_3N	H_3BO_3	1 : 2.0 : 2.0 : 2.0 : 2.0	67 : 10
40	2.5% $Pd_2(dba)_3$	10% dppb	Et_3N	H_3BO_3	1 : 2.0 : 2.0 : 2.0 : 2.0	66 : 8
41	5% $Pd(dba)_2$	10% dppb	Et_3N	H_3BO_3	1 : 2.0 : 2.0 : 2.0 : 2.0	59 : 8
42	5% PEPPSI	10% dppb	Et_3N	H_3BO_3	1 : 2.0 : 2.0 : 2.0 : 2.0	0 : 0
43	5% Neolyst	10% dppb	Et_3N	H_3BO_3	1 : 2.0 : 2.0 : 2.0 : 2.0	<2 : 0
44	5% $Pd(OAc)_2$	10% dppm	Et_3N	H_3BO_3	1 : 2.0 : 2.0 : 2.0 : 2.0	9 : 2
45	5% $Pd(OAc)_2$	10% dppe	Et_3N	H_3BO_3	1 : 2.0 : 2.0 : 2.0 : 2.0	0 : 0
46	5% $Pd(OAc)_2$	10% dppp	Et_3N	H_3BO_3	1 : 2.0 : 2.0 : 2.0 : 2.0	5 : <2
47	5% $Pd(OAc)_2$	10% dpppe	Et_3N	H_3BO_3	1 : 2.0 : 2.0 : 2.0 : 2.0	44 : 21
48	5% $Pd(OAc)_2$	10% dpphex	Et_3N	H_3BO_3	1 : 2.0 : 2.0 : 2.0 : 2.0	18 : 33
49	5% $Pd(OAc)_2$	10% BINAP	Et_3N	H_3BO_3	1 : 2.0 : 2.0 : 2.0 : 2.0	27 : 27
50	5% $Pd(OAc)_2$	10% DPEPhos	Et_3N	H_3BO_3	1 : 2.0 : 2.0 : 2.0 : 2.0	47 : 14
51	5% $Pd(OAc)_2$	10% XantPhos	Et_3N	H_3BO_3	1 : 2.0 : 2.0 : 2.0 : 2.0	26 : 3
52	5% $Pd(OAc)_2$	10% dppf	Et_3N	H_3BO_3	1 : 2.0 : 2.0 : 2.0 : 2.0	41 : 8
53	5% $Pd(OAc)_2$	20% PCy_3HBF_4	Et_3N	H_3BO_3	1 : 2.0 : 2.0 : 2.0 : 2.0	15 : 68
54	5% $Pd(OAc)_2$	20% PCy_2Ph	Et_3N	H_3BO_3	1 : 2.0 : 2.0 : 2.0 : 2.0	13 : 87
55	5% $Pd(OAc)_2$	20% $PCyPh_2$	Et_3N	H_3BO_3	1 : 2.0 : 2.0 : 2.0 : 2.0	17 : 72
56	5% $Pd(OAc)_2$	20% PPh_3	Et_3N	H_3BO_3	1 : 2.0 : 2.0 : 2.0 : 2.0	24 : 61
57	5% $Pd(OAc)_2$	20% DavePhos	Et_3N	H_3BO_3	1 : 2.0 : 2.0 : 2.0 : 2.0	<2 : <2
58	5% $Pd(OAc)_2$	20% XPhos	Et_3N	H_3BO_3	1 : 2.0 : 2.0 : 2.0 : 2.0	<2 : <2
59	5% $Pd(OAc)_2$	20% SPhos	Et_3N	H_3BO_3	1 : 2.0 : 2.0 : 2.0 : 2.0	<2 : <2
60	5% $Pd(OAc)_2$	10% dppb	Et_3N	H_3BO_3	1 : 1.2 : 1.2 : 1.2 : 1.2	48 : 7
61	5% $Pd(OAc)_2$	10% dppb	Et_3N	H_3BO_3	1 : 1.5 : 1.5 : 1.5 : 1.5	79 : 6
62	5% $Pd(OAc)_2$	10% dppb	Et_3N	H_3BO_3	1 : 1.5 : 4.5 : 2.0 : 2.0	79 : 9
63	5% $Pd(OAc)_2$	10% dppb	Et_3N	H_3BO_3	1 : 2.0 : 1.5 : 1.5 : 1.5	82 : 8
64	5% $Pd(OAc)_2$	10% dppb	Et_3N	H_3BO_3	1 : 2.0 : 2.0 : 1.5 : 1.5	84 : 8
65	5% $Pd(OAc)_2$	10% dppb	Et_3N	H_3BO_3	1 : 2.0 : 2.0 : 1.0 : 2.0	82 : 15
66	5% $Pd(OAc)_2$	10% dppb	Et_3N	H_3BO_3	1 : 2.0 : 2.0 : 1.5 : 2.0	82 : 11
67	5% $Pd(OAc)_2$	10% dppb	Et_3N	H_3BO_3	1 : 2.0 : 2.0 : 4.0 : 2.0	77 : 14

68	5% $Pd(OAc)_2$	10% dppb	Et_3N	H_3BO_3	1 : 2.0 : 4.0 : 2.0 : 2.0	75 : 10
69	5% $Pd(OAc)_2$	10% dppb	Et_3N	H_3BO_3	1 : 2.0 : 4.0 : 4.0 : 2.0	82 : 10
70	5% $Pd(OAc)_2$	10% dppb	Et_3N	H_3BO_3	1 : 3.0 : 1.5 : 2.0 : 2.0	77 : 14
71	5% $Pd(OAc)_2$	10% dppb	Et_3N	H_3BO_3	1 : 3.0 : 4.5 : 2.0 : 2.0	63 : 12
72	5% $Pd(OAc)_2$	10% dppb	Et_3N	H_3BO_3	1 : 2.0 : 1.5 : 1.5 : 1.5	72 : 15
73[h]	5% $Pd(OAc)_2$	10% dppb	Et_3N	H_3BO_3	1 : 2.0 : 1.5 : 1.5 : 1.5	48 : 10
74[i]	5% $Pd(OAc)_2$	10% dppb	Et_3N	H_3BO_3	1 : 2.0 : 1.5 : 1.5 : 1.5	38 : 11

[a]Conditions: carboxylic acid (1.0 equiv), boronic acid (1.2-4.0 equiv), base (1.5-4.5 equiv), 1,4-dioxane (0.20 M), 160 °C, 15 h; [b]Determined by ^{1}H NMR and/or GC-MS; [c]140 °C; [d]Toluene; [e]0.10 M; [f]0.50 M; [g]100 mg MS; [h]120 °C; [i]100 °C. **3** = 1-(4'-methoxy-[1,1'-biphenyl]-4-yl)ethan-1-one; **3'** = 1-(4-(4-methoxybenzoyl)phenyl)ethan-1-one.

Transparent Methods

Computational Details

All density functional theory (DFT) calculations were performed with Gaussian 09 package (Frisch et al., 2010). Geometry optimizations of all the minima and transition states were carried out at the B3LYP (Becke et al., 1993; Lee et al., 1988) level of theory, with the LANL2DZ (Hay et al., 1985; Wadt et al., 1985; Hay et al., 1985) basis set for Pd and the 6-31G(d) basis set for the other atoms. Vibrational frequencies were computed at the same level of theory to evaluate its zero-point vibrational energy (ZPVE) and thermal corrections at 298 K, and to check whether each optimized structure is an energy minimum or a transition state. On the basis of the gas-phase optimized structures, the single point energies were calculated with the M06 functional developed by Truhlar and coworkers (Zhao et al., 2008; Zhao et al., 2008) and a mixed basis set of SDD (von Szentpaly et al., 1982; Dolg et al., 1987; Schwerdtfeger et al., 1898) for Pd and 6-311+G(d,p) for other atoms. Solvation energy corrections were calculated using the SMD model (Marenich et al., 2009) with 1,4-dioxane as the solvent. The 3D diagrams of computed species were generated using CYLView (Legault, 2009). In order to adjust the Gibbs free energies from 1 atm to 1 mol/L, a correction of $RT\ln(c_s/c_g)$ (about 1.9 kcal/mol) is added to energies of all species. c_s is the standard molar concentration in solution (1 mol/L), c_g is the standard molar concentration in gas phase (0.0446 mol/L), and R is the gas constant. Extensive conformational searches are conducted to ensure that the most stable conformers are located.

List of Known Compounds/General Methods

All starting materials reported in the manuscript have been previously described in literature or prepared by the method reported previously. All experiments involving palladium were performed using standard Schlenk techniques under argon atmosphere unless stated otherwise. All solvents were purchased at the highest commercial grade and used as received or after purification by passing through activated alumina columns or distillation from sodium/benzophenone under nitrogen. All solvents were deoxygenated prior to use. All other chemicals were purchased at the highest commercial grade and used as received. Reaction glassware was oven-dried at 140 °C for at least 24 h or flame-dried prior to use, allowed to cool under vacuum and purged with argon (three cycles). All products were identified using ^{1}H NMR analysis and comparison with authentic samples. GC and/or GC/MS analysis was used for volatile products. All yields refer to yields determined by ^{1}H NMR and/or GC or GC/MS using an internal standard (optimization) and isolated yields (preparative runs) unless stated otherwise. ^{1}H NMR and ^{13}C NMR spectra were recorded in $CDCl_3$ on Bruker spectrometers at 500 (^{1}H NMR) and 125 MHz (^{13}C NMR). All shifts are reported in parts per million (ppm) relative to residual $CHCl_3$ peak (7.27 and 77.2 ppm, ^{1}H NMR and ^{13}C NMR, respectively). All coupling constants (*J*) are reported in hertz (Hz). Abbreviations are: s, singlet; d, doublet; t, triplet; q, quartet; brs, broad singlet. GC-MS chromatography was performed using Agilent HP6890 GC System and Agilent 5973A inert XL EI/CI MSD using helium as the carrier gas at a flow rate of 1 mL/min and an initial oven temperature of 50 °C. The injector temperature was 250 °C. The detector temperature was 250 °C. For runs with the initial oven temperature of 50 °C, temperature was increased with a 10 °C/min ramp after 50 °C hold for 3 min to a final temperature of 220 °C, then hold at 220 °C for 15 min (splitless mode of injection, total run time of 22.0 min). High-resolution mass spectra (HRMS) were measured on a 7T Bruker Daltonics FT-MS instrument (for HRMS). Melting point was measured on MeltEMP (laboratory devices). All flash chromatography was performed using silica gel, 60 Å, 300 mesh. TLC analysis was carried out on glass plates coated with silica gel 60 F254, 0.2 mm thickness. The plates were visualized using a 254 nm ultraviolet lamp or aqueous potassium permanganate solutions. ^{1}H NMR and ^{13}C NMR data are given for all compounds. ^{1}H NMR, ^{13}C NMR and HRMS data are reported for all new compounds.

Experimental Procedures and Characterization Data

General Procedure for Decarbonylative Suzuki-Miyaura Coupling of Carboxylic Acids. An oven-dried vial equipped with a stir bar was charged with carboxylic acid (neat, 1.0 equiv), boronic acid (neat, typically, 2.0 equiv), $Pd(OAc)_2$ (typically, 5 mol%), ligand (typically, 10 mol%), triethylamine (typically, 1.5 equiv), boric acid (typically, 1.5 equiv) and trimethylacetic anhydride (typically, 1.5 equiv), placed under a positive pressure of argon, and subjected to three evacuation/backfilling cycles under high vacuum. Dioxane (0.20 M) was added with vigorous stirring at room temperature, the reaction mixture was placed in a preheated oil bath at 160 °C, and stirred for the indicated time at 160 °C.

Representative Procedure for Decarbonylative Suzuki-Miyaura Coupling of Carboxylic Acids. An oven-dried vial equipped with a stir bar was charged with 4-acetylbenzoic acid (neat, 32.9 mg, 0.20 mmol), phenylboronic acid (neat, 48.8 mg, 0.40 mmol, 2.0 equiv), $Pd(OAc)_2$ (2.3 mg, 5 mol%), 1,4-bis(diphenylphosphino)butane (8.6 mg, 10 mol%), triethylamine (30.4 mg, 0.30 mmol, 1.5 equiv), boric acid (18.6 mg, 0.30 mmol, 1.5 equiv) and trimethylacetic anhydride (55.9 mg, 0.30 mmol, 1.5 equiv), placed under a positive pressure of argon, and subjected to three evacuation/backfilling cycles under high vacuum. Dioxane (1.0 mL, 0.20 M) was added with vigorous stirring at room temperature, the reaction mixture was placed in a preheated oil bath at 160 °C, and stirred for 15 h at 160 °C. After the indicated time, the reaction mixture was cooled down to room temperature, diluted with CH_2Cl_2 (10 mL), filtered, and concentrated. Purification by chromatography on silica gel (ethyl acetate/hexane) afforded the title product. Yield 83% (32.6 mg). White solid. Characterization data are included in the section below.

Representative Procedure for Decarbonylative Suzuki-Miyaura Coupling of Carboxylic Acids. Gram Scale. An oven-dried vial equipped with a stir bar was charged with probenecid (*p*-(dipropylsulfamoyl)benzoic acid, neat, 1.00 g, 3.50 mmol), phenylboronic acid (neat, 0.855 g, 7.00 mmol, 2.0 equiv), $Pd(OAc)_2$ (39.3 mg, 5 mol%), 1,4-bis(diphenylphosphino)butane (149.3 mg, 10 mol%), triethylamine (0.531 g, 5.25 mmol, 1.5 equiv), boric acid (0.324 g, 5.25 mmol, 1.5 equiv) and trimethylacetic anhydride (0.978 g, 5.25 mmol, 1.5 equiv), placed under a positive pressure of argon, and subjected to three evacuation/backfilling cycles under high vacuum. Dioxane (17.5 mL, 0.20 M) was added with vigorous stirring at room temperature, the reaction

mixture was placed in a preheated oil bath at 160 °C, and stirred for 15 h at 160 °C. After the indicated time, the reaction mixture was cooled down to room temperature, diluted with CH_2Cl_2 (50 mL), filtered, and concentrated. Purification by chromatography on silica gel (ethyl acetate/hexane) afforded the title product. Yield 86% (0.958 g). White solid. Characterization data are included in the section below.

Mechanistic Studies

A series of synthetic studies were performed to gain insight into the reaction mechanism and investigate factors involved in controlling the Pd-catalyzed decarbonylative Suzuki-Miyaura coupling of carboxylic acids (Schemes S1-S6).

(1) To investigate whether benzoic pivalic anhydride was a possible reaction intermediate, benzoic pivalic anhydride **1S** was prepared and subjected to the reaction conditions (Scheme S1). Formation of product **3S** from **1S** was observed using Pd-catalysis, suggesting that **1S** could be a competent intermediate. Moreover, benzoic anhydride served as a competent intermediate under Pd-catalyzed conditions (45% yield, not shown).

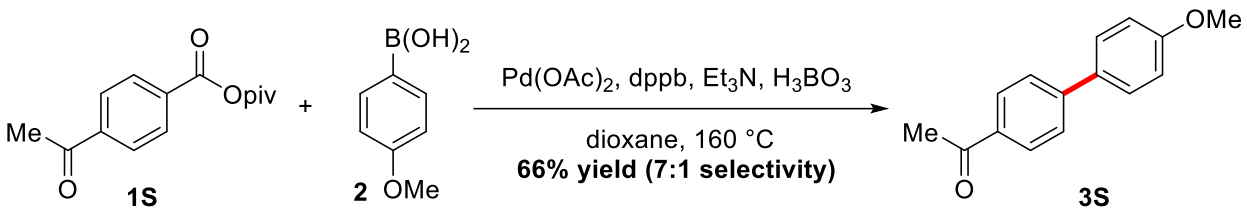

Scheme S1. Decarbonylative Suzuki-Miyaura of benzoic pivalic anhydride, related to Figure 1. *Conditions:* ***1S*** *(1.0 equiv), 4-MeO-C_6H_4-$B(OH)_2$ (2.0 equiv), $Pd(OAc)_2$ (5 mol%), dppb (10 mol%), Et_3N (2.0 equiv), H_3BO_3 (2.0 equiv), dioxane (0.20 M), 160 °C, 15 h.*

(2) To investigate electronic effect on the decarbonylative coupling, intermolecular competition experiments between differently substituted carboxylic acids were conducted (Scheme S2). The experiments revealed that electron-deficient arenes are inherently more reactive than their electron-rich counterparts, consistent with facility of metal insertion and decarbonylation.

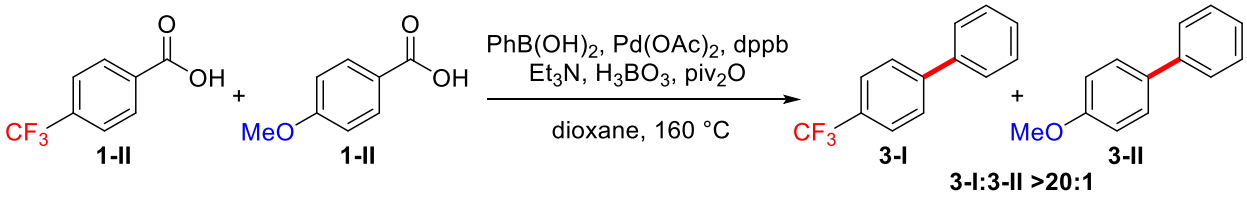

Scheme S2. Intermolecular competition experiments in decarbonylative Suzuki-Miyaura coupling of carboxylic acids, related to Figure 1. *Conditions:* ***1*** *(1.0 equiv each), $PhB(OH)_2$*

(0.5 equiv), $Pd(OAc)_2$ (5 mol%), dppb (10 mol%), Et_3N (1.5 equiv), H_3BO_3 (1.5 equiv), piv_2O (1.5 equiv), dioxane (0.20 M), 160 °C, 15 h.

(3) To investigate steric effect on the decarbonylative coupling, intermolecular competition experiments between differently substituted carboxylic acids were conducted (Scheme S3). The experiments revealed that sterically-hindered carboxylic acids react preferentially, consistent with decarbonylation favored by steric demand of acylpalladium complexes.

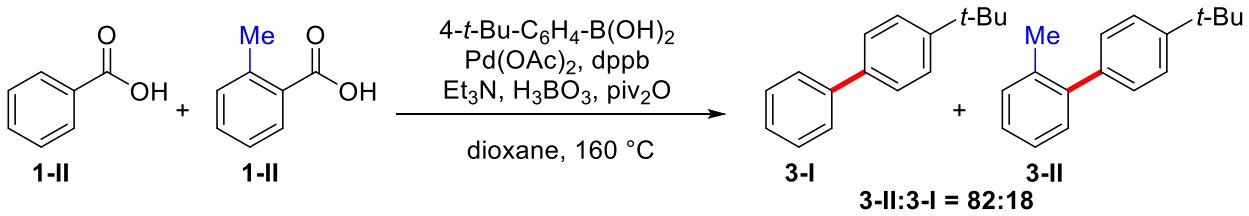

Scheme S3. Intermolecular competition experiments in decarbonylative Suzuki-Miyaura coupling of carboxylic acids, related to Figure 1. *Conditions: **1** (1.0 equiv each), 4-t-Bu-C_6H_4-$B(OH)_2$ (0.5 equiv), $Pd(OAc)_2$ (5 mol%), dppb (10 mol%), Et_3N (1.5 equiv), H_3BO_3 (1.5 equiv), piv_2O (1.5 equiv), dioxane (0.20 M), 160 °C, 15 h.*

(4) To investigate electronic effect on the boronic acid component on the decarbonylative coupling, intermolecular competition experiments between differently substituted boronic acids were conducted (Scheme S4). The experiments revealed that electron-rich boronic acids are inherently more reactive than their electron-deficient counterparts, consistent with facility of transmetallation.

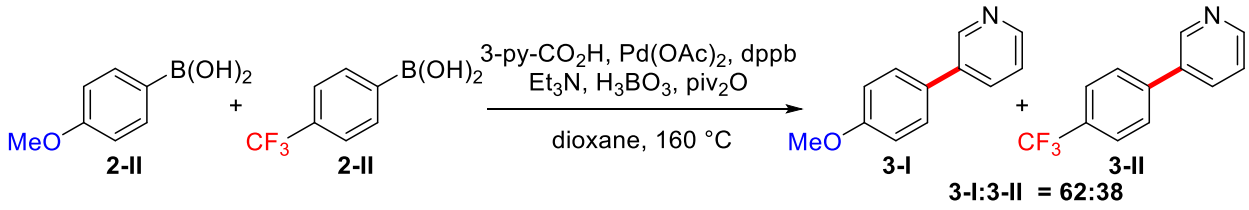

Scheme S4. Intermolecular competition experiments in decarbonylative Suzuki-Miyaura coupling of carboxylic acids, related to Figure 1. *Conditions: **2** (1.0 equiv each), 3-py-CO_2H (0.5 equiv), $Pd(OAc)_2$ (5 mol%), dppb (10 mol%), Et_3N (1.5 equiv), H_3BO_3 (1.5 equiv), piv_2O (1.5 equiv), dioxane (0.20 M), 160 °C, 15 h.*

(5) To investigate steric effect on the boronic acid component on the decarbonylative coupling, intermolecular competition experiments between differently substituted boronic acids were conducted (Scheme S5). The experiments revealed that electron-rich boronic acids are inherently more reactive than their electron-deficient counterparts, consistent with decarbonylation favored by steric demand of acylpalladium complexes.

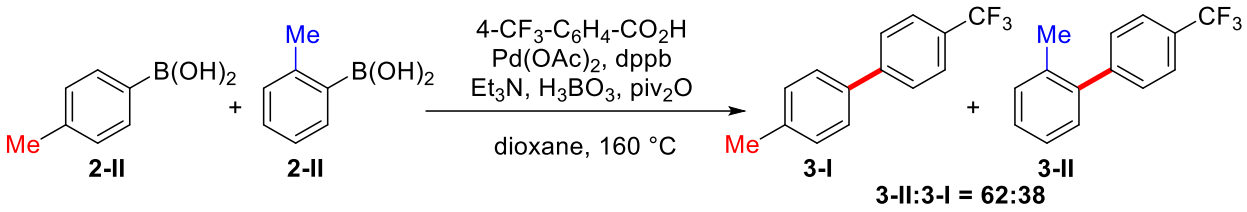

Scheme S5. Intermolecular competition experiments in decarbonylative Suzuki-Miyaura coupling of carboxylic acids, related to Figure 1. *Conditions: **2** (1.0 equiv each), 4-CF_3-C_6H_4-CO_2H (0.5 equiv), $Pd(OAc)_2$ (5 mol%), dppb (10 mol%), Et_3N (1.5 equiv), H_3BO_3 (1.5 equiv), piv_2O (1.5 equiv), dioxane (0.20 M), 160 °C, 15 h.*

(6) To investigate the effect of low catalytic loading on the decarbonylative coupling, the cross-coupling was conducted at 0.25 mol% of $Pd(OAc)_2$ (Scheme S6). Formation of product **3b** from **1b** was observed without a noticeable decrease in yield, consistent with the high efficiency of this cross-coupling. The high catalytic efficiency is characteristic to Pd catalysis and bodes well for the future development of protocols in the redox-neutral decarbonylative cross-coupling manifold of carboxylic acids.

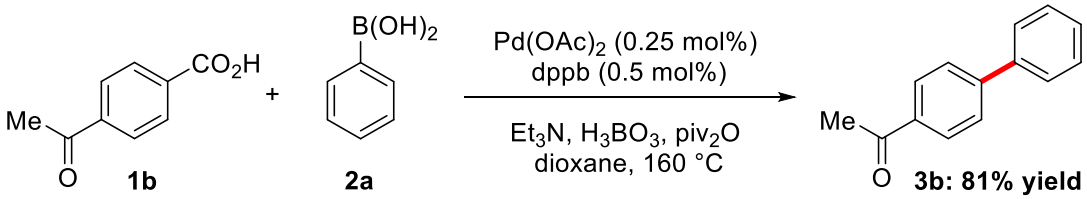

Scheme S6. Decarbonylative Suzuki-Miyaura coupling of carboxylic acids at low catalyst loading, related to Figure 1. *Conditions: **1** (1.0 equiv), $PhB(OH)_2$ (2.0 equiv), $Pd(OAc)_2$ (0.25 mol%), dppb (0.5 mol%), Et_3N (1.5 equiv), H_3BO_3 (1.5 equiv), piv_2O (1.5 equiv), dioxane, 160 °C, 15 h.*

Characterization Data of Cross-Coupling Products

4-(Methoxycarbonyl)benzoic acid and phenylboronic acid (3a, Figure 3, Entry 1)

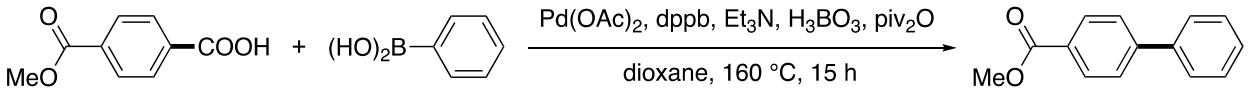

1a **2a** **3a**

According to the general procedure, the reaction of 4-(methoxycarbonyl)benzoic acid (0.20 mmol), phenylboronic acid (2.0 equiv), $Pd(OAc)_2$ (5 mol%), 1,4-bis(diphenylphosphino)butane (10 mol%), triethylamine (1.5 equiv), H_3BO_3 (1.5 equiv) and trimethylacetic anhydride (1.5 equiv) in 1,4-dioxane (0.20 M) for 15 h at 160 °C, afforded after work-up and chromatography the title compound in 92% yield (39.1 mg). White solid. **^{1}H NMR (500 MHz, $CDCl_3$)** δ 8.15-8.13 (d, *J* = 8.3 Hz, 2 H), 7.70-7.68 (d, *J* = 8.3 Hz, 2 H), 7.66-7.65 (d, *J* = 7.6 Hz, 2 H), 7.51-7.48 (t, *J* = 7.4 Hz, 2 H), 7.44-7.41 (t, *J* = 7.4 Hz, 1 H), 3.97 (s, 3 H). **^{13}C NMR (125 MHz, $CDCl_3$)** δ 167.02, 145.65, 140.02, 130.13, 128.95, 128.92, 128.17, 127.30, 127.07, 52.15. The spectral data matched those reported in the literature (Liu et al., 2018).

4-Acetylbenzoic acid and phenylboronic acid (3b, Figure 3, Entry 2)

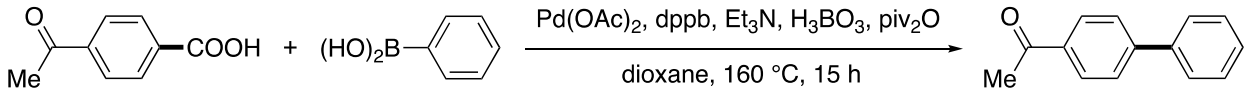

1b **2a** **3b**

According to the general procedure, the reaction of 4-acetylbenzoic acid (0.20 mmol), phenylboronic acid (2.0 equiv), $Pd(OAc)_2$ (5 mol%), 1,4-bis(diphenylphosphino)butane (10 mol%), triethylamine (1.5 equiv), H_3BO_3 (1.5 equiv) and trimethylacetic anhydride (1.5 equiv) in 1,4-dioxane (0.20 M) for 15 h at 160 °C, afforded after work-up and chromatography the title compound in 83% yield (32.6 mg). White solid. **^{1}H NMR (500 MHz, $CDCl_3$)** δ 8.07-8.05 (d, *J* = 8.2 Hz, 2 H), 7.72-7.71 (d, *J* = 8.3 Hz, 2 H), 7.66-7.65 (d, *J* = 7.8 Hz, 2 H), 7.52-7.49 (t, *J* = 7.4 Hz, 2 H), 7.44-7.42 (t, *J* = 7.4 Hz, 1 H), 2.67 (s, 3 H). **^{13}C NMR (125 MHz, $CDCl_3$)** δ 197.79, 145.81, 139.90, 135.87, 128.98, 128.94, 128.26, 127.30, 127.25, 26.69. The spectral data matched those reported in the literature (Shi et al., 2016).

4-Formylbenzoic acid and phenylboronic acid (3c, Figure 3, Entry 3)

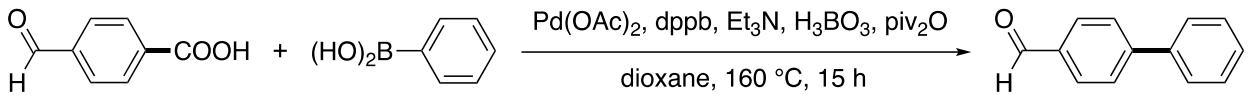

1c **2a** **3c**

According to the general procedure, the reaction of 4-formylbenzoic acid (0.20 mmol), phenylboronic acid (2.0 equiv), $Pd(OAc)_2$ (5 mol%), 1,4-bis(diphenylphosphino)butane (10 mol%), triethylamine (1.5 equiv), H_3BO_3 (1.5 equiv) and trimethylacetic anhydride (1.5 equiv) in 1,4-dioxane (0.20 M) for 15 h at 160 °C, afforded after work-up and chromatography the title compound in 82% yield (29.9 mg). White solid. **^{1}H NMR (500 MHz, $CDCl_3$)** δ 10.09 (s, 1 H), 7.99-7.98 (d, *J* = 8.2 Hz, 2 H), 7.79-7.78 (d, *J* = 8.1 Hz, 2 H), 7.67-7.66 (d, *J* = 7.4 Hz, 2 H), 7.53-7.50 (t, *J* = 7.4 Hz, 2 H), 7.46-7.43 (t, *J* = 7.2 Hz, 1 H). **^{13}C NMR (125 MHz, $CDCl_3$)** δ 191.98, 147.24, 139.75, 135.22, 130.30, 129.04, 128.50, 127.72, 127.39. The spectral data matched those reported in the literature (Kadam et al., 2018).

4-(Trifluoromethyl)benzoic acid and phenylboronic acid (3d, Figure 3, Entry 4)

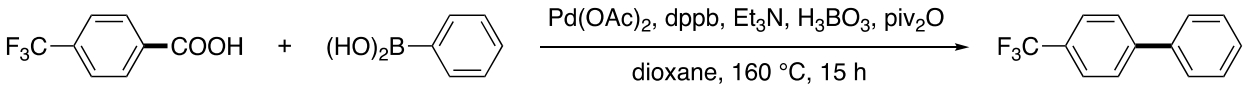

1d **2a** **3d**

According to the general procedure, the reaction of 4-(trifluoromethyl)benzoic acid (0.20 mmol), phenylboronic acid (2.0 equiv), $Pd(OAc)_2$ (5 mol%), 1,4-bis(diphenylphosphino)butane (10 mol%), triethylamine (1.5 equiv), H_3BO_3 (1.5 equiv) and trimethylacetic anhydride (1.5 equiv) in 1,4-dioxane (0.20 M) for 15 h at 160 °C, afforded after work-up and chromatography the title compound in 91% yield (40.5 mg). White solid. **^{1}H NMR (500 MHz, $CDCl_3$)** δ 7.73 (s, 4 H), 7.64-7.63 (d, *J* = 7.6 Hz, 2 H), 7.52-7.49 (t, *J* = 7.5 Hz, 2 H), 7.46-7.43 (t, *J* = 7.4 Hz, 1 H). **^{13}C NMR (125 MHz, $CDCl_3$)** δ 144.75, 139.79, 129.36 (q, J^F = 32.3 Hz), 129.01, 128.21, 127.44, 127.30, 125.73 (q, J^F = 3.7 Hz), 124.34 (q, J^F = 270.2 Hz). **^{19}F NMR (471 MHz, $CDCl_3$)** δ -62.39. The spectral data matched those reported in the literature (Shi et al., 2016).

4-(Tosyloxy)benzoic acid and phenylboronic acid (3e, Figure 3, Entry 5)

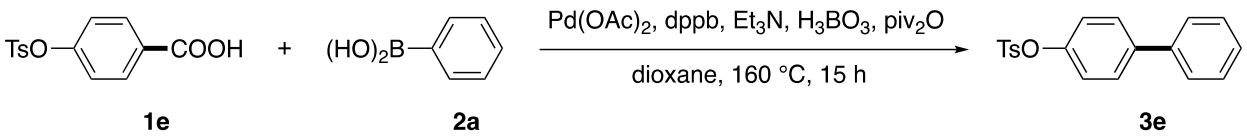

1e **2a** **3e**

According to the general procedure, the reaction of 4-(tosyloxy)benzoic acid (0.20 mmol), phenylboronic acid (2.0 equiv), $Pd(OAc)_2$ (5 mol%), 1,4-bis(diphenylphosphino)butane (10 mol%), triethylamine (1.5 equiv), H_3BO_3 (1.5 equiv) and trimethylacetic anhydride (1.5 equiv) in 1,4-dioxane (0.20 M) for 15 h at 160 °C, afforded after work-up and chromatography the title compound in 94% yield (61.0 mg). White solid. **^{1}H NMR (500 MHz, $CDCl_3$)** δ 7.79-7.76 (t, *J* = 6.9 Hz, 4 H), 7.55-7.50 (m, 3 H), 7.47-7.44 (t, *J* = 7.5 Hz, 1 H), 7.39-7.34 (m, 3 H), 7.15-7.13 (d, *J* = 8.4 Hz, 1 H), 7.08-7.06 (d, *J* = 8.4 Hz, 1 H), 2.48 (s, 3 H). **^{13}C NMR (125 MHz, $CDCl_3$)** δ 149.02, 140.18, 137.13, 132.74, 131.73, 129.96, 129.79, 128.87, 128.58, 128.25, 127.08, 122.67, 21.74. The spectral data matched those reported in the literature (Lv et al., 2018).

4-Cyanobenzoic acid and phenylboronic acid (3f, Figure 3, Entry 6)

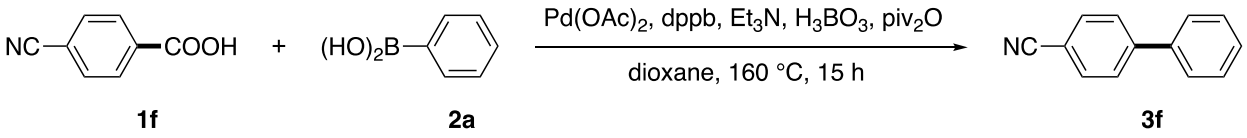

1f **2a** **3f**

According to the general procedure, the reaction of 4-cyanobenzoic acid (0.20 mmol), phenylboronic acid (2.0 equiv), $Pd(OAc)_2$ (5 mol%), 1,4-bis(diphenylphosphino)butane (10 mol%), triethylamine (1.5 equiv), H_3BO_3 (1.5 equiv) and trimethylacetic anhydride (1.5 equiv) in 1,4-dioxane (0.20 M) for 15 h at 160 °C, afforded after work-up and chromatography the title compound in 62% yield (22.3 mg). White solid. **^{1}H NMR (500 MHz, $CDCl_3$)** δ 7.76-7.70 (m, 4 H), 7.62-7.61 (d, *J* = 7.4 Hz, 2 H), 7.53-7.50 (t, *J* = 7.3 Hz, 2 H), 7.47-7.44 (t, *J* = 7.2 Hz, 1 H). **^{13}C NMR (125 MHz, $CDCl_3$)** δ 145.70, 139.20, 132.62, 129.13, 128.68, 127.76, 127.25, 118.97, 110.94. The spectral data matched those reported in the literature (Gan et al., 2018).

2-Methylbenzoic acid and 4-methoxyphenylboronic acid (3g, Figure 3, Entry 7)

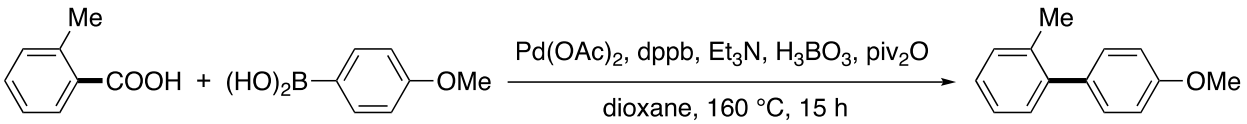

1g **2b** **3g**

According to the general procedure, the reaction of 2-methylbenzoic acid (0.20 mmol), 4-methoxyphenylboronic acid (2.0 equiv), $Pd(OAc)_2$ (5 mol%), 1,4-bis(diphenylphosphino)butane (10 mol%), triethylamine (1.5 equiv), H_3BO_3 (1.5 equiv) and trimethylacetic anhydride (1.5 equiv) in 1,4-dioxane (0.20 M) for 15 h at 160 °C, afforded after work-up and chromatography the title compound in 80% yield (31.8 mg). White solid. **^{1}H NMR (500 MHz, $CDCl_3$)** δ 7.30-7.26 (m, 6 H), 7.00-6.98 (d, *J* = 8.6 Hz, 2 H), 3.89 (s, 3 H), 2.31 (s, 3 H). **^{13}C NMR (125 MHz, $CDCl_3$)** δ 158.52, 141.56, 135.51, 134.39, 130.31, 130.27, 129.92, 126.99, 125.77, 113.50, 55.30, 20.56. The spectral data matched those reported in the literature (Simpson et al., 2018).

2-(Methylthio)benzoic acid and 4-methoxyphenylboronic acid (3h, Figure 3, Entry 8)

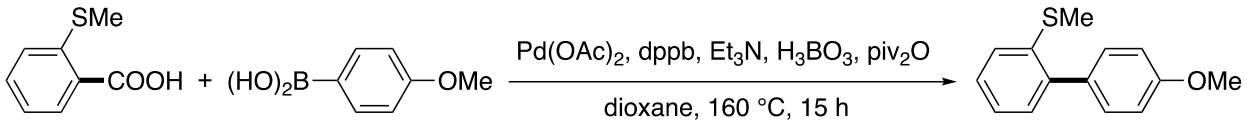

1h **2b** **3h**

According to the general procedure, the reaction of 2-(methylthio)benzoic acid (0.20 mmol), 4-methoxyphenylboronic acid (2.0 equiv), $Pd(OAc)_2$ (5 mol%), 1,4-bis(diphenylphosphino)butane (10 mol%), triethylamine (1.5 equiv), H_3BO_3 (1.5 equiv) and trimethylacetic anhydride (1.5 equiv) in 1,4-dioxane (0.20 M) for 15 h at 160 °C, afforded after work-up and chromatography the title compound in 97% yield (44.7 mg). White solid. **^{1}H NMR (500 MHz, $CDCl_3$)** δ 7.39-7.33 (m, 3 H), 7.30-7.29 (d, *J* = 9.5 Hz, 1 H), 7.24-7.20 (m, 2 H), 7.01-6.99 (d, *J* = 8.6 Hz, 2 H), 3.89 (s, 3 H), 2.40 (s, 3 H). **^{13}C NMR (125 MHz, $CDCl_3$)** δ 159.06, 140.56, 137.30, 132.93, 130.47, 130.07, 127.69, 125.09, 124.69, 113.54, 55.28, 16.00. The spectral data matched those reported in the literature (Sugahara et al., 2014).

2-Methoxybenzoic acid and phenylboronic acid (3i, Figure 3, Entry 9)

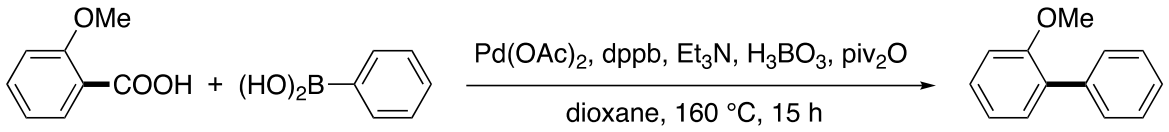

1i **2a** **3i**

According to the general procedure, the reaction of 2-methoxybenzoic acid (0.20 mmol), phenylboronic acid (2.0 equiv), $Pd(OAc)_2$ (5 mol%), 1,4-bis(diphenylphosphino)butane (10 mol%), triethylamine (1.5 equiv), H_3BO_3 (1.5 equiv) and trimethylacetic anhydride (1.5 equiv) in 1,4-dioxane (0.20 M) for 15 h at 160 °C, afforded after work-up and chromatography the title compound in 55% yield (20.3 mg). White solid. **^{1}H NMR (500 MHz, $CDCl_3$)** δ 7.58-7.57 (d, *J* = 7.6 Hz, 2 H), 7.47-7.44 (t, *J* = 7.5 Hz, 2 H), 7.38-7.35 (t, *J* = 7.1 Hz, 3 H), 7.09-7.06 (t, *J* = 7.5 Hz, 1 H), 7.04-7.02 (d, *J* = 8.6 Hz, 1 H), 3.85 (s, 3 H). **^{13}C NMR (125 MHz, $CDCl_3$)** δ 156.49, 138.57, 130.92, 130.75, 129.57, 128.64, 128.01, 126.94, 120.85, 111.25, 55.58. The spectral data matched those reported in the literature (Simpson et al., 2018).

1-Naphthoic acid and phenylboronic acid (3j, Figure 3, Entry 10)

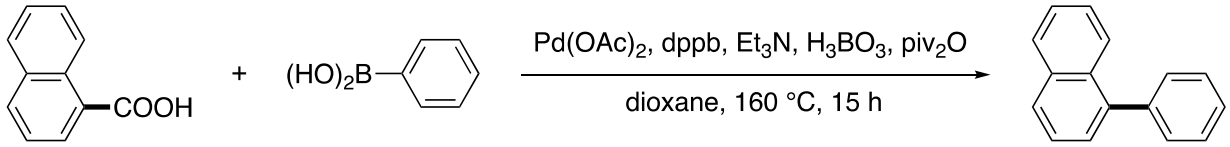

1j **2a** **3j**

According to the general procedure, the reaction of 1-naphthoic acid (0.20 mmol), phenylboronic acid (2.0 equiv), $Pd(OAc)_2$ (5 mol%), 1,4-bis(diphenylphosphino)butane (10 mol%), triethylamine (1.5 equiv), H_3BO_3 (1.5 equiv) and trimethylacetic anhydride (1.5 equiv) in 1,4-dioxane (0.20 M) for 15 h at 160 °C, afforded after work-up and chromatography the title compound in 77% yield (31.5 mg). White solid. **^{1}H NMR (500 MHz, $CDCl_3$)** δ 7.95-7.94 (d, *J* = 8.6 Hz, 2 H), 7.91-7.89 (d, *J* = 8.2 Hz, 1 H), 7.58-7.51 (m, 6 H), 7.48-7.45 (m, 3 H). **^{13}C NMR (125 MHz, $CDCl_3$)** δ 140.79, 140.29, 133.82, 131.64, 130.10, 128.28, 127.65, 127.26, 126.95, 126.05, 126.04, 125.79, 125.40. The spectral data matched those reported in the literature (Shi et al., 2016).

2-Naphthoic acid and 4-methoxyphenylboronic acid (3k, Figure 3, Entry 11)

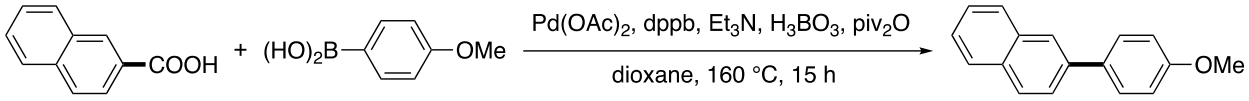

1k **2b** **3k**

According to the general procedure, the reaction of 2-naphthoic acid (0.20 mmol), 4-methoxyphenylboronic acid (2.0 equiv), $Pd(OAc)_2$ (5 mol%), 1,4-bis(diphenylphosphino)butane (10 mol%), triethylamine (1.5 equiv), H_3BO_3 (1.5 equiv) and trimethylacetic anhydride (1.5 equiv) in 1,4-dioxane (0.20 M) for 15 h at 160 °C, afforded after work-up and chromatography the title compound in 60% yield (28.2 mg). White solid. **^{1}H NMR (500 MHz, $CDCl_3$)** δ 8.02 (s, 1 H), 7.93-7.87 (m, 3 H), 7.76-7.74 (dd, *J* = 8.5 Hz, 1 H), 7.70-7.69 (d, *J* = 8.7 Hz, 2 H), 7.54-7.48 (m, 2 H), 7.07-7.05 (d, *J* = 8.7 Hz, 2 H), 3.91 (s, 3 H). **^{13}C NMR (125 MHz, $CDCl_3$)** δ 159.27, 138.17, 133.77, 133.66, 132.33, 128.45, 128.36, 128.07, 127.64, 126.25, 125.66, 125.46, 125.05, 114.34, 55.41. The spectral data matched those reported in the literature (Muto et al., 2015).

Quinoline-6-carboxylic acid and phenylboronic acid (3l, Figure 3, Entry 12)

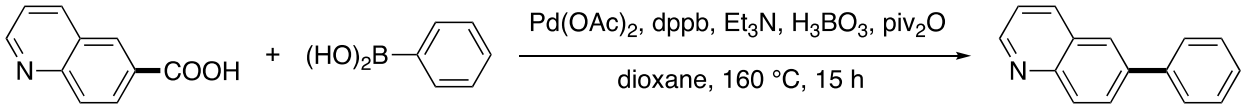

1l **2a** **3l**

According to the general procedure, the reaction of quinoline-6-carboxylic acid (0.20 mmol), phenylboronic acid (2.0 equiv), $Pd(OAc)_2$ (5 mol%), 1,4-bis(diphenylphosphino)butane (10 mol%), triethylamine (1.5 equiv), H_3BO_3 (1.5 equiv) and trimethylacetic anhydride (1.5 equiv) in 1,4-dioxane (0.20 M) for 15 h at 160 °C, afforded after work-up and chromatography the title compound in 76% yield (31.2 mg). White solid. **^{1}H NMR (500 MHz, $CDCl_3$)** δ 8.95-8.95 (d, *J* = 2.7 Hz, 1 H), 8.25-8.20 (m, 2 H), 8.03-8.01 (m, 2 H), 7.76-7.74 (d, *J* = 7.5 Hz, 2 H), 7.55-7.52 (t, *J* = 7.5 Hz, 2 H), 7.47-7.42 (m, 2 H). **^{13}C NMR (125 MHz, $CDCl_3$)** δ 150.40, 147.70, 140.35, 139.37, 136.28, 129.92, 129.27, 128.99, 128.49, 127.78, 127.49, 125.51, 121.50. The spectral data matched those reported in the literature (Okura et al., 2018).

Nicotinic acid and phenylboronic acid (3m, Figure 3, Entry 13)

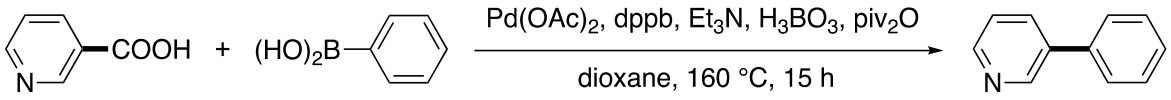

1m **2a** **3m**

According to the general procedure, the reaction of nicotinic acid (0.20 mmol), phenylboronic acid (2.0 equiv), $Pd(OAc)_2$ (5 mol%), 1,4-bis(diphenylphosphino)butane (10 mol%), triethylamine (1.5 equiv), H_3BO_3 (1.5 equiv) and trimethylacetic anhydride (1.5 equiv) in 1,4-dioxane (0.20 M) for 15 h at 160 °C, afforded after work-up and chromatography the title compound in 92% yield (28.6 mg). White solid. **^{1}H NMR (500 MHz, $CDCl_3$)** δ 8.88 (s, 1 H), 8.63-8.62 (d, *J* = 4.5 Hz, 1 H), 7.91-7.90 (d, *J* = 7.9 Hz, 1 H), 7.62-7.61 (d, *J* = 7.5 Hz, 2 H), 7.53-7.50 (t, *J* = 7.5 Hz, 2 H), 7.45-7.42 (t, *J* = 7.4 Hz, 1 H), 7.41-7.38 (m, 1 H). **^{13}C NMR (125 MHz, $CDCl_3$)** δ 148.49, 148.37, 137.87, 136.67, 134.39, 129.10, 128.12, 127.18, 123.56. The spectral data matched those reported in the literature (Muto et al., 2015).

Picolinic acid and 4-methoxyphenylboronic acid (3n, Figure 3, Entry 14)

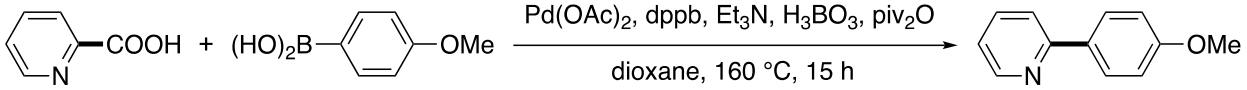

1n **2b** **3n**

According to the general procedure, the reaction of picolinic acid (0.20 mmol), 4-methoxyphenylboronic acid (2.0 equiv), $Pd(OAc)_2$ (5 mol%), 1,4-bis(diphenylphosphino)butane (10 mol%), triethylamine (1.5 equiv), H_3BO_3 (1.5 equiv) and trimethylacetic anhydride (1.5 equiv) in 1,4-dioxane (0.20 M) for 15 h at 160 °C, afforded after work-up and chromatography the title compound in 75% yield (27.8 mg). White solid. **^{1}H NMR (500 MHz, $CDCl_3$)** δ 8.68-8.67 (d, *J* = 4.5 Hz, 1 H), 7.99-7.97 (d, *J* = 8.7 Hz, 2 H), 7.75-7.72 (t, *J* = 7.8 Hz, 1 H), 7.70-7.68 (m, 1 H), 7.21-7.18 (t, *J* = 6.0 Hz, 1 H), 7.03-7.02 (d, *J* = 8.7 Hz, 2 H), 3.89 (s, 3 H). **^{13}C NMR (125 MHz, $CDCl_3$)** δ 160.47, 157.15, 149.56, 136.68, 132.06, 128.18, 121.42, 119.83, 114.13, 55.37. The spectral data matched those reported in the literature (Muto et al., 2015).

4-(Dibenzo[*b,d*]furan-4-yl)benzoic acid and 4-methoxyphenylboronic acid (3o, Figure 3, Entry 15)

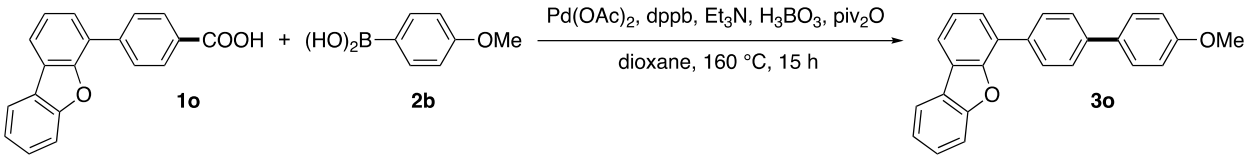

According to the general procedure, the reaction of 4-(dibenzo[*b,d*]furan-4-yl)benzoic acid (0.20 mmol), 4-methoxyphenylboronic acid (2.0 equiv), $Pd(OAc)_2$ (5 mol%), 1,4-bis(diphenylphosphino)butane (10 mol%), triethylamine (1.5 equiv), H_3BO_3 (1.5 equiv) and trimethylacetic anhydride (1.5 equiv) in 1,4-dioxane (0.20 M) for 15 h at 160 °C, afforded after work-up and chromatography the title compound in 78% yield (54.7 mg). *New compound.* White solid. **Mp** = 189-191 °C. **^{1}H NMR (500 MHz, $CDCl_3$)** δ 8.04-8.00 (t, *J* = 7.9 Hz, 3 H), 7.98-7.97 (d, *J* = 7.5 Hz, 1 H), 7.77-7.75 (d, *J* = 8.2 Hz, 2 H), 7.69-7.64 (m, 4 H), 7.52-7.46 (m, 2 H), 7.41-7.38 (t, *J* = 7.4 Hz, 1 H), 7.06-7.04 (d, *J* = 8.6 Hz, 2 H), 3.90 (s, 3 H). **^{13}C NMR (125 MHz, $CDCl_3$)** δ 159.31, 156.22, 153.44, 140.25, 134.77, 133.35, 129.14, 128.16, 127.25, 126.96, 126.69, 125.56, 124.97, 124.24, 123.26, 122.80, 120.70, 119.63, 114.32, 111.89, 55.39. **HRMS** calcd for $C_{25}H_{18}O_2Na$ (M^+ + Na) 350.1301, found 350.1314.

4-(Dibenzo[*b,d*]thiophen-4-yl)benzoic acid and 4-methoxyphenylboronic acid (3p, Figure 3, Entry 16)

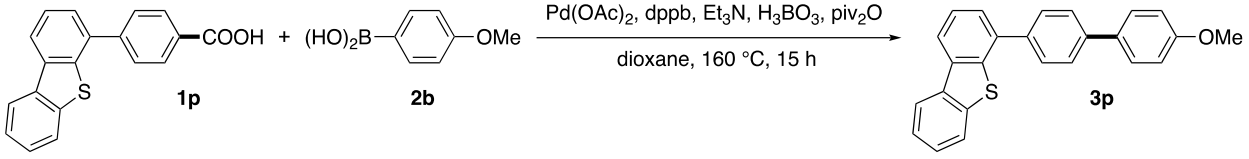

According to the general procedure, the reaction of 4-(dibenzo[*b,d*]thiophen-4-yl)benzoic acid (0.20 mmol), 4-methoxyphenylboronic acid (2.0 equiv), $Pd(OAc)_2$ (5 mol%), 1,4-bis(diphenylphosphino)butane (10 mol%), triethylamine (1.5 equiv), H_3BO_3 (1.5 equiv) and trimethylacetic anhydride (1.5 equiv) in 1,4-dioxane (0.20 M) for 15 h at 160 °C, afforded after work-up and chromatography the title compound in 73% yield (53.5 mg). *New compound.* White solid. **Mp** = 198-200 °C. **^{1}H NMR (500 MHz, $CDCl_3$)** δ 8.24-8.19 (m, 2 H), 7.89-7.87 (m, 1 H), 7.84-7.83 (d, *J* = 8.1 Hz, 2 H), 7.75-7.73 (d, *J* = 8.2 Hz, 2 H), 7.66-7.65 (d, *J* = 8.7 Hz, 2 H), 7.62-7.59 (t, *J* = 7.5 Hz, 1 H), 7.57-7.55 (m, 1 H), 7.52-7.48 (m, 2 H), 7.06-7.04 (d, *J* = 8.6 Hz, 2 H), 3.91 (s, 3 H). **^{13}C NMR (125 MHz, $CDCl_3$)** δ 159.38, 140.48, 139.63, 138.93, 138.59,

136.73, 136.30, 135.84, 133.22, 128.63, 128.16, 127.05, 126.83, 126.81, 125.14, 124.39, 122.63, 121.75, 120.43, 114.34, 55.38. **HRMS** calcd for $C_{25}H_{18}OSNa$ (M^+ + Na) 366.1073, found 366.1065.

4'-(Trifluoromethyl)-[1,1'-biphenyl]-4-carboxylic acid and phenylboronic acid (3q, Figure 3, Entry 17)

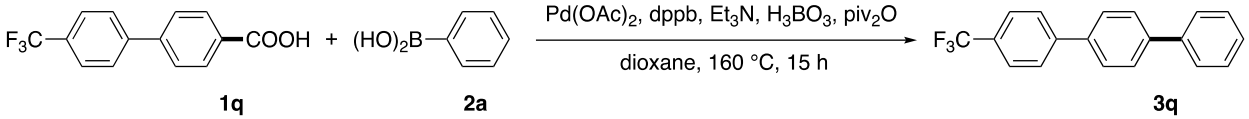

1q **2a** **3q**

According to the general procedure, the reaction of 4'-(trifluoromethyl)-[1,1'-biphenyl]-4-carboxylic acid (0.20 mmol), phenylboronic acid (2.0 equiv), $Pd(OAc)_2$ (5 mol%), 1,4-bis(diphenylphosphino)butane (10 mol%), triethylamine (1.5 equiv), H_3BO_3 (1.5 equiv) and trimethylacetic anhydride (1.5 equiv) in 1,4-dioxane (0.20 M) for 15 h at 160 °C, afforded after work-up and chromatography the title compound in 78% yield (46.6 mg). White solid. **^{1}H NMR (500 MHz, $CDCl_3$)** δ 7.78-7.70 (m, 8 H), 7.68-7.66 (d, *J* = 7.8 Hz, 2 H), 7.51-7.48 (t, *J* = 7.5 Hz, 2 H), 7.42-7.39 (t, *J* = 7.4 Hz, 1 H). **^{13}C NMR (125 MHz, $CDCl_3$)** δ 144.23, 141.12, 140.41, 138.60, 129.05 (q, J^F = 56.8 Hz), 128.90, 127.72, 127.65, 127.61, 127.51 (q, J^F = 220.7 Hz), 127.29, 127.09, 125.78 (q, J^F = 4.4 Hz). **^{19}F NMR (471 MHz, $CDCl_3$)** δ -62.40. The spectral data matched those reported in the literature (Nakamura et al., 2015).

(*E*)-2-Styrylbenzoic acid and 4-methoxyphenylboronic acid (3r, Figure 3, Entry 18)

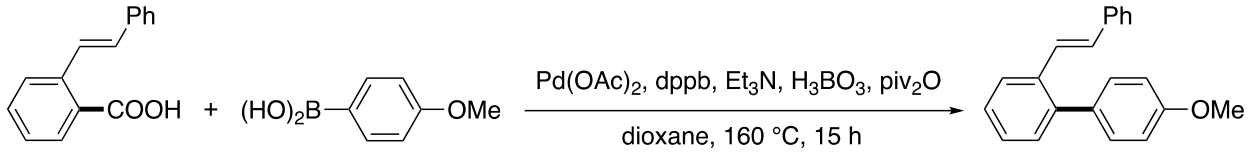

1r **2b** **3r**

According to the general procedure, the reaction of (*E*)-2-styrylbenzoic acid (0.20 mmol), 4-methoxyphenylboronic acid (2.0 equiv), $Pd(OAc)_2$ (5 mol%), 1,4-bis(diphenylphosphino)butane (10 mol%), triethylamine (1.5 equiv), H_3BO_3 (1.5 equiv) and trimethylacetic anhydride (1.5 equiv) in 1,4-dioxane (0.20 M) for 15 h at 160 °C, afforded after work-up and chromatography the title compound in 82% yield (47.0 mg). White solid. **^{1}H NMR (500 MHz, $CDCl_3$)** δ 7.78-7.76 (d, *J* = 7.4 Hz, 1 H), 7.43-7.33 (m, 9 H), 7.27-7.24 (t, *J* = 7.4 Hz, 1 H), 7.19-7.16 (d, *J* = 16.3 Hz, 1 H), 7.09-7.05 (d, *J* = 16.3 Hz, 1 H), 7.02-7.00 (d, *J* = 8.6 Hz, 2 H), 3.91 (s, 3 H). **^{13}C**

NMR (125 MHz, $CDCl_3$) δ 158.85, 140.82, 137.70, 135.48, 133.29, 131.02, 130.29, 129.27, 128.65, 128.07, 127.55, 127.45, 127.25, 126.55, 125.91, 113.59, 55.34. The spectral data matched those reported in the literature (Veld et al., 1978).

[1,1'-Biphenyl]-2-carboxylic acid and 4-methoxyphenylboronic acid (3s, Figure 3, Entry 19)

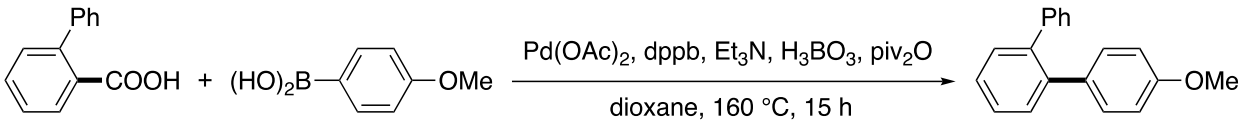

1s **2b** **3s**

According to the general procedure, the reaction of [1,1'-biphenyl]-2-carboxylic acid (0.20 mmol), 4-methoxyphenylboronic acid (2.0 equiv), $Pd(OAc)_2$ (5 mol%), 1,4-bis(diphenylphosphino)butane (10 mol%), triethylamine (1.5 equiv), H_3BO_3 (1.5 equiv) and trimethylacetic anhydride (1.5 equiv) in 1,4-dioxane (0.20 M) for 15 h at 160 °C, afforded after work-up and chromatography the title compound in 56% yield (29.2 mg). White solid. **^{1}H NMR (500 MHz, $CDCl_3$)** δ 7.45-7.43 (m, 4 H), 7.27-7.21 (m, 3 H), 7.19-7.18 (m, 2 H), 7.09-7.08 (d, *J* = 8.6 Hz, 2 H), 6.79-6.78 (d, *J* = 8.6 Hz, 2 H), 3.80 (s, 3 H). **^{13}C NMR (125 MHz, $CDCl_3$)** δ 158.30, 141.74, 140.49, 140.16, 133.91, 130.94, 130.64, 130.55, 129.89, 127.91, 127.48, 127.14, 126.38, 113.35, 55.18. The spectral data matched those reported in the literature (Yadav et al., 2017).

Benzoic acid and 4-methoxyphenylboronic acid (3t, Figure 3, Entry 20)

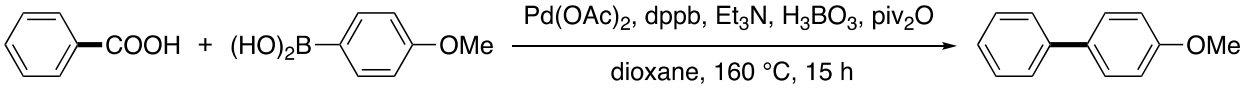

1t **2b** **3t**

According to the general procedure, the reaction of benzoic acid (0.20 mmol), 4-methoxyphenylboronic acid (2.0 equiv), $Pd(OAc)_2$ (5 mol%), 1,4-bis(diphenylphosphino)butane (10 mol%), triethylamine (1.5 equiv), H_3BO_3 (1.5 equiv) and trimethylacetic anhydride (1.5 equiv) in 1,4-dioxane (0.20 M) for 15 h at 160 °C, afforded after work-up and chromatography the title compound in 51% yield (18.8 mg). White solid. **^{1}H NMR (500 MHz, $CDCl_3$)** δ 7.59-7.55 (m, 4 H), 7.46-7.43 (t, *J* = 7.6 Hz, 2 H), 7.34-7.31 (t, *J* = 7.4 Hz, 1 H), 7.02-7.00 (d, *J* = 8.7 Hz, 2 H), 3.88 (s, 3 H). **^{13}C NMR (125 MHz, $CDCl_3$)** δ 159.15, 140.85, 133.80, 128.73, 128.17,

126.76, 126.67, 114.21, 55.37. The spectral data matched those reported in the literature (Song et al., 2018).

4-Chlorobenzoic acid and 4-methoxyphenylboronic acid (3u, Figure 3, Entry 21)

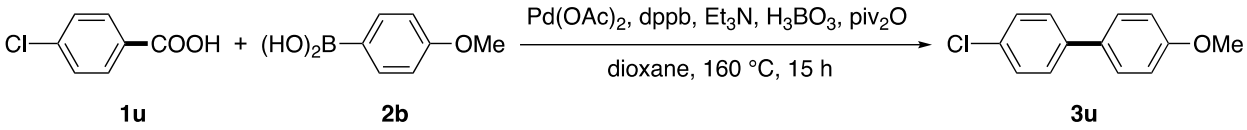

1u **2b** **3u**

According to the general procedure, the reaction of 4-chlorobenzoic acid (0.20 mmol), 4-methoxyphenylboronic acid (2.0 equiv), $Pd(OAc)_2$ (5 mol%), 1,4-bis(diphenylphosphino)butane (10 mol%), triethylamine (1.5 equiv), H_3BO_3 (1.5 equiv) and trimethylacetic anhydride (1.5 equiv) in 1,4-dioxane (0.20 M) for 15 h at 160 °C, afforded after work-up and chromatography the title compound in 59% yield (25.8 mg). White solid. **^{1}H NMR (500 MHz, $CDCl_3$)** δ 7.52-7.49 (t, *J* = 8.3 Hz, 4 H), 7.41-7.39 (d, *J* = 8.5 Hz, 2 H), 7.01-6.99 (d, *J* = 8.7 Hz, 2 H), 3.88 (s, 3 H). **^{13}C NMR (125 MHz, $CDCl_3$)** δ 159.38, 139.29, 132.69, 132.52, 128.85, 128.03, 127.95, 114.33, 55.39. The spectral data matched those reported in the literature (Keaveney et al., 2018).

3-(Methoxycarbonyl)benzoic acid and phenylboronic acid (3v, Figure 3, Entry 22)

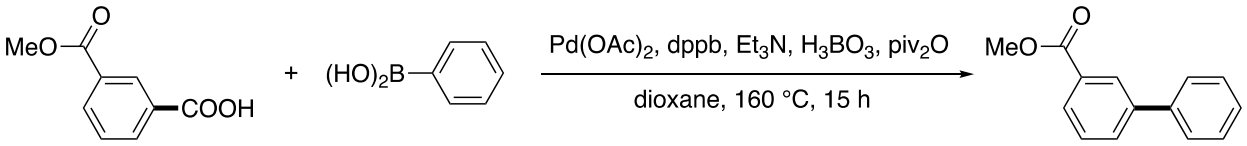

1v **2a** **3v**

According to the general procedure, the reaction of 3-(methoxycarbonyl)benzoic acid (0.20 mmol), phenylboronic acid (2.0 equiv), $Pd(OAc)_2$ (5 mol%), 1,4-bis(diphenylphosphino)butane (10 mol%), triethylamine (1.5 equiv), H_3BO_3 (1.5 equiv) and trimethylacetic anhydride (1.5 equiv) in 1,4-dioxane (0.20 M) for 15 h at 160 °C, afforded after work-up and chromatography the title compound in 52% yield (22.1 mg). White solid. **^{1}H NMR (500 MHz, $CDCl_3$)** δ 8.31 (s, 1 H), 8.06-8.04 (d, *J* = 7.8 Hz, 1 H), 7.82-7.81 (d, *J* = 7.7 Hz, 1 H), 7.66-7.65 (d, *J* = 7.5 Hz, 2 H), 7.56-7.53 (t, *J* = 7.7 Hz, 1 H), 7.51-7.48 (t, *J* = 7.7 Hz, 2 H), 7.42-7.39 (t, *J* = 7.4 Hz, 1 H), 3.98 (s, 3 H). **^{13}C NMR (125 MHz, $CDCl_3$)** δ 167.09, 141.50, 140.14, 131.56, 130.71, 128.91, 128.88, 128.37, 128.30, 127.77, 127.19, 52.23. The spectral data matched those reported in the literature (Yadav et al., 2017).

3-Acetylbenzoic acid and phenylboronic acid (3w, Figure 3, Entry 23)

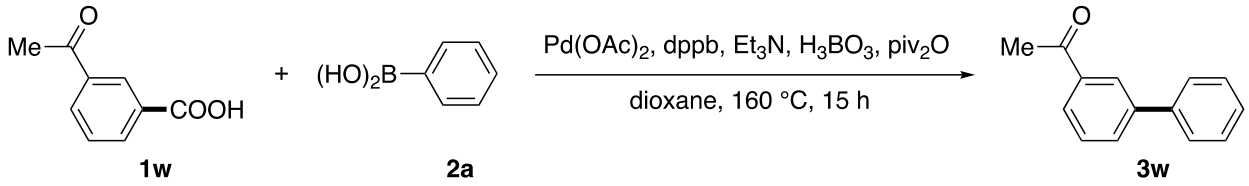

1w **2a** **3w**

According to the general procedure, the reaction of 3-acetylbenzoic acid (0.20 mmol), phenylboronic acid (2.0 equiv), $Pd(OAc)_2$ (5 mol%), 1,4-bis(diphenylphosphino)butane (10 mol%), triethylamine (1.5 equiv), H_3BO_3 (1.5 equiv) and trimethylacetic anhydride (1.5 equiv) in 1,4-dioxane (0.20 M) for 15 h at 160 °C, afforded after work-up and chromatography the title compound in 68% yield (26.7 mg). White solid. **^{1}H NMR (500 MHz, $CDCl_3$)** δ 8.21 (s, 1 H), 7.97-7.96 (d, *J* = 7.7 Hz, 1 H), 7.83-7.81 (d, *J* = 7.6 Hz, 1 H), 7.66-7.64 (d, *J* = 7.3 Hz, 2 H), 7.58-7.55 (t, *J* = 7.7 Hz, 1 H), 7.51-7.48 (t, *J* = 7.4 Hz, 2 H), 7.43-7.40 (t, *J* = 7.4 Hz, 1 H), 2.69 (s, 3 H). **^{13}C NMR (125 MHz, $CDCl_3$)** δ 198.12, 141.75, 140.21, 137.66, 131.77, 129.07, 128.95, 127.84, 127.22, 127.21, 126.99, 26.79. The spectral data matched those reported in the literature (Liu et al., 2018).

3-Chlorobenzoic acid and phenylboronic acid (3x, Figure 3, Entry 24)

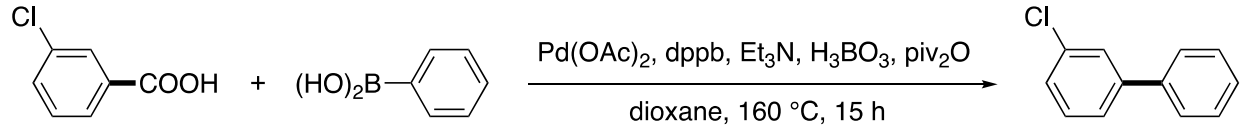

1x **2a** **3x**

According to the general procedure, the reaction of 3-chlorobenzoic acid (0.20 mmol), phenylboronic acid (2.0 equiv), $Pd(OAc)_2$ (5 mol%), 1,4-bis(diphenylphosphino)butane (10 mol%), triethylamine (1.5 equiv), H_3BO_3 (1.5 equiv) and trimethylacetic anhydride (1.5 equiv) in 1,4-dioxane (0.20 M) for 15 h at 160 °C, afforded after work-up and chromatography the title compound in 55% yield (20.8 mg). White solid. **^{1}H NMR (500 MHz, $CDCl_3$)** δ 7.60-7.58 (m, 3 H), 7.50-7.46 (m, 3 H), 7.41-7.38 (m, 2 H), 7.35-7.34 (m, 1 H). **^{13}C NMR (125 MHz, $CDCl_3$)** δ 143.09, 139.83, 134.66, 130.00, 128.91, 127.88, 127.32, 127.27, 127.13, 125.32. The spectral data matched those reported in the literature (Keaveney et al., 2018).

4-(Trifluoromethoxy)benzoic acid and 4-methoxyphenylboronic acid (3y, Figure 3, Entry 25)

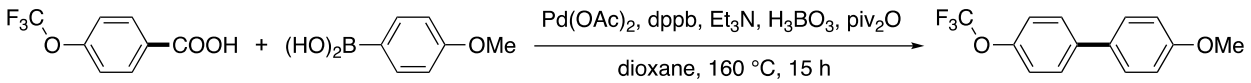

1y **2b** **3y**

According to the general procedure, the reaction of 4-(trifluoromethoxy)benzoic acid (0.20 mmol), 4-methoxyphenylboronic acid (2.0 equiv), $Pd(OAc)_2$ (5 mol%), 1,4-bis(diphenylphosphino)butane (10 mol%), triethylamine (1.5 equiv), H_3BO_3 (1.5 equiv) and trimethylacetic anhydride (1.5 equiv) in 1,4-dioxane (0.20 M) for 15 h at 160 °C, afforded after work-up and chromatography the title compound in 95% yield (51.0 mg). White solid. **^{1}H NMR (500 MHz, $CDCl_3$)** δ 7.58-7.57 (d, *J* = 8.6 Hz, 2 H), 7.53-7.51 (d, *J* = 8.6 Hz, 2 H), 7.29-7.28 (d, *J* = 8.1 Hz, 2 H), 7.02-7.00 (d, *J* = 8.6 Hz, 2 H), 3.88 (s, 3 H). **^{13}C NMR (125 MHz, $CDCl_3$)** δ 159.44, 148.20, 139.64, 132.38, 128.17, 127.97, 121.25, 120.56 (q, J^F = 255.3 Hz), 114.34, 55.37. **^{19}F NMR (471 MHz, $CDCl_3$)** δ -57.83. The spectral data matched those reported in the literature (Liu et al., 2013).

4-(Benzoyloxy)benzoic acid and 4-methoxyphenylboronic acid (3z, Figure 3, Entry 26)

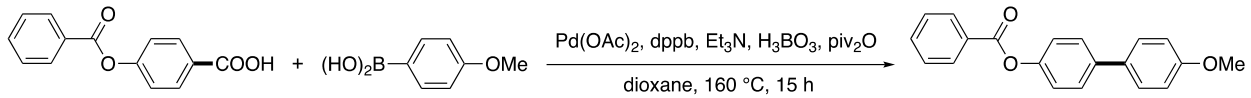

1z **2b** **3z**

According to the general procedure, the reaction of 4-(benzoyloxy)benzoic acid (0.20 mmol), 4-methoxyphenylboronic acid (2.0 equiv), $Pd(OAc)_2$ (5 mol%), 1,4-bis(diphenylphosphino)butane (10 mol%), triethylamine (1.5 equiv), H_3BO_3 (1.5 equiv) and trimethylacetic anhydride (1.5 equiv) in 1,4-dioxane (0.20 M) for 15 h at 160 °C, afforded after work-up and chromatography the title compound in 71% yield (43.3 mg). White solid. **^{1}H NMR (500 MHz, $CDCl_3$)** δ 8.26-8.25 (d, *J* = 7.3 Hz, 2 H), 7.69-7.66 (t, *J* = 7.5 Hz, 1 H), 7.63-7.61 (d, *J* = 8.6 Hz, 2 H), 7.57-7.54 (m, 4 H), 7.30-7.28 (d, *J* = 8.6 Hz, 2 H), 7.02-7.01 (d, *J* = 8.7 Hz, 2 H), 3.89 (s, 3 H). **^{13}C NMR (125 MHz, $CDCl_3$)** δ 165.31, 159.22, 149.92, 138.71, 133.63, 133.00, 130.96, 130.22, 128.60, 128.19, 127.80, 121.93, 114.27, 55.38. The compound has been previously reported (van Alpen et al., 1931).

Probenecid and phenylboronic acid (3aa, Figure 3, Entry 27)

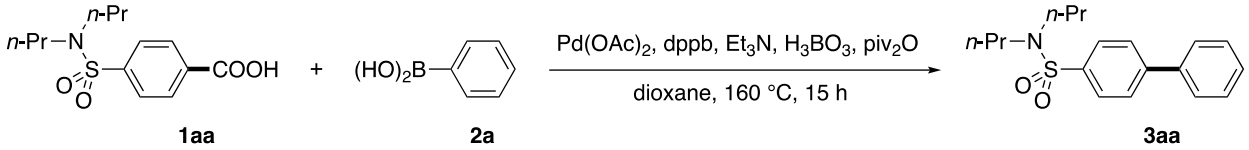

1aa **2a** **3aa**

According to the general procedure, the reaction of probenecid (0.20 mmol), phenylboronic acid (2.0 equiv), $Pd(OAc)_2$ (5 mol%), 1,4-bis(diphenylphosphino)butane (10 mol%), triethylamine (1.5 equiv), H_3BO_3 (1.5 equiv) and trimethylacetic anhydride (1.5 equiv) in 1,4-dioxane (0.20 M) for 15 h at 160 °C, afforded after work-up and chromatography the title compound in 90% yield (57.2 mg). *New compound.* White solid. **Mp** = 50-51 °C. **^{1}H NMR (500 MHz, $CDCl_3$)** δ 7.90-7.88 (d, *J* = 8.4 Hz, 2 H), 7.73-7.71 (d, *J* = 8.4 Hz, 2 H), 7.64-7.62 (d, *J* = 7.2 Hz, 2 H), 7.51-7.48 (t, *J* = 7.4 Hz, 2 H), 7.44-7.41 (t, *J* = 7.3 Hz, 1 H), 3.16-3.13 (t, *J* = 7.6 Hz, 4 H), 1.65-1.57 (m, 4 H), 0.93-0.90 (t, *J* = 7.4 Hz, 6 H). **^{13}C NMR (125 MHz, $CDCl_3$)** δ 145.09, 139.38, 138.77, 129.05, 128.41, 127.59, 127.58, 127.29, 50.16, 22.13, 11.24. **HRMS** calcd for $C_{18}H_{23}NO_2SNa$ (M^+ + Na) 340.1347, found 340.1383.

Flufenamic acid and 4-methoxyphenylboronic acid (3ab, Figure 3, Entry 28)

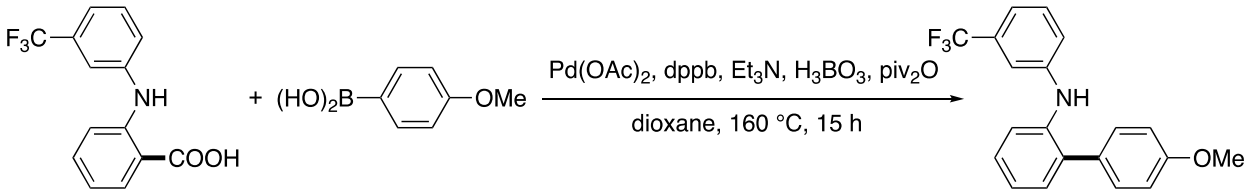

1ab **2b** **3ab**

According to the general procedure, the reaction of flufenamic acid (0.20 mmol), 4-methoxyphenylboronic acid (2.0 equiv), $Pd(OAc)_2$ (5 mol%), 1,4-bis(diphenylphosphino)butane (10 mol%), triethylamine (1.5 equiv), H_3BO_3 (1.5 equiv) and trimethylacetic anhydride (1.5 equiv) in 1,4-dioxane (0.20 M) for 15 h at 160 °C, afforded after work-up and chromatography the title compound in 60% yield (41.2 mg). *New compound.* White solid. **Mp** = 144-145 °C. **^{1}H NMR (500 MHz, $CDCl_3$)** δ 7.40-7.29 (m, 6 H), 7.24 (s, 1 H), 7.18-7.08 (m, 3 H), 7.00-6.98 (d, *J* = 8.7 Hz, 2 H), 5.69 (s, 1 H), 3.87 (s, 3 H). **^{13}C NMR (125 MHz, $CDCl_3$)** δ 159.17, 144.38, 138.93, 132.53, 131.77 (q, J^F = 31.8 Hz), 131.13, 130.38, 129.81, 128.07, 124.10 (q, J^F = 270.8 Hz), 122.45, 119.94, 119.07, 118.75, 116.91 (q, J^F = 3.8 Hz), 114.38, 113.42 (q, J^F = 3.9 Hz),

55.34. **^{19}F NMR (471 MHz, $CDCl_3$)** δ -62.85. **HRMS** calcd for $C_{20}H_{16}ONF_3Na$ (M^+ + Na) 343.1179, found 343.1165.

4-((*N*-(2,4-Difluorophenyl)-2-(3-(trifluoromethyl)phenoxy)nicotinamido)methyl)benzoic acid and 4-methoxyphenylboronic acid (3ac, Figure 3, Entry 29)

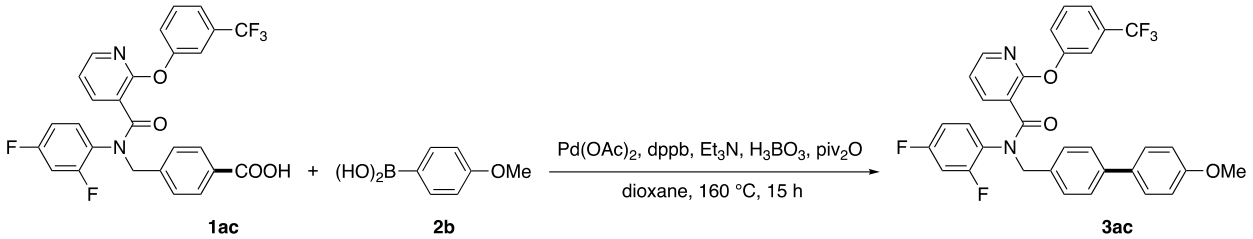

According to the general procedure, the reaction of 4-((*N*-(2,4-difluorophenyl)-2-(3-(trifluoromethyl)phenoxy)nicotinamido)methyl)benzoic acid (0.20 mmol), 4-methoxyphenylboronic acid (2.0 equiv), $Pd(OAc)_2$ (5 mol%), 1,4-bis(diphenylphosphino)butane (10 mol%), triethylamine (1.5 equiv), H_3BO_3 (1.5 equiv) and trimethylacetic anhydride (1.5 equiv) in 1,4-dioxane (0.20 M) for 15 h at 160 °C, afforded after work-up and chromatography the title compound in 66% yield (78.0 mg). *New compound.* White solid. **Mp** = 300-302 °C. **^{1}H NMR (500 MHz, $CDCl_3$)** δ 8.04 (s, 1 H), 7.87-7.85 (d, J = 7.1 Hz, 1 H), 7.53-7.48 (m, 4 H), 7.37-7.30 (m, 4 H), 7.17-7.16 (m, 2 H), 7.05-6.99 (m, 4 H), 6.72-6.68 (t, J = 9.0 Hz, 1 H), 6.66-6.63 (t, J = 7.7 Hz, 1 H), 5.55-5.52 (d, J = 14.3 Hz, 1 H), 4.72-4.70 (d, J = 14.4 Hz, 1 H), 3.81 (s, 3 H). **^{13}C NMR (125 MHz, $CDCl_3$)** δ 167.15, 160.02 (q, J^F = 268.0 Hz), 159.92 (q, J^F = 269.5 Hz), 157.42, 156.45, 153.22, 148.44, 138.78, 138.04, 134.75, 131.91 (q, J^F = 32.6 Hz), 131.39 (d, J^F = 9.5 Hz), 130.79, 130.07, 130.01, 129.70, 128.75, 128.57, 128.19, 124.65, 121.61 (q, J^F = 3.8 Hz), 121.25, 120.88, 118.78, 118.37 (q, J^F = 3.8 Hz), 111.33, 104.85 (q, J^F = 24.2 Hz), 55.54, 52.32. **^{19}F NMR (471 MHz, $CDCl_3$)** δ -62.69, -107.80, -113.93. **HRMS** calcd for $C_{33}H_{23}N_2O_3F_5Na$ (M^+ + Na) 613.1521, found 613.1527.

4-((((*S*)-2,5,7,8-Tetramethyl-2-((4*R*,8*R*)-4,8,12-trimethyltridecyl)chroman-6-yl)oxy)methyl) benzoic acid and 4-methoxyphenylboronic acid (3ad, Figure 3, Entry 30)

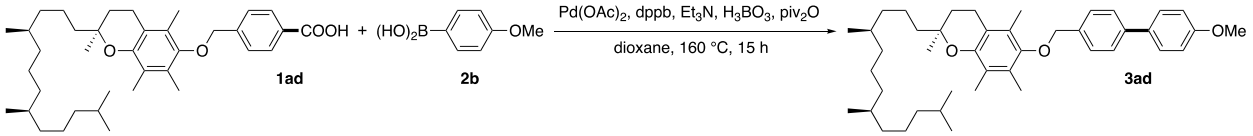

According to the general procedure, the reaction of 4-((((*S*)-2,5,7,8-tetramethyl-2-((4*R*,8*R*)-4,8,12-trimethyltridecyl)chroman-6-yl)oxy)methyl)benzoic acid (0.20 mmol), 4-methoxyphenylboronic acid (2.0 equiv), $Pd(OAc)_2$ (5 mol%), 1,4-bis(diphenylphosphino)butane (10 mol%), triethylamine (1.5 equiv), H_3BO_3 (1.5 equiv) and trimethylacetic anhydride (1.5 equiv) in 1,4-dioxane (0.20 M) for 15 h at 160 °C, afforded after work-up and chromatography the title compound in 61% yield (76.5 mg). *New compound.* White solid. **Mp** = 145-147 °C. **^{1}H NMR (500 MHz, $CDCl_3$)** δ 7.62-7.57 (m, 6 H), 7.03-7.01 (d, *J* = 8.6 Hz, 2 H), 4.75 (s, 2 H), 3.89 (s, 3 H), 2.64-2.61 (t, *J* = 6.6 Hz, 2 H), 2.27 (s, 3 H), 2.22 (s, 3 H), 2.14 (s, 3 H), 1.89-1.77 (m, 2 H), 1.55-1.53 (m, 3 H), 1.45-1.38 (m, 3 H), 1.35-1.28 (m, 12 H), 1.18-1.14 (m, 3 H), 1.13-1.09 (m, 3 H), 0.90-0.87 (m, 12 H). **^{13}C NMR (125 MHz, $CDCl_3$)** δ 159.20, 148.17, 140.39, 136.47, 133.56, 128.16, 127.96, 127.75, 126.82, 125.98, 122.96, 117.62, 114.25, 114.18, 74.85, 74.49, 55.38, 40.11, 39.39, 37.48, 37.44, 37.41, 37.31, 32.82, 32.73, 31.35, 28.00, 24.83, 24.46, 23.92, 22.73, 22.64, 20.71, 19.77, 19.70, 12.91, 12.05, 11.84. **HRMS** calcd for $C_{43}H_{62}O_3Na$ (M^+ + Na) 649.4591, found 649.4616.

4-Methyl-[1,1'-biphenyl]-2-carboxylic acid and 4-methoxyphenylboronic acid (3ae, Figure 3, Entry 31)

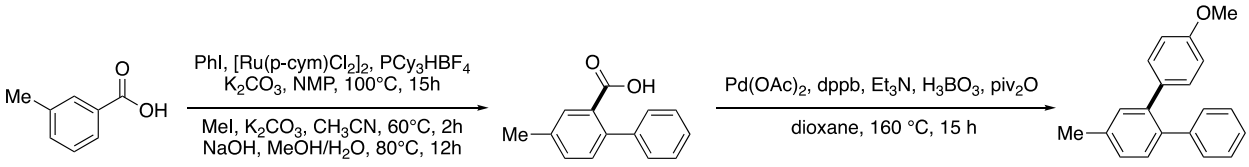

1ae **1af** **3ae**

According to the general procedure (Huang et al., 2016), *m*-toluic acid (1.0 mmol) was reacted with iodobenzene (1.5 equiv), $[Ru(p\text{-cym})Cl_2]_2$ (4 mol%), tricyclohexylphosphine tetrafluoroborate (8 mol%) and K_2CO_3 (1.0 equiv) in *N*-methyl-2-pyrrolidone (0.20 M) for 15 h at 100 °C. The reaction mixture was charged with iodomethane (3.0 equiv), K_2CO_3 (2.5 equiv) and acetonitrile (0.50 M) and heated for 2 h at 60 °C. Work-up and chromatography afforded methyl 4-methyl-[1,1'-biphenyl]-2-carboxylate in 93% yield (210.5 mg). A 20 mL vial was charged with methyl 4-methyl-[1,1'-biphenyl]-2-carboxylate (0.93 mmol), NaOH (10.0 equiv), methanol (1 mL) and water (10 mL) and heated for 12 h at 80 °C. The organic solvent was removed and the reaction mixture was acidified with HCl (6.0 *N*, 5 mL). The precipitate was filtered and washed with water (3 × 10 mL) to afford the product in 90% yield (177.7 mg).

White solid. The reaction of 4-methyl-[1,1'-biphenyl]-2-carboxylic acid (0.20 mmol), 4-methoxyphenyl boronic acid (2.0 equiv), $Pd(OAc)_2$ (5 mol%), 1,4-bis(diphenylphosphino)butane (10 mol%), triethylamine (1.5 equiv), H_3BO_3 (1.5 equiv) and trimethylacetic anhydride (1.5 equiv) in 1,4-dioxane (0.20 M) for 15 h at 160 °C, afforded after work-up and chromatography the title compound in 52% yield (28.6 mg). White solid. **^{1}H NMR (500 MHz, $CDCl_3$)** δ 7.39-7.37 (d, *J* = 10.6 Hz, 1 H), 7.34-7.32 (d, *J* = 7.7 Hz, 1 H), 7.25-7.22 (t, *J* = 7.3 Hz, 4 H), 7.16-7.15 (d, *J* = 6.7 Hz, 2 H), 7.08-7.07 (d, *J* = 8.4 Hz, 2 H), 6.78-6.77 (d, *J* = 8.3 Hz, 2 H), 3.80 (s, 3 H), 2.45 (s, 3 H). **^{13}C NMR (125 MHz, $CDCl_3$)** δ 158.27, 141.68, 139.98, 137.69, 137.15, 134.03, 131.30, 130.89, 130.58, 129.90, 128.16, 127.85, 126.16, 113.32, 55.17, 21.10. The spectral data matched those reported in the literature (Campo et al., 2007).

3'-Methoxy-[1,1'-biphenyl]-3-carboxylic acid and 2-methoxyphenylboronic acid (3af, Figure 3, Entry 32)

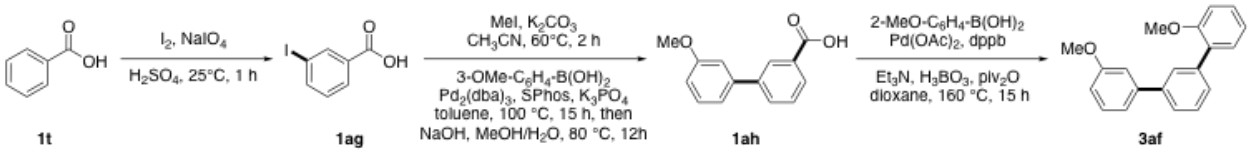

According to the general procedure (Kraszkiewicz et al., 2006), iodine (3.0 mmol) and $NaIO_4$ (1.0 mmol) were dropwise added to stirred 95% H_2SO_4 (15.0 mL). Stirring was continued for 30 min at 25 °C to give a dark brown iodinating solution containing ca. 7.0 mmol (1.17 equiv) of the I^+ intermediate. Benzoic acid (6.0 mmol) was added in one portion to the iodinating solution containing the I^+ intermediate (1.17 equiv) and the resulting solution was stirred for 1 h at 25 °C. Then the reaction mixture was slowly poured into stirred ice water (50 g). The crude solid product was filtered and washed with water (3 × 10 mL) to afforded 3-iodobenzoic acid in 72% yield (1.072 g). White solid. According to the general procedure (Huang et al., 2016), 3-iodobenzoic acid (4.32 mmol), was charged with iodomethane (3.0 equiv), K_2CO_3 (2.5 equiv) and acetonitrile (10.0 mL) and heated for 2 h at 60 °C. Work-up and chromatography afforded methyl 3-iodobenzoate in 91% yield (1.031 g). According to the general procedure (Barder et al., 2005), the reaction of 3-iodobenzoate (1.0 mmol), (3-methoxyphenyl)boronic acid (1.5 equiv), $Pd_2(dba)_3$ (1 mol%), SPhos (4 mol%) and K_3PO_4 (2.0 equiv) in toluene (0.25 M) for 15 h at 100 °C, afforded after work-up and chromatography methyl 3'-methoxy-[1,1'-biphenyl]-3-carboxylate in 98% yield (237.4 mg). White solid. A 20 mL vial was charged with methyl 3'-

methoxy-[1,1'-biphenyl]-3-carboxylate (0.98 mmol), NaOH (10.0 equiv) in methanol (1 mL) and water (10 mL) and heated for 12 h at 80 °C. The organic solvent was removed and the reaction mixture was acidified with HCl (6.0 *N*, 5 mL). The precipitate was filtered and washed with water (3 × 10 mL) to afford the product in 89% yield (199.1 mg). White solid. The reaction of 3'-methoxy-[1,1'-biphenyl]-3-carboxylic acid (0.20 mmol), 2-methoxyphenylboronic acid (2.0 equiv), $Pd(OAc)_2$ (5 mol%), 1,4-bis(diphenylphosphino)butane (10 mol%), triethylamine (1.5 equiv), H_3BO_3 (1.5 equiv) and trimethylacetic anhydride (1.5 equiv) in 1,4-dioxane (0.20 M) for 15 h at 160 °C, afforded after work-up and chromatography the title compound in 67% yield (38.9 mg). *New compound.* Colorless oil. **^{1}H NMR (500 MHz, $CDCl_3$)** δ 7.78 (s, 1 H), 7.59-7.55 (t, *J* = 8.1 Hz, 2 H), 7.52-7.49 (t, *J* = 7.5 Hz, 1 H), 7.42-7.36 (m, 3 H), 7.27-7.25 (d, *J* = 7.5 Hz, 1 H), 7.20 (s, 1 H), 7.10-7.07 (t, *J* = 7.3 Hz, 1 H), 7.05-7.04 (d, *J* = 8.1 Hz, 1 H), 6.94-6.93 (d, *J* = 7.8 Hz, 1 H), 3.90 (s, 3 H), 3.86 (s, 3 H). **^{13}C NMR (125 MHz, $CDCl_3$)** δ 159.94, 156.53, 142.96, 140.89, 139.00, 130.94, 130.59, 129.71, 128.78, 128.70, 128.53, 128.36, 125.85, 120.88, 119.83, 112.98, 112.72, 111.26, 55.61, 55.32. **HRMS** calcd for $C_{20}H_{18}O_2Na$ (M^+ + Na) 313.1199, found 313.1202.

Quinoline-6-carboxylic acid and 2-naphthylboronic acid (3ag, Figure 3, Entry 33)

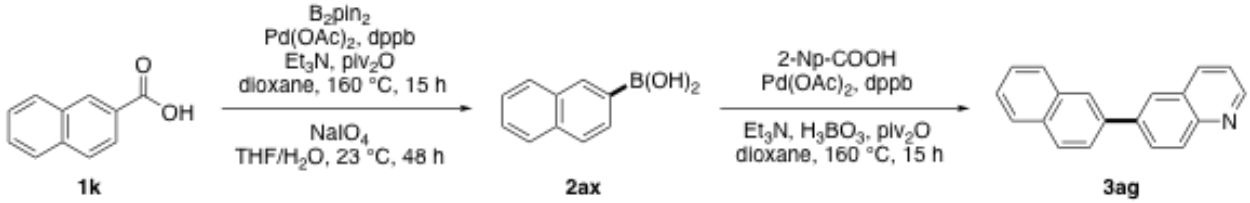

According to the general procedure (Liu et al., 2018), the reaction of 2-naphthoic acid (1.0 mmol), bis(pinacolato)diboron (3.0 equiv), $Pd(OAc)_2$ (5 mol%), 1,4-bis(diphenylphosphino)butane (10 mol%), triethylamine (3.0 equiv) and trimethylacetic anhydride (3.0 equiv) in 1,4-dioxane (0.20 M) for 15 h at 160 °C, afforded after work-up and chromatography 4,4,5,5-tetramethyl-2-(naphthalen-2-yl)-1,3,2-dioxaborolane in 76% yield (193.2 mg). White solid. According to the general procedure (Crawford et al., 2012), the reaction of 4,4,5,5-tetramethyl-2-(naphthalen-2-yl)-1,3,2-dioxaborolane (0.76 mmol), $NaIO_4$ (3.0 equiv) in THF/H_2O (2.8 mL/0.7 mL) for 48 h at room temperature, afforded after work-up 2-naphthylboronic acid in 86% yield (112.4 mg). The reaction of 2-naphthylboronic acid (0.20 mmol), quinoline-6-carboxylic acid (1.0 equiv), $Pd(OAc)_2$ (5 mol%), 1,4-

bis(diphenylphosphino)butane (10 mol%), triethylamine (1.5 equiv), H_3BO_3 (1.5 equiv) and trimethylacetic anhydride (1.5 equiv) in 1,4-dioxane (0.20 M) for 15 h at 160 °C, afforded after work-up and chromatography the title compound in 72% yield (36.8 mg). *New compound.* White solid. **Mp** = 144-146 °C. **^{1}H NMR (500 MHz, $CDCl_3$)** δ 8.97 (s, 1 H), 8.28-8.24 (t, *J* = 8.8 Hz, 2 H), 8.20 (s, 1 H), 8.16 (s, 2 H), 8.01-7.96 (m, 2 H), 7.93-7.89 (m, 2 H), 7.57-7.54 (m, 2 H), 7.49-7.47 (m, 1 H). **^{13}C NMR (125 MHz, $CDCl_3$)** δ 150.46, 147.77, 139.25, 137.63, 136.28, 133.71, 132.83, 130.03, 129.41, 128.72, 128.54, 128.30, 127.72, 126.54, 126.39, 126.29, 125.80, 125.55, 121.56. **HRMS** calcd for $C_{19}H_{13}NNa$ (M^+ + Na) 278.0940, found 278.0961.

[1,1'-Biphenyl]-4-carboxylic acid and 2-methoxyphenylboronic acid (3ah, Figure 3, Entry 34)

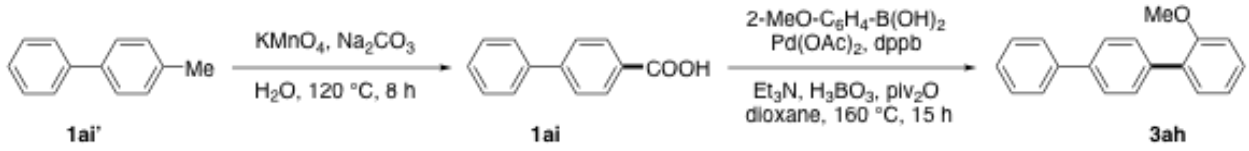

According to the general procedure (Ni et al., 2016), methyl 4-methyl-1,1'-biphenyl (2.0 mmol) was reacted with $KMnO_4$ (2.5 equiv), Na_2CO_3 (1.0 equiv) in H_2O (0.2 M) for 8 h at 120 °C. The reaction mixture was filtered through a pad of celite, and the filtrate was acidified with HCl (6.0 *N*, 5 mL). The precipitate was filtered and washed with water (3 × 10 mL) to afford [1,1'-biphenyl]-4-carboxylic acid in 87% yield (344.9 mg). White solid. The reaction of [1,1'-biphenyl]-4-carboxylic acid (0.20 mmol), 2-methoxyphenylboronic acid (2.0 equiv), $Pd(OAc)_2$ (5 mol%), 1,4-bis(diphenylphosphino)butane (10 mol%), triethylamine (1.5 equiv), H_3BO_3 (1.5 equiv) and trimethylacetic anhydride (1.5 equiv) in 1,4-dioxane (0.20 M) for 15 h at 160 °C, afforded after work-up and chromatography the title compound in 92% yield (47.9 mg). White solid. **^{1}H NMR (500 MHz, $CDCl_3$)** δ 7.70-7.66 (m, 6 H), 7.51-7.48 (t, *J* = 7.2 Hz, 2 H), 7.43-7.37 (m, 3 H), 7.11-7.08 (t, *J* = 7.3 Hz, 1 H), 7.06-7.04 (d, *J* = 8.2 Hz, 1 H), 3.88 (s, 3 H). **^{13}C NMR (125 MHz, $CDCl_3$)** δ 156.58, 141.07, 139.78, 137.57, 130.85, 130.27, 129.95, 128.78, 128.73, 127.21, 127.16, 126.81, 120.93, 111.29, 55.61. The spectral data matched those reported in the literature (Miguez et al., 2007).

Nicotinic acid and 4-acetylphenylboronic acid (3ai, Figure 4, Entry 35)

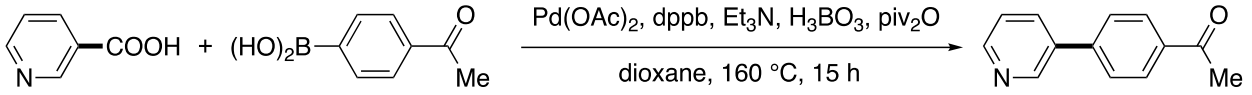

1m **2c** **3ai**

According to the general procedure, the reaction of nicotinic acid (0.20 mmol), 4-acetylphenylboronic acid (2.0 equiv), $Pd(OAc)_2$ (5 mol%), 1,4-bis(diphenylphosphino)butane (10 mol%), triethylamine (1.5 equiv), H_3BO_3 (1.5 equiv) and trimethylacetic anhydride (1.5 equiv) in 1,4-dioxane (0.20 M) for 15 h at 160 °C, afforded after work-up and chromatography the title compound in 86% yield (34.0 mg). White solid. **^{1}H NMR (500 MHz, $CDCl_3$)** δ 8.91 (s, 1 H), 8.68-8.67 (d, *J* = 4.0 Hz, 1 H), 8.11-8.09 (d, *J* = 8.2 Hz, 2 H), 7.95-7.94 (d, *J* = 7.9 Hz, 1 H), 7.72-7.71 (d, *J* = 8.3 Hz, 2 H), 7.45-7.42 (m, 1 H), 2.68 (s, 3 H). **^{13}C NMR (125 MHz, $CDCl_3$)** δ 197.59, 149.30, 148.32, 142.35, 136.56, 135.50, 134.56, 129.16, 127.32, 123.73, 26.72. The spectral data matched those reported in the literature (Adak et al., 2011).

Nicotinic acid and 4-(methoxycarbonyl)phenylboronic acid (3aj, Figure 4, Entry 36)

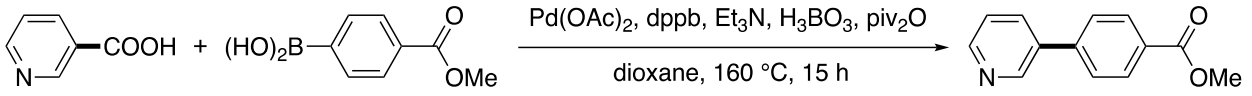

1m **2d** **3aj**

According to the general procedure, the reaction of nicotinic acid (0.20 mmol), 4-(methoxycarbonyl)phenylboronic acid (2.0 equiv), $Pd(OAc)_2$ (5 mol%), 1,4-bis(diphenylphosphino)butane (10 mol%), triethylamine (1.5 equiv), H_3BO_3 (1.5 equiv) and trimethylacetic anhydride (1.5 equiv) in 1,4-dioxane (0.20 M) for 15 h at 160 °C, afforded after work-up and chromatography the title compound in 98% yield (41.8 mg). White solid. **^{1}H NMR (500 MHz, $CDCl_3$)** δ 8.90 (s, 1 H), 8.66-8.65 (d, *J* = 3.8 Hz, 1 H), 8.17-8.15 (d, *J* = 8.3 Hz, 2 H), 7.93-7.92 (d, *J* = 7.9 Hz, 1 H), 7.68-7.66 (d, *J* = 8.3 Hz, 2 H), 7.42-7.40 (m, 1 H), 3.96 (s, 3 H). **^{13}C NMR (125 MHz, $CDCl_3$)** δ 166.73, 149.26, 148.35, 142.22, 135.56, 134.52, 130.37, 129.76, 127.10, 123.68, 52.26. The spectral data matched those reported in the literature (Muto et al., 2015).

Nicotinic acid and 4-formylphenylboronic acid (3ak, Figure 4, Entry 37)

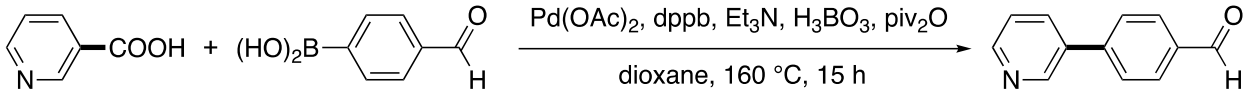

1m **2e** **3ak**

According to the general procedure, the reaction of nicotinic acid (0.20 mmol), 4-formylphenylboronic acid (2.0 equiv), $Pd(OAc)_2$ (5 mol%), 1,4-bis(diphenylphosphino)butane (10 mol%), triethylamine (1.5 equiv), H_3BO_3 (1.5 equiv) and trimethylacetic anhydride (1.5 equiv) in 1,4-dioxane (0.20 M) for 15 h at 160 °C, afforded after work-up and chromatography the title compound in 72% yield (26.4 mg). White solid. **^{1}H NMR (500 MHz, $CDCl_3$)** δ 10.11 (s, 1 H), 8.93 (s, 1 H), 8.70-8.69 (d, *J* = 4.0 Hz, 1 H), 8.04-8.02 (d, *J* = 8.1 Hz, 2 H), 7.97-7.95 (d, *J* = 7.9 Hz, 1 H), 7.80-7.78 (d, *J* = 8.1 Hz, 2 H), 7.46-7.44 (m, 1 H). **^{13}C NMR (125 MHz, $CDCl_3$)** δ 191.73, 149.56, 148.40, 143.77, 135.83, 135.36, 134.63, 130.49, 127.79, 123.76. The spectral data matched those reported in the literature (Rao et al., 2018).

Nicotinic acid and 4-(trifluoromethyl)phenylboronic acid (3al, Figure 4, Entry 38)

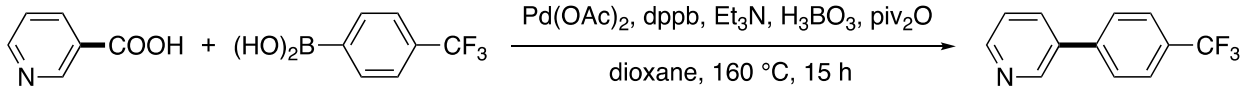

1m **2f** **3al**

According to the general procedure, the reaction of nicotinic acid (0.20 mmol), 4-(trifluoromethyl)phenylboronic acid (2.0 equiv), $Pd(OAc)_2$ (5 mol%), 1,4-bis(diphenylphosphino)butane (10 mol%), triethylamine (1.5 equiv), H_3BO_3 (1.5 equiv) and trimethylacetic anhydride (1.5 equiv) in 1,4-dioxane (0.20 M) for 15 h at 160 °C, afforded after work-up and chromatography the title compound in 82% yield (36.6 mg). White solid. **^{1}H NMR (500 MHz, $CDCl_3$)** δ 8.88 (s, 1 H), 8.68-8.67 (d, *J* = 3.8 Hz, 1 H), 7.92-7.91 (d, *J* = 7.9 Hz, 1 H), 7.77-7.71 (m, 4 H), 7.44-7.42 (m, 1 H). **^{13}C NMR (125 MHz, $CDCl_3$)** δ 149.39, 148.36, 141.41, 135.32, 134.54, 130.26 (q, J^F = 32.6 Hz), 127.52, 126.07 (q, J^F = 3.6 Hz), 124.10 (q, J^F = 270.4 Hz), 123.72. **^{19}F NMR (471 MHz, $CDCl_3$)** δ -62.58. The spectral data matched those reported in the literature (Muto et al., 2015).

Nicotinic acid and 4-cyanophenylboronic acid (3am, Figure 4, Entry 39)

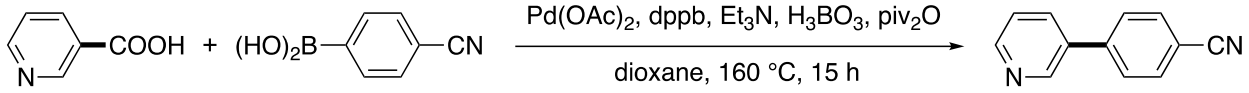

1m **2g** **3am**

According to the general procedure, the reaction of nicotinic acid (0.20 mmol), 4-cyanophenylboronic acid (2.0 equiv), $Pd(OAc)_2$ (5 mol%), 1,4-bis(diphenylphosphino)butane (10 mol%), triethylamine (1.5 equiv), H_3BO_3 (1.5 equiv) and trimethylacetic anhydride (1.5 equiv) in 1,4-dioxane (0.20 M) for 15 h at 160 °C, afforded after work-up and chromatography the title compound in 70% yield (25.3 mg). White solid. **^{1}H NMR (500 MHz, $CDCl_3$)** δ 8.88 (s, 1 H), 8.70-8.69 (d, *J* = 4.0 Hz, 1 H), 7.92-7.91 (d, *J* = 7.9 Hz, 1 H), 7.81-7.79 (d, *J* = 8.4 Hz, 2 H), 7.72-7.71 (d, *J* = 8.4 Hz, 2 H), 7.46-7.44 (m, 1 H). **^{13}C NMR (125 MHz, $CDCl_3$)** δ 149.73, 148.22, 142.32, 134.85, 134.56, 132.91, 127.82, 123.85, 118.56, 111.99. The spectral data matched those reported in the literature (Wang et al., 2015).

Nicotinic acid and 4-methoxyphenylboronic acid (3an, Figure 4, Entry 40)

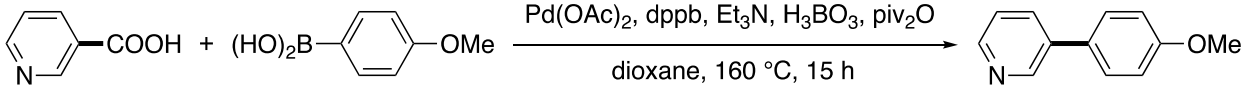

1m **2h** **3an**

According to the general procedure, the reaction of nicotinic acid (0.20 mmol), 4-methoxyphenylboronic acid (2.0 equiv), $Pd(OAc)_2$ (5 mol%), 1,4-bis(diphenylphosphino)butane (10 mol%), triethylamine (1.5 equiv), H_3BO_3 (1.5 equiv) and trimethylacetic anhydride (1.5 equiv) in 1,4-dioxane (0.20 M) for 15 h at 160 °C, afforded after work-up and chromatography the title compound in 75% yield (27.8 mg). White solid. **^{1}H NMR (500 MHz, $CDCl_3$)** δ 8.84 (s, 1 H), 8.57-8.56 (d, *J* = 4.6 Hz, 1 H), 7.86-7.84 (m, 1 H), 7.55-7.53 (d, *J* = 8.6 Hz, 2 H), 7.37-7.34 (m, 1 H), 7.04-7.03 (d, *J* = 8.7 Hz, 2 H), 3.88 (s, 3 H). **^{13}C NMR (125 MHz, $CDCl_3$)** δ 159.78, 148.00, 147.88, 136.27, 133.88, 130.27, 128.24, 123.52, 114.57, 55.40. The spectral data matched those reported in the literature (Muto et al., 2015).

Nicotinic acid and 4-fluorophenylboronic acid (3ao, Figure 4, Entry 41)

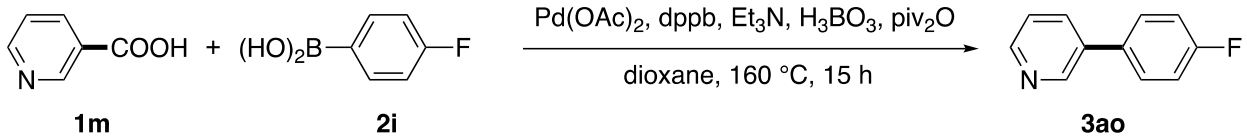

1m **2i** **3ao**

According to the general procedure, the reaction of nicotinic acid (0.20 mmol), 4-fluorophenylboronic acid (2.0 equiv), $Pd(OAc)_2$ (5 mol%), 1,4-bis(diphenylphosphino)butane (10 mol%), triethylamine (1.5 equiv), H_3BO_3 (1.5 equiv) and trimethylacetic anhydride (1.5 equiv) in 1,4-dioxane (0.20 M) for 15 h at 160 °C, afforded after work-up and chromatography the title compound in 76% yield (26.4 mg). White solid. **^{1}H NMR (500 MHz, $CDCl_3$)** δ 8.83 (s, 1 H), 8.62-8.61 (d, J = 3.8 Hz, 1 H), 7.86-7.84 (d, J = 7.9 Hz, 1 H), 7.58-7.55 (m, 2 H), 7.40-7.37 (m, 1 H), 7.21-7.18 (t, J = 8.6 Hz, 2 H). **^{13}C NMR (125 MHz, $CDCl_3$)** δ 162.95 (d, J^F = 246.3 Hz), 148.48, 148.14, 135.78, 134.25, 133.98, 128.86 (d, J^F = 8.1 Hz), 123.61, 116.10 (d, J^F = 21.5 Hz). **^{19}F NMR (471 MHz, $CDCl_3$)** δ -114.19. The spectral data matched those reported in the literature (Muto et al., 2015).

Nicotinic acid and 2-fluorophenylboronic acid (3ap, Figure 4, Entry 42)

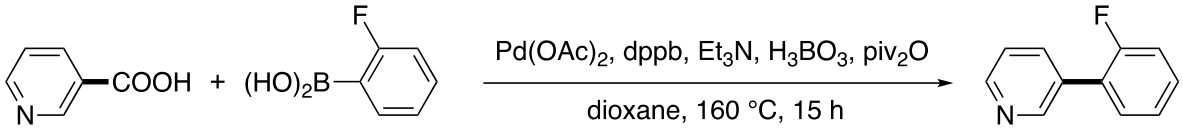

1m **2j** **3ap**

According to the general procedure, the reaction of nicotinic acid (0.20 mmol), 2-fluorophenylboronic acid (2.0 equiv), $Pd(OAc)_2$ (5 mol%), 1,4-bis(diphenylphosphino)butane (10 mol%), triethylamine (1.5 equiv), H_3BO_3 (1.5 equiv) and trimethylacetic anhydride (1.5 equiv) in 1,4-dioxane (0.20 M) for 15 h at 160 °C, afforded after work-up and chromatography the title compound in 90% yield (31.2 mg). White solid. **^{1}H NMR (500 MHz, $CDCl_3$)** δ 8.82 (s, 1 H), 8.64-8.64 (d, J = 3.9 Hz, 1 H), 7.91-7.90 (d, J = 7.8 Hz, 1 H), 7.48-7.39 (m, 3 H), 7.30-7.27 (t, J = 6.0 Hz, 1 H), 7.24-7.20 (t, J = 9.0 Hz, 1 H). **^{13}C NMR (125 MHz, $CDCl_3$)** δ 159.87 (d, J^F = 247.1 Hz), 149.65 (d, J^F = 3.1 Hz), 148.77, 136.37 (d, J^F = 3.3 Hz), 134.10 (d, J^F = 8.5 Hz), 131.68, 130.51 (d, J^F = 3.2 Hz), 129.99 (d, J^F = 8.2 Hz), 124.71 (d, J^F = 3.7 Hz), 123.29, 116.32 (d, J^F = 22.2 Hz). **^{19}F NMR (471 MHz, $CDCl_3$)** δ -117.94. The spectral data matched those reported in the literature (Roesner et al., 2016).

Nicotinic acid and 2,4-difluorophenylboronic acid (3aq, Figure 4, Entry 43)

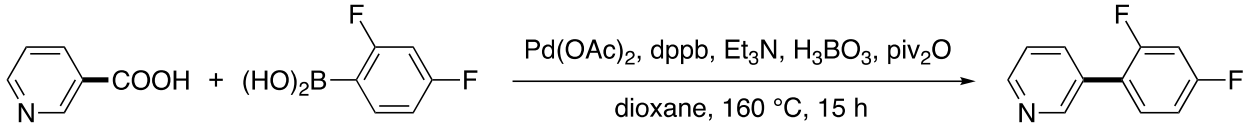

1m **2k** **3aq**

According to the general procedure, the reaction of nicotinic acid (0.20 mmol), 2,4-difluorophenylboronic acid (2.0 equiv), $Pd(OAc)_2$ (5 mol%), 1,4-bis(diphenylphosphino)butane (10 mol%), triethylamine (1.5 equiv), H_3BO_3 (1.5 equiv) and trimethylacetic anhydride (1.5 equiv) in 1,4-dioxane (0.20 M) for 15 h at 160 °C, afforded after work-up and chromatography the title compound in 80% yield (30.6 mg). *New compound.* White solid. **Mp** = 54-56 °C. **^{1}H NMR (500 MHz, $CDCl_3$)** δ 8.77 (s, 1 H), 8.64-8.64 (d, J = 3.8 Hz, 1 H), 7.86-7.84 (dd, J = 7.8 Hz, 1 H), 7.46-7.39 (m, 2 H), 7.04-6.96 (m, 2 H). **^{13}C NMR (125 MHz, $CDCl_3$)** δ 162.88 (dd, J^F = 249.0 Hz), 159.95 (dd, J^F = 249.7 Hz), 149.52 (d, J^F = 2.9 Hz), 148.89, 136.24 (d, J^F = 3.2 Hz), 131.28 (dd, J^F = 9.5 Hz), 130.89, 123.35, 121.93 (dd, J^F = 13.9 Hz), 112.04 (dd, J^F = 21.2 Hz), 104.71 (dd, J^F = 25.5 Hz). **^{19}F NMR (471 MHz, $CDCl_3$)** δ -109.66, -113.37. **HRMS** calcd for $C_{11}H_7NF_2Na$ (M^+ + Na) 214.0439, found 214.0431.

Nicotinic acid and 2-methoxyphenylboronic acid (3ar, Figure 4, Entry 44)

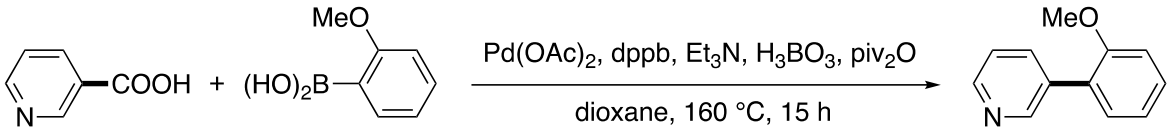

1m **2l** **3ar**

According to the general procedure, the reaction of nicotinic acid (0.20 mmol), 2-methoxyphenylboronic acid (2.0 equiv), $Pd(OAc)_2$ (5 mol%), 1,4-bis(diphenylphosphino)butane (10 mol%), triethylamine (1.5 equiv), H_3BO_3 (1.5 equiv) and trimethylacetic anhydride (1.5 equiv) in 1,4-dioxane (0.20 M) for 15 h at 160 °C, afforded after work-up and chromatography the title compound in 77% yield (28.6 mg). White solid. **^{1}H NMR (500 MHz, $CDCl_3$)** δ 8.81 (s, 1 H), 8.60-8.59 (d, J = 3.9 Hz, 1 H), 7.91-7.90 (d, J = 7.9 Hz, 1 H), 7.42-7.34 (m, 3 H), 7.10-7.07 (t, J = 7.5 Hz, 1 H), 7.04-7.03 (d, J = 8.3 Hz, 1 H), 3.85 (s, 3 H). **^{13}C NMR (125 MHz, $CDCl_3$)** δ 156.57, 150.20, 147.81, 137.14, 134.42, 130.67, 129.66, 126.87, 123.04, 121.08, 111.30, 55.53. The spectral data matched those reported in the literature (Zhang et al., 2017).

Nicotinic acid and 3-methoxyphenylboronic acid (3as, Figure 4, Entry 45)

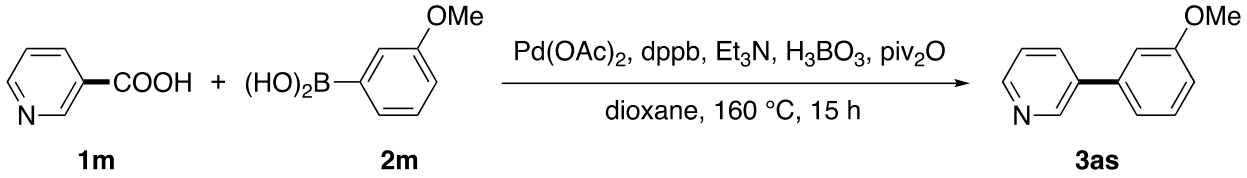

1m **2m** **3as**

According to the general procedure, the reaction of nicotinic acid (0.20 mmol), 3-methoxyphenylboronic acid (2.0 equiv), $Pd(OAc)_2$ (5 mol%), 1,4-bis(diphenylphosphino)butane (10 mol%), triethylamine (1.5 equiv), H_3BO_3 (1.5 equiv) and trimethylacetic anhydride (1.5 equiv) in 1,4-dioxane (0.20 M) for 15 h at 160 °C, afforded after work-up and chromatography the title compound in 86% yield (31.9 mg). White solid. **^{1}H NMR (500 MHz, $CDCl_3$)** δ 8.87 (s, 1 H), 8.62-8.61 (d, *J* = 4.2 Hz, 1 H), 7.90-7.88 (d, *J* = 7.9 Hz, 1 H), 7.44-7.37 (m, 2 H), 7.20-7.18 (d, *J* = 7.4 Hz, 1 H), 7.13 (s, 1 H), 6.99-6.96 (m, 1 H), 3.90 (s, 3 H). **^{13}C NMR (125 MHz, $CDCl_3$)** δ 160.15, 148.60, 148.35, 139.32, 136.56, 134.45, 130.16, 123.55, 119.62, 113.43, 112.98, 55.38. The spectral data matched those reported in the literature (Muto et al., 2015).

Nicotinic acid and 3,4-dimethoxyphenylboronic acid (3at, Figure 4, Entry 46)

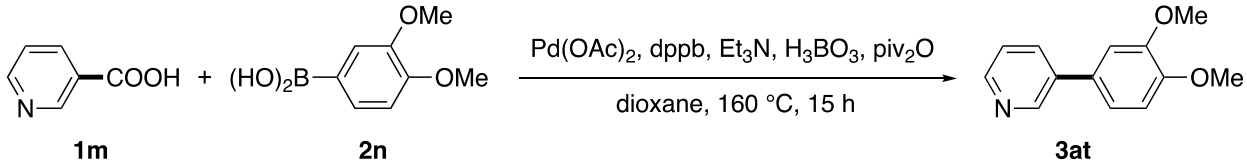

1m **2n** **3at**

According to the general procedure, the reaction of nicotinic acid (0.20 mmol), 3,4-dimethoxyphenylboronic acid (2.0 equiv), $Pd(OAc)_2$ (5 mol%), 1,4-bis(diphenylphosphino)butane (10 mol%), triethylamine (1.5 equiv), H_3BO_3 (1.5 equiv) and trimethylacetic anhydride (1.5 equiv) in 1,4-dioxane (0.20 M) for 15 h at 160 °C, afforded after work-up and chromatography the title compound in 84% yield (36.2 mg). White solid. **^{1}H NMR (500 MHz, $CDCl_3$)** δ 8.85 (s, 1 H), 8.59-8.58 (d, *J* = 4.0 Hz, 1 H), 7.87-7.86 (d, *J* = 7.9 Hz, 1 H), 7.38-7.36 (m, 1 H), 7.18-7.16 (m, 1 H), 7.11-7.11 (d, *J* = 1.8 Hz, 1 H), 7.01-7.00 (d, *J* = 8.3 Hz, 1 H), 3.99 (s, 3 H), 3.96 (s, 3 H). **^{13}C NMR (125 MHz, $CDCl_3$)** δ 149.47, 149.29, 148.07, 148.00, 136.54, 134.07, 130.69, 123.53, 119.63, 111.70, 110.28, 56.04. The spectral data matched those reported in the literature (Muto et al., 2015).

Nicotinic acid and 3-(trifluoromethyl)phenylboronic acid (3au, Figure 4, Entry 47)

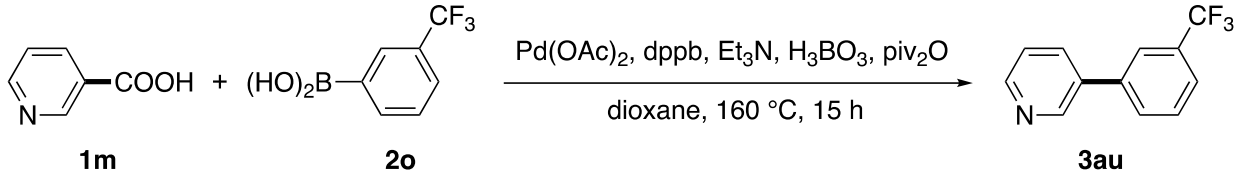

1m **2o** **3au**

According to the general procedure, the reaction of nicotinic acid (0.20 mmol), 3-(trifluoromethyl)phenylboronic acid (2.0 equiv), $Pd(OAc)_2$ (5 mol%), 1,4-bis(diphenylphosphino)butane (10 mol%), triethylamine (1.5 equiv), H_3BO_3 (1.5 equiv) and trimethylacetic anhydride (1.5 equiv) in 1,4-dioxane (0.20 M) for 15 h at 160 °C, afforded after work-up and chromatography the title compound in 87% yield (38.9 mg). White solid. **^{1}H NMR (500 MHz, $CDCl_3$)** δ 8.92 (s, 1 H), 8.72-8.71 (d, *J* = 4.1 Hz, 1 H), 7.96-7.95 (d, *J* = 7.9 Hz, 1 H), 7.85 (s, 1 H), 7.80-7.78 (d, *J* = 7.7 Hz, 1 H), 7.72-7.70 (d, *J* = 7.5 Hz, 1 H), 7.66-7.63 (t, *J* = 7.8 Hz, 1 H), 7.49-7.46 (m, 1 H). **^{13}C NMR (125 MHz, $CDCl_3$)** δ 148.69, 147.73, 138.47, 135.63, 134.96, 131.79, 131.53, 130.47, 129.71, 128.08, 124.99 (q, J^F = 3.4 Hz), 124.02 (q, J^F = 3.7 Hz). **^{19}F NMR (471 MHz, $CDCl_3$)** δ -62.71. The spectral data matched those reported in the literature (Barder et al., 2005).

Nicotinic acid and 3-acetylphenylboronic acid (3av, Figure 4, Entry 48)

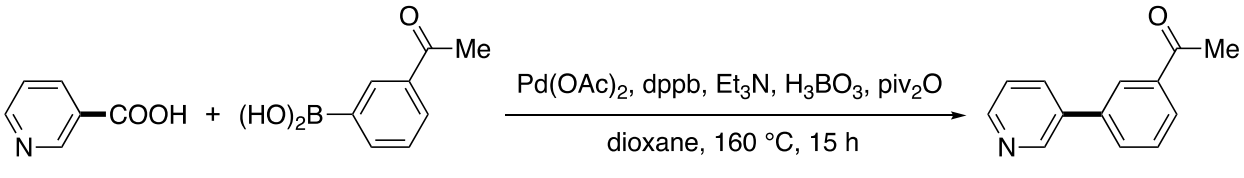

1m **2p** **3av**

According to the general procedure, the reaction of nicotinic acid (0.20 mmol), 3-acetylphenylboronic acid (2.0 equiv), $Pd(OAc)_2$ (5 mol%), 1,4-bis(diphenylphosphino)butane (10 mol%), triethylamine (1.5 equiv), H_3BO_3 (1.5 equiv) and trimethylacetic anhydride (1.5 equiv) in 1,4-dioxane (0.20 M) for 15 h at 160 °C, afforded after work-up and chromatography the title compound in 98% yield (38.7 mg). White solid. **^{1}H NMR (500 MHz, $CDCl_3$)** δ 8.90 (s, 1 H), 8.66-8.66 (d, *J* = 3.9 Hz, 1 H), 8.20 (s, 1 H), 8.02-8.01 (d, *J* = 7.7 Hz, 1 H), 7.95-7.93 (d, *J* = 7.9 Hz, 1 H), 7.82-7.80 (d, *J* = 7.7 Hz, 1 H), 7.63-7.60 (t, *J* = 7.8 Hz, 1 H), 7.44-7.41 (m, 1 H), 2.69 (s, 3 H). **^{13}C NMR (125 MHz, $CDCl_3$)** δ 197.78, 149.02, 148.29, 138.43, 137.90, 135.76,

134.52, 131.67, 129.44, 128.05, 126.92, 123.69, 26.77. The spectral data matched those reported in the literature (Kuriyama et al., 2013).

Nicotinic acid and thiophen-3-ylboronic acid (3aw, Figure 4, Entry 49)

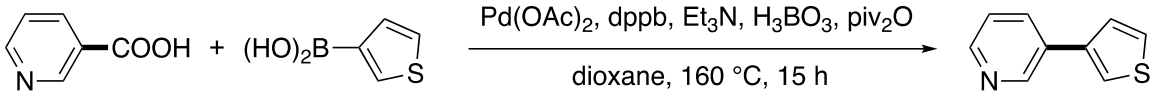

1m **2q** **3aw**

According to the general procedure, the reaction of nicotinic acid (0.20 mmol), thiophen-3-ylboronic acid (2.0 equiv), $Pd(OAc)_2$ (5 mol%), 1,4-bis(diphenylphosphino)butane (10 mol%), triethylamine (1.5 equiv), H_3BO_3 (1.5 equiv) and trimethylacetic anhydride (1.5 equiv) in 1,4-dioxane (0.20 M) for 15 h at 160 °C, afforded after work-up and chromatography the title compound in 80% yield (25.8 mg). White solid. **^{1}H NMR (500 MHz, $CDCl_3$)** δ 8.90 (s, 1 H), 8.56-8.55 (d, *J* = 4.6 Hz, 1 H), 7.90-7.88 (d, *J* = 7.9 Hz, 1 H), 7.55-7.55 (d, *J* = 1.4 Hz, 1 H), 7.48-7.46 (m, 1 H), 7.42-7.41 (m, 1 H), 7.36-7.34 (m, 1 H). **^{13}C NMR (125 MHz, $CDCl_3$)** δ 148.21, 147.68, 138.80, 133.61, 131.60, 127.02, 125.93, 123.68, 121.48. The spectral data matched those reported in the literature (Muto et al., 2015).

Nicotinic acid and naphthalen-2-ylboronic acid (3ax, Figure 4, Entry 50)

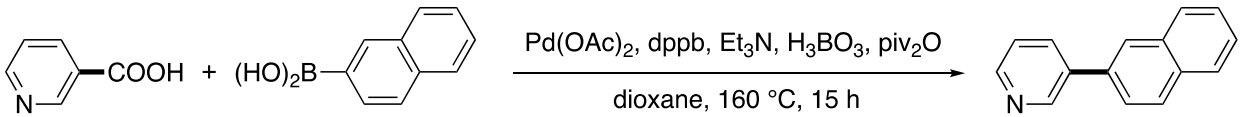

1m **2r** **3ax**

According to the general procedure, the reaction of nicotinic acid (0.20 mmol), naphthalen-2-ylboronic acid (2.0 equiv), $Pd(OAc)_2$ (5 mol%), 1,4-bis(diphenylphosphino)butane (10 mol%), triethylamine (1.5 equiv), H_3BO_3 (1.5 equiv) and trimethylacetic anhydride (1.5 equiv) in 1,4-dioxane (0.20 M) for 15 h at 160 °C, afforded after work-up and chromatography the title compound in 86% yield (35.3 mg). White solid. **^{1}H NMR (500 MHz, $CDCl_3$)** δ 9.01 (s, 1 H), 8.66-8.65 (d, *J* = 4.1 Hz, 1 H), 8.08 (s, 1 H), 8.04-8.02 (d, *J* = 7.9 Hz, 1 H), 8.00-7.98 (d, *J* = 8.5 Hz, 1 H), 7.95-7.94 (d, *J* = 7.1 Hz, 1 H), 7.92-7.91 (d, *J* = 8.2 Hz, 1 H), 7.75-7.74 (d, *J* = 8.5 Hz, 1 H), 7.58-7.54 (m, 2 H), 7.45-7.43 (m, 1 H). **^{13}C NMR (125 MHz, $CDCl_3$)** δ 148.61, 148.55, 136.63, 135.17, 134.61, 133.61, 132.90, 128.92, 128.26, 127.74, 126.64, 126.48, 126.20, 125.06, 123.64. The spectral data matched those reported in the literature (Muto et al., 2015).

Nicotinic acid and 6-methoxynaphthalen-2-ylboronic acid (3ay, Figure 4, Entry 51)

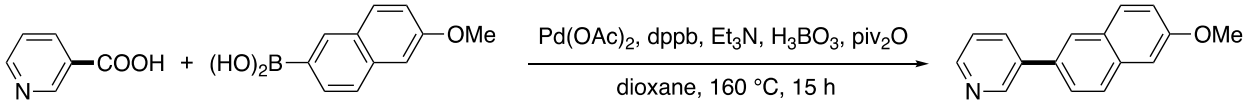

1m **2s** **3ay**

According to the general procedure, the reaction of nicotinic acid (0.20 mmol), 6-methoxynaphthalen-2-ylboronic acid (2.0 equiv), $Pd(OAc)_2$ (5 mol%), 1,4-bis(diphenylphosphino)butane (10 mol%), triethylamine (1.5 equiv), H_3BO_3 (1.5 equiv) and trimethylacetic anhydride (1.5 equiv) in 1,4-dioxane (0.20 M) for 15 h at 160 °C, afforded after work-up and chromatography the title compound in 98% yield (46.2 mg). White solid. **^{1}H NMR (500 MHz, $CDCl_3$)** δ 9.00 (s, 1 H), 8.64-8.63 (d, *J* = 4.0 Hz, 1 H), 8.03-8.00 (m, 2 H), 7.88-7.83 (m, 2 H), 7.71-7.70 (d, *J* = 8.4 Hz, 1 H), 7.44-7.42 (m, 1 H), 7.23-7.20 (m, 2 H), 3.98 (s, 3 H). **^{13}C NMR (125 MHz, $CDCl_3$)** δ 158.16, 148.22, 148.01, 136.81, 134.57, 134.18, 132.83, 129.78, 129.11, 127.73, 126.00, 125.50, 123.69, 119.56, 105.61, 55.39. The spectral data matched those reported in the literature (Lucas et al., 2008).

Nicotinic acid and dibenzo[*b,d*]furan-4-ylboronic acid (3az, Figure 4, Entry 52)

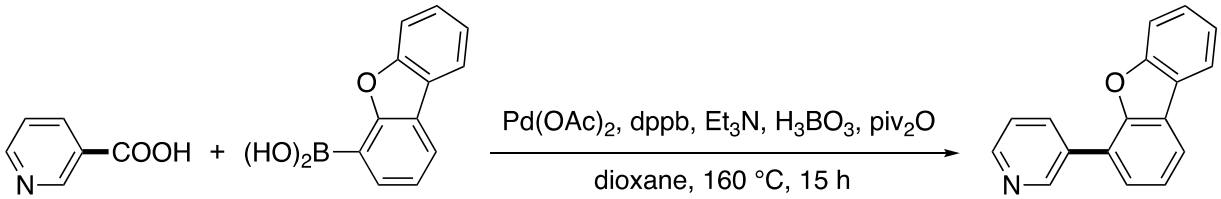

1m **2t** **3az**

According to the general procedure, the reaction of nicotinic acid (0.20 mmol), dibenzo[*b,d*]furan-4-ylboronic acid (2.0 equiv), $Pd(OAc)_2$ (5 mol%), 1,4-bis(diphenylphosphino)butane (10 mol%), triethylamine (1.5 equiv), H_3BO_3 (1.5 equiv) and trimethylacetic anhydride (1.5 equiv) in 1,4-dioxane (0.20 M) for 15 h at 160 °C, afforded after work-up and chromatography the title compound in 69% yield (33.9 mg). White solid. **^{1}H NMR (500 MHz, $CDCl_3$)** δ 9.19 (s, 1 H), 8.69-8.69 (d, *J* = 3.8 Hz, 1 H), 8.28-8.26 (d, *J* = 7.9 Hz, 1 H), 8.03-8.00 (m, 2 H), 7.64-7.62 (m, 2 H), 7.53-7.47 (m, 3 H), 7.42-7.39 (t, *J* = 7.6 Hz, 1 H). **^{13}C NMR (125 MHz, $CDCl_3$)** δ 156.17, 153.37, 149.65, 148.82, 135.98, 132.26, 127.54, 126.52, 125.19, 123.98, 123.51, 123.43, 123.03, 122.36, 120.81, 120.62, 111.89. The spectral data matched those reported in the literature (Ramakrishna et al., 2017).

Nicotinic acid and dibenzo[*b,d*]thiophen-4-ylboronic acid (3ba, Figure 4, Entry 53)

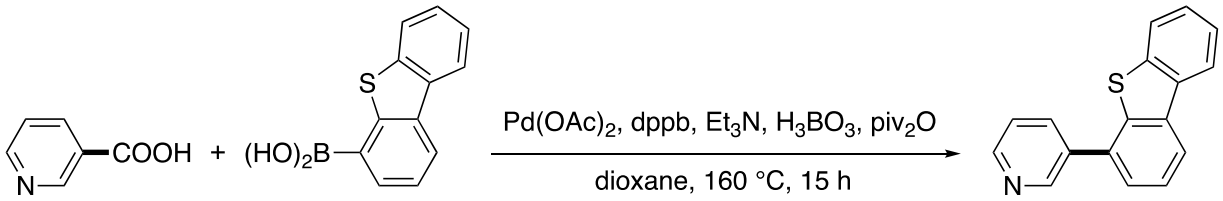

1m **2u** **3ba**

According to the general procedure, the reaction of nicotinic acid (0.20 mmol), dibenzo[*b,d*]thiophen-4-ylboronic acid (2.0 equiv), $Pd(OAc)_2$ (5 mol%), 1,4-bis(diphenylphosphino)butane (10 mol%), triethylamine (1.5 equiv), H_3BO_3 (1.5 equiv) and trimethylacetic anhydride (1.5 equiv) in 1,4-dioxane (0.20 M) for 15 h at 160 °C, afforded after work-up and chromatography the title compound in 65% yield (34.0 mg). *New compound.* White solid. **Mp** = 128-129 °C. **^{1}H NMR (500 MHz, $CDCl_3$)** δ 9.00 (s, 1 H), 8.73-8.72 (d, *J* = 3.7 Hz, 1 H), 8.24-8.22 (d, *J* = 7.8 Hz, 2 H), 8.11-8.10 (d, *J* = 7.8 Hz, 1 H), 7.88-7.86 (m, 1 H), 7.63-7.60 (t, *J* = 7.5 Hz, 1 H), 7.53-7.47 (m, 4 H). **^{13}C NMR (125 MHz, $CDCl_3$)** δ 149.35, 149.21, 139.30, 138.75, 136.52, 136.31, 135.62, 135.53, 133.40, 127.09, 127.05, 125.29, 124.64, 123.54, 122.73, 121.86, 121.27. **HRMS** calcd for $C_{17}H_{11}NS$ (M^+) 261.0607, found 261.0596.

4-(Methoxycarbonyl)benzoic acid and *p*-tolylboronic acid (3bb, Figure 4, Entry 54)

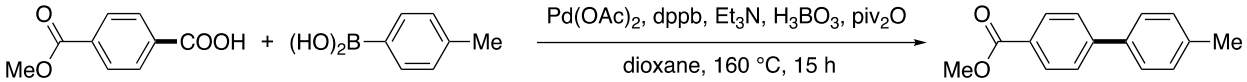

1a **2v** **3bb**

According to the general procedure, the reaction of 4-(methoxycarbonyl)benzoic acid (0.20 mmol), *p*-tolylboronic acid (2.0 equiv), $Pd(OAc)_2$ (5 mol%), 1,4-bis(diphenylphosphino)butane (10 mol%), triethylamine (1.5 equiv), H_3BO_3 (1.5 equiv) and trimethylacetic anhydride (1.5 equiv) in 1,4-dioxane (0.20 M) for 15 h at 160 °C, afforded after work-up and chromatography the title compound in 91% yield (41.2 mg). White solid. **^{1}H NMR (500 MHz, $CDCl_3$)** δ 8.13-8.11 (d, *J* = 8.3 Hz, 2 H), 7.68-7.66 (d, *J* = 8.3 Hz, 2 H), 7.56-7.55 (d, *J* = 8.0 Hz, 2 H), 7.31-7.29 (d, *J* = 7.9 Hz, 2 H), 3.96 (s, 3 H), 2.44 (s, 3 H). **^{13}C NMR (125 MHz, $CDCl_3$)** δ 167.08, 145.59, 138.13, 137.10, 130.10, 129.67, 128.60, 127.12, 126.81, 52.11, 21.18. The spectral data matched those reported in the literature (Kloss et al., 2018).

4-(Methoxycarbonyl)benzoic acid and 4-(*tert*-butyl)phenylboronic acid (3bc, Figure 4, Entry 55)

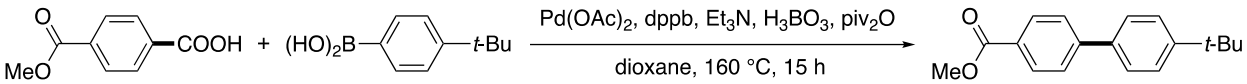

1a **2w** **3bc**

According to the general procedure, the reaction of 4-(methoxycarbonyl)benzoic acid (0.20 mmol), 4-(*tert*-butyl)phenylboronic acid (2.0 equiv), $Pd(OAc)_2$ (5 mol%), 1,4-bis(diphenylphosphino)butane (10 mol%), triethylamine (1.5 equiv), H_3BO_3 (1.5 equiv) and trimethylacetic anhydride (1.5 equiv) in 1,4-dioxane (0.20 M) for 15 h at 160 °C, afforded after work-up and chromatography the title compound in 82% yield (44.1 mg). White solid. **^{1}H NMR (500 MHz, $CDCl_3$)** δ 8.13-8.12 (d, *J* = 8.3 Hz, 2 H), 7.70-7.68 (d, *J* = 8.3 Hz, 2 H), 7.62-7.60 (d, *J* = 8.3 Hz, 2 H), 7.53-7.51 (d, *J* = 8.4 Hz, 2 H), 3.97 (s, 3 H), 1.40 (s, 9 H). **^{13}C NMR (125 MHz, $CDCl_3$)** δ 167.09, 151.36, 145.49, 137.06, 130.09, 128.63, 126.94, 126.85, 125.92, 52.11, 34.65, 31.34. The spectral data matched those reported in the literature (Miao et al., 2017).

4-(Methoxycarbonyl)benzoic acid and *o*-tolylboronic acid (3bd, Figure 4, Entry 56)

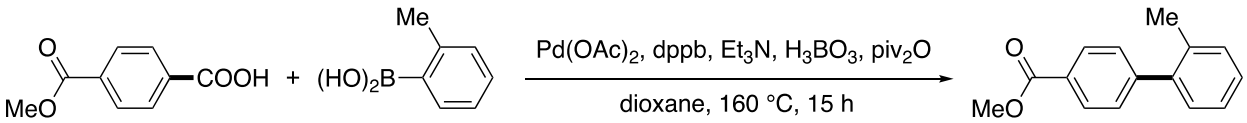

1a **2x** **3bd**

According to the general procedure, the reaction of 4-(methoxycarbonyl)benzoic acid (0.20 mmol), *o*-tolylboronic acid (2.0 equiv), $Pd(OAc)_2$ (5 mol%), 1,4-bis(diphenylphosphino)butane (10 mol%), triethylamine (1.5 equiv), H_3BO_3 (1.5 equiv) and trimethylacetic anhydride (1.5 equiv) in 1,4-dioxane (0.20 M) for 15 h at 160 °C, afforded after work-up and chromatography the title compound in 76% yield (34.4 mg). White solid. **^{1}H NMR (500 MHz, $CDCl_3$)** δ 8.13-8.11 (d, *J* = 8.0 Hz, 2 H), 7.44-7.42 (d, *J* = 7.9 Hz, 2 H), 7.31-7.25 (m, 4 H), 3.98 (s, 3 H), 2.30 (s, 3 H). **^{13}C NMR (125 MHz, $CDCl_3$)** δ 167.09, 146.78, 140.88, 135.19, 130.51, 129.54, 129.43, 129.29, 128.61, 127.85, 125.92, 52.15, 20.40. The spectral data matched those reported in the literature (Luan et al., 2017).

4-(Methoxycarbonyl)benzoic acid and 2-(trifluoromethyl)phenylboronic acid (3be, Figure 4, Entry 57)

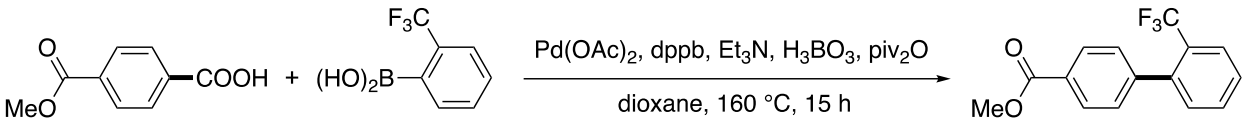

1a **2y** **3be**

According to the general procedure, the reaction of 4-(methoxycarbonyl)benzoic acid (0.20 mmol), 2-(trifluoromethyl)phenylboronic acid (2.0 equiv), $Pd(OAc)_2$ (5 mol%), 1,4-bis(diphenylphosphino)butane (10 mol%), triethylamine (1.5 equiv), H_3BO_3 (1.5 equiv) and trimethylacetic anhydride (1.5 equiv) in 1,4-dioxane (0.20 M) for 15 h at 160 °C, afforded after work-up and chromatography the title compound in 85% yield (47.7 mg). White solid. **^{1}H NMR (500 MHz, $CDCl_3$)** δ 8.11-8.10 (d, *J* = 8.1 Hz, 2 H), 7.80-7.78 (d, *J* = 7.8 Hz, 1 H), 7.62-7.59 (t, *J* = 7.4 Hz, 1 H), 7.54-7.51 (t, *J* = 7.7 Hz, 1 H), 7.44-7.42 (d, *J* = 8.0 Hz, 2 H), 7.35-7.34 (d, *J* = 7.5 Hz, 1 H), 3.97 (s, 3 H). **^{13}C NMR (125 MHz, $CDCl_3$)** δ 166.89, 144.50, 140.31, 131.61, 131.43, 129.50, 129.08, 128.40 (d, J^F = 30.1 Hz), 127.88, 126.21 (d, J^F = 5.2 Hz), 124.00 (d, J^F = 272.3 Hz), 52.19. **^{19}F NMR (471 MHz, $CDCl_3$)** δ -56.81. The spectral data matched those reported in the literature (Tang et al., 2015).

4-(Methoxycarbonyl)benzoic acid and 2-formylphenylboronic acid (3bf, Figure 4, Entry 58)

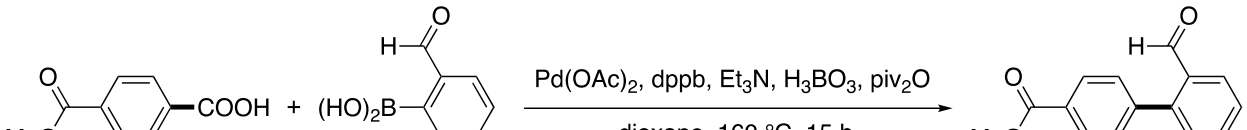

1a **2z** **3bf**

According to the general procedure, the reaction of 4-(methoxycarbonyl)benzoic acid (0.20 mmol), 2-formylphenylboronic acid (2.0 equiv), $Pd(OAc)_2$ (5 mol%), 1,4-bis(diphenylphosphino)butane (10 mol%), triethylamine (1.5 equiv), H_3BO_3 (1.5 equiv) and trimethylacetic anhydride (1.5 equiv) in 1,4-dioxane (0.20 M) for 15 h at 160 °C, afforded after work-up and chromatography the title compound in 73% yield (35.1 mg). White solid. **^{1}H NMR (500 MHz, $CDCl_3$)** δ 9.99 (s, 1 H), 8.18-8.16 (d, *J* = 8.2 Hz, 2 H), 8.08-8.07 (d, *J* = 7.7 Hz, 1 H), 7.71-7.68 (t, *J* = 7.1 Hz, 1 H), 7.59-7.55 (t, *J* = 7.6 Hz, 1 H), 7.50-7.46 (t, *J* = 8.4 Hz, 3 H), 3.99 (s, 3 H). **^{13}C NMR (125 MHz, $CDCl_3$)** δ 191.79, 166.68, 144.69, 142.48, 133.72, 133.67,

130.63, 130.11, 129.89, 129.67, 128.45, 127.99, 52.33. The spectral data matched those reported in the literature (Zhao et al., 2007).

4-(Methoxycarbonyl)benzoic acid and 3,5-dichlorophenylboronic acid (3bg, Figure 4, Entry 59)

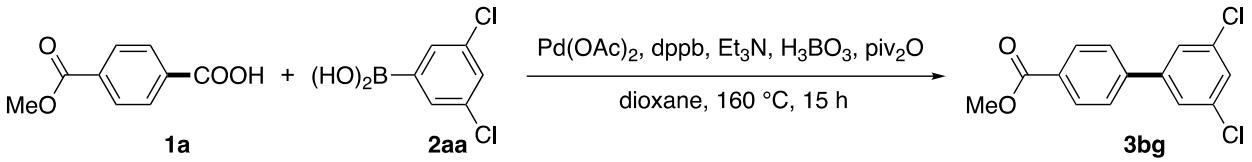

1a 2aa 3bg

According to the general procedure, the reaction of 4-(methoxycarbonyl)benzoic acid (0.20 mmol), 3,5-dichlorophenylboronic acid (2.0 equiv), $Pd(OAc)_2$ (5 mol%), 1,4-bis(diphenylphosphino)butane (10 mol%), triethylamine (1.5 equiv), H_3BO_3 (1.5 equiv) and trimethylacetic anhydride (1.5 equiv) in 1,4-dioxane (0.20 M) for 15 h at 160 °C, afforded after work-up and chromatography the title compound in 62% yield (34.9 mg). White solid. **^{1}H NMR (500 MHz, $CDCl_3$)** δ 8.15-8.13 (d, *J* = 7.5 Hz, 2 H), 7.64-7.62 (d, *J* = 7.2 Hz, 2 H), 7.51 (s, 2 H), 7.41 (s, 1 H), 3.97 (s, 3 H). **^{13}C NMR (125 MHz, $CDCl_3$)** δ 166.63, 143.00, 142.81, 135.53, 130.32, 128.14, 127.99, 127.07, 125.81, 52.27. The spectral data matched those reported in the literature (Ishiyama et al., 2003).

4-(Methoxycarbonyl)benzoic acid and 3,4-difluorophenylboronic acid (3bh, Figure 4, Entry 60)

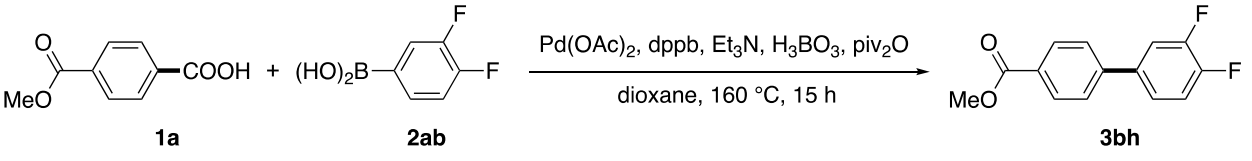

1a 2ab 3bh

According to the general procedure, the reaction of 4-(methoxycarbonyl)benzoic acid (0.20 mmol), 3,4-difluorophenylboronic acid (2.0 equiv), $Pd(OAc)_2$ (5 mol%), 1,4-bis(diphenylphosphino)butane (10 mol%), triethylamine (1.5 equiv), H_3BO_3 (1.5 equiv) and trimethylacetic anhydride (1.5 equiv) in 1,4-dioxane (0.20 M) for 15 h at 160 °C, afforded after work-up and chromatography the title compound in 83% yield (41.2 mg). White solid. **^{1}H NMR (500 MHz, $CDCl_3$)** δ 8.14-8.12 (d, *J* = 7.5 Hz, 2 H), 7.62-7.61 (d, *J* = 7.4 Hz, 2 H), 7.47-7.43 (t, *J* = 8.6 Hz, 1 H), 7.36 (s, 1 H), 7.30-7.25 (m, 1 H), 3.97 (s, 3 H). **^{13}C NMR (125 MHz, $CDCl_3$)** δ 166.75, 151.53 (dd, J^F = 19.1 Hz), 149.55 (dd, J^F = 20.4 Hz), 143.43, 137.12 (dd, J^F = 5.6 Hz),

130.27, 129.49, 126.90, 123.29 (dd, J^F = 6.2 Hz), 117.78 (d, J^F = 17.3 Hz), 116.26 (d, J^F = 17.8 Hz), 52.22. **^{19}F NMR (471 MHz, $CDCl_3$)** δ -137.01, -138.70. The spectral data matched those reported in the literature (Tang et al., 2015).

4-(Methoxycarbonyl)benzoic acid and benzo[*d*][*1,3*]dioxol-5-ylboronic acid (3bi, Figure 4, Entry 61)

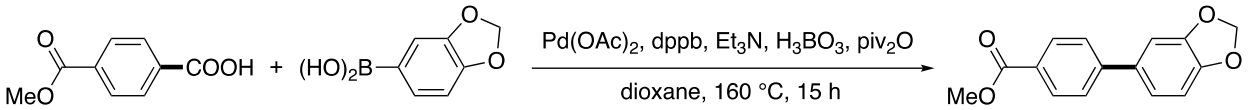

1a **2ac** **3bi**

According to the general procedure, the reaction of 4-(methoxycarbonyl)benzoic acid (0.20 mmol), benzo[*d*][*1,3*]dioxol-5-ylboronic acid (2.0 equiv), $Pd(OAc)_2$ (5 mol%), 1,4-bis(diphenylphosphino)butane (10 mol%), triethylamine (1.5 equiv), H_3BO_3 (1.5 equiv) and trimethylacetic anhydride (1.5 equiv) in 1,4-dioxane (0.20 M) for 15 h at 160 °C, afforded after work-up and chromatography the title compound in 90% yield (46.2 mg). White solid. **^{1}H NMR (500 MHz, $CDCl_3$)** δ 8.10-8.09 (d, *J* = 7.6 Hz, 2 H), 7.61-7.59 (d, *J* = 7.5 Hz, 2 H), 7.14-7.12 (m, 2 H), 6.93-6.92 (d, *J* = 7.7 Hz, 1 H), 6.04 (s, 2 H), 3.96 (s, 3 H). **^{13}C NMR (125 MHz, $CDCl_3$)** δ 166.99, 148.34, 147.83, 145.30, 134.28, 130.11, 128.54, 126.69, 121.06, 108.72, 107.65, 101.34, 52.10. The spectral data matched those reported in the literature (Wu et al., 2013).

4-(Trifluoromethyl)benzoic acid and 3-chlorophenylboronic acid (3bj, Figure 4, Entry 62)

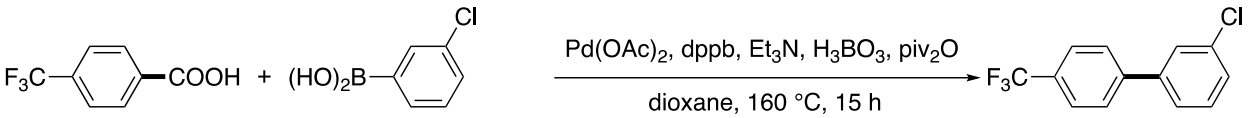

1d **2ad** **3bj**

According to the general procedure, the reaction of 4-(trifluoromethyl)benzoic acid (0.20 mmol), 3-chlorophenylboronic acid (2.0 equiv), $Pd(OAc)_2$ (5 mol%), 1,4-bis(diphenylphosphino)butane (10 mol%), triethylamine (1.5 equiv), H_3BO_3 (1.5 equiv) and trimethylacetic anhydride (1.5 equiv) in 1,4-dioxane (0.20 M) for 15 h at 160 °C, afforded after work-up and chromatography the title compound in 65% yield (33.4 mg). White solid. **^{1}H NMR (500 MHz, $CDCl_3$)** δ 7.74-7.68 (m, 4 H), 7.61 (s, 1 H), 7.51-7.49 (d, *J* = 7.1 Hz, 1 H), 7.43-7.40 (m, 2 H). **^{13}C NMR (125 MHz, $CDCl_3$)** δ 143.31, 141.58, 134.96, 130.24, 129.99 (q, J^F = 32.4 Hz), 128.23, 127.45,

127.29, 125.88 (q, J^F = 3.6 Hz), 125.45, 124.17 (q, J^F = 270.4 Hz). **^{19}F NMR (471 MHz, $CDCl_3$)** δ -62.50. The spectral data matched those reported in the literature (Sun et al., 2018).

4-(Trifluoromethyl)benzoic acid and 4-chlorophenylboronic acid (3bk, Figure 4, Entry 63)

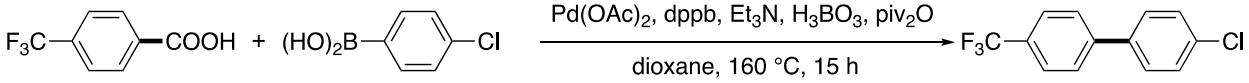

1d **2ae** **3bk**

According to the general procedure, the reaction of 4-(trifluoromethyl)benzoic acid (0.20 mmol), 4-chlorophenylboronic acid (2.0 equiv), $Pd(OAc)_2$ (5 mol%), 1,4-bis(diphenylphosphino)butane (10 mol%), triethylamine (1.5 equiv), H_3BO_3 (1.5 equiv) and trimethylacetic anhydride (1.5 equiv) in 1,4-dioxane (0.20 M) for 15 h at 160 °C, afforded after work-up and chromatography the title compound in 54% yield (27.8 mg). White solid. **^{1}H NMR (500 MHz, $CDCl_3$)** δ 7.73-7.67 (m, 4 H), 7.56-7.55 (d, J = 8.5 Hz, 2 H), 7.48-7.46 (d, J = 8.6 Hz, 2 H). **^{13}C NMR (125 MHz, $CDCl_3$)** δ 143.50, 138.20, 134.46, 129.20, 128.65 (d, J^F = 32.8 Hz), 128.53, 127.29, 125.86 (d, J^F = 3.5 Hz), 124.20 (d, J^F = 270.3 Hz). **^{19}F NMR (471 MHz, $CDCl_3$)** δ -62.48. The spectral data matched those reported in the literature (Keaveney et al., 2018).

3-Chlorobenzoic acid and *m*-tolylboronic acid (3bl, Figure 4, Entry 64)

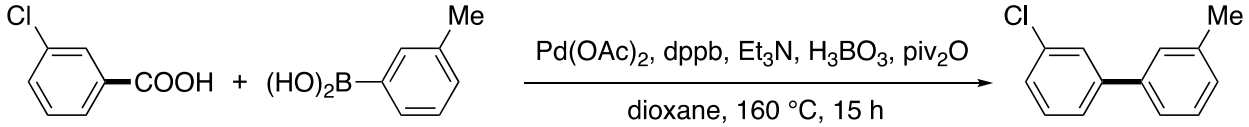

1x **2af** **3bl**

According to the general procedure, the reaction of 3-chlorobenzoic acid (0.20 mmol), *m*-tolylboronic acid (2.0 equiv), $Pd(OAc)_2$ (5 mol%), 1,4-bis(diphenylphosphino)butane (10 mol%), triethylamine (1.5 equiv), H_3BO_3 (1.5 equiv) and trimethylacetic anhydride (1.5 equiv) in 1,4-dioxane (0.20 M) for 15 h at 160 °C, afforded after work-up and chromatography the title compound in 73% yield (29.6 mg). White solid. **^{1}H NMR (500 MHz, $CDCl_3$)** δ 7.60 (s, 1 H), 7.50-7.48 (d, J = 7.6 Hz, 1 H), 7.41-7.33 (m, 5 H), 7.23-7.21 (d, J = 7.0 Hz, 1 H), 2.45 (s, 3 H). **^{13}C NMR (125 MHz, $CDCl_3$)** δ 143.23, 139.82, 138.55, 134.60, 129.93, 128.81, 128.62, 127.91, 127.31, 127.17, 125.32, 124.23, 21.52. The spectral data matched those reported in the literature (Goossen et al., 2004).

3-Chlorobenzoic acid and 3-fluorophenylboronic acid (3bm, Figure 4, Entry 65)

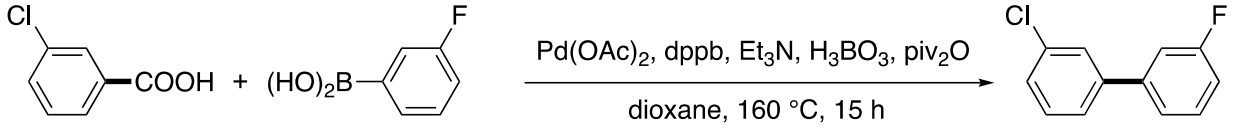

1x **2ag** **3bm**

According to the general procedure, the reaction of 3-chlorobenzoic acid (0.20 mmol), 3-fluorophenylboronic acid (2.0 equiv), $Pd(OAc)_2$ (5 mol%), 1,4-bis(diphenylphosphino)butane (10 mol%), triethylamine (1.5 equiv), H_3BO_3 (1.5 equiv) and trimethylacetic anhydride (1.5 equiv) in 1,4-dioxane (0.20 M) for 15 h at 160 °C, afforded after work-up and chromatography the title compound in 77% yield (31.9 mg). White solid. **^{1}H NMR (500 MHz, $CDCl_3$)** δ 7.58 (s, 1 H), 7.48-7.36 (m, 5 H), 7.30-7.28 (m, 1 H), 7.11-7.08 (m, 1 H). **^{13}C NMR (125 MHz, $CDCl_3$)** δ 163.19 (d, J^F = 244.6 Hz), 142.06 (d, J^F = 7.6 Hz), 141.78 (d, J^F = 2.1 Hz), 134.82, 130.41 (d, J^F = 8.4 Hz), 130.12, 127.87, 127.29, 125.27, 122.76 (d, J^F = 2.8 Hz), 114.71 (d, J^F = 21.0 Hz), 114.07 (d, J^F = 22.1 Hz). **^{19}F NMR (471 MHz, $CDCl_3$)** δ -112.71. The spectral data matched those reported in the literature (Sun et al., 2018).

4-(Methoxycarbonyl)benzoic acid and 2,6-dimethoxyphenylboronic acid (3bn, Figure 4, Entry 66)

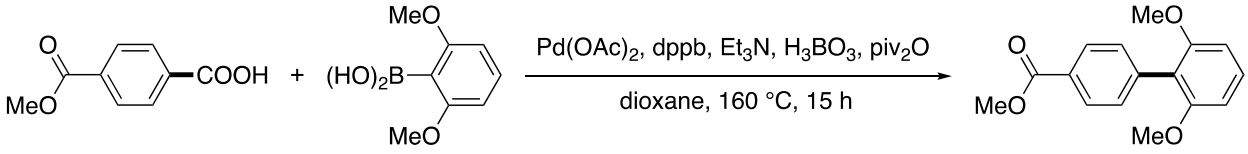

1a **2ah** **3bn**

According to the general procedure, the reaction of 4-(methoxycarbonyl)benzoic acid (0.20 mmol), 2,6-dimethoxyphenylboronic acid (2.0 equiv), $Pd(OAc)_2$ (5 mol%), 1,4-bis(diphenylphosphino)butane (10 mol%), triethylamine (1.5 equiv), H_3BO_3 (1.5 equiv) and trimethylacetic anhydride (1.5 equiv) in 1,4-dioxane (0.20 M) for 15 h at 160 °C, afforded after work-up and chromatography the title compound in 90% yield (49.1 mg). White solid. **^{1}H NMR (500 MHz, $CDCl_3$)** δ 8.11-8.09 (d, J = 8.3 Hz, 2 H), 7.46-7.45 (d, J = 8.3 Hz, 2 H), 7.35-7.31 (t, J = 8.4 Hz, 1 H), 6.69-6.68 (d, J = 8.4 Hz, 2 H), 3.95 (s, 3 H), 3.76 (s, 6 H). **^{13}C NMR (125 MHz, $CDCl_3$)** δ 167.27, 157.52, 139.46, 131.11, 129.31, 128.94, 128.38, 118.53, 104.23, 55.91, 52.00. The spectral data matched those reported in the literature (Michelet et al., 2017).

4-Acetylbenzoic acid and 2,6-dimethoxyphenylboronic acid (3bo, Figure 4, Entry 67)

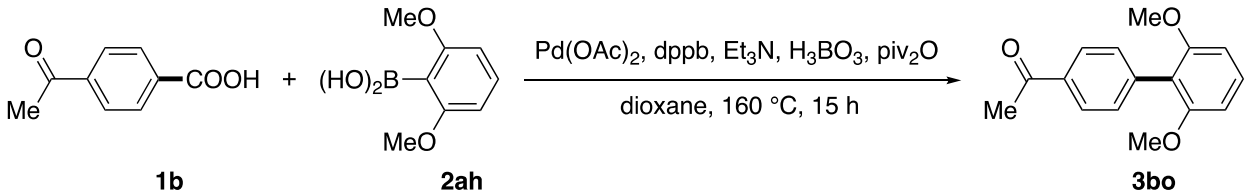

1b **2ah** **3bo**

According to the general procedure, the reaction of 4-acetylbenzoic acid (0.20 mmol), 2,6-dimethoxyphenylboronic acid (2.0 equiv), $Pd(OAc)_2$ (5 mol%), 1,4-bis(diphenylphosphino)butane (10 mol%), triethylamine (1.5 equiv), H_3BO_3 (1.5 equiv) and trimethylacetic anhydride (1.5 equiv) in 1,4-dioxane (0.20 M) for 15 h at 160 °C, afforded after work-up and chromatography the title compound in 90% yield (46.2 mg). White solid. **^{1}H NMR (500 MHz, $CDCl_3$)** δ 8.03-8.02 (d, *J* = 8.2 Hz, 2 H), 7.49-7.48 (d, *J* = 8.1 Hz, 2 H), 7.35-7.32 (t, *J* = 8.4 Hz, 1 H), 6.70-6.68 (d, *J* = 8.4 Hz, 2 H), 3.77 (s, 6 H), 2.65 (s, 3 H). **^{13}C NMR (125 MHz, $CDCl_3$)** δ 198.00, 157.51, 139.75, 135.44, 131.30, 129.40, 127.75, 118.37, 104.22, 55.92, 26.62. The spectral data matched those reported in the literature (Xu et al., 2010).

4-Formylbenzoic acid and 2,6-dimethoxyphenylboronic acid (3bp, Figure 4, Entry 68)

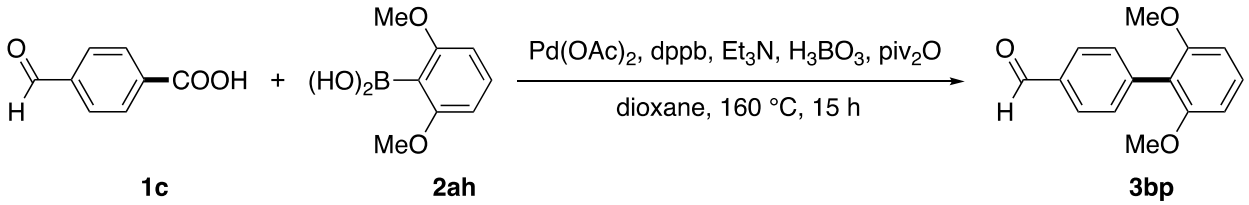

1c **2ah** **3bp**

According to the general procedure, the reaction of 4-formylbenzoic acid (0.20 mmol), 2,6-dimethoxyphenylboronic acid (2.0 equiv), $Pd(OAc)_2$ (5 mol%), 1,4-bis(diphenylphosphino)butane (10 mol%), triethylamine (1.5 equiv), H_3BO_3 (1.5 equiv) and trimethylacetic anhydride (1.5 equiv) in 1,4-dioxane (0.20 M) for 15 h at 160 °C, afforded after work-up and chromatography the title compound in 64% yield (31.0 mg). White solid. **^{1}H NMR (500 MHz, $CDCl_3$)** δ 10.07 (s, 1 H), 7.95-7.93 (d, *J* = 8.0 Hz, 2 H), 7.56-7.55 (d, *J* = 8.0 Hz, 2 H), 7.37-7.33 (t, *J* = 8.4 Hz, 1 H), 6.71-6.69 (d, *J* = 8.4 Hz, 2 H), 3.77 (s, 6 H). **^{13}C NMR (125 MHz, $CDCl_3$)** δ 192.26, 157.46, 141.27, 134.82, 131.81, 129.59, 129.09, 118.19, 104.21, 55.90. The spectral data matched those reported in the literature (Heijnen et al., 2019).

4-(Trifluoromethyl)benzoic acid and 2,6-dimethoxyphenylboronic acid (3bq, Figure 4, Entry 69)

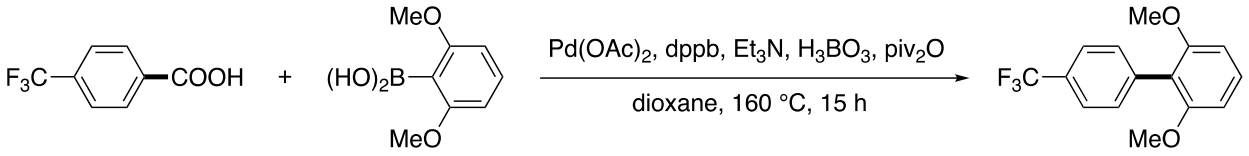

1d **2ah** **3bq**

According to the general procedure, the reaction of 4-(trifluoromethyl)benzoic acid (0.20 mmol), 2,6-dimethoxyphenylboronic acid (2.0 equiv), $Pd(OAc)_2$ (5 mol%), 1,4-bis(diphenylphosphino)butane (10 mol%), triethylamine (1.5 equiv), H_3BO_3 (1.5 equiv) and trimethylacetic anhydride (1.5 equiv) in 1,4-dioxane (0.20 M) for 15 h at 160 °C, afforded after work-up and chromatography the title compound in 85% yield (48.0 mg). White solid. **^{1}H NMR (500 MHz, $CDCl_3$)** δ 7.68-7.66 (d, *J* = 8.1 Hz, 2 H), 7.50-7.48 (d, *J* = 8.0 Hz, 2 H), 7.36-7.33 (t, *J* = 8.4 Hz, 1 H), 6.70-6.69 (d, *J* = 8.4 Hz, 2 H), 3.77 (s, 6 H). **^{13}C NMR (125 MHz, $CDCl_3$)** δ 157.52, 138.10, 131.37, 129.39, 128.67 (q, J^F = 31.9 Hz), 124.55 (q, J^F = 3.8 Hz), 124.48 (q, J^F = 270.2 Hz), 118.09, 104.20, 55.89. **^{19}F NMR (471 MHz, $CDCl_3$)** δ -62.38. The spectral data matched those reported in the literature (Pinxterhuis et al., 2016).

4-Cyanobenzoic acid and 2,6-dimethoxyphenylboronic acid (3br, Figure 4, Entry 70)

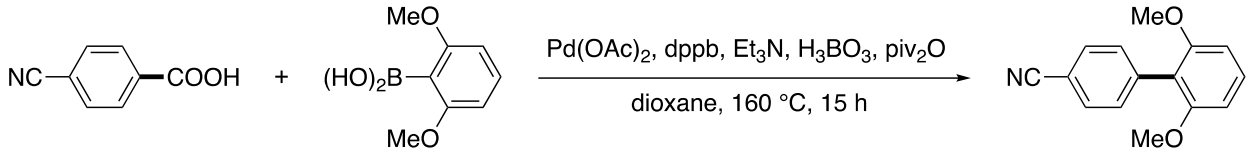

1f **2ah** **3br**

According to the general procedure, the reaction of 4-cyanobenzoic acid (0.20 mmol), 2,6-dimethoxyphenylboronic acid (2.0 equiv), $Pd(OAc)_2$ (5 mol%), 1,4-bis(diphenylphosphino)butane (10 mol%), triethylamine (1.5 equiv), H_3BO_3 (1.5 equiv) and trimethylacetic anhydride (1.5 equiv) in 1,4-dioxane (0.20 M) for 15 h at 160 °C, afforded after work-up and chromatography the title compound in 61% yield (29.2 mg). White solid. **^{1}H NMR (500 MHz, $CDCl_3$)** δ 7.70-7.68 (d, *J* = 8.0 Hz, 2 H), 7.49-7.48 (d, *J* = 8.0 Hz, 2 H), 7.36-7.33 (t, *J* = 8.3 Hz, 1 H), 6.69-6.68 (d, *J* = 8.4 Hz, 2 H), 3.76 (s, 6 H). **^{13}C NMR (125 MHz, $CDCl_3$)** δ 157.33, 139.54, 131.93, 131.38, 129.80, 119.38, 117.55, 110.29, 104.17, 55.87. The spectral data matched those reported in the literature (Liu et al., 2013).

4-(Tosyloxy)benzoic acid and 2,6-dimethoxyphenylboronic acid (3bs, Figure 4, Entry 71)

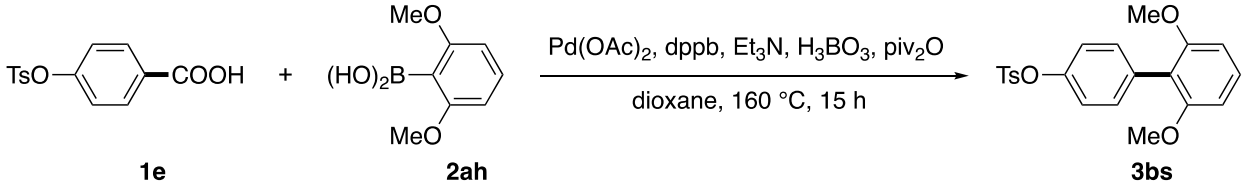

1e **2ah** **3bs**

According to the general procedure, the reaction of 4-(tosyloxy)benzoic acid (0.20 mmol), 2,6-dimethoxyphenylboronic acid (2.0 equiv), $Pd(OAc)_2$ (5 mol%), 1,4-bis(diphenylphosphino)butane (10 mol%), triethylamine (1.5 equiv), H_3BO_3 (1.5 equiv) and trimethylacetic anhydride (1.5 equiv) in 1,4-dioxane (0.20 M) for 15 h at 160 °C, afforded after work-up and chromatography the title compound in 78% yield (60.0 mg). *New compound.* White solid. **Mp** = 146-147 °C. **^{1}H NMR (500 MHz, $CDCl_3$)** δ 7.81-7.79 (d, *J* = 8.1 Hz, 2 H), 7.36-7.34 (d, *J* = 8.1 Hz, 2 H), 7.29-7.28 (d, *J* = 8.4 Hz, 3 H), 7.04-7.02 (d, *J* = 8.5 Hz, 2 H), 6.67-6.65 (d, *J* = 8.4 Hz, 2 H), 3.74 (s, 6 H), 2.48 (s, 3 H). **^{13}C NMR (125 MHz, $CDCl_3$)** δ 157.54, 148.29, 145.12, 133.05, 132.89, 132.28, 129.69, 129.03, 128.57, 121.39, 118.17, 104.26, 55.87, 21.72. **HRMS** calcd for $C_{21}H_{20}O_5SNa$ (M^+ + Na) 407.0924, found 407.0925.

Quinoline-6-carboxylic acid and 2,6-dimethoxyphenylboronic acid (3bt, Figure 4, Entry 72)

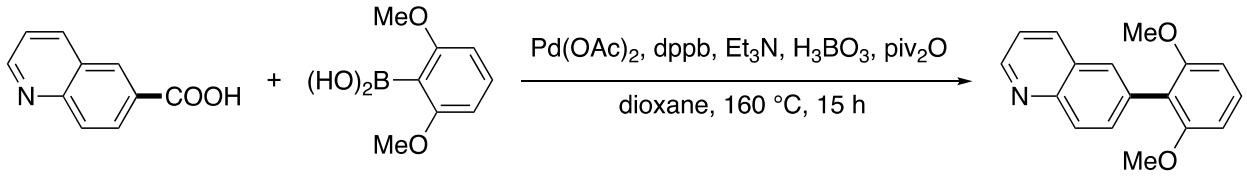

1l **2ah** **3bt**

According to the general procedure, the reaction of quinoline-6-carboxylic acid (0.20 mmol), 2,6-dimethoxyphenylboronic acid (2.0 equiv), $Pd(OAc)_2$ (5 mol%), 1,4-bis(diphenylphosphino)butane (10 mol%), triethylamine (1.5 equiv), H_3BO_3 (1.5 equiv) and trimethylacetic anhydride (1.5 equiv) in 1,4-dioxane (0.20 M) for 15 h at 160 °C, afforded after work-up and chromatography the title compound in 75% yield (39.8 mg). *New compound.* White solid. **Mp** = 104-106 °C. **^{1}H NMR (500 MHz, $CDCl_3$)** δ 8.93-8.92 (d, *J* = 2.9 Hz, 1 H), 8.19-8.14 (m, 2 H), 7.84 (s, 1 H), 7.75-7.73 (dd, *J* = 8.7 Hz, 1 H), 7.42-7.34 (m, 2 H), 6.74-6.72 (d, *J* = 8.4 Hz, 2 H), 3.77 (s, 6 H). **^{13}C NMR (125 MHz, $CDCl_3$)** δ 157.77, 150.05, 147.41, 136.27, 133.26, 132.69, 129.59, 129.19, 128.37, 128.10, 120.84, 118.65, 104.29, 55.95. **HRMS** calcd for $C_{17}H_{15}NO_2$ (M^+) 265.1097, found 265.1093.

1-Naphthoic acid and 2,6-dimethoxyphenylboronic acid (3bu, Figure 4, Entry 73)

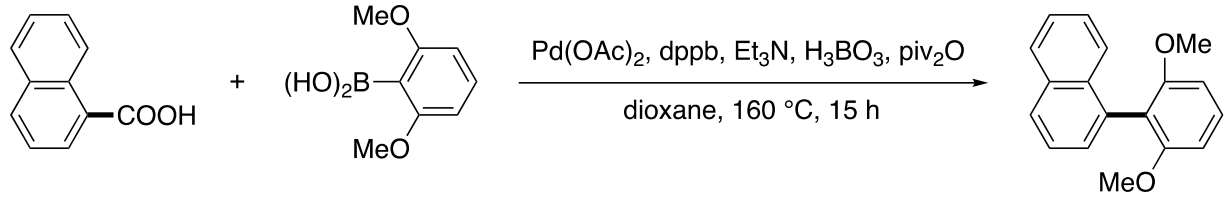

1j **2ah** **3bu**

According to the general procedure, the reaction of 1-naphthoic acid (0.20 mmol), 2,6-dimethoxyphenylboronic acid (2.0 equiv), $Pd(OAc)_2$ (5 mol%), 1,4-bis(diphenylphosphino)butane (10 mol%), triethylamine (1.5 equiv), H_3BO_3 (1.5 equiv) and trimethylacetic anhydride (1.5 equiv) in 1,4-dioxane (0.20 M) for 15 h at 160 °C, afforded after work-up and chromatography the title compound in 41% yield (21.7 mg). White solid. **^{1}H NMR (500 MHz, $CDCl_3$)** δ 7.91-7.87 (m, 2 H), 7.58-7.55 (m, 1 H), 7.50-7.35 (m, 5 H), 6.76-6.74 (d, *J* = 8.4 Hz, 2 H), 3.66 (s, 6 H). **^{13}C NMR (125 MHz, $CDCl_3$)** δ 158.50, 133.57, 132.68, 132.59, 129.11, 128.18, 128.05, 127.45, 126.02, 125.47, 125.42, 125.35, 117.73, 104.21, 55.95. The spectral data matched those reported in the literature (Pinxterhuis et al., 2016).

2-Methylbenzoic acid and 2-methoxyphenylboronic acid (3bv, Figure 4, Entry 74)

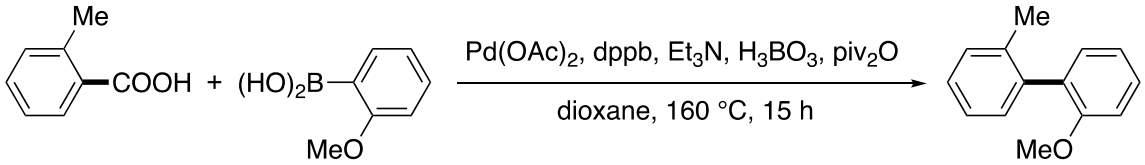

1g **2l** **3bv**

According to the general procedure, the reaction of 2-methylbenzoic acid (0.20 mmol), 2-methoxyphenylboronic acid (2.0 equiv), $Pd(OAc)_2$ (5 mol%), 1,4-bis(diphenylphosphino)butane (10 mol%), triethylamine (1.5 equiv), H_3BO_3 (1.5 equiv) and trimethylacetic anhydride (1.5 equiv) in 1,4-dioxane (0.20 M) for 15 h at 160 °C, afforded after work-up and chromatography the title compound in 31% yield (12.3 mg). White solid. **^{1}H NMR (500 MHz, $CDCl_3$)** δ 7.38-7.35 (m, 1 H), 7.28-7.23 (m, 3 H), 7.21-7.20 (d, *J* = 7.2 Hz, 1 H), 7.18-7.16 (dd, *J* = 7.4 Hz, 1 H), 7.05-7.02 (t, *J* = 7.4 Hz, 1 H), 7.00-6.98 (d, *J* = 8.3 Hz, 1 H), 3.79 (s, 3 H), 2.16 (s, 3 H). **^{13}C NMR (125 MHz, $CDCl_3$)** δ 156.62, 138.64, 136.83, 131.02, 130.88, 130.01, 129.58, 128.55, 127.29, 125.44, 120.45, 110.68, 55.42, 19.91. The spectral data matched those reported in the literature (Teng et al., 2018).

Probenecid and 6-methoxypyridin-3-ylboronic acid (3bw, Figure 4, Entry 75)

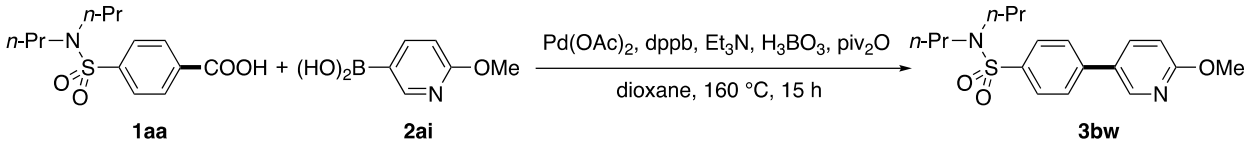

According to the general procedure, the reaction of probenecid (0.20 mmol), 6-methoxypyridin-3-ylboronic acid (2.0 equiv), $Pd(OAc)_2$ (5 mol%), 1,4-bis(diphenylphosphino)butane (10 mol%), triethylamine (1.5 equiv), H_3BO_3 (1.5 equiv) and trimethylacetic anhydride (1.5 equiv) in 1,4-dioxane (0.20 M) for 15 h at 160 °C, afforded after work-up and chromatography the title compound in 74% yield (51.6 mg). *New compound.* White solid. **Mp** = 108-110 °C. **^{1}H NMR (500 MHz, $CDCl_3$)** δ 8.44-8.44 (d, *J* = 1.7 Hz, 1 H), 7.90-7.88 (d, *J* = 8.2 Hz, 2 H), 7.84-7.82 (dd, *J* = 8.6 Hz, 1 H), 7.67-7.65 (d, *J* = 8.2 Hz, 2 H), 6.88-6.87 (d, *J* = 8.6 Hz, 1 H), 4.02 (s, 3 H), 3.15-3.12 (t, *J* = 7.6 Hz, 4 H), 1.65-1.57 (m, 4 H), 0.93-0.90 (t, *J* = 7.3 Hz, 6 H). **^{13}C NMR (125 MHz, $CDCl_3$)** δ 164.29, 145.38, 141.83, 138.90, 137.40, 128.34, 127.81, 126.97, 111.19, 53.71, 50.15, 22.13, 11.22. **HRMS** calcd for $C_{18}H_{24}N_2O_3SNa$ (M^+ + Na) 371.1400, found 371.1376.

Probenecid and 5-acetylthiophen-2-ylboronic acid (3bx, Figure 4, Entry 76)

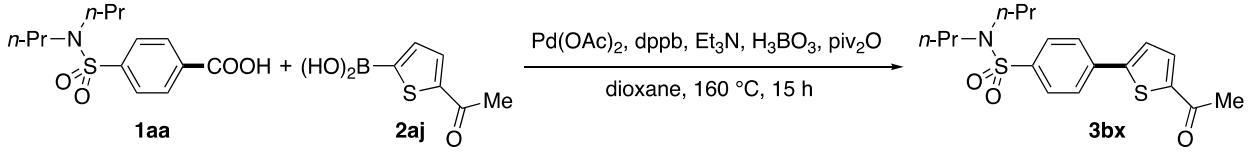

According to the general procedure, the reaction of probenecid (0.20 mmol), 5-acetylthiophen-2-ylboronic acid (2.0 equiv), $Pd(OAc)_2$ (5 mol%), 1,4-bis(diphenylphosphino)butane (10 mol%), triethylamine (1.5 equiv), H_3BO_3 (1.5 equiv) and trimethylacetic anhydride (1.5 equiv) in 1,4-dioxane (0.20 M) for 15 h at 160 °C, afforded after work-up and chromatography the title compound in 93% yield (68.0 mg). *New compound.* White solid. **Mp** = 148-150 °C. **^{1}H NMR (500 MHz, $CDCl_3$)** δ 7.87-7.85 (d, *J* = 8.5 Hz, 2 H), 7.78-7.77 (d, *J* = 8.4 Hz, 2 H), 7.71-7.70 (d, *J* = 3.9 Hz, 1 H), 7.44-7.43 (d, *J* = 3.9 Hz, 1 H), 3.14-3.11 (t, *J* = 7.7 Hz, 4 H), 2.60 (s, 3 H), 1.63-1.55 (m, 4 H), 0.92-0.89 (t, *J* = 7.4 Hz, 6 H). **^{13}C NMR (125 MHz, $CDCl_3$)** δ 190.54, 150.09, 144.61, 140.25, 136.95, 133.36, 127.90, 126.57, 125.40, 50.07, 26.67, 22.06, 11.21. **HRMS** calcd for $C_{18}H_{23}NO_3S_2Na$ (M^+ + Na) 388.1012, found 388.1011.

Probenecid and pyrene-1-boronic acid (3by, Figure 4, Entry 77)

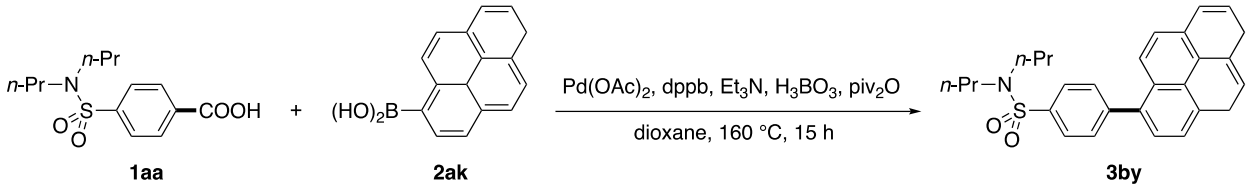

1aa 2ak 3by

According to the general procedure, the reaction of probenecid (0.20 mmol), pyrene-1-boronic acid (2.0 equiv), $Pd(OAc)_2$ (5 mol%), 1,4-bis(diphenylphosphino)butane (10 mol%), triethylamine (1.5 equiv), H_3BO_3 (1.5 equiv) and trimethylacetic anhydride (1.5 equiv) in 1,4-dioxane (0.20 M) for 15 h at 160 °C, afforded after work-up and chromatography the title compound in 81% yield (71.6 mg). *New compound.* White solid. **Mp** = 363-365 °C. **^{1}H NMR (500 MHz, $CDCl_3$)** δ 8.27-8.25 (m, 2 H), 8.23-8.21 (d, *J* = 7.5 Hz, 1 H), 8.17-8.12 (m, 2 H), 8.09-8.05 (m, 3 H), 8.04-8.02 (d, *J* = 8.2 Hz, 2 H), 7.99-7.97 (d, *J* = 7.9 Hz, 1 H), 7.80-7.78 (d, *J* = 8.2 Hz, 2 H), 3.26-3.23 (t, *J* = 7.6 Hz, 4 H), 1.73-1.66 (m, 4 H), 1.00-0.97 (t, *J* = 7.4 Hz, 6 H). **^{13}C NMR (125 MHz, $CDCl_3$)** δ 145.44, 139.02, 135.68, 131.45, 131.19, 131.12, 130.87, 128.39, 128.11, 127.96, 127.34, 127.18, 126.26, 125.55, 125.20, 124.96, 124.79, 124.72, 124.49, 50.28, 22.25, 11.29. **HRMS** calcd for $C_{28}H_{29}NO_2S$ (M^+) 443.1914, found 443.1898.

Probenecid and 3-cyanophenylboronic acid (3bz, Figure 4, Entry 78)

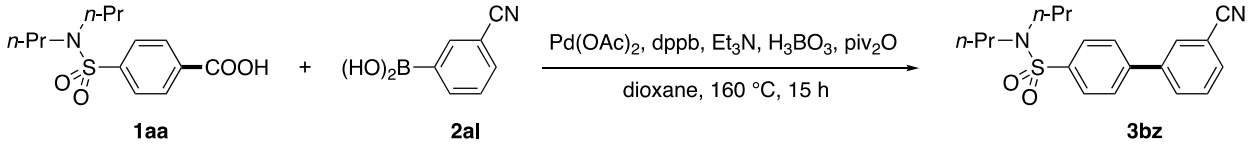

1aa 2al 3bz

According to the general procedure, the reaction of probenecid (0.20 mmol), 3-cyanophenylboronic acid (2.0 equiv), $Pd(OAc)_2$ (5 mol%), 1,4-bis(diphenylphosphino)butane (10 mol%), triethylamine (1.5 equiv), H_3BO_3 (1.5 equiv) and trimethylacetic anhydride (1.5 equiv) in 1,4-dioxane (0.20 M) for 15 h at 160 °C, afforded after work-up and chromatography the title compound in 98% yield (67.2 mg). *New compound.* Colorless oil. **^{1}H NMR (500 MHz, $CDCl_3$)** δ 7.94-7.91 (t, *J* = 8.4 Hz, 3 H), 7.86-7.85 (d, *J* = 7.9 Hz, 1 H), 7.73-7.70 (t, *J* = 10.0 Hz, 3 H), 7.64-7.61 (t, *J* = 7.8 Hz, 1 H), 3.16-3.13 (t, *J* = 7.6 Hz, 4 H), 1.64-1.57 (m, 4 H), 0.93-0.90 (t, *J* = 7.4 Hz, 6 H). **^{13}C NMR (125 MHz, $CDCl_3$)** δ 142.62, 140.74, 140.15, 131.73, 131.62, 130.87, 129.95, 127.89, 127.67, 118.46, 113.37, 50.08, 22.07, 11.22. **HRMS** calcd for $C_{19}H_{22}N_2O_2SNa$ (M^+ + Na) 365.1294, found 365.1288.

Probenecid and *m*-tolylboronic acid (3ca, Figure 4, Entry 79)

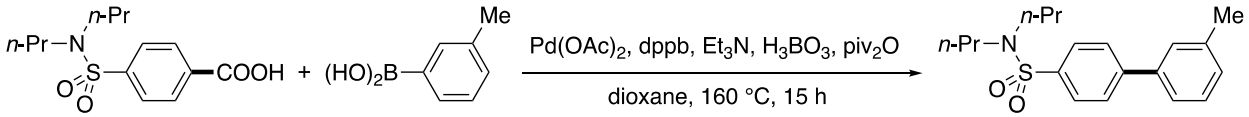

1aa **2af** **3ca**

According to the general procedure, the reaction of probenecid (0.20 mmol), *m*-tolylboronic acid (2.0 equiv), $Pd(OAc)_2$ (5 mol%), 1,4-bis(diphenylphosphino)butane (10 mol%), triethylamine (1.5 equiv), H_3BO_3 (1.5 equiv) and trimethylacetic anhydride (1.5 equiv) in 1,4-dioxane (0.20 M) for 15 h at 160 °C, afforded after work-up and chromatography the title compound in 88% yield (58.4 mg). *New compound.* Colorless oil. **^{1}H NMR (500 MHz, $CDCl_3$)** δ 7.89-7.87 (d, *J* = 8.4 Hz, 2 H), 7.72-7.71 (d, *J* = 8.3 Hz, 2 H), 7.44-7.42 (d, *J* = 9.4 Hz, 2 H), 7.40-7.37 (t, *J* = 7.5 Hz, 1 H), 7.26-7.24 (d, *J* = 7.3 Hz, 1 H), 3.14-3.11 (t, *J* = 7.6 Hz, 4 H), 2.60 (s, 3 H), 1.63-1.55 (m, 4 H), 0.92-0.89 (t, *J* = 7.4 Hz, 6 H). **^{13}C NMR (125 MHz, $CDCl_3$)** δ 145.25, 139.41, 138.71, 138.64, 129.13, 128.94, 128.06, 127.58, 127.53, 124.41, 50.12, 22.11, 21.53, 11.23. **HRMS** calcd for $C_{19}H_{25}NO_2SNa$ (M^+ + Na) 354.1498, found 354.1485.

Probenecid and 4-hydroxyphenylboronic acid (3cb, Figure 4, Entry 80)

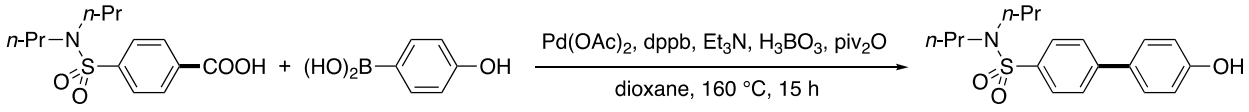

1aa **2am** **3cb**

According to the general procedure, the reaction of probenecid (0.20 mmol), 4-hydroxyphenylboronic acid (2.0 equiv), $Pd(OAc)_2$ (5 mol%), 1,4-bis(diphenylphosphino)butane (10 mol%), triethylamine (1.5 equiv), H_3BO_3 (1.5 equiv) and trimethylacetic anhydride (1.5 equiv) in 1,4-dioxane (0.20 M) for 15 h at 160 °C, afforded after work-up and chromatography the title compound in 50% yield (33.4 mg). *New compound.* White solid. **Mp** = 82-84 °C. **^{1}H NMR (500 MHz, $CDCl_3$)** δ 8.35-8.34 (d, *J* = 8.4 Hz, 2 H), 7.98-7.96 (d, *J* = 8.4 Hz, 2 H), 7.49-7.46 (t, *J* = 7.8 Hz, 2 H), 7.25-7.24 (d, *J* = 7.8 Hz, 2 H), 3.17-3.14 (t, *J* = 7.7 Hz, 4 H), 1.63-1.56 (m, 4 H), 0.93-0.90 (t, *J* = 7.4 Hz, 6 H). **^{13}C NMR (125 MHz, $CDCl_3$)** δ 163.90, 144.92, 132.88, 130.81, 129.64, 127.19, 126.28, 121.52, 49.96, 21.96, 11.19. **HRMS** calcd for $C_{18}H_{23}NO_3SK$ (M^+ + K) 372.1036, found 372.1049.

Probenecid and 3,5-difluorophenylboronic acid (3cc, Figure 4, Entry 81)

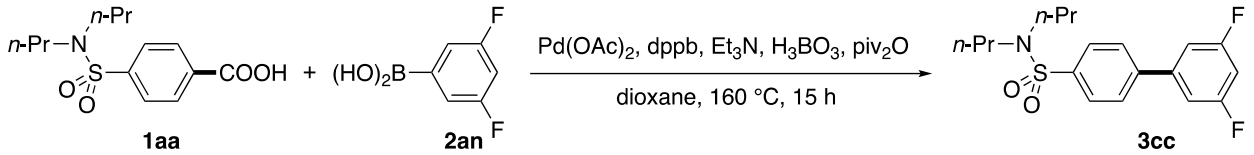

1aa 2an 3cc

According to the general procedure, the reaction of probenecid (0.20 mmol), 3,5-difluorophenylboronic acid (2.0 equiv), $Pd(OAc)_2$ (5 mol%), 1,4-bis(diphenylphosphino)butane (10 mol%), triethylamine (1.5 equiv), H_3BO_3 (1.5 equiv) and trimethylacetic anhydride (1.5 equiv) in 1,4-dioxane (0.20 M) for 15 h at 160 °C, afforded after work-up and chromatography the title compound in 65% yield (46.0 mg). *New compound.* Colorless oil. **^{1}H NMR (500 MHz, $CDCl_3$)** δ 7.92-7.90 (d, J = 8.4 Hz, 2 H), 7.69-7.67 (d, J = 8.4 Hz, 2 H), 7.15-7.14 (d, J = 6.3 Hz, 2 H), 6.90-6.85 (m, 1 H), 3.15-3.12 (t, J = 7.6 Hz, 4 H), 1.63-1.56 (m, 4 H), 0.93-0.90 (t, J = 7.4 Hz, 6 H). **^{13}C NMR (125 MHz, $CDCl_3$)** δ 163.41 (dd, J^F = 247.6 Hz), 142.60 (d, J^F = 2.1 Hz), 140.16, 132.20, 128.00 (d, J^F = 238.7 Hz), 127.68 (d, J^F = 26.1 Hz), 110.29 (d, J^F = 26.0 Hz), 103.64 (dd, J^F = 25.2 Hz), 50.09, 22.07, 11.20. **^{19}F NMR (471 MHz, $CDCl_3$)** δ -108.81. **HRMS** calcd for $C_{18}H_{21}NO_2SF_2Na$ (M^+ + Na) 376.1153, found 376.1148.

Flufenamic acid and 2-methoxyphenylboronic acid (3cd, Figure 4, Entry 82)

1ab 2l 3cd

According to the general procedure, the reaction of flufenamic acid (0.20 mmol), 2-methoxyphenylboronic acid (2.0 equiv), $Pd(OAc)_2$ (5 mol%), 1,4-bis(diphenylphosphino)butane (10 mol%), triethylamine (1.5 equiv), H_3BO_3 (1.5 equiv) and trimethylacetic anhydride (1.5 equiv) in 1,4-dioxane (0.20 M) for 15 h at 160 °C, afforded after work-up and chromatography the title compound in 56% yield (38.5 mg). *New compound.* White solid. **Mp** = 135-137 °C. **^{1}H NMR (500 MHz, $CDCl_3$)** δ 7.42-7.39 (t, J = 7.6 Hz, 2 H), 7.38-7.27 (m, 4 H), 7.15-7.06 (m, 5 H), 7.02-7.01 (d, J = 8.2 Hz, 1 H), 5.98 (s, 1 H), 3.74 (s, 3 H). **^{13}C NMR (125 MHz, $CDCl_3$)** δ 156.41, 144.99, 139.95, 131.85, 131.80, 131.57 (q, J^F = 32.4 Hz), 130.81, 129.57, 129.32,

128.32, 128.01, 124.17 (q, J^F = 270.7 Hz), 122.60, 121.37, 119.53, 119.48, 116.21 (q, J^F = 3.7 Hz), 112.94 (q, J^F = 3.6 Hz), 111.16, 55.64. **^{19}F NMR (471 MHz, $CDCl_3$)** δ -62.83. **HRMS** calcd for $C_{20}H_{16}NOF_3$ (M^+) 343.1179, found 343.1165.

Flufenamic acid and 2-fluorophenylboronic acid (3ce, Figure 4, Entry 83)

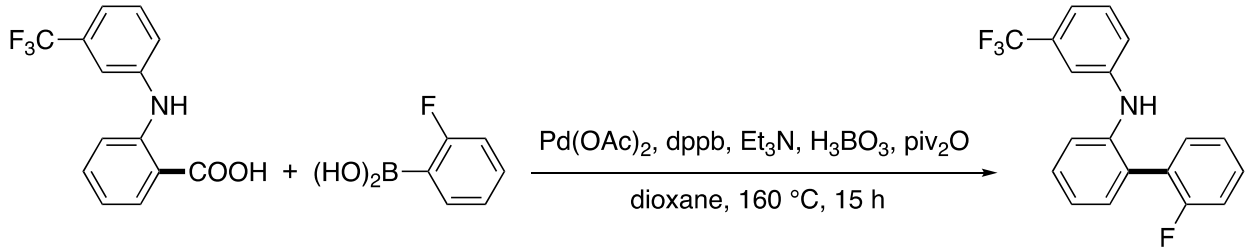

1ab **2j** **3ce**

According to the general procedure, the reaction of flufenamic acid (0.20 mmol), 2-fluorophenylboronic acid (2.0 equiv), $Pd(OAc)_2$ (5 mol%), 1,4-bis(diphenylphosphino)butane (10 mol%), triethylamine (1.5 equiv), H_3BO_3 (1.5 equiv) and trimethylacetic anhydride (1.5 equiv) in 1,4-dioxane (0.20 M) for 15 h at 160 °C, afforded after work-up and chromatography the title compound in 74% yield (49.1 mg). *New compound.* Colorless oil. **^{1}H NMR (500 MHz, $CDCl_3$)** δ 7.42-7.30 (m, 6 H), 7.25-7.11 (m, 6 H), 5.63 (s, 1 H). **^{13}C NMR (125 MHz, $CDCl_3$)** δ 159.87 (d, J^F = 245.0 Hz), 144.31, 139.82, 131.91 (d, J^F = 3.4 Hz), 131.72, 131.67 (q, J^F = 31.9 Hz), 129.79 (d, J^F = 8.1 Hz), 129.70, 129.12, 127.43, 126.21 (d, J^F = 15.9 Hz), 124.66 (d, J^F = 3.5 Hz), 124.08 (q, J^F = 270.8 Hz), 122.61, 120.11, 119.48, 116.94 (q, J^F = 3.7 Hz), 116.05 (d, J^F = 22.2 Hz), 113.63 (q, J^F = 3.8 Hz). **^{19}F NMR (471 MHz, $CDCl_3$)** δ -62.86, -114.15. **HRMS** calcd for $C_{19}H_{13}NF_4$ (M^+) 331.0979, found 331.0995.

Supplemental References

Frisch, M. J. et al. (2010). Gaussian 09, Revision D 01. (Gaussian Inc).

Becke, A. D. (1993). Density-functional thermochemistry. III. The role of exact exchange. J. Chem. Phys. *98*, 5648-5652.

Lee, C., Yang, W., and Parr, R. G. (1988). Development of the Colle-Salvetti correlation-energy formula into a functional of the electron density. Phys. Rev. B: Condens. Matter Mater. Phys. *37*, 785-789.

Hay, P. J., and Wadt, W. R. (1985). *Ab initio* effective core potentials for molecular calculations. Potentials for the transition metal atoms Sc to Hg. J. Chem. Phys. *82*, 270-283.

Wadt, W. R., and Hay, P. J. (1985). *Ab initio* effective core potentials for molecular calculations. Potentials for main group elements Na to Bi. J. Chem. Phys. *82*, 284-298.

Hay, P. J., and Wadt, W. R. (1985). *Ab initio* effective core potentials for molecular calculations. Potentials for K to Au including the outermost core orbitals. J. Chem. Phys. *82*, 299-310.

Zhao, Y., and Truhlar, D. G. (2008). The M06 suite of density functionals for main group thermochemistry, thermochemical kinetics, noncovalent interactions, excited etates, and transition elements: Two new functionals and systematic testing of four M06-class functionals and 12 other functionals. Theor. Chem. Acc. *120*, 215-241.

Zhao, Y., and Truhlar, D. G. (2008). Density functionals with broad applicability in chemistry. Acc. Chem. Res. *41*, 157-167.

von Szentpaly, L., Fuentealba, P., Preuss, H., and Stoll, H. (1982). Pseudopotential calculations on Rb^{+}_{2}, Cs^{+}_{2}, RbH^{+}, CsH^{+} and the mixed alkali dimer ions. Chem. Phys. Lett. *93*, 555-559.

Dolg, M., Wedig, U., Stoll, H., and Preuss, H. (1987). Energy-adjusted ab initio pseudopotentials for the first row transition elements. J. Chem. Phys. *86*, 866-872.

Schwerdtfeger, P., Dolg, M., Schwarz, W. H. E., Bowmaker, G. A., and Boyd, P. D. W. (1989). Relativistic effects in gold chemistry. I. Diatomic gold compounds. J. Chem. Phys. *91*, 1762-

1774.

Marenich, A. V., Cramer, C. J., and Truhlar, D. G. (2009). Universal solvation model based on solute electron density and on a continuum model of the solvent defined by the bulk dielectric constant and atomic surface tensions. J. Phys. Chem. B *113*, 6378-6396.

Legault, C. Y. (2009). CYLview, 1.0b. (Université de Sherbrooke).

Liu, C., Li, G., Shi, S., Meng, G., Lalancette, R., Szostak, R., and Szostak, M. (2018). Acyl and Decarbonylative Suzuki Coupling of N-Acetyl Amides: Electronic Tuning of Twisted, Acyclic Amides in Catalytic Carbon-Nitrogen Bond Cleavage. ACS Catal. *8*, 9131-9139.

Shi, S., Meng, G., and Szostak, M. (2016). Synthesis of Biaryls via Nickel Catalyzed Suzuki-Miyaura Coupling of Amides by Carbon-Nitrogen Cleavage. Angew. Chem. Int. Ed. *55*, 6959-6963.

Kadam, V. D., Feng, B., Chen, X., Liang, W., Zhou, F., Liu, Y., Gao, G., and You, J. (2018). Cascade C-H Annulation Reaction of Benzaldehydes, Anilines, and Alkynes toward Dibenzo[a,f]quinolizinium Salts: Discovery of Photostable Mitochondrial Trackers at the Nanomolar Level. Org. Lett. *20*, 7071-7075.

Lv, L., Zhu, D., Tang, J., Qiu, Z., Li, C. C., Gao, J., and Li, C. J. (2018). Cross-Coupling of Phenol Derivatives with Umpolung Aldehydes Catalyzed by Nickel. ACS Catal. *8*, 4622-4627.

Gan, Y., Wang, G., Xie, X., and Liu, Y. (2018). Nickel-Catalyzed Cyanation of Phenol Derivatives with $Zn(CN)_2$ Involving C-O Bond Cleavage. J. Org. Chem. *83*, 14036-14048.

Simpson, Q., Sinclair, M. J. G., Lupton, D. W., Chaplin, A. B., and Hooper, J. F. (2018). Oxidative Cross-Coupling of Boron and Antimony Nucleophiles via Palladium(I). Org. Lett. *20*, 5537-5540.

Sugahara, T., Murakami, K., Yorimitsu, H., and Osuka, A. (2014). Palladium-Catalyzed Amination of Aryl Sulfides with Anilines. Angew. Chem. Int. Ed. *53*, 9329-9333.

Muto, K., Yamaguchi, J., Musaev, D. G., and Itami, K. (2015). Decarbonylative organoboron cross-coupling of esters by nickel catalysis. Nat. Commun. *6*, 7508.

Okura, K., Teranishi, T., Yoshida, Y., and Shirakawa, E. (2018). Electron-Catalyzed Cross-Coupling of Arylboron Compounds with Aryl Iodides. Angew. Chem. Int. Ed. *57*, 7186-7190.

Nakamura, K., Yasui, K., Tobisu, M., and Chatani, N. (2015). Rhodium-catalyzed cross-coupling of aryl carbamates with arylboron reagents. Tetrahedron *71*, 4484-4489.

Veld, P. H. G., and Laarhoven, W. H. (1978). Substituent effects in the photocyclization of 2-styrylbiphenyls. J. Chem. Soc., Perkin, Trans. 2. 922-927.

Yadav, M. R., Nagaoka, M., Kashihara, M., Zhong, R. L., Miyazaki, T., Sakaki, S., and Nakao, Y. (2017). The Suzuki-Miyaura Coupling of Nitroarenes. J. Am. Chem. Soc. *139*, 9423-9426.

Song, H. J., Jiang, W. T., Zhou, Q. L., Xu, M. Y., and Xiao, B. (2018). Structure-Modified Germatranes for Pd-Catalyzed Biaryl Synthesis. ACS Catal. *8*, 9287-9291.

Keaveney, S. T., Kundu, G., and Schoenebeck, F. (2018). Modular Functionalization of Arenes in a Triply Selective Sequence: Rapid C(sp^2) and C(sp^3) Coupling of C-Br, C-OTf, and C-Cl Bonds Enabled by a Single Palladium(I) Dimer. Angew. Chem. Int. Ed. *57*, 12573-12577.

Liu, W., Liu, P., Lv, L., and Li, C. J. (2018). Metal-Free and Redox-Neutral Conversion of Organotrifluoroborates into Radicals Enabled by Visible Light. Angew. Chem. Int. Ed. *57*, 13499-13503.

Liu, J. B., Yan, H., Chen, H. X., Luo, Y., Weng, J., and Lu, G. (2013). Palladium-catalyzed Suzuki cross-coupling of N'-tosyl arylhydrazines. Chem. Commun. *49*, 5268-5270.

Van Alphen, J. (1931). Primary addition products in indirect substitution in the benzene nucleus. III. Addition products of 4,4'-dialkoxybiphenyls with nitric acid. *Recl. Trav. Chim. Pays-Bas. 50*, 657-658.

Huang, L., and Weix, D. J. (2016). Ruthenium-Catalyzed C-H Arylation of Diverse Aryl Carboxylic Acids with Aryl and Heteroaryl Halides. Org. Lett. *18*, 5432-5435.

Campo, M. A., Zhang, H., Yao, T., Ibdah, A., McCulla, R. D., Huang, Q., Zhao, J., Jenks, W. S., and Larock, R. C. (2007). Aryl to Aryl Palladium Migration in the Heck and Suzuki Coupling of o-Halobiaryls. J. Am. Chem. Soc. *129*, 6298-6307.

Kraszkiewicz, L., Sosnowski, M., and Skulski, L. (2006). Oxidative Iodination of Deactivated Arenes in Concentrated Sulfuric Acid with I_2/$NaIO_4$ and KI/$NaIO_4$ Iodinating Systems. Synthesis 1195-1199.

Barder, T. E., Walker, S. D., Martinelli, J. R., and Buchwald, S. L. (2005). Catalysts for Suzuki-Miyaura Coupling Processes: Scope and Studies of the Effect of Ligand Structure. J. Am. Chem. Soc. *127*, 4685-4696.

Liu, C., Ji, C. L., Hong, X., and Szostak, M. (2018). Palladium-Catalyzed Decarbonylative Borylation of Carboxylic Acids: Tuning Reaction Selectivity by Computation. Angew. Chem. Int. Ed. *57*, 16721-16726.

Crawford, A. G., Liu, Z., Mkhalid, I. A. I., Thibault, M. H., Schwarz, N., Alcaraz, G., Steffen, A., Collings, J. C., Batsanov, A. S., Howard, J. A. K., and Marder, T. B. (2012). Synthesis of 2- and 2,7-Functionalized Pyrene Derivatives: An Application of Selective C-H Borylation. Chem. Eur. J. *18*, 5022-5035.

Ni, J., Li, J., Fan, Z., and Zhang, A. (2016). Cobalt-Catalyzed Carbonylation of C(sp^2)-H Bonds with Azodicarboxylate as the Carbonyl Source. Org. Lett. *18*, 5960-5963.

Miguez, J. M. A., Adrio, L. A., Sousa-Pedrares, A., Vila, J. M., and Hii, K. K. (2007). A Practical and General Synthesis of Unsymmetrical Terphenyls. J. Org. Chem. *72*, 7771-7774.

Adak, L., and Yoshikai, N. (2011). Cobalt-Catalyzed Preparation of Arylindium Reagents from Aryl and Heteroaryl Bromides. J. Org. Chem. *76*, 7563-7568.

Rao, B., Chong, C. C., and Kinjo, R. (2018). Metal-Free Regio- and Chemoselective Hydroboration of Pyridines Catalyzed by 1,3,2-Diazaphosphenium Triflate. J. Am. Chem. Soc. *140*, 652-656.

Wang, D. Y., Wang, C., and Uchiyama, M. (2015). Stannyl-Lithium: A Facile and Efficient Synthesis Facilitating Further Applications. J. Am. Chem. Soc. *137*, 10488-10491.

Roesner, S., and Buchwald, S. L. (2016). Continuous-Flow Synthesis of Biaryls by Negishi Cross-Coupling of Fluoro- and Trifluoromethyl-Substituted (Hetero)arenes. Angew. Chem. Int. Ed. *55*, 10463-10467.

Zhang, Z., Tanaka, K., and Yu, J. Q. (2017). Remote site-selective C-H activation directed by a catalytic bifunctional template. Nature *543*, 538-542.

Kuriyama, M., Matsuo, S., Shinozawa, M., and Onomura, O. (2013). Ether-Imidazolium Carbenes for Suzuki-Miyaura Cross-Coupling of Heteroaryl Chlorides with Aryl/Heteroarylboron Reagents. Org. Lett. *15*, 2716-2719.

Lucas, S., Heim, R., Negri, M., Antes, I., Ries, C., Schewe, K. E., Bisi, A., Gobbi, S., and Hartmann, R. W. (2008). Novel Aldosterone Synthase Inhibitors with Extended Carbocyclic Skeleton by a Combined Ligand-Based and Structure-Based Drug Design Approach. J. Med. Chem. *51*, 6138-6149.

Ramakrishna, V., Rani, M. J., and Reddy, N. D. (2017). A Zwitterionic Palladium(II) Complex as a Precatalyst for Neat-Water-Mediated Cross-Coupling Reactions of Heteroaryl, Benzyl, and Aryl Acid Chlorides with Organoboron Reagents. Eur. J. Org. Chem. 7238-7255.

Kloss, F., Neuwirth, T., Haensch, V. G., and Hertweck, C. (2018). Metal-Free Synthesis of Pharmaceutically Important Biaryls by Photosplicing. Angew. Chem. Int. Ed. *57*, 14476-14481.

Miao, W., and Chan, T. H. (2003). Exploration of Ionic Liquids as Soluble Supports for Organic Synthesis. Demonstration with a Suzuki Coupling Reaction. Org. Lett. *5*, 5003-5005.

Luan, Y. X., Zhang, T., Yao, W. W., Lu, K., Kong, L. Y., Lin, Y. T., and Ye, M. (2017). Amide-Ligand-Controlled Highly para-Selective Arylation of Monosubstituted Simple Arenes with Arylboronic Acids. J. Am. Chem. Soc. *139*, 1786-1789.

Tang, R. J., He, Q., and Yang, L. (2015). Metal-free oxidative decarbonylative coupling of aromatic aldehydes with arenes: direct access to biaryls. Chem. Commun. *51*, 5925-5928.

Zhao, J., Yue, D., Campo, M. A., and Larock, R. C. (2007). An Aryl to Imidoyl Palladium Migration Process Involving Intramolecular C-H Activation. J. Am. Chem. Soc. *129*, 5288-5295.

Ishiyama, T., Nobuta, Y., Hartwig, J. F., and Miyaura, N. (2003). Room temperature borylation of arenes and heteroarenes using stoichiometric amounts of pinacolborane catalyzed by iridium complexes in an inert solvent. Chem. Commun. 2924-2925.

Wu, J., Zhang, D., Chen, L., Li, J., Wang, J., Ning, C., Yu, N., Zhao, F., Chen, D., Chen, X., Chen, K., Jiang, H., Liu, H., and Liu, D. (2013). Discovery and Mechanism Study of SIRT1 Activators that Promote the Deacetylation of Fluorophore-Labeled Substrate J. Med. Chem. *56*, 761-780.

Sun, K. X., He, Q. W., Xu, B. B., Wu, X. T., and Lu, J. M. (2018). Synthesis of N-Heterocyclic Carbene-Pd(II)-2-Methyl-4,5-dihydrooxazole Complexes and Their Application Toward Highly Chemoselective Mono-Suzuki-Miyaura Coupling of Dichlorobenzenes. Asian J. Org. Chem. *7*, 781-787.

Goossen, L. J., and Paetzold, J. (2004). New synthesis of biaryls via Rh-catalyzed decarbonylative Suzuki-coupling of carboxylic anhydrides with arylboroxines. Adv. Synth. Catal. *346*, 1665-1668.

Michelet, B., Deldaele, C., Kajouj, S., Moucheron, C., and Evano, G. (2017). A General Copper Catalyst for Photoredox Transformations of Organic Halides. Org. Lett. *19*, 3576-3579.

Xu, X., Xu, B., Li, Y., and Hong, S. H. (2010). Abnormal N-Heterocyclic Carbene Promoted Suzuki-Miyaura Coupling Reaction: A Comparative Study. Organometallics *29*, 6343-6349.

Heijnen, D., Helbert, H., Luurtsema, G., Elsinga, P. H., and Feringa, B. L. (2019). Synthesis of substituted benzaldehydes via a two-step, one-pot reduction/cross-coupling procedure. Chem. Commun. *21*, 4087-4091.

Pinxterhuis, E. B., Giannerini, M., Hornillos, V., and Feringa, B. L. (2016). Fast, greener and scalable direct coupling of organolithium compounds with no additional solvents. Nat. Commun. *7*, 11698.

Liu, Z., Dong, N., Xu, M., Sun, Z., and Tu, T. (2013). Mild Negishi Cross-Coupling Reactions Catalyzed by Acenaphthoimidazolylidene Palladium Complexes at Low Catalyst Loadings. J. Org. Chem. *78*, 7436-7444.

Teng, Q., Wu, W., Duong, H. A., and Huynh, H. V. (2018). Ring-expanded N-heterocyclic carbenes as ligands in iron-catalysed cross-coupling reactions of arylmagnesium reagents and aryl chlorides. Chem. Commun. *54*, 6044-6047.